



**The role of PADs in the biogenesis of prostate cancer
microvesicles which play a dysfunctional role on DC
biology and the therapeutic potential of skeletal
muscle microvesicles on prostate cancer cells**

Presented by

Sharadkumar Rajnikant Kholia

Thesis submitted in partial fulfilment of the requirement

for the degree of

DOCTOR OF PHILOSOPHY (Ph.D)

Director of Studies: Prof. Jameel M. Inal

Second Supervisor: Dr Sigrun Lange (UCL)

Cellular and Molecular Immunology Research Centre (CMIRC)

School of Human Sciences, Faculty of Life Sciences and Computing

London Metropolitan University

April 2014

Contents

Acknowledgements	1
Abstract	4
Original Publications	6
Abbreviations	7
1. Introduction.....	9
1.1 Microvesicles.....	10
1.1.1 Definition, Size and History	10
1.1.2 MV biogenesis	11
1.1.3 Apoptotic bodies differ from MVs	16
1.1.4 Exosomes: definition, release and function.....	18
1.1.5 Pathological implications of MVs.....	20
1.2 Peptidylarginine Deiminase (PAD)	24
1.2.1 Traits and Tissue Expression of PAD Isotypes	25
1.2.2 The role of PAD in Human Disease	28
1.3 Human Skeletal muscle cells (HSkMC) and Cancer	32
1.4 Dendritic cells in the Cancer Microenvironment	33
1.4.1 Subsets of Dendritic cells.....	34
1.4.2 Tumour infiltration of Dendritic cells	35
1.4.3 Apoptosis and dysfunction of DCs in the tumour environment.....	37
1.5 Aim.....	41
2. Methodologies	43
2.1 Eukaryotic Cell lines and Culturing.....	44
2.1.1 Cell Growth Medium (CGM).....	44
2.1.2 Non-Adherent Cell lines	44
2.1.3 Adherent Cell lines	45
2.1.4 Maintaining Non-Adherent Cell lines.....	48
2.1.5 Maintaining Adherent Cell lines.....	48
2.1.6 Freezing of eukaryotic cells	49
2.1.7 Thawing of cells	50

2.2 Biochemical Methods	51
2.2.1 Flow cytometry	51
2.2.2 Preparation of Normal Human Serum (NHS)	52
2.2.3 Purification of Microvesicles (MVs) from conditioned medium (Constitutively released MVs)	52
2.2.4 Induction and purification of MVs	53
2.2.5 Determination of Protein Concentration	54
2.2.6 Preparation of cell lysates	54
2.2.7 Sample preparation for SDS-Polyacrylamide Gel Electrophoresis (SDS-PAGE)	55
2.2.8 SDS-PAGE Protein Molecular Weight Standards	55
2.2.9 SDS-Polyacrylamide Gel Electrophoresis	56
2.2.10 Western Blotting Analysis	57
2.2.11 Immunochemical Protein Detection using the ECL System	58
2.2.12 Mass Spectrometry Analysis	58
2.3 Statistical Analysis	60
3. The Effect of HSkMC MVs on prostate Cancer Cells	61
3.1 Introduction	62
3.2 Methodologies	63
3.2.1 The effect of NHS on MV release	63
3.2.2 Annexin V labelling of MVs	63
3.2.3 Electron microscopy	64
3.2.4 HSkMC cell differentiation	65
3.2.5 Proliferation assay	66
3.2.6 Cell migration assay	67
3.2.7 Mass Spectrometry analysis of myoblast and myocyte MVs	68
3.3 Results	69
3.3.1 The effect of sublytic complement on the release of MVs	69
3.3.2 HSkMC and cancer	73
3.3.3 Summary of the apoptotic effect of HSkMC MVs on PC3M cells	90

4. The role of Peptidylarginine deiminase on microvesiculation	92
4.1 Introduction	93
4.2 Methodologies.....	95
4.2.1 PAD isotype expression in cancer and non-cancerous cells.....	95
4.2.2 The Effect of PAD inhibition on MV release	97
4.2.3 F95 Immunoprecipitation (IP).....	98
4.2.4 Western blot analysis of citrullinated proteins from PC3M cells stimulated for microvesiculation.....	100
4.2.5 Mass Spectrometry analysis of citrullinated proteins from PC3M cells stimulated for microvesiculation.....	101
4.2.6 Role of chloramidine on the cytotoxic effect of methotrexate on cancer cells.....	101
4.3 Results	103
4.3.1 PAD 2 and 4 are expressed in K562, PC3 and PNT2 cells.....	103
4.3.2 PAD activation is needed for microvesiculation of cancer and non-cancer cells.....	108
4.3.3 During MV release from K562 cells the cytoskeletal protein β - Actin is deiminated by PAD enzyme	119
4.3.4 PAD inhibition reduces deimination levels of proteins in PC3 cells stimulated to microvesiculate with BzATP	122
4.3.5 Mass Spectrometry analysis of deiminated proteins from PC3 cells stimulated for microvesiculation.....	125
4.3.6 The PAD and microvesiculation inhibitor chloramidine sensitizes erythroleukaemic K562 cells to cancer drug mediated cytotoxicity.....	130
4.3.7 The PAD and microvesiculation inhibitor chloramidine renders PC3 cells more sensitive to cancer drug mediated cytotoxicity	134
4.3.8 Summary of the role of PAD on microvesiculation and PAD inhibitors on the viability of cancer cells.....	136

5. The role of iC3b deposition on apoptotic cancer cells and their MVs in inhibiting DC maturation with the aim of developing novel immunotherapeutic strategies to inhibit tolerance of tumour cells	139
5.1 Introduction	140
5.2 Methodologies.....	142
5.2.1 Heat Induced Apoptosis assay.....	142
5.2.2 iC3b deposition assay.....	142
5.2.3 Fluorescence microscopy analysis of iC3b deposition on cells.....	144
5.2.4 Western blot analysis of iC3b deposition on cells	144
5.2.5 Detection of iC3b on MVs from apoptotic cells.....	145
5.2.6 Isolation of MVs with or without iC3b from cancer cells	145
5.2.7 Western blot analysis of iC3b expression on MVs from apoptotic cells	146
5.2.8 Isolation of peripheral blood mononuclear cells from whole blood.....	146
5.2.9 Isolation of CD14 ⁺ monocytes from PBMC	147
5.2.10 Differentiation of CD14 ⁺ monocytes to immature DC (iDC).....	148
5.2.11 The effect of iC3b opsonised apoptotic cells on iDC maturation.....	148
5.2.12 The effect of iC3b rich apoptotic cell MVs on DC maturation.....	149
5.3 Results	151
5.3.1 Cancer cell apoptosis assay	151
5.3.2 Deposition of iC3b on cancerous apoptotic cells.....	157
5.3.3 The complement inhibitory peptide Complement C2 receptor trispanning (CRIT) and its role in inhibiting the deposition of iC3b on cancer cells.....	166
5.3.4 Blocking exposed phosphatidylserine inhibits the deposition of iC3b on apoptotic cancer cells	171
5.3.5 iC3b is also deposited on MVs released from apoptotic cancer cells.....	175
5.3.6 Isolation of CD14 ⁺ monocytes from healthy blood donors	178
5.3.7 Differentiation of CD14 ⁺ monocytes to iDCs	179
5.3.8 iC3b opsonised apoptotic cells inhibit iDC maturation	181

5.3.9 iC3b-rich apoptotic MVs inhibit the maturation of iDCs	184
5.3.10 The effect of cancer cell MVs on DC maturation.....	187
5.3.11 Summary of the effect of iC3b and cancer cell derived MVs on DC cell maturation	190
6. Discussion	194
6.1 MVs and/or exosomes released from human myocytes induce apoptosis of highly metastatic PC3M cells	196
6.2 The potential role of PADs in MV biogenesis	202
6.3 iC3b from apoptotic cancer cells and MVs have an effect on DC phenotype and function	208
6.4 Summary and concluding remarks.....	214
7. Appendix	216
7.1 Additional figures.....	216
7.2 Materials.....	217
7.2.1 Chemicals	217
7.3 Equipment.....	218
7.4 Antibodies	219
7.5 Experimental Solutions.....	220
7.5.1 Mammalian cell freeze medium	220
7.5.2 HSkMC cell freezing medium.....	220
7.5.3 Lysis Buffer pH 7.4.....	220
7.5.4 SDS PAGE Solutions.....	220
7.5.5 Immunofluorescence antibody dilution buffers.....	223
7.5.6 Annexin V binding buffer – pH 7.4	224
8. References	225

Acknowledgements

First and foremost I would like to thank Bhagwan Swaminarayan and my beloved guru HDH Pramukh Swami Maharaj for their blessings and guidance towards completing this PhD.

I would also like to offer my sincerest gratitude to Prof. Jameel Inal, the director of my studies, for giving me the opportunity to work under his supervision. Not only did he patiently provide the vision, encouragement and advice necessary for me to progress through the programme and complete my thesis, but also as a friend and mentor gave me strength and motivation during the uphill moments of this PhD. His ability to listen with patience, Humility, and enthusiasm to name a few are qualities that are truly inspirational which makes him an ideal role model to have for a successful career in research. I truly would like to apologise for any inconvenience that I may have caused him during my journey as a PhD student.

I would also like to thank my second supervisor Dr Sigrun Lange for her expert guidance and advice towards the completion of my projects and thesis as well as for kindly providing antibodies that were essential towards the success of the research project. My sincere thanks to Dr Ephraim Ansa-Addo, who, not only as a supervisor gave me guidance and advice, but also as a friend and colleague supported me throughout my studies. I often remember the Skype calls we had regarding experiments during the late or early hours of the day due to the time difference between the UK and USA. His passion and zeal for science together with his high standards of working

makes him an inspiration for all to follow. A special thanks to London Metropolitan University for awarding me the VC scholarship without which this PhD would have not been possible.

I would also like to specially thank all the members of CMIRC including, Dr. Samireh Jorfi for her help in the lab as well as motivation, Dr. Dan Stratton for helping me out in times of need, Dr. Ahmad Zia Haidery for being a true companion in the lab, Dr. Samuel Antwi-Baffour and Ryan Grant for your friendship, help, support and advice as well as motivation and encouragement during difficult times throughout the programme. A special thanks to Dr. Ravi Velaga for all his help and advice in learning various molecular biology techniques. Over the past years we have truly become more like friends rather than colleagues. Wish you all the best for the future and hope to keep in touch. I would also like to thank members of the MRU especially Dr. Elyn and Dr. Daniel for their support and friendship and would like to wish them good luck for the future. Special thanks to my colleagues in the research lab: Ali, Suam, Xinyu, Marta, Roberta and Simona for their support and friendship. I truly wish you all the best and good luck for the future.

My special thanks also go to all the technical staff both past and present including Eric, Dr. Brigitte, Sophie, Ruth, Hannah, John Morgan and Crowder, Louis Stott, Lubica, Brian Whiting and Kennedy. Each one of you played a vital role in making my studies successful. I would also like to thank Sheelagh Heugh, Dr. Kenneth White, Prof. Chris Palmer, Dr. Garry McLean,

Dr. Samir Nuseibeh and Dr. Nick Wardle for their expert advice and support throughout my PhD. I would also like to extend my gratitude to the staff of the postgraduate research office including Doreen Henry for their admin support throughout the programme.

My heart felt appreciation to my father the late Rajnikant Kholia and my mother Kusumben Kholia for their love, support and blessings which became my inspiration and was my driving force. I would also like to thank my Uncle Rajendra Kholia and Aunt Damyanti Kholia who have treated me like a son. This PhD would have not been possible without their love, support and encouragement. Not to forget my dear sister Runita who has been with me as a pillar of support together with the rest of the Kholia family. I would also like to thank my cousin Jay Kacha who helped me in designing and completing the diagrams for the thesis. Last but not least, I would like to apologise and thank all those who I may have missed out but have played an important role in the successful completion of my studies.

Finally, I would like to dedicate this work to my beloved Guru HDH Pramukh Swami Maharaj, my family and friends. I hope that this work makes you all proud.

“Education is the manifestation of perfection that is already present in man”

HDH Pramukh Swami Maharaj

Abstract

Microvesicles (MVs) are small, plasma membrane derived vesicles that are shed constitutively or upon activation from both normal and malignant cells. Apart from physiological roles, MVs have also been implicated to play a role in various pathologies particularly cancer. Aspects of MV biogenesis and function have therefore become emerging targets for further research and cancer therapy.

In light with the current research this thesis reports for the first time a novel function of peptidylarginine deiminase (PAD) isozymes (elevated in cancer cells) in the biogenesis of MVs. It was reported here that during the stimulation of cancer cells to microvesiculate, PAD expression and deimination of cytoskeletal-actins is increased. Inhibiting the enzyme with pan-PAD inhibitor chloramidine, abrogated the deimination of cytoskeletal actins as well as reduced the release of MVs. Furthermore, combining chloramidine with anticancer drug methotrexate increased the cytotoxic effect of the drug synergistically on different types of cancer cells.

It is also reported for the first time the cytotoxic and anti-proliferative effects of myocyte MVs on prostate cancer cells. Treating prostate cancer cells with MVs from myocytes reduced proliferation and induced apoptosis. Furthermore mass spectrometry analysis of the MVs revealed a candidate protein gelsolin that has been reported to exhibit anti-tumourigenic properties.

This thesis reveals the role of iC3b rich apoptotic cancer cells and their MVs on regulating the phenotype and function of dendritic cells (DC). iC3b rich apoptotic cells prevented the maturation of DCs which was reversed by blocking the iC3b receptor on the DC, or by inhibiting factor I and factor H mediated cleavage of C3b to iC3b using the CRIT-H17 peptide. Furthermore, it was also observed that DCs treated with either iC3b rich apoptotic cell MVs or healthy cancer cell MVs produced elevated levels of the anti-inflammatory cytokine IL-10. iDCs or DCs producing IL-10 levels have been reported to have immunosuppressive properties that are pro-tumourigenic.

Together these results suggest important functions of MVs and their cargo that could have the potential of becoming future therapeutic options in anti-cancer treatments.

Original Publications

- i. Inal JM, Ansa-Addo EA, Stratton D, Kholia S, Antwi-Baffour SS, Jorfi S, Lange S. (2012) Microvesicles in health and disease. *Arch Immunol Ther Exp (Warsz)*. **60(2)**, 107-21.
- ii. Grant R, Ansa-Addo E, Stratton D, Antwi-Baffour S, Jorfi S, Kholia S, Krige L, Lange S, Inal J. (2011) A filtration-based protocol to isolate human plasma membrane-derived vesicles and exosomes from blood plasma. *J Immunol Methods* **31**, 371(1-2).
- iii. Antwi-Baffour S, Kholia S, Aryee YK, Ansa-Addo EA, Stratton D, Lange S, Inal JM. (2010). Human plasma membrane-derived vesicles inhibit the phagocytosis of apoptotic cells--possible role in SLE. *Biochem Biophys Res Commun*. **23**, 398(2).

Public presentations

- iv. Kholia S, and Inal, J.M (2012) Human Skeletal muscle derived microvesicles induce apoptosis in highly metastatic prostate cancer cells. Presented at the Microvesiculation and Disease conference 13th-14th September 2012, London Metropolitan University, UK, Sponsored by Biochemical Society.
- v. Kholia S, and Inal, J.M (2012) Human Skeletal muscle derived microvesicles induce apoptosis in highly metastatic prostate cancer cells. Presented at the 3rd Postgraduates Research Symposium held at London Metropolitan University on 12th July 2012

Abbreviations

AML	Acute myelocytic leukaemia
Anx V	Annexin V
BSA	Bovine serum albumin
Calp	Calpeptin
CD4	Cluster of differentiation 4
Cl-am	Chloramidine
CPT	Camptothecin
DAPI	4',6-diamidino-2-phenylindole
DMSO	Dimethyl sulfoxide
DNA	Deoxyribonucleic acid
DTT	Dithiothreitol
ECM	Extracellular matrix
ECS	Extracellular space
ELISA	Enzyme Linked immunosorbent assay
ER	Endoplasmic reticulum
FACS	Fluorescent activated cell sorter
FasL	Fas ligand
FasR	Fas receptor
FGF-1	Fibroblast growth factor -1
fmk	Fluoromethylketone
FSC	Forward scatter
<i>g</i>	G-force
Gal-3	Galectin-3
GM-CSF	Granulocyte macrophage - colony stimulating factor
Hsp	Heat-shock protein
HUVECs	Human umbilical vein endothelial cells
IL-4	Interleukin-4
LMP-1	Latent membrane protein-I
MAC	Membrane attack complex
MHC	Major histocompatibility complex
MMP	Matrix metalloproteinase
MPs	Microparticles
mRNA	messenger Ribonucleic acid
MVs	Microvesicles
MVBs	Multivesicular bodies
NET	Neutrophil extracellular trap
NHS	Normal human serum
NI	Non-Induced
PAD	Peptidylarginine deiminase
PB	Peripheral blood

PBB	Permeabilisation buffer
PBMCs	Peripheral blood mononuclear cells
PBS	Phosphate buffered saline
PBS-T	Phosphate buffered saline – Tween 20
PC	Phosphatidylcholine
PE	Phosphatidylethanolamine
PI3K	Phosphatidylinositol-3-kinases
PIP ₂	Phosphatidylinositol 4,5-bisphosphate
PL	Phospholipid
PM	Plasma membrane
PS	Phosphatidylserine
RBCs	Red Blood Cells
RNA	Ribonucleic acid
ROCK 1	Rho associated kinase 1
RT	Room temperature
SD	Standard deviation
SDS	Sodium dodecyl sulphate
SSc	Side scatter
SM	Sphingomyelin
TAA	Tumour associated antigens
TEMED	Triamine urine N, N, N-tetramethylethylenediamine
TGF-β1	Transforming growth factor-β 1
TNFα	Tumor necrosis factor-α
TfR	Transferrin receptor
TTP	Thrombocytopenic purpura
TPA	Tissue plasminogen activator
uPA	urokinase Plasminogen Activator
VEGF	Vascular endothelial growth factor
v/v	Volume per volume
w/v	Weight per volume
Z-DEVD-fmk	Benzyloxycarbonyl-Asp-Glu-Val-Asp (OMe)fluoromethylketone
Z-VAD-fmk	Benzyloxycarbonyl-Val-Ala-Asp (OMe) fluoromethylketone

1. Introduction

1.1 Microvesicles

The field of Microvesicles (MVs) has gained interest over the last decade, and is constantly gaining momentum as more and more researchers become aware of this field. Various publications have been released over the years describing the molecular and functional characteristics of MVs, suggesting their importance as a key role player in various cell processes rather than just inert bi-products of cellular activation (3-5).

1.1.1 Definition, Size and History

Microvesicles are defined as intact, submicron, phospholipid-rich vesicles that are ubiquitously released from the cell membranes of diverse cell types upon stimulation and/or apoptosis (6). These vesicles are released from the cellular plasma membrane through membrane shedding as they are constantly challenged in the cellular environment by various factors ranging from chemical to physical stress conditions. This leads to a variety of MVs being formed that differ in size and composition depending on the status and origin of the cell. As a result, a plethora of terms have been used to describe these sub-cellular fragments in a host of reports ranging from microvesicles, microparticles, vesicles and ectosomes, to Plasma Membrane derived Vesicles (7).

The work on MVs began in the 1940's when Chargaff et al. first recognized a sub-cellular precipitable factor in platelet-free plasma. They observed that this factor could accelerate the production of the coagulation protein thrombin (8). Later Wolf and co-workers also noticed the presence of the

sub-cellular factor in platelet-free plasma and termed it "platelet dust". They also confirmed that the platelet dust had procoagulant properties and further demonstrated a linear correlation between the levels of the platelet dust and the original platelet count of the blood samples. This was later established by electron microscopy where small MVs were seen budding from the distal ends of activated platelets (9).

In the past decade scientists have discovered MVs originating from various other cells including monocytes, endothelial cells, and red blood cells. Recent research has further shown that there could be a possibility of most of the other cell types in our body producing MVs (10).

1.1.2 MV biogenesis

1.1.2.1 Cell membrane phospholipids and the enzymatic control of asymmetry

Before looking at how MVs are produced, it is important to understand the normal constitution of the cell membrane and how it is maintained in a normal physiologically active cell.

The plasma membrane phospholipid bi-layer of cells is composed of highly specific phospholipids that are distributed in a precise manner. A form of asymmetry is constantly maintained in a dynamic manner in that phosphatidylcholine (PC) and sphingomyelin (SM) are located on the external leaflet of the plasma membrane whereas phosphatidylserine (PS) and phosphatidylethanolamine (PE) are positioned on the inner leaflet (6).

The conservation of this asymmetry is essential for cell survival and physiology, and is achieved by a combination of five transmembrane enzymes (**Fig 1.1 A - D**) that are also implicated in MV production (6).

Gelsolin

A calcium regulated enzyme that is ubiquitous and plays a multifunctional role in regulating cell structure, metabolism, as well as signal transduction by acting as a transcriptional cofactor (11). It has also been implicated in the biogenesis of MV release by removing proteins that cap the ends of actin filaments of the platelet cytoskeleton. This in turn allows actin to reorganize and hence causes platelet activation and contraction together with MV generation. The enzyme is activated by increased levels of cytosolic calcium (1,6).

Aminophospholipid translocase

This is an ATP-dependent enzyme that is involved in the constant transportation of PS and PE from the outer leaflet of the cell membrane to the inner leaflet, one molecule of ATP being required for the transfer of each PS molecule. The enzyme is inhibited by increased levels of cytosolic calcium (12).

Floppase

This is another ATP-dependent enzyme that is thought to work in conjunction with aminophospholipid translocase. Its main action is to transport lipids from

the inner to the outer leaflet; however its full function is not currently well understood (6).

Lipid Scramblase

The function of this enzyme is to allow the movement of phospholipids across the cell membrane. The enzyme is activated during increased levels of intracellular calcium which simultaneously inhibits aminophospholipid translocase (13). This therefore causes a loss of membrane asymmetry and a stable expression of PS is maintained on the outer membrane which is a hallmark of MV production (6). This enzyme is thought to play an important role in platelet coagulant activity and MV production. Patients who have Scott syndrome and therefore have a mutation in the lipid scramblase enzyme have shown a defect in platelet coagulation activity as well as a reduction in MV levels. This is due to reduced PS expression on the outer leaflet leading to reduced production of MVs, and thus establishing the importance of the enzyme in MV formation (14).

Calpain

This enzyme is a cysteine protease of the papainase family. It is activated during increased levels of cytosolic calcium either through extracellular sources or through the endoplasmic reticulum (ER). Calpain when activated translocates to intracellular membranes from the cytosol where cleavage of actin-cytoskeletal proteins such as talin and α -actinin results in the rearrangement of long actin filaments therefore leading to loss of membrane asymmetry and subsequent release of MVs (**Fig 1.1**)(15,16).

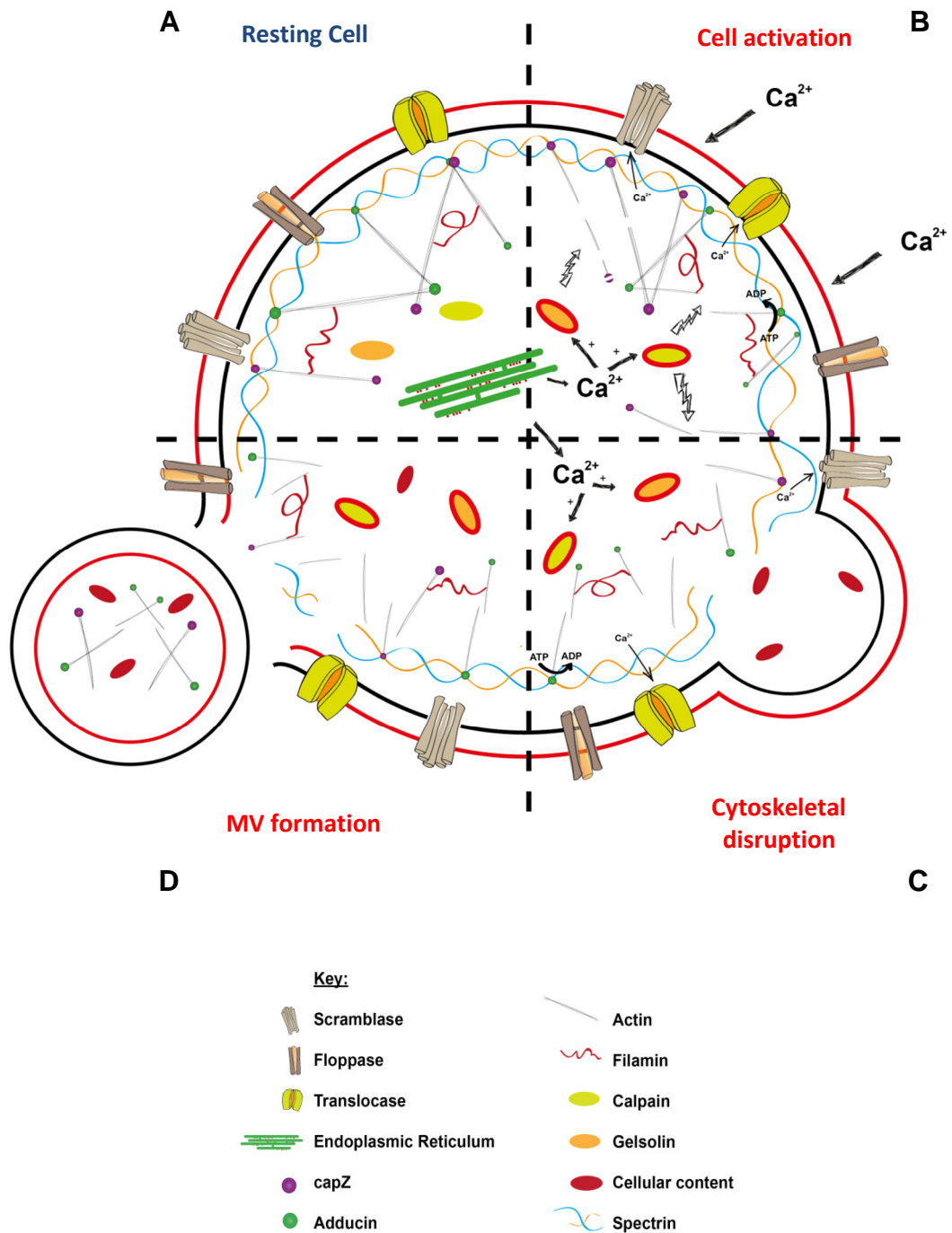


Fig 1.1: Mechanism of Microvesicle release. A) Representation of the resting cell: Scramblase is inactive while Translocase and Floppase are active maintaining membrane asymmetry. **B) Cell Activation:** Scramblase, Calpain and Gelsolin are activated due to calcium release from ER. Calpain cleaves long actin filaments, whilst gelsolin cleaves actin capping proteins. Translocase is inactivated. Membrane asymmetry is therefore compromised. **C) Cytoskeletal Disruption:** protein anchorage to the cytoskeleton is disrupted allowing membrane budding. **D) MV formation:** increased phosphatidylserine is exposed on the MV external surface. **Note-**Cell and MV size is not to scale.

1.1.2.2 Mechanism of MV formation

MVs are released from the cell surface membrane following either cell activation or apoptosis due to chemical stimuli such as cytokines, endotoxins or a physical stimulus such as shear stress (17).

On cell activation there is a rise in cytosolic calcium concentration. This consequently leads to the activation of enzymes such as calpain, gelsolin, scramblase as well as protein kinases. Simultaneously enzymes such as translocase (**Fig 1.1 B**), and phosphatases are inhibited, therefore resulting in cytoskeletal reorganisation, loss of membrane asymmetry, membrane blebbing and MV formation and release (17).

During programmed cell death, the release of MVs is associated with membrane blebbing, which is a characteristic feature of apoptosis. There are some kinases that have been identified to play a role in membrane blebbing (18). One such kinase is the Rho associated kinase 1 (ROCK-1) which is thought to play a key role in the blebbing of MVs (19). The ROCK kinases are activated by GTP-bound Rho and are important mediators of cytoskeletal modifications such as myosin light chain phosphorylation and actin myosin coupling to the plasma membrane. Experiments carried out with mouse fibroblasts and human epithelial breast cancer cells stimulated by tumour necrosis factor α (TNF α) induced apoptosis, showed a decrease in MV blebbing on application of a ROCK 1 activity inhibitor (Y27632) (19) suggesting that the ROCK kinases play a role in MV formation in apoptosis. Furthermore, inhibition of caspases by benzyloxycarbonyl-Val-Ala-Asp

(OMe) fluoromethylketone (z-VAD-fmk) resulted in the abrogation of ROCK-1 activity and subsequently microvesiculation, therefore suggesting a role of caspases (involved in apoptosis) in the release of microvesicles through the activation of ROCK-1 (19). In addition, a study carried out by colleagues at the Cellular and Molecular Immunology Research Centre (CMIRC) observed a similar effect on healthy THP1 monocytes whereby microvesiculation of THP1 cells by normal human serum (sublytic complement) was abrogated by the Rho kinase inhibitor Y27632, therefore suggesting the involvement of the enzyme during microvesiculation in healthy cells as well (20).

As mentioned earlier cell activation and apoptosis causes an imbalance in the asymmetry of the cell membrane and due to this the MVs have a rich phospholipid bi-layer consisting of PS on the outside. PS has therefore become a key marker for identifying MVs whereas other MV proteins and markers are generally used to identify the cellular origin, as different cell types express different markers and proteins on their surfaces (6,17).

1.1.3 Apoptotic bodies differ from MVs

Apoptosis is a controlled mechanism of cell death in the normal physiology of a cell. During this controlled cell death a cell passes through several stages from condensation of nuclear chromatin, to membrane blebbing and eventually the disintegration and packaging of cellular content into distinct membrane enclosed vesicles known as apoptotic bodies (21). Whereas MVs and exosomes (sec 1.1.4) are secreted during normal cellular processes, apoptotic bodies are restricted to cells undergoing apoptosis. Like

microvesicles apoptotic bodies also express PS on the outer leaflet, which facilitates their recognition and clearance by phagocytic cells (i.e. macrophages). Other than usually carrying fragmented DNA and organelles, they are also easily distinguishable from MVs by their larger mean diameter ranging from 500-4000 nm (22).

As aforementioned, the exposure of PS on the outer leaflet of the plasma membrane due to the deactivation of flippase and activation of scramblase, subsequently, leads to microvesiculation. However, other observations suggest that this phenomenon does not always follow exposure of PS simply because the required threshold of cytosolic Ca^{2+} for microvesiculation is higher than for exposure of PS on the outer leaflet (23).

Furthermore, Simak *et al* reported in their study that on treating human umbilical vein endothelial cells (HUVEC) with lower concentrations of camptothecin (CPT), a topoisomerase-I inhibitor, released a variety of phenotypically different populations of PS⁺ MVs that were limited to the early stages of apoptosis whereby the detection of PS on the cells as well as DNA fragmentation was not observed (24). Interestingly, they also observed that on inhibiting myosin adenosine triphosphatase (MAT), CPT-mediated release of MVs was further enhanced. Simply put, the use of a myosin light chain inhibitor failed to inhibit CPT-induced release of MVs. Earlier reports explaining the mechanisms of apoptotic blebbing have suggested the dependency of apoptotic blebbing on the activities of MAT and myosin light chain kinase (25). This therefore indicates that MVs that are released at the early stage of pro-apoptotic stimulation are produced via a different

mechanism than apoptotic blebbing, which results in the release of apoptotic bodies.

1.1.4 Exosomes: definition, release and function

First described by Rose Johnstone *et al* in the 1980s, exosomes were thought to be a means by which reticulocytes remove unwanted proteins from the plasma membrane (26). Since then various studies have uncovered the role of these vesicles as important mediators of intercellular communication at both a physiological and pathological level (3).

Exosomes are a homogenous population of small membrane vesicles released by eukaryotic cells and are often confused with MVs. They have a much narrower size range than MVs, ranging from 50-100 nm in diameter and are coated with a lipid bilayer (3). Like MVs, exosomes are also released from cells upon activation but have a different mechanism of release through microvesicular bodies (MVBs) (27).

Invagination of the MVB membrane creates an enclosed compartment known as intraluminal vesicles (ILVs) containing proteins sequestered to the limiting membrane of MVBs, which are then either secreted as exosomes or degraded after fusion with lysosomes (28). Two distinct pathways have been identified that lead to the formation of ILVs. Components of the endosomal sorting complex required for transport (ESCRT) machinery have been shown to be involved in the inward budding and cleavage of bud necks of the limiting membrane of MVBs therefore forming ILVs (29). A second ESCRT-independent exosomal pathway has been discovered by Trajkovic *et al*

whereby sphingomyelin hydrolysis occurs by neutral Sphingomyelin phosphodiesterase (Smase) activity which generates ceramide. The cone-shaped structure of ceramide is postulated to induce a spontaneous negative curvature that occurs on the cytosolic leaflet of the endosomal membrane resulting in an inward budding into the endosome thereby forming ILVs which are then secreted as exosomes upon MVB fusion with the plasma membrane (27).

Exosomes can be active and function in various processes such as antigen presentation or mediate target cell killing. They have a density range from 1.13 g/cm³ to 1.19 g/cm³ and carry protein biomarkers as in the original cell (3). Some proteins can be found on the surface of the plasma membrane or in the cytoplasm of nearly all exosomes regardless of the cell type from which they were isolated (3). These are referred to as exosomal markers to help differentiate exosomes from other types of vesicles. These include membrane transport and fusion proteins (Annexins, GTPases, flotillin), heat shock proteins (Hsc70, HSP 90), MVB biogenesis proteins (Alix, TSG101) and tetraspanins – including CD9, CD63, CD81 and CD82, which represent the most abundant protein families present in exosomes (30,31).

Since their discovery, it has been becoming increasingly evident that exosomes through their function as extracellular vehicles play specialized roles in both physiological and pathological environments (32). Physiologically they are thought to function as the messengers, delivering various effectors or signalling macromolecules at an intercellular level.

Pathologically the same intercellular function of exosomes has linked them with an important role in cancer progression as mediators of immune suppression, angiogenesis and metastasis. Nevertheless, the current understanding of exosome biogenesis and function has opened doors to understand the biology of cancer as well as development of novel anticancer therapies (33).

1.1.5 Pathological implications of MVs

1.1.5.1 MVs and Cancer

Over the past century cancer has constantly been an increasing burden globally and has become one of the leading causes of death both in the developed and developing world (34). Over the last decade MVs have been implicated to play a role directly or indirectly in the pathogenesis of various diseases cancer being one of them (35-37). The presence of MVs in cancer patients had already been noticed since the late 1970s (38), and, various investigators have also shown elevated levels of MVs in the blood from cancer patients as opposed to healthy people (39-41). Therefore it was only a matter of time before the role of MVs in cancer biology was actually determined.

1.1.5.1.1 Cellular Survival

Various cells have been shown to release MVs as a protective mechanism against intracellular stress such as would occur with apoptotic enzymes. Caspase 3 is one of the primary enzymes involved in apoptosis in normal cell

physiology, and recently various researchers have reported the presence of this enzyme in conditioned medium of viable cell cultures (42,43). Furthermore, analysis of MVs from the conditioned medium confirmed them as having substantial quantities of caspase 3 enzyme. On the basis of this information, various researchers postulated that the cells release caspase 3 via MVs in order to prevent intracellular accumulation and hence escape from its apoptotic effects. This hypothesis was strengthened by Hussein et al who reported that on blocking the release of MVs, cells indeed accumulate caspase 3 and undergo apoptosis (44). As cancer cells retain the majority of cellular function akin to their non-cancerous counterparts, this mechanism may be one way by which cancer cells escape cell death.

Cancer cells have also been shown to be resistant to a variety of chemotherapeutic drugs. Shedden *et al* showed in their study that cancer cells insensitive to chemotherapy express more genes related to membrane shedding as opposed to the chemo-sensitive cells. They also reported that MVs from the chemo-insensitive cells contained high levels of the chemotherapeutic drug doxorubicin (45). Safeaei and colleagues also conducted a similar study on another resistant chemotherapeutic drug, cisplatin. They demonstrated that cisplatin-insensitive cells released MVs that contained 2.6 fold more cisplatin compared to MVs released by cisplatin-sensitive cells (46). This evidence therefore suggested that cancer cells probably eject the drug through the release of MVs in order to escape from the detrimental effects of chemotherapeutic agents and that this might provide a possible mechanism for multidrug resistance.

Another way by which cancer cells have been shown to survive is by escaping immuno surveillance. The tumour environment is well known to be resistant to complement attacks, although the micro-tumours are more susceptible to complement. In 1988, Sims and co-workers, suggested a mechanism known as "complement resistance" whereby cells exposed to complement C5b-9 complex survived complement lysis by releasing MVs rich in C5b-9 (47). Various researchers later showed that cancer cells use the same mechanism to evade the complement system (48,49). This mechanism was however further enhanced by the cancer cells through shedding MVs rich in the complement inhibitor protein CD46, which inactivates complement C4b and C3b proteins (50). Hence not only would the cancer cells prevent complement from attacking but would also inactivate it.

Apart from inactivating complement, cancer cells have also been shown to suppress the immune system by releasing MVs rich in immuno-modulatory molecules such as Fas ligand (which diminishes the function of the adaptive immune system) and Latent membrane protein-I (LMP-I) which inhibits leukocyte proliferation (51-53). Various other mechanisms have been identified through which cancer cells evade the immune system via MVs. These include releasing MVs that fuse with monocyte plasma membranes so impairing differentiation of monocytes into antigen presenting cells. Another mechanism involves MVs exchanging surface lipids and proteins such as integrins which in turn mask cells as non-cancerous enabling them to effectively evade immuno surveillance (54-56).

1.1.5.1.2 Invasive growth and metastasis

After successfully evading the immune system, not only do cancers proliferate and grow into large tumours, but they spread to other parts of the body through metastasis.

For a tumour to grow it is essential for it to degrade the extracellular matrix (ECM). In a physiological setting this is achieved by proteases such as matrix metalloproteinase 2 (MMP-2) and MMP-9 as well as urokinase Plasminogen Activator (uPA) which degrades the basement membrane collagen as well as various components of the ECM such as fibrin. One mechanism by which cancer cells break down the ECM is through the release of MVs that are rich in MMP-2 and MMP-9 as well as uPA (57). This was demonstrated by Graves *et al* who reported elevated levels of MVs rich in MMPs and uPA from patients with late stage ovarian carcinoma as opposed to patients in early stage ovarian carcinoma. Furthermore, inhibiting the MMPs and uPA in these MVs virtually eliminated the ability of the MVs to support tumour invasiveness (57).

Together with ECM degradation, MVs have also been shown to aid cancer cells in angiogenesis. It is a well established fact that not only do cancer patients have elevated levels of MVs in their blood but also that these MVs are rich in tissue factor, which is a procoagulant factor that contributes to fibrin formation. The fibrin eventually protects the tumour against the immune system and forms a matrix to support angiogenesis (58,59). This procoagulant effect of MVs has also been shown to indirectly activate the

release of growth factors such as vascular endothelial growth factor (VEGF). One way by which cancer cell MVs are likely to activate growth factors was reported by Baj *et al* who showed that these MVs carried mRNA encoding for growth factors such as VEGF and hepatocyte growth factor. The MVs would then fuse with monocytes and transfer the nucleic acids to induce production of these growth factors (60,61).

Whether or not MVs promote cancer cell metastasis has not yet been studied extensively. However one can postulate that the MVs probably aid in cancer metastasis indirectly through the immunosuppressive and angiogenic effects of the cancer cell derived MVs seen earlier.

1.2 Peptidylarginine Deiminase (PAD)

Amongst all the post translational modifications that occur in proteins, deimination alternatively known as citrullination has become a centre point of investigation amid researchers for its role in physiology and pathology.

Deimination is the posttranslational conversion of protein-bound arginine and methylarginine residues that are positively charged to the neutral amino acid citrulline. Citrulline is a nonstandard amino acid that has no transfer-ribonucleic acid (tRNA) molecule coded for it and therefore is not integrated into proteins during translation. This irreversible posttranslational modification is mediated by calcium regulated peptidylarginine deiminases (PADs) that in response to elevated calcium levels cause protein bound deimination in target proteins, leading to structural and functional changes (62-64).

The process of citrullination, or protein deimination, was first described in 1977 by Llewellyn-Smith *et al*, and the PADs are thought to be the only group of enzymes to citrullinate proteins as part of post translational modification (65).

In mammals, five isoforms of PAD (i.e. PADs 1-4, and 6) have been identified that exhibit tissue-specific expression patterns and vary in their subcellular localization (63,66,67). In humans, the PAD genes are localized to a well organized gene cluster at 1p36.13 which interestingly is also identified to be the cluster region for the tumour suppressor gene RUNX3 also implicated in cancer (68). All isotypes of PAD exhibit extensive mutual homologies, with approximately 50 to 60% sequence identity at the amino acid level. However, the tissue distribution patterns of each of the isotypes are relatively selective as are their target cellular proteins (69,70).

1.2.1 Traits and Tissue Expression of PAD Isotypes

PAD1 is primarily expressed in the epidermis and the uterus. In the epidermis, PAD1 plays an important role in skin homeostasis. It is involved in the citrullination of cytokeratin (70). This allows the modulation of cornification in the epidermis together with the maintenance of the barrier function of the keratinized superficial epidermal cell layers. As a consequence there is a reduction in the flexibility of the keratin cytoskeleton, therefore stimulating the cornification of the epidermis (71,72).

PAD2 is broadly expressed in multiple organs of the body, the most extensive being the skeletal muscle, female reproductive tissues, cells of the

haematopoietic lineage, spleen, secretory glands and the brain (72-74). The main substrates of PAD2 are vimentin (in macrophages and skeletal muscle) and Myelin Basic Protein (MBP) (in the central nervous system) (75,76). Vimentin is an intermediate filament that provides support to cell organelles in conjunction with the cytoskeleton in a healthy cell. This function is possible due to the polymerisation and depolymerisation of the filaments which is regulated by reversible phosphorylation of specific sites on the vimentin molecule (77). Citrullination by PAD2 causes disintegration of the vimentin-cytoskeleton in macrophages and therefore apoptosis (75).

PAD2 is the isoform of PAD that is highly expressed in the brain, with MBP as its primary substrate. MBP is a major constituent of the myelin sheath that insulates the axons of nerve cells. This protein has been shown to be citrullinated in the white matter of healthy subjects, where approximately 19% of MBP molecules were citrullinated (78). However this proportion was found to have increased in patients with multiple sclerosis, therefore suggesting a more pathological role of PAD2 in neurodegenerative diseases (78).

PAD3 has been shown to be expressed in hair follicles and epithelium where it targets trychohyaline which is a major structural protein of the inner root sheath cells of hair follicles. Citrullination of trychohyaline allows efficient cross-linking with keratin filaments thereby forming a solid matrix that guides the directional growth of the hair fibre (79). Furthermore, filaggrin a keratin binding filament based protein in epithelial cells has also been linked as a substrate for PAD3 citrullination in epidermal homeostasis (71).

PAD6 is a relatively novel member of the PAD enzyme group that has been recently discovered in embryo and egg cells (80). It is therefore considered as a maternal effect enzyme and is essential for the early stage development of the embryo (81).

To date, **PAD4** has been the focus of many biochemical studies, making it the most characterised isoform of PAD. Physiologically, the enzyme is expressed mainly in haematopoietic progenitor cells, and cells of the immune system such as granulocytes, monocytes and natural killer cells. It is the only isoform to contain a classic nuclear localization signal and is commonly localised in the nucleus of the cell (75,82-84) but recently other PAD isozymes (PAD2 and PAD3) have also been reported in the nucleus (85-87). PAD4 has also been shown to have a variety of roles in the body. PAD4 is a transcriptional co-regulator for a range of factors such as p53, p300, p21 and ELK1. The regulatory function of PAD4 is thought to be mediated by citrullination of the N-terminal tails of various histone proteins. PAD4 also acts as co-mediator of gene transcription and epigenetic cross talk with histone deacetylase 2 (HDAC2) (to regulate p53 gene activity during DNA damage) and has been postulated to play a role in apoptosis. PAD4 has been shown to translocate to the nucleus in response to upregulated TNF α (88) as well as playing a role in the formation of neutrophil extracellular traps (NETs) which is an essential part of the innate immune system during bacterial infection (82,89,90).

1.2.2 The role of PAD in Human Disease

As seen above, protein citrullination via PAD enzymes has been shown to regulate numerous physiological functions. However when dysregulated, citrullination has also been shown to be associated with various human autoimmune diseases such as rheumatoid arthritis, psoriasis, multiple sclerosis, and recently cancer (89,91-93).

Psoriasis occurs due to a rapid abnormal proliferation of keratinocytes which then migrate from the basal layer to the surface of the skin. The skin cannot shed these cells effectively which accumulate in thick dry plaques which then become inflamed and itchy. In normal keratinocytes, PAD1 citrullinates keratin K1 during terminal differentiation which allows the keratin filaments to be more compact and therefore normal cornification of the epidermis occurs. In psoriatic plaques, the keratinocytes lack citrullinated K1 keratin filaments therefore indicating the involvement of PAD1 in the pathology. However, it is not yet clear whether the increased proliferation of keratinocytes prevents the necessary citrullination by PAD or whether an inactive abnormal PAD is the actual cause of the proliferation of the keratinocytes (94).

Rheumatoid arthritis (RA) is a common autoimmune disease characterized by chronic inflammation and infiltration of immune cells to the synovial joints due to the presence of antibodies to auto-antigens. 80% of blood samples analysed from patients with RA has shown the presence of auto-antibodies against citrullinated proteins with a RA specificity of 99% (95). Furthermore, these auto-antibodies have been detected in the early stages of the disease

and therefore have become an ideal diagnostic marker for RA. Their appearance at the site of inflammation indicates the presence of citrullinated proteins such as extravascular citrullinated fibrin which in turn drives the maturation of anti-peptidylcitrulline specific B cells locally (95-99).

One explanation for the citrullinated proteins could be the imbalance in oxygen metabolism at the site of inflammation. One area would be rich in oxygen partially due to the production of reactive oxygen species, and other areas would be hypoxic, both of which would lead to stress and eventually death at a cellular level. Due to inflammation the area is rich in white blood cells such as granulocytes and macrophages which express PAD4 and PAD2 enzymes respectively. Once these cells are stressed and eventually die due to the oxygen imbalance there is a possibility of leakage of the PAD enzymes in to the surrounding areas, and as the extracellular matrix is rich in Ca^{2+} ions, the PAD enzymes would be activated leading to aberrant citrullination of extracellular proteins such as fibrin (67,75,95,98).

The presence of both citrullinated proteins and autoantibodies leads to the formation of antigen-antibody immune complexes which eventually exacerbates the disease.

Multiple Sclerosis (MS) is a chronic inflammatory disorder of the central nervous system, characterised by damage to the myelin sheath causing demyelination of the axons hence loss of function (78). The myelin sheath is composed of lipid-protein complexes in a ratio of approximately 3:1. 85% of

the total protein content of the myelin sheath is composed of myelin binding protein (MBP) and lipophilin (100).

MBP is a highly positively charged molecule that interacts strongly with negatively charged phospholipids such as phosphatidylserine, an interaction that is essential for the formation of normal myelin sheath (100). Citrullination of MBP by PAD2 affects this lipid binding ability by reducing its highly cationic state, therefore causing the structure to unfold. This makes the protein more prone to degradation by the proteinase enzyme cathepsin D (four times more than uncitrullinated MBP) known to be localised in the central nervous system myelin of MS patients with elevated activity (101). In rare cases of MS (Marburg type), 80% of the MBP is citrullinated making it severely unfolded. This not only reduces the capability of forming a stable form of myelin, but also increases the degradation rate by cathepsin D to about 45 times than normal (102). Therefore PAD mediated citrullination is implemented as a mechanism of pathogenesis of multiple sclerosis. Various researchers have reported low doses of the anti-cancer drug Paclitaxel to inhibit citrullination of MBP by PAD2 and therefore attenuate the related clinical symptoms together with remyelination of damaged sheaths (103,104). This therefore provides new insight to the aetiology of the disease which may contribute towards development of more effective drugs for the treatment of demyelinating diseases.

1.2.2.1 PAD and Cancer

Out of all the PAD isozymes, PAD2 and PAD4 have been linked with cancer, both being reported to be over expressed in blood and tissues of patients suffering from malignant tumours (85,105,106).

Chang *et al* reported in their study a significant expression of the PAD4 enzyme in many tumours particularly adenocarcinoma. They further reported that not only was PAD4 co-located with cytokeratin (CK), an established tumour marker, but also that various isoforms of CK (8, 18, and 19) had been citrullinated which made them resistant to caspase mediated cleavage. It was postulated that CK could be a substrate of PAD4 and could contribute through the disruption of apoptosis in cancer tumours by caspase-mediated cleavage of CK (cleavage of CK leads to cell cytoskeleton disassembly, cell shrinkage and therefore cell death) (107).

PAD4 has also been linked with the regulation of oestrogen receptor target gene activity mediated by oestrogen stimulation via histone tail citrullination (108). In addition to this, the isozyme has also been shown to act as a cofactor in epidermal growth factor (EGF) mediated target gene activity. Zhang *et al.* reported that treating MCF-7 cells with EGF lead to PAD4 mediated citrullination of *ELK1* oncogene thereby facilitating subsequent phosphorylation by ERK1/2 and therefore activating the expression of the proto-oncogene *c-fos* (109). Given that both oestrogen and EGF are mitogens in cancer, this observation provides an insight into the role of PAD in cancer.

PAD4 has also been shown to interact with *p53* and influence the expression of its target genes (110-113). Wang *et al.* recently reported the involvement of PAD4 in the repression of *p53* target genes. On inhibiting the enzyme an increase in the expression of *p21*, *C1P1*, and *WAF1* was noticed subsequently causing cell cycle arrest and apoptosis. In addition, the induction of *p21*, cell cycle arrest, and apoptosis by the depletion of PAD4 was *p53* dependent (113). On the basis of these findings PAD4 potentially plays a crucial role in cancer biology.

Given that both PAD activation and microvesiculation are calcium dependant events that are elevated in certain human diseases such as autoimmune diseases and cancer, we hypothesize that an interaction between the two are involved in cancer progression.

1.3 Human Skeletal muscle cells (HskMC) and Cancer

The human skeletal muscle contributes to approximately 40 percent of the total body mass and is also one of the most highly vascularised tissues of the body. Considering these two factors, one would expect skeletal muscle to be the number one region for cancer metastasis. Surprisingly, this is not the case. It is well established in the field of cancer medicine and research that malignant cancers rarely metastasize to the skeletal muscle (114-116). A retrograde study conducted over 3 decades ago concluded that out of all the soft tissue sarcomas (muscle) examined, only 1.6% were of metastatic origin (116).

In the past decade, various researchers have tried to elucidate the cellular and molecular mechanisms contributing to the rarity of secondary metastasis in skeletal muscles but it still remains elusive. Some have postulated that high levels of lactic acid produced by skeletal muscle cells not only makes them unresponsive to the lactic acid secreted by invasive cancer cells for tumour angiogenesis (117), but that the chemical creates a toxic environment that is unfavourable for tumour development (118). In addition, other groups have reported the cytotoxic effects of conditioned media collected from skeletal muscle cells on cancer cells, whilst, some have identified several factors including a molecule known as adenosine reported to be the cause of these cytotoxic effects. However, skeletal muscle cell conditioned media without adenosine, still induced cytotoxicity in target cells, implying the possible involvement of other molecules that have the same effect (119-121).

On this basis, we reasoned to further investigate the possible effect of human skeletal muscle cells derived microvesicles on the proliferation and growth of cancer cells.

1.4 Dendritic cells in the Cancer Microenvironment

First described by Ralph Steinman about thirty years ago, dendritic cells (DCs) are antigen-presenting cells (APC) which play a crucial role in both the innate and the adaptive immune responses. They are considered to be potent "professional" antigen presenters that have the ability to uptake,

process, and present multiple different types of antigens to antigen specific resting naïve T lymphocytes (60,122).

1.4.1 Subsets of Dendritic cells

Dendritic cells originate from haematopoietic progenitor cells located in the bone marrow and then migrate to different non lymphoid tissues and organs in an immature state. Upon maturation with different stimuli, they migrate to the lymphoid tissues to induce a T cell mediated immune response (123).

Since their discovery, four main subtypes have been generally recognised: classical or conventional DCs (cDCs), plasmacytoid DCs (pDCs), Langerhans cells and monocyte-derived DCs (124). Usually these subsets demonstrate a diverse morphology, phenotype and function depending on different environmental milieus. Nevertheless, they often share the ability to either stimulate or inactivate T cell proliferation and response (123,125). For instance, in spite of the accepted function of cDCs as activators of T cell response, various researchers have shown that cDCs together with migratory DCs, inflammatory DCs, and tissue resident DCs may induce tolerance in the immature stage or under certain conditions (125-127).

Similarly, pDCs whose primary function is to suppress an immune response and induce tolerance by blocking proliferation of naïve and antigen-specific CD4+ and CD8+ T cells and activating the proliferation of T regulatory cells, have been shown to induce immune responses by presenting antigens to cytotoxic T lymphocytes (128-130).

Over the years it has become an accepted paradigm that DC function is primarily dependent on maturation. However, there is evidence now to suggest that DCs can function in a multitude of states rather than just the phenotypically immature or mature state depending on the microenvironment they are in (131).

Therefore, DCs can be classified as a group of antigen-presenting cells with functional plasticity to immuno-stimulate or immuno-suppress or both, regardless of their maturation status, instead depending on the micro-environmental stimuli affecting DC differentiation, maturation, activation, and polarization. Recently, the tumour microenvironment has been accepted as such a setting that could influence all aspects of DC biology and therefore influence survival of the tumour from the immune system (132).

1.4.2 Tumour infiltration of Dendritic cells

The immune system has been shown to be involved in the detection and elimination of emerging tumours. As antigen presenting cells, DCs contribute towards this function by infiltrating primary tumour lesions and initiating antitumour immune responses (122).

This function has been evidently shown to significantly prolong survival and reduce metastasis related recurrence in patients with oral, head and neck tumours, lung, bladder, gastric and oesophageal carcinomas (133). Furthermore, analysing tumourigenic glandular epithelium and its surrounding affected tissue by immunohistochemistry showed an inversely proportional relationship between infiltrating DCs and the clinical stage of the

tumour together with lymph node metastasis (134). The relationship between tumour infiltrating DCs and well differentiated, less invasive tumours observed in these together with other findings (134-137) not only reciprocates the important function of DCs in cancer but also reveals a new function of DCs as prognostic and survival markers in cancer patients (133).

The accepted paradigm of DC mediated tumour specific T cell activation is that the T cells are activated in the lymph node and then migrate to the tumour. However, it has been recently reported that naïve T cells can infiltrate tumours and undergo activation *in situ*. For instance, Becker *et al* have recently shown that targeting lymphotoxin- α to mouse melanoma, induced formation of a lymphoid like tissue rich in clonally expanded T-cells, suggesting that T-cell priming occurred in the tumour rather than lymph nodes (138). In relation to this, other researchers have also shown recruitment, proliferation and differentiation of naïve T cells into cytotoxic effectors in various murine tumours in the absence of inflammatory signals (139). Therefore, these findings demonstrate a possible role of tumour infiltrating DCs in activation of tumour specific T cells and so justify the clinical significance of elevated levels of DCs in the tumour microenvironment.

Despite DCs playing such a crucial role in aiding the immune system to tackle tumours, cancers are still able to develop immune resistance and progress in an uncontrollable manner.

1.4.3 Apoptosis and dysfunction of DCs in the tumour environment

There is abundant evidence supporting the connection between reduced levels of DCs and tumour aggressiveness for a wide array of tumours. For instance, researchers in 1984 reported a marked increase in the presence of Langerhans cells (a type of DC in skin) in benign skin lesions compared to malignant tumours that had depleted levels of DCs that were grossly stunted and deformed (140). Since then various authors have reported similar observations, Toriyama *et al* for example reporting a significant reduction in Langerhans cells in malignant melanoma (141).

Esche *et al*, in their study reported that tumour derived factors could induce apoptosis in mouse and human models *in-vitro* and *ex-vivo* (142), which was confirmed by other researchers (143-145). Furthermore, not only DCs but also precursors of DCs were associated with tumour mediated apoptosis (146). Together with this, the presence of apoptotic DCs in the blood of patients with early stage breast cancer has been shown to be significantly higher compared to healthy volunteers (147). Tumour induced apoptosis of DCs and their precursors, therefore seems to be a key process for immune system evasion and tumour survival.

Another way that cancers are able to bypass the anti-tumour immune response is by impairing the functional differentiation and activation of DCs. Physiologically, DCs are present in an immature state. When exposed to an antigen or danger signal, they mature and transform into specialized antigen presenting cells (148). However, several groups have reported abnormal or

inhibited function of DCs isolated from animals and patients with cancer. Chaux *et al* observed that DCs associated with tumours expressed low levels of co-stimulatory molecules (149). Similarly, additional studies have disclosed further abnormalities such as suppressed endocytic activity, aberrant antigen processing and presenting ability, atypical motility and suppressed IL12 production (essential in activating T Lymphocytes) (132,150-153). These results therefore suggest a unique mechanism by which tumour cells can escape DC mediated anti-tumour responses.

Other than inducing apoptosis and rendering DCs dysfunctional, tumour microenvironments have been shown to alter the functions of DCs from antigen presentation to tolerance induction (154). This tolerogenic property is mainly attributed to immature DCs which have been reported to be elevated in the peripheral blood of patients with lung, breast, oesophageal and cancers of the head and neck (155). Certain subsets of immature DCs reduce the proliferation or induce anergy of antigen specific CD4+ and CD8+ T cells by insufficient production of cytokine and co-stimulatory signals. Alternatively, they could activate the generation of T regulatory cells (abrogate immune responses) by the release of anti-inflammatory cytokines such as IL10 and TGF- β (126,156,157). Even though these mechanisms play a crucial role in regulating autoimmunity (123), in the tumour environment, these mechanisms could down regulate anti-tumour activity and promote tumour progression (158). For example, Ghiringelli *et al.* have reported the recruitment of myeloid immature DCs by tumour cells to draining lymph nodes whereby they selectively promote T regulatory cell proliferation

through the release of TGF- β (159). This therefore confirms the ability of tumour cells in converting immature DCs into regulatory DCs as a means to avoid an anti-tumour response. Hence, various factors present in the tumour microenvironment play a significant role in either deactivating tumour infiltrating anti-tumour DCs by apoptosis or bring about their dysfunction or by converting them into regulatory cells that suppress the anti-tumour response, allowing tumour survival and progression.

Further to this, apoptotic cancer cells have been shown to induce tolerance in DC cells (160). Physiologically, apoptosis is a non-inflammatory process whereby apoptotic cells are cleared up by phagocytes such as DCs and macrophages. This process is very crucial for tissue homeostasis. Deficiencies in the recognition and phagocytosis of apoptotic cells have been shown to result in autoimmune diseases (161).

Immunotherapy is one of the most recent advances in cancer treatment. It involves using the immune system to induce a strong and specific immunological response against tumours (162). One strategy is to load tumour antigens on DCs as they act as nature's adjuvants and activate T cells thereby initiating immune responses. However, one issue in optimizing DC vaccines is the choice of tumour associated antigens (TAA) for DC loading (163). The majority of TAAs are over expressed products of normal cellular genes; as such, self-tolerance mechanisms have hindered their use for the induction of effective antitumour response (163).

1.4.3.1 iC3b opsonised apoptotic cancer cells mediate dysfunction of DC cells

When a cell undergoes apoptosis it expresses phosphatidylserine on the surface that acts as a marker to attract phagocytes. Concurrently, activation of the complement system also allows the plasma serine protease factor I and factor H mediated cleavage of C3b to iC3b which is the ligand of the complement receptors CR3 and CR4 present on DCs and macrophages (164). When iC3b opsonises apoptotic cells, it is through the iC3b-CR3 interaction that enhances clearance of apoptotic cells by DCs and macrophages (164). The clearance results in an immuno-modulatory effect whereby the release of anti-inflammatory cytokines is triggered, and inflammatory cytokines is inhibited leading to T cell tolerance (165). Furthermore, there is evidence that this tolerance may be a result of prevention of DC maturation during iC3b opsonisation of DCs (166).

Chemotherapy as well as immunotherapy induces apoptosis in tumour cells. A study conducted by Schmidt *et al.* showed that apoptotic tumour cells release iC3b thereby preventing full maturation of DC cells and inducing tolerance *invitro* and *invivo* (160). As MVs are rich in phosphatidylserine and have been shown to carry various factors and molecules from the parent cell, it would be of interest to investigate the involvement of microvesicles in apoptotic cell induced tolerance of DC cells.

Tumour derived microvesicles as aforementioned have also been implicated in tumour survival by playing an active role in various mechanisms such as

chemotherapy resistance, complement resistance, angiogenesis and T cell suppression via apoptosis (45,46,48,49,52,167). Furthermore, Valenti *et al.* has also showed that cancer cell-derived microvesicles are able to fuse with plasma membranes of monocytes, thereby impairing their differentiation to antigen-presenting cells (54).

On the basis of this information, it would be interesting to investigate whether tumour derived microvesicles play a role in apoptosis, dysfunctioning and conversion of DC cells in the tumour microenvironment for the purpose of tumour survival and progression.

1.5 Aim

In the past decade, researchers have established the involvement of MVs in the pathophysiology of various diseases (168). It is also a well-established fact that MVs are greatly elevated in patients with cancers and play a role in the survival, growth and spread of these cancers (169).

As aforementioned, the involvement of the post transcriptional modification enzyme Peptidylarginine deiminase (PAD) in cancer biology has come to light. The involvement of the tumour microenvironment in relation to DC related anti-tumour function has also been elucidated to a certain extent, and a novel anti-tumourigenic role of certain factors released by skeletal muscle has also been identified.

On the basis of this information, the aim of this project was to determine the relationship if any between PAD and microvesiculation in both cancerous and non-cancerous cells.

I also propose to investigate whether tumour derived microvesicles play a role in apoptosis, dysfunctioning and conversion of DC cells in the tumour microenvironment for the purpose of tumour survival and progression. Thirdly, aim to establish whether microvesicles derived from skeletal muscle express any anti-tumourigenic properties as mentioned earlier that could be implicated as a form of therapy for cancer.

2. Methodologies

2.1 Eukaryotic Cell lines and Culturing

2.1.1 Cell Growth Medium (CGM)

The RPMI 1640 supplemented growth medium was used to cultivate all the cell lines mentioned apart from Human Skeletal muscle cell line (Special medium required). RPMI 1640 medium with phenol red, containing 2.05 mM glutamine, sodium pyruvate, and sodium bicarbonate was supplemented with 10% foetal bovine serum (FBS) (v/v) in 500 ml volumes and stored at 4°C.

The prophylactic use of antibiotics has been implicated to interfere with various cellular mechanisms resulting in changes to cellular morphology, and metabolic processes (170). This would make the standardized conditions in cell culture incomparable. Therefore, antibiotics (1% penicillin/streptomycin and 1% kanamycin) were added separately in the medium only during the first week of cell culture.

2.1.2 Non-Adherent Cell lines

2.1.2.1 THP-1 Cells

An Acute Monocytic Leukaemic cell line derived from human origin. The cell line is non-adherent in nature and is adopted for microvesicle cancer research. It was obtained from the Health Protection Agency Culture Collections (formerly known as European Collection of Cell Cultures (ECCAC) cat no - 88081201).

2.1.2.2 K562 Cells

This human cell line is derived from the pleural effusion of a 53 year old female with chronic myelogenous leukaemia in terminal blast crisis. The Population is highly undifferentiated and of the granulocytic series. Recent studies have shown the K562 blasts are multipotential, haematopoietic malignant cells that spontaneously differentiate into recognisable progenitors of the erythrocyte, granulocyte and monocytic series (171). The cell line was obtained from ECCAC (cat no - 89121407).

2.1.3 Adherent Cell lines

2.1.3.1 PC3 - Prostate Cancer Cell line

A highly tumorigenic cell line initiated from bone metastasis of a grade IV Human prostate adenocarcinoma (HPA) from a 62 year old male Caucasian. The cell line is adherent in nature and is ideal as a model to study cancer metastasis. This cell line was obtained from Sigma Aldrich (Cat no - 90112714-1VL).

2.1.3.2 PC3M – Prostate Cancer Cell line

A highly metastatic variant of the PC3 cell line established from secondary metastatic origin from a patient with grade IV HPA. This cell line was kindly gifted by Prof. Chris Palmer (London Metropolitan University).

2.1.3.3 PNT2 – Normal Human Prostate Cell line

An adherent cell line derived from normal adult prostate epithelial cells which have been immortalised, and was adopted as a comparative control together with the highly metastatic cancer cell line (PC3 and PC3M). The cell line was obtained from ECCAC UK (same as above).

2.1.3.4 MCF7 – Breast Cancer Cell Line

An adherent cell line isolated from a pleural effusion from a Caucasian woman suffering from a breast adenocarcinoma. MCF7 was adopted as it is a well-established cell line in the study of cancer metastasis. The cell line was also obtained from ECCAC UK.

2.1.3.5 Human Skeletal Muscle cell line (HskMC)

A primary cell line that is isolated from the human limb skeletal muscle. The cells were ordered from the ECCAC (catalogue no - 06090718).

2.1.3.5.1 Maintaining HskMC cells

Due to the sensitive nature of these cells, the procedure for cell culturing was followed according to ECCAC protocols.

The HskMC cells were cultured in a special skeletal muscle growth medium that was ordered from PromoCell (Germany). As these cells are adherent in nature, washing and culturing is done in the culture flask.

The culturing was done under sterile conditions in a microbiology safety cabinet to prevent contamination. The supernatant was first discarded and

the cells washed 2 times with 10ml prewarmed RPMI. 20 ml of prewarmed HSkMC complete growth medium (5% FBS) was then added to each of the 50 ml T-75 flasks containing the cells and incubated in 37°C, 5% CO₂ humidified conditions.

As cells grow and multiply they release waste products which must be removed consecutively to keep them healthy and viable. In order to do this the cells were first examined under a microscope to check for bacterial contamination and then washed and maintained as mentioned above. If the cells were 85 - 90% confluent, they had to be split. To detach the cells, they were washed twice with pre warmed RPMI, 5ml of 5% Trypsin-EDTA was then added to the 50ml flasks and incubated for 2-5 minutes at room temperature. The flasks were examined at 2 minute intervals with an inverted microscope for cell detachment. Once 90% of the cells were detached, the flasks were tapped slightly and 20 ml of skeletal growth medium (with 5% serum) was added to inhibit trypsin activity.

The cell suspension was centrifuged twice at 220 *g* for 5 minutes at 21°C, the second time with serum free RPMI. The pellet was then resuspended in 20 ml of skeletal muscle growth medium and gently pipetted to break up clumps of cells. A further 20 ml of medium was then added and the cells transferred into two T-75 culture flasks (i.e. Cells from a single flask were split to two flasks). The flasks were then incubated at 37°C, 5% CO₂ humidified conditions.

In order to maintain continuous cell growth and viability, the cells were subcultured every other day. In case of weekend feeding the volume was increased to 35 ml to avoid stressing out the cells.

2.1.4 Maintaining Non-Adherent Cell lines

Non-adherent cells were maintained in growth medium containing RPMI 1640 supplemented with 10% FBS. In addition, cells were occasionally maintained for a week in growth medium supplemented with 1% penicillin-streptomycin and 1% kanamycin at 37°C in 5% CO₂ humidified conditions, to prevent any possible bacterial and mycobacterial contamination. The cells were split, depending on confluency every 3 to 5 days by washing twice with serum-free RPMI 1640. In summary, the cells were transferred into 50 ml centrifuge tubes and spun at 160 g for 5 min. The resulting supernatant was discarded and cells were gently resuspended in the remaining medium, serum-free RPMI being added and cells centrifuged as before. The resulting supernatant was also discarded and cell pellets resuspended in the appropriate volume of growth medium. Cells were then seeded in the desired dilution into new 75 cm² culture flasks. Cells were only cultured in medium supplemented with kanamycin for a week to avoid development of resistance to the antibiotic.

2.1.5 Maintaining Adherent Cell lines

Adherent cells were also maintained at 37°C with 5% CO₂, in RPMI growth medium. These cells were also split depending on confluency every 3 to 5 days. Cells were washed twice by replacing CGM with serum-free RPMI and

addition of 0.25% (v/v) trypsin/EDTA in RPMI. After 10 min incubation at 37°C, the flask was tapped several times to detach the cells and growth medium was added to inactivate the trypsin. The trypsin solution was removed by centrifugation at 200 g for 5 min followed by one wash in serum-free RPMI. Cell pellets were resuspended in the appropriate GM volume and seeded in the desired dilution into new culture flasks. Growing cells with a viability of 95% or higher were used in every experiment. The number of cells and viability were determined before the start of every experiment using the Guava EasyCyte flow cytometer (ViaCount assay, Guava Technologies).

All three cell lines apart from HSkMC were cultured in the same complete growth medium comprising of 500 ml of sterile RPMI 1640 with 2.05 mM L-glutamine, and 10% FBS (50 ml). In order to avoid contamination, 1% of penicillin/streptomycin (1000µg/ml), and 1% of kanamycin (1000µg/ml) was also added only for the first week after thawing.

As all three cell lines are adherent in nature, washing and culturing was carried out in the culture flask, under sterile conditions in a microbiology safety cabinet to prevent contamination. The supernatant was first discarded. The cells were then washed three times with 10ml prewarmed RPMI. 20 ml of prewarmed CGM was then added to each of the 50 ml flasks and the cells were incubated in 37°C, 5% CO₂ humidified conditions.

2.1.6 Freezing of eukaryotic cells

To prepare frozen stocks for long term storage, non-adherent cells grown to almost 100% confluency were washed twice (160 g, 5 min) with serum-free

RPMI and cell number determined using Guava ViaCount. Cells were carefully resuspended in freezing mix, transferred into cryo-vials (Greiner) at 1×10^7 cells/ml in 1ml volumes and immediately placed on ice. The cryo-vials were frozen at -80°C in polystyrene containers, which ensure a temperature decrease of 1°C per minute. For long-term storage the deep frozen cryo-vials were transferred to liquid nitrogen cell storage tanks. Adherent cells were also frozen by a similar procedure except that cells were first trypsinised to bring them into suspension, as described earlier. Suspended cells were washed by centrifugation at 200 g for 5 min , resuspended in the freeze mix and transferred into cryo-vials.

2.1.7 Thawing of cells

To defrost cells, cryo-vials were removed from liquid nitrogen and immediately thawed in a water-bath at 37°C . After cleaning the lid with 70% ethanol, the content was transferred to a 15 ml centrifuge tube containing 9 ml of fresh growth medium, prewarmed to 37°C and cells were pelleted by centrifugation at the appropriate speed (160 g for non-adherent cells or 200 g for adherent cells, 5 min). To remove DMSO, the medium was discarded and the pellet was resuspended in fresh growth medium. The cells were then placed into culture flasks of the same size as had been used prior to freezing, and incubated at 37°C with 5% CO_2 .

2.2 Biochemical Methods

2.2.1 Flow cytometry

The Guava EasyCyte Flow cytometer (Guava Technologies, UK) allows complex biological studies such as cell counting and viability testing, white blood cell phenotyping, cytokine detection, cell activation marker analysis and other complex molecular analyses to be performed simultaneously. This saves time, but also generates accurate results.

Flow cytometry provides data which is associated with size (forward scatter), and granularity (side scatter) and therefore analysis of the characteristics of microvesicles could also be performed. PS expressed on the surface of MVs is detected by annexin V binding assays. Moreover, large numbers of MVs can be analysed in small samples and various antigens can be detected at the same time using antibodies.

The Guava flow cytometer can be used to perform ten different assays; however, for these studies only three assays were implemented. These were the ViaCount assay (for counting cells and determining viability), Express Plus assay (for cell activation marker analysis, cytokine expression, studies on protein-protein interaction) and Nexin assay (for reporting apoptosis).

2.2.1.1 Cell counting and viability assessment

Cell number and viability were determined using the ViaCount assay, which distinguishes between viable and non-viable cells based on the differential permeabilities of two DNA-binding dyes in the Guava ViaCount reagent. The nuclear dye only stains nucleated cells, while the viability dye brightly stains

dying or dead cells. This proprietary combination of dyes enables the Guava ViaCount assay to distinguish viable, apoptotic and dead cells. Cell debris is excluded from results based on negative staining with the nuclear dye.

2.2.2 Preparation of Normal Human Serum (NHS)

NHS (from human AB plasma - Sigma Aldrich) was thawed at 4°C and filtered with a 0.22 µm syringe filter. NHS that was required to be MV free was then centrifuged as per section 2.2.3 (The supernatant in this case NHS was kept and the pellet discarded) and then frozen in 1 ml aliquots in a -80°C freezer for later use.

For heat inactivating NHS, 0.22 µm filtered NHS was heated in a water bath at 56°C on a shaker for 1 h. The heat inactivated NHS (HI NHS) was then frozen in 1 ml aliquots in a -80°C freezer for later use (for iC3b deposition experiments – sec 5.3.2).

2.2.3 Purification of Microvesicles (MVs) from conditioned medium (Constitutively released MVs)

Conditioned medium from cells cultured with 10% FBS at 37°C and 5% CO₂, was centrifuged once at 200 g for 5 min to remove the cells. The supernatant was then centrifuged at 4,000 g for 1 h to remove cell debris and apoptotic bodies. The supernatant was then centrifuged at 25,000 g for 2 h to pellet MVs. Pelleted MVs were washed once by resuspending in sterile 0.1µm membrane filtered PBS and centrifuged again at 25,000 g for 2 h. The MV pellet was resuspended in sterile 0.1µm membrane filtered PBS and

quantified, or analysed for PS exposure or stored in -80°C freezer for later use.

2.2.4 Induction and purification of MVs

Alternatively, microvesiculation was induced by treating the cells with an inducing agent. The cells were washed twice at 200 g for 5 min and preincubated at 37°C in 5% CO₂ for 1 h. Cells were centrifuged in order to remove any background MVs released during the pre-incubation step. Pelleted cells were resuspended in pre-warmed RPMI (37°C) supplemented with 0.5 mM CaCl₂, and seeded into 24-well plates at 1x10⁶ cells/well in 1 ml reaction volumes. Cells were stimulated to microvesiculate by addition of the specific inducing agents (either 10% NHS or 300µM 2'(3')-O-(4-benzoylbenzoyl) adenosine-5'-triphosphate (BzATP)) and incubated at 37°C for 30 min with shaking. The reaction was stopped by placing on ice for 1 min and transferred into 1.5 ml microcentrifuge tubes. Cells were pelleted by low speed centrifugation at 200 g for 5 min followed by 4,000 g for 60 min for the removal of cell debris and apoptotic bodies. MVs were isolated from the resulting supernatant by ultracentrifugation at 25,000 g for 2 h. This speed parameter was found to pellet MVs without much contamination with aggregated exosomes. MVs isolated were resuspended in 200 µl of sterile 0.1µm membrane filtered PBS and quantified by flow cytometry or stored at -80°C freezer for later use.

2.2.5 Determination of Protein Concentration

The concentration of protein was determined using the BCA Protein Assay Kit (Pierce, Thermo Scientific, UK). It uses a combination of the biuret reaction (reduction of Cu^{2+} ions to Cu^+ ions by proteins in an alkaline medium) and the colorimetric detection of the Cu^+ cations by a bicinchoninic acid-containing colour reagent. Following the manufacturer's instructions, 10 μl of protein samples were diluted in double distilled water (ddH₂O; dilution 1:5) and added to 200 μl working solution consisting of a mixture of kit reagent A and reagent B (ratio 50:1 respectively). In parallel, a dilution series of a 0.5 $\mu\text{g}/\mu\text{l}$ BSA stock solution in ddH₂O was prepared and used as standard in later evaluation. Applied concentrations were 0, 62.5, 125, 250, 500, 750, 1000, 1500 and 2000 $\mu\text{g}/\text{ml}$ BSA in 500 μl ddH₂O. Volumes equal to samples were added to 200 μl of a mixture of kit reagent A and B (ratio 50:1) in a 96 well plate followed by incubation at 37°C for 30 min. After incubation at room temperature for 10 min to cool samples, A_{540} readings were taken on a FLUOstar Omega microplate reader. Protein concentrations of the unknown samples were determined by interpolation on a standard curve multiplied by a dilution factor of 5.

2.2.6 Preparation of cell lysates

Cells (1×10^7) to be lysed were sedimented by centrifugation (160 *g*, 5 min at 15°C). The pellet was washed once by careful resuspension in RPMI followed by centrifugation. After that, cells were counted using a haemocytometer and lysis was performed to give a protein concentration

equivalent to 2×10^6 cells/10 μ l. If defined amounts of protein were required, the pellet was subjected to detergent based lysis followed by determination of total protein concentration (sec 3.2.4). Briefly, cell lysis was performed by resuspension of the pellet in Radioimmunoprecipitation assay buffer (RIPA buffer) containing HALT protease inhibitor cocktail (1:100 dilutions in RIPA buffer). To solubilise membrane proteins, samples were repeatedly pipetted and left on ice for 30 min after which they were repeatedly pipetted once more and left on ice for a further 30 min. Insoluble material was then sedimented by centrifugation at 13,000 rpm for 10 min at 4°C (1730R microcentrifuge, 7-6020-111-130 fixed angle rotor, Labogene). The total protein concentration was determined of the resultant supernatant and then subjected to sodium dodecyl sulphate polyacrylamide gel electrophoresis (SDS-PAGE) analysis.

2.2.7 Sample preparation for SDS-Polyacrylamide Gel Electrophoresis (SDS-PAGE)

Sodium dodecyl sulphate (SDS) sample buffer (4X) was added to samples in a ratio of 1:3 followed by incubation at 95°C for 4 min. Before loading the samples onto the gel, a centrifugation step was performed (2,000 g, 2 min) to collect all liquid at the bottom of the reaction microtube and loaded into the gel wells.

2.2.8 SDS-PAGE Protein Molecular Weight Standards

As a protein molecular weight standard, prestained Protein-Marker I (BioRad) was used. Prestained markers, ranging from 10 to 194 kDa or 10 to

250 kDa were used when analysing gels by Western blot using the enhanced chemiluminescence (ECL) detection system. Markers were applied by loading 5 µl into wells.

2.2.9 SDS-Polyacrylamide Gel Electrophoresis

To separate proteins which were denatured by SDS according to their molecular masses, SDS-PAGE was performed as described (Laemmli, 1970) using the Mini PROTEAN III Electrophoresis System (Bio-Rad). Gels with dimensions of 102 x 73 mm and a thickness of 0.75 mm were cast between two glass plates by pouring freshly prepared 8% separating gel solution containing acrylamide/bisacrylamide into the gel cassette fixed in a casting frame. Unpolymerized separating gel solution was overlaid with H₂O-saturated butanol to achieve an even surface. After polymerization, H₂O-saturated butanol was poured off, washed twice with deionised water, and the excess water was blotted using a filter paper (Whatman 3 MM, Whatman AG). Then unpolymerized stacking gel was poured into the gel cassette and a plastic comb was inserted from the top, to form the loading wells in the stacking gel.

After polymerization, the gels were used immediately. To perform electrophoresis, the gel was placed into the electrode assembly device inside a clamping frame in the tank of the Mini PROTEAN III system. Electrophoresis running buffer was added to the inner and outer chambers of the tank and the plastic comb was carefully removed. Wells were washed with the running buffer to remove any free unpolymerized

acrylamide/bisacrylamide. Samples (total protein concentration added varied according to the experiment) were loaded into the wells of the stacking gel using extra long loading pipette tips. Electrophoretic separation was performed at 100 V (constant voltage) until the bromophenol blue front of the SDS sample buffer reached the end of the resolving gel. Gels were either stained with Coomassie Brilliant Blue or transferred onto nitrocellulose membrane for Western blotting analysis.

2.2.10 Western Blotting Analysis

Proteins separated by SDS-PAGE were transferred to a Hybond C nitrocellulose membrane for further analysis using a semidry transfer device (Bio-Rad Sartoblot system). A Hybond C nitrocellulose membrane and two pieces of blotting paper (Whatman 3 MM, BioRad) were cut to the size of the separating gel. Blotting paper, nitrocellulose membrane and the sandwich-blotting cassette were equilibrated in Sartoblot buffer. One piece of blotting paper was placed on the cathode plate, and the nitrocellulose membrane was placed on top of the blotting paper. The gel was removed from between the sandwich-blotting cassette and placed on top of the membrane, and a second blotting paper was also placed on top of the gel. Having removed air bubbles, the anode plate, also dampened with the Sartoblot buffer was used to complete the sandwich. Electroblothing was carried out at 150mA (constant Amps) for 1.5 h.

2.2.11 Immunochemical Protein Detection using the ECL System

Western blotting was performed as described above using hybond C nitrocellulose membrane (Amersham Biosciences). The membrane was incubated in blocking buffer for 1 h at room temperature or at 4°C, overnight, on a shaker. Following blocking, the membrane was rinsed with PBS-T and incubated with the primary antibody in the desired dilution for 1 h at room temperature on a shaker. Three 10 min washing steps with PBS-T were performed and the membrane was incubated with isotype matched HRP conjugated secondary antibody in the desired dilution for 1 h at room temperature on a shaker. After three 10 min washes with phosphate buffer saline and 0.2% Tween 20 (PBS-T), visualization was performed using ECL system (Amersham Pharmacia). The ECL solutions (reagent A and B) were mixed at equal volumes and the membrane was incubated with the mixture for 2 min at room temperature and chemiluminescence detected using the UVP ChemiDoc-It system (UVP systems, UK).

2.2.12 Mass Spectrometry Analysis

2.2.12.1 In-solution Trypsin Digestion

The samples were denatured by the addition of 20µl of 100mM Tris-HCl buffer (pH 7.2) supplemented with 5 M dithioerythritol (DTT) and 6 M urea at room temperature for 60 min on a shaker. Free thiol groups in the samples were then carboamidomethylated by the addition of 6 µl of 100 mM Tris-HCL (pH 7.8) supplemented with 5 M iodoacetamide for 45 min. This was followed by further incubating the samples with 180 µl of 1 µg sequence grade trypsin

dissolved in ddH₂O for 12-16 h at 37°C. The samples were then centrifuged and the supernatant collected and analysed by Mass spectrometry (172). Prior to analysis each digest was spiked with 1 pmol of an enolase tryptic digestion (*Saccharomyces cerevisiae*), which acted as an internal standard for the quantitation of each protein.

2.2.12.2 MSe Label-Free Quantitation

The processed samples (sec 2.2.12.1 above) were identified and quantified by direct analysis using a nanoAcquity UPLC (Ultra Performance Liquid Chromatography) and QTOF (Quadrupole Time-of-flight) Premier mass spectrometer (Waters Corporation, Manchester, UK).

Briefly, the samples were trapped and desalted using a Symmetry C18 5 µm, 5mm x 300 µm precolumn in 0.1% formic acid for a total time of 4 min at a rate of 4 µl/min and then eluted. The elute was then separated using a 15 cm x 75 µm C18 reverse phase analytical column using a gradient of 3-40% acetonitrile containing 0.1% formic acid over a period of 120 min at a flow rate of 250 nl/min. The column was washed and regenerated at 300 nl/min for 10 min using 99% acetonitrile containing 0.1% formic acid. After the removal of all non-peptide and non-polar materials, the column was re-equilibrated under the initial starting conditions for 20 min. All columns were maintained at 35°C (173).

After purification the samples were analysed in positive ion mode with the QTOF operated in v-mode with a typical resolving power of 10,000 fwhm after the calibration of the TOF analyser. Accurate mass LC-MS were

collected in a data-independent and alternating, low and collision energy mode. The data was then processed using the ProteinLynx GlobalServer version 2.4 (Waters, UK) (173).

2.3 Statistical Analysis

Statistical analysis for all data presented was performed by the unpaired *t*-test for repeated measures using GraphPad Prism version 5.00 for Windows (GraphPad Software, San Diego, USA). Statistical correlations between data values were also determined using GraphPad Prism software. Differences giving a value of $P < 0.05$ with confidence interval of 95% were considered statistically significant.

3. The Effect of HSkMC MVs on prostate Cancer Cells

3.1 Introduction

Over the last decade, research in the field of MVs has dramatically increased and scientists are reporting the involvement of MVs not only in normal physiology but also in virtually every disease state possible in the human body; they have been implicated in cancer (61), as well as autoimmune diseases (174) to name a few. Nevertheless, MVs have also been shown to be useful in therapy. Recently, Biancone *et al* reported the therapeutic potential of MVs derived from mesenchymal stem cells to repair damaged tissue by inhibiting apoptosis and stimulating cell proliferation (175). Others have also reported the potential role of MVs as carriers of pharmacological and genetic therapeutic agents (176).

As aforementioned, skeletal muscle is one of the most vascularised tissues in the body and yet it is also one of the tissues that is rarely affected by cancer metastasis (119). Over the years, researchers have postulated various reasons for this rarity such as high levels of lactic acid that is toxic to metastatic cancer cells (117), and low molecular weight factors, such as adenosine released by skeletal muscle, that have cytotoxic effects on metastasising cancer cells (119,120). Nevertheless, no definite mechanism has been identified as of yet.

On the basis of this information, we proposed to investigate whether HSkMC cells release MVs and whether they have cancer cell cytotoxic and anti-proliferative properties.

3.2 Methodologies

3.2.1 The effect of NHS on MV release

To determine the effect of NHS on microvesiculation, PNT2, PC3M, and MCF7 cells were seeded into two 24-well plates in triplicate. Briefly, 2.5×10^5 cells (per well) were first trypsinised, quantified and checked for viability before being seeded. 1 ml of CGM was added to each of the wells and incubated at 37°C, 5% CO₂ humidified conditions overnight to allow the cells to settle in the new environment.

On the day of experiment the cells were first washed twice with pre-warmed PBS and resuspended in fresh serum-free RPMI supplemented with 0.5mM CaCl₂. The cells were then stimulated with 5% NHS and further incubated at 37°C, for 30 min (shaking).

After the incubation period the plate was removed and placed on ice for 1 minute to stop any further reactions. The supernatant from each well was then transferred to sterile 1.5 ml Eppendorf tubes and placed on ice. The tubes were then centrifuged at 200 g for 5 minutes to remove any cell debris. The supernatant was treated as mentioned in sec 2.2.4 to isolate MVs from the supernatant. At this point the pellet of MVs was suspended in 200 µl of sterile PBS and quantified using Guava Express plus.

3.2.2 Annexin V labelling of MVs

Isolated MVs were resuspended in annexin V binding buffer and annexin V-FITC (1:200) (R&D Systems) was added or not (control) in a 200 µl final

volume. Sample was then incubated at RT for 30 min with shaking and centrifuged at 25,000 *g* for 2 h to pellet MVs. Samples were analysed immediately using Guava Express plus.

3.2.3 Electron microscopy

3.2.3.1 Sample preparation for EM analysis

All processing steps were carried out in a fume cupboard, as hazardous chemicals were being used. Pure isolated MVs were separately fixed and treated with agar resin. The polymerised blocks were sent for cutting, staining, examination and image capture at the London School of Hygiene and Tropical Medicine (LSHTM), Electron Microscopy Unit. Ultra-thin sections were cut on a Leica Ultracut R ultra microtome and picked up onto Pioloform film copper grids. The sections were then stained for 10 min in Reynolds Lead Citrate stain (177) before washing in ultrapure MilliQ water and examining on a Jeol JEM – 1200 Ex II Electron Microscope. Digital images were taken with a 1K, side-mounted AMT Digital camera (Advanced Microscopy Techniques Corp. 3 Electronics Ave., Danvers, MA 01923 USA, supplied by Deben UK limited, IP30 9QS).

3.2.3.2 Negative staining

Pure isolated MVs samples for negative staining were also taken to the EM Unit at the LSHTM and stained with 2% aqueous uranyl acetate or 2% phosphotungstic acid (PTA) pH 6.8 + aqueous Bacitracin (300 µg/ ml diluted 1:10 in the negative stain acts as a spreading agent). Using fine tipped

Watchmaker forceps to handle the 400 mesh copper grids with a Pioloform support film (Grids and Pioloform powder from Agar Scientific Limited, Essex CM24 8DA), the grids were pre-treated with 1% aqueous Alcian Blue 8GX for 10 minutes before rinsing in MilliQ water. 5 μ l of the sample MVs were placed on the grids for 1 min. This was then removed by touching the grid edge with a strip of filter paper and replaced with 5 μ l of the stain for a further 1 min. The stain was then removed in the same way and the grid was allowed to air-dry, before examination on the Transmission Electron Microscope. Digital images were recorded using the AMT digital camera previously described for the examination of stained ultrathin sections.

3.2.4 HSkMC cell differentiation

The Human skeletal muscle cell line is supplied in an undifferentiated form known as myoblasts and can only be cultured in this undifferentiated form. However for this investigation both the undifferentiated (myoblast) and the differentiated (myocytes) were required. In order to differentiate the myoblasts to myocytes a special differentiation medium is required. The medium was ordered from PromoCell (catalogue no C-23061) as, having found several other protocols to be unsatisfactory their protocol for differentiation was preferred for ease of use.

Once the cells reached 80-90% confluency, they were washed three times with prewarmed RPMI. 20 ml of prewarmed Dulbecco's modified Eagle's medium (DMEM) supplemented with 2% horse serum medium was added to the cells and incubated at 37°C for 24 hrs. After 24 hr, the medium was

changed to special skeletal differentiation medium (PromoCell). This differentiation medium was changed every 2-3 days as per the manufacturer's protocol.

The cells were then monitored under the microscope every other day to detect any changes in cell morphology leading to differentiation. According to the manufacturer's (PromoCell) protocol, extensive formation of multinucleated syncytia is supposed to be observed after 8-14 days, as a sign of differentiation.

3.2.5 Proliferation assay

In order to understand the effect of supernatant collected from undifferentiated and differentiated HSkMC cells, PC3M cells were seeded in to two 24-well plates at 5×10^4 cells per well in triplicate and incubated overnight at 37°C. On the day of the experiment cells in the plate were first observed under a light microscope for cell attachment or possible contamination and then washed three times with prewarmed RPMI. Cells were then resuspended in RPMI 1640 complete growth medium containing 10% FBS and 1% penicillin/streptomycin (RPMI-CGM). The volume of complete growth medium added was adjusted according to treatments to obtain a final volume of 1ml. The appropriate treatments were then added to the wells in triplicates and the plates incubated at 37°C for 72 hrs.

3.2.5.1 Post experimental analysis

After 72 hr the plates were first observed under the microscope to check for contamination. The supernatant was then collected from each well and transferred to 15 ml conical tubes (one tube for each triplicate treatment). The wells were washed twice with Dulbecco's Phosphate Buffered Saline (DPBS), which was then retained in the designated 15 ml conical tubes containing the supernatant. The tubes were then centrifuged at 400 x g for 5 minutes to pellet the apoptotic cells from the supernatant and the DPBS used for washing the cells. During the period of centrifugation the cells in the plates were trypsinised (200 µl of 0.25% Trypsin/EDTA) at 37°C for 5 min to detach the cells and transferred to the 15 ml tubes and centrifuged again.

After centrifugation of the 15 ml tubes, the supernatant was discarded and the pellet resuspended in 300 µl of CGM, which was then transferred to the designated treatment wells (100 µl/well) in triplicate. A ViaCount assay was then carried out as described earlier.

3.2.6 Cell migration assay

To investigate the effect of MVs derived from Human Skeletal muscle cells and PC3M cells on PC3M cells, 1×10^5 PC3M cells were seeded in triplicate in 12-well plates, 24 hr prior to setting up the experiment.

On the day of the experiment, the cells seeded the night before were first observed under a microscope for cell attachment and contamination. The cells were washed three times with prewarmed RPMI and resuspended in

1ml of RPMI. A scratch was made in the centre of all the wells using a sterile yellow pipette tip and confirmed under a microscope. The cells were washed one more time to remove any cellular debris due to the scratch and resuspended in 1ml of CGM, followed by addition of 30 µg/ml of either HSkMC or PC3M MVs to the wells in triplicate. The remaining wells that had cells seeded served as control. Before incubation, bright field images were taken of the scratch for every well to calculate the migration index. The plates were then incubated at 37°C for 24 hr.

After 24 hr the plates were first observed under the microscope for any contamination and then washed once with prewarmed RPMI to remove any cell debris. Individual wells were then viewed under the fluorescence microscope and bright field images were taken of the scratch area in order to calculate the migration index.

3.2.7 Mass Spectrometry analysis of myoblast and myocyte MVs

In order to identify and compare proteins carried by microvesicles from myoblast and myocytes, MVs isolated from both the skeletal muscle subtypes were subjected to mass spectrometry analysis.

Supernatant collected from healthy myoblasts and myocytes were subjected to differential centrifugation (sec 2.2.3) and the MVs isolated were lysed with RIPA buffer (sec 2.2.6). The MV lysates were then analysed by mass spectroscopy (sec 2.2.12).

3.3 Results

3.3.1 The effect of sublytic complement on the release of MVs

Reports from several investigators have suggested that sublytic levels of complement can stimulate the release of MVs from different cell types. To determine this effect, HSkMC, PNT2, PC3M and MCF7 cells were treated with RPMI + 0.5 mM CaCl₂ in the presence or absence of 5% NHS. The cells were then incubated in 37°C, 5% CO₂ humidified conditions for 30 minutes. Released MVs were isolated by differential centrifugation of the supernatant from each of the treatments and analysed by flow cytometry.

Microvesicles are identified in flow cytometry by their size and granularity, as assessed by the logarithmic amplification of forward scatter (FSC) and side scatter (SSC) signals respectively. A typical FSC vs. SSC dot plot (**Fig 3.1 A**) was observed showing size heterogeneity and granularity as described previously (20,178). This suggested that MVs rather than cell debris had been isolated.

Another way to identify MVs by flow cytometry is by annexin V staining. PS expression on the membrane surface is indicative of membrane asymmetry, and early apoptosis. However, during microvesiculation, the loss of cell membrane asymmetry, results in inversion of the bi-layer. Phosphatidylcholine (PC) and sphingomyelin normally expressed on the outer membrane are inverted onto the inner leaflet whereas phosphatidylethanolamine (PE) and PS on the inner leaflet are exposed on the outer membrane surface. Using flow cytometry isolated MVs from PC3M

cells were found to express PS on the outer leaflet by staining with annexin V-FITC (**Fig 3.1 B**). Annexin V staining was repeated for MVs isolated from other cell types and found to correspond with values reported here (data not shown). This was further ascertained by electron microscopy whereby purified MVs from THP-1 cells were fixed and subjected to electron microscopy (EM). Electron microscopy revealed the size and shape of microvesicles ranging from 1.2 μm to 0.4 μm in size (**Fig 3.1 C**).

Incubation of HSkMC, PNT2, PC3M, and MCF7 with 5% NHS significantly increased MV release from an average of 4.3×10^4 MVs/ml (for all three cell lines) to 4.3×10^5 MVs/ml for HSkMC cells, 4.7×10^5 MVs/ml for PNT2, 6.6×10^5 MVs/ml for PC3M, and about 1.2×10^6 MVs/ml for MCF7 (**Fig 3.2**). This therefore indicates that sublytic complement in the form of NHS has a stimulatory effect increasing microvesiculation from both non-cancerous (PNT2 and HSkMC) and cancerous cell lines (PC3M and MCF7). However the analysis also showed another trend that was interesting. On comparing the amount of MVs released from the non-cancerous prostate cell line (PNT2) with both the cancer cell lines after treatment with NHS, it can be seen that the cancer cell lines had more MVs released, with MCF7 showing a significant 3-fold increased production compared to PNT2 and HSkMC cells (**Fig 3.2**). This data indicates that cancer cells likely produce more MVs than normal cells once activated.

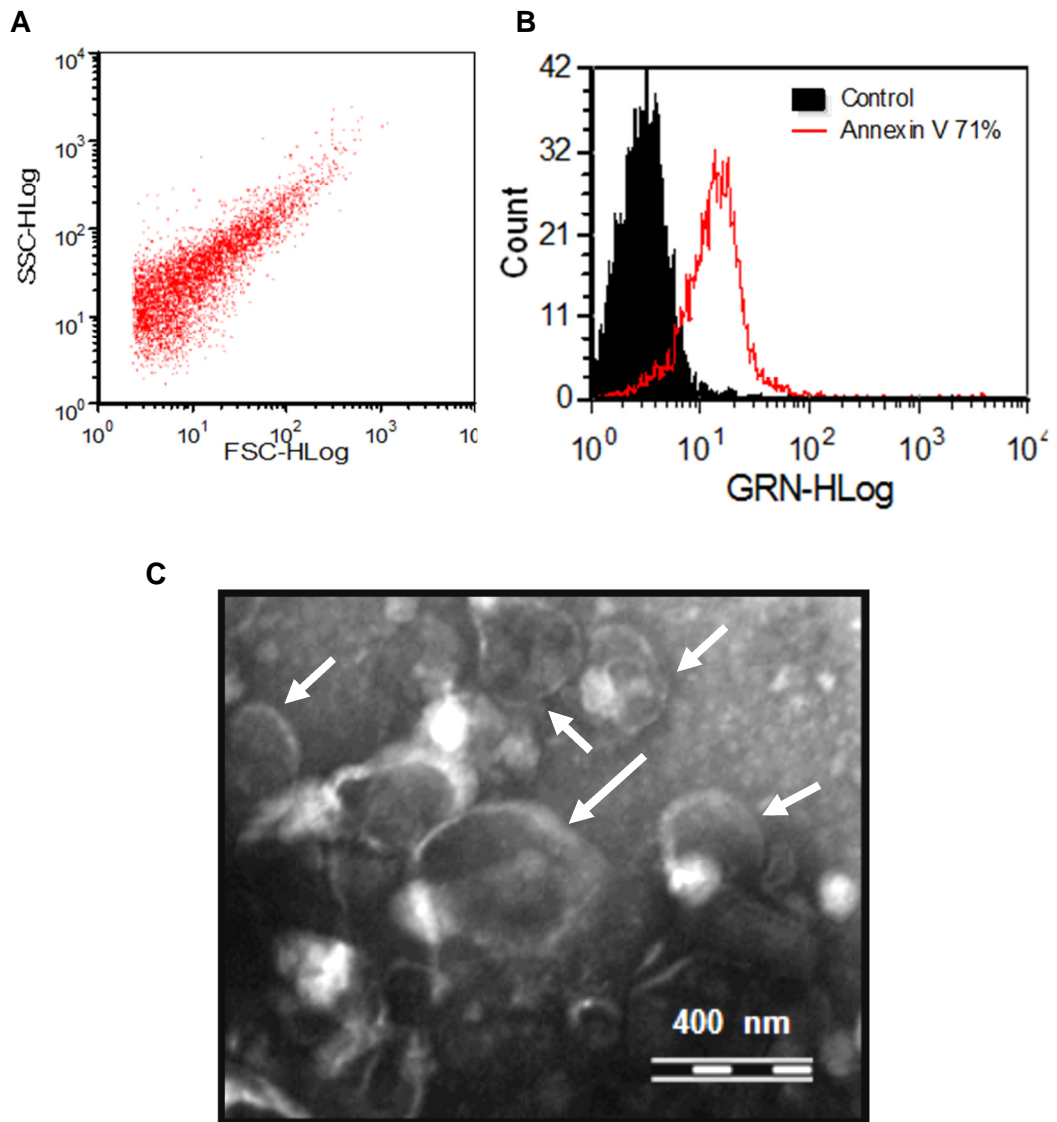


Fig 3.1: Characterisation of MVs. **A)** A typical FSC vs SSC dot plot of MVs obtained after treating PC3M cells with 5% NHS (in the presence of 0.5mM CaCl₂). MVs were isolated by differential centrifugation and analysed by flow cytometry. The vesicles were identified by their size and granularity, as assessed by the logarithmic amplification of forward (FSC) and side scatter (SSC) signals. **B)** Isolated MVs were analysed for PS expression by staining with annexin V -FITC. The resulting histogram show approximately 71% of labelled MVs to be AnV-FITC positive. Unlabelled MVs, shown in black were used as a negative control. All experiments were repeated several times, with similar results. **C)** Electron microscopy image showing purified microvesicles (white arrows) isolated from THP-1 cells.

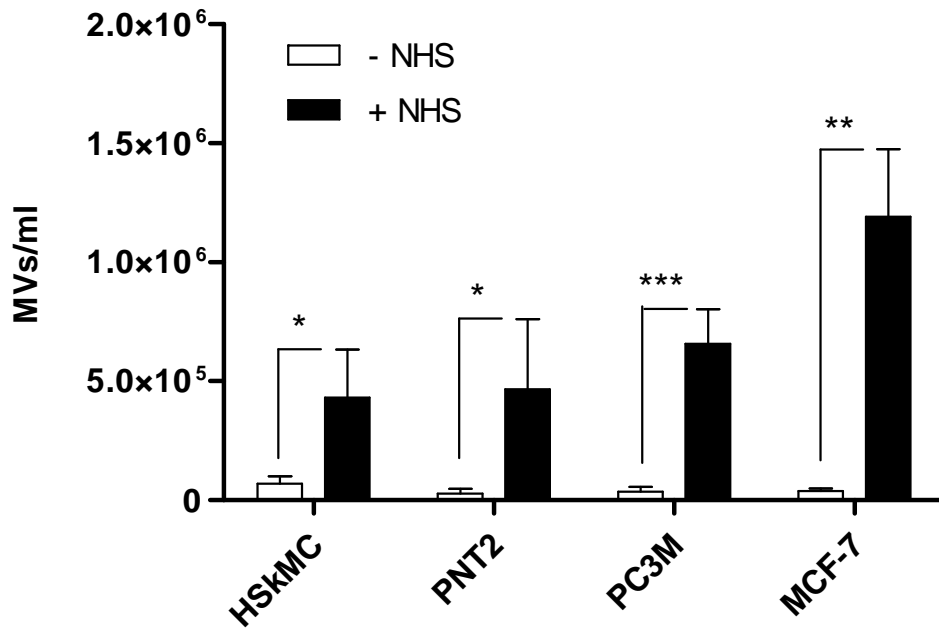


Fig 3.2: The Effect of NHS on microvesiculation in non-cancerous and cancerous cell lines. HSkMC, PNT2, PC3M, and MCF-7 cells were treated with or without 5% NHS (control) and incubated at 37°C for 30 minutes. MVs isolated from the experiment were then analysed by flow cytometry. The data represents the mean \pm standard deviation of one of two experiments performed in triplicates. * p <0.05, ** p <0.01, *** p <0.001 were considered statistically significant.

3.3.2 HSkMC and cancer

3.3.2.1 HSkMC differentiation

The Human skeletal muscle cell line comes in an undifferentiated myoblast form and can only be cultured in this undifferentiated form. However for our investigation both myoblast and the differentiated form myocytes was required.

In order to differentiate the myoblasts to myocytes, cells confluent at 80-90% were first grown for 24 hr in Dulbecco's modified Eagle's medium supplemented with 2% horse serum. After 24 hr, the cells were then grown in skeletal muscle cell differentiation medium, the medium being changed every 2-3 days. The culture was monitored every other day to detect any changes in cell morphology leading to differentiation. Extensive formation of multinucleated syncytia is supposed to then be observed after 8-14 days, as a sign of differentiation.

The cells in **Fig 3.3 A** represent the myoblasts just before inducing differentiation. There were no changes observed up to 24 h after inducing differentiation. However, on the second day the cells appeared to be much more prominent and larger in size compared to their undifferentiated counterparts. Between day 4 and 5 the cells were aligned next to each other, taking on the appearance of striations. Few changes were observed up to day 7 when we observed large skeletal muscle cells fused together with multiple nuclei, forming syncytia (**Fig 3.3B**).

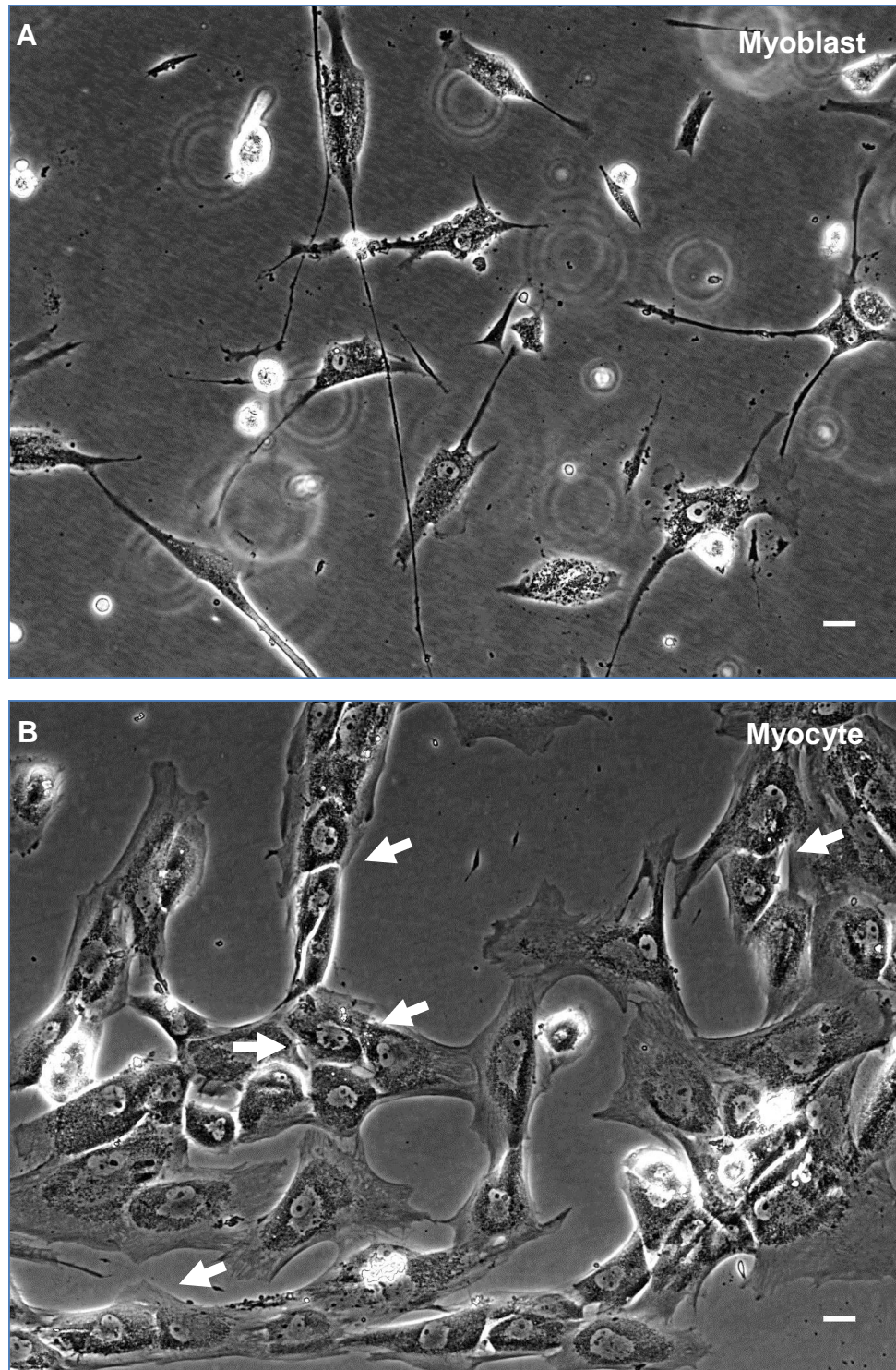


Fig 3.3: Differentiation of HSkMC cells. (A) Bright field image of HSkMC cells (Myoblasts) prior to inducing differentiation with differentiation medium. **(B)** Bright field image of differentiated HSkMC cells (Myocytes) after day 7 of inducing differentiation. White arrows show fusion and formation of syncytia. Scale bar - 50 μ m.

3.3.2.2 The cytotoxic effect of HSkMC supernatant on PC3M cells

To determine the effect of skeletal muscle supernatant on highly metastatic prostate cancer cells, PC3M cells were seeded in 24-well plates and incubated overnight at 37°C. The following day, cells were washed three times, resuspended in CGM and treated with supernatant from healthy myoblast or myocyte cells with or without MVs at total protein concentrations of 0.5 mg/ml, 1 mg/ml, or 2 mg/ml. Cells with CGM or DMEM with 15% horse serum (myocyte differentiation medium (DF)) served as controls. The plates were then incubated for 72 hr at 37°C. Following incubation, the cells were processed and analysed for apoptosis with Guava ViaCount reagent by flow cytometry.

On analysing the data (**Fig 3.4**), three significant trends could be recognized. Looking at the effect of myocyte supernatant on PC3M cells, it can be seen that there was a gradual significant increase in the percentage apoptosis in a dose dependant manner from 10% at a low concentration of 0.5mg/ml of supernatant with microvesicles, to a maximum of about 27% for 2 mg/ml of supernatant without microvesicles (**Fig 3.4**). Conversely, PC3M cells treated with HSkMC differentiation medium as control showed approximately 3% apoptosis. The differentiation medium was preferred as control since differentiated HSkMC cells are maintained in this medium after differentiation, and conditioned medium for MV isolation also comprises of this medium.

The second trend was observed when comparing PC3M cells treated with myoblast supernatant (s/n) or myocyte s/n. Cells treated with myocyte s/n containing MVs showed an overall significant increase in apoptosis from an average of 8.7% (0.5 mg/ml) to 14% (2 mg/ml) with increasing concentrations (**Fig 3.5 A**) compared to cells treated with myoblast supernatant containing MVs which showed lower levels of apoptosis at an average of 3.4% (0.5 mg/ml) to 8.4% (2 mg/ml) (**Fig 3.5 A**). Furthermore, on comparing apoptotic levels at a higher concentration of supernatant (2 mg/ml), myocyte supernatant significantly increased the apoptotic levels by 6% (almost 2-fold) compared to myoblast supernatant (**Fig 3.5 B**).

Cells treated with myocyte supernatant with MVs removed by filtration also showed a dose dependent increasing effect on PC3M cell cytotoxicity. As the concentration was increased from 0.5 mg/ml to 2 mg/ml the percentage of apoptotic cells increased from 11% to 27% (**Fig 3.6 A**). On the other hand, cells treated with myoblast supernatant without MVs showed only a slight increase from 5% (MB s/n 0.5 mg/ml) to about 8% (MB s/n 2 mg/ml) (**Fig 3.6 A**). Furthermore, a comparison between the apoptotic effect elicited at high concentrations (2 mg/ml) of exposure to the supernatants revealed a 3.5-fold increase in apoptosis of PC3M cells by myocyte MV-free supernatant (25%) compared to myoblast supernatant (7.2%) (**Fig 3.6 B**). This data therefore suggests that supernatant from myocytes with or without MVs was clearly having a more cytotoxic effect on PC3M cells compared to that of myoblast supernatant.

The third trend that was noticed was between cells exposed to myocyte supernatant with and without microvesicles. Although there was a gradual increase in apoptosis from 9% (MC s/n 0.5 mg/ml) to 14% (MC s/n 2 mg/ml) in cells exposed to supernatant with microvesicles (**Fig 3.5 A**), the effect was much higher when exposed to supernatant without microvesicles with an apoptotic range from 11% (MC s/n MV free 0.5 mg/ml) to approximately 27% (MC s/n MV free 1 mg/ml and 2 mg/ml) (**Fig 3.4, 3.6 B**). Simply put, supernatant that was filtered through a 0.2 μ m pore size filter to remove microvesicles elicited greater apoptosis to PC3M cells, as opposed to supernatant containing MVs, thus implying the presence of a small molecule and/or exosomes released by myocytes into the supernatant, which would be in the filtrate.

On comparing the effect of myoblast supernatant on PC3M cells, no significant difference was observed compared to cells treated only with CGM (**Fig 3.4**), therefore indicating that myoblasts do not release any active substance that would have the same inhibitory effect on PC3M cells as myocyte supernatant. The CGM treatment was chosen as a control to compare with myoblast supernatant since myoblasts were cultured in CGM and so the components of the supernatant would be similar to that of CGM.

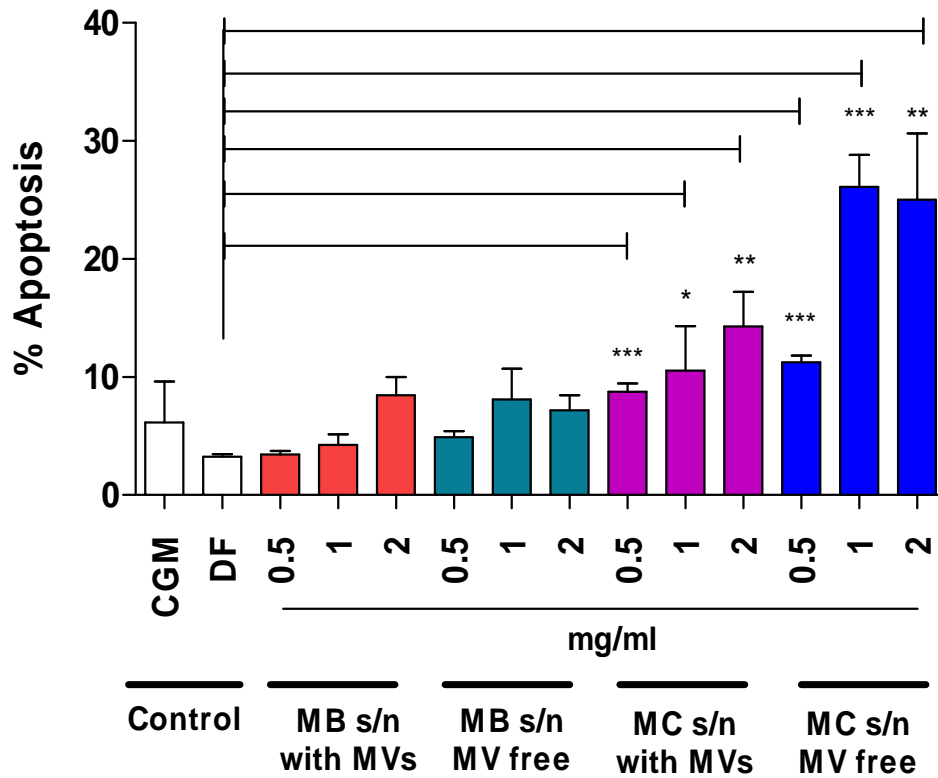


Fig 3.4: Human Skeletal muscle cell supernatant induces apoptosis in highly metastatic prostate cancer cells. PC3M cells were treated with either complete growth medium (CGM), skeletal muscle differentiation medium (DF - DMEM + 15% HS), supernatant from myoblast (MB s/n) or myocytes (MC s/n) with or without microvesicles (MV) and incubated at 37°C for 72 hrs. The cells were then stained with Guava ViaCount reagent and analysed by flow cytometry. The data represents the mean ± standard deviation of one of two experiments performed in triplicate. *: P < 0.05 was considered statistically significant. **: P < 0.005, ***: P < 0.0001.

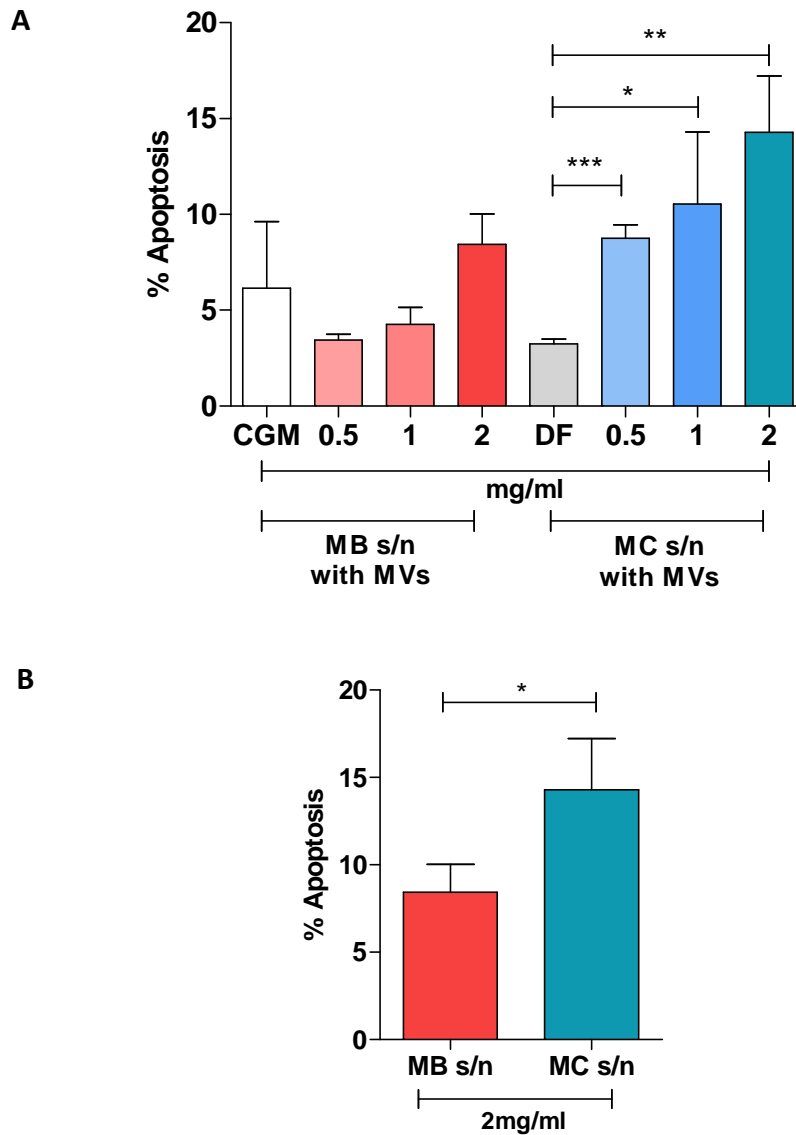


Fig 3.5: Comparison between the apoptotic effect of Human Skeletal muscle cell supernatant with MVs on highly metastatic prostate cancer cells. A) PC3M cells were treated with either complete growth medium (CGM), skeletal muscle differentiation medium (DF-DMEM+15% HS), various protein concentrations of supernatant (s/n) from myoblast (MB) or myocytes (MC) containing MVs and incubated at 37°C for 72 hrs. The cells were then stained with Guava ViaCount reagent and analysed by flow cytometry. **B)** Comparison of the apoptotic effect elicited by MB s/n and MC s/n at high protein concentration (2mg/ml) on PC3M cells. The data represents the mean \pm standard deviation of one of two experiments performed in triplicate. *: P < 0.05 was considered statistically significant. **: P < 0.005, ***: P < 0.0001.

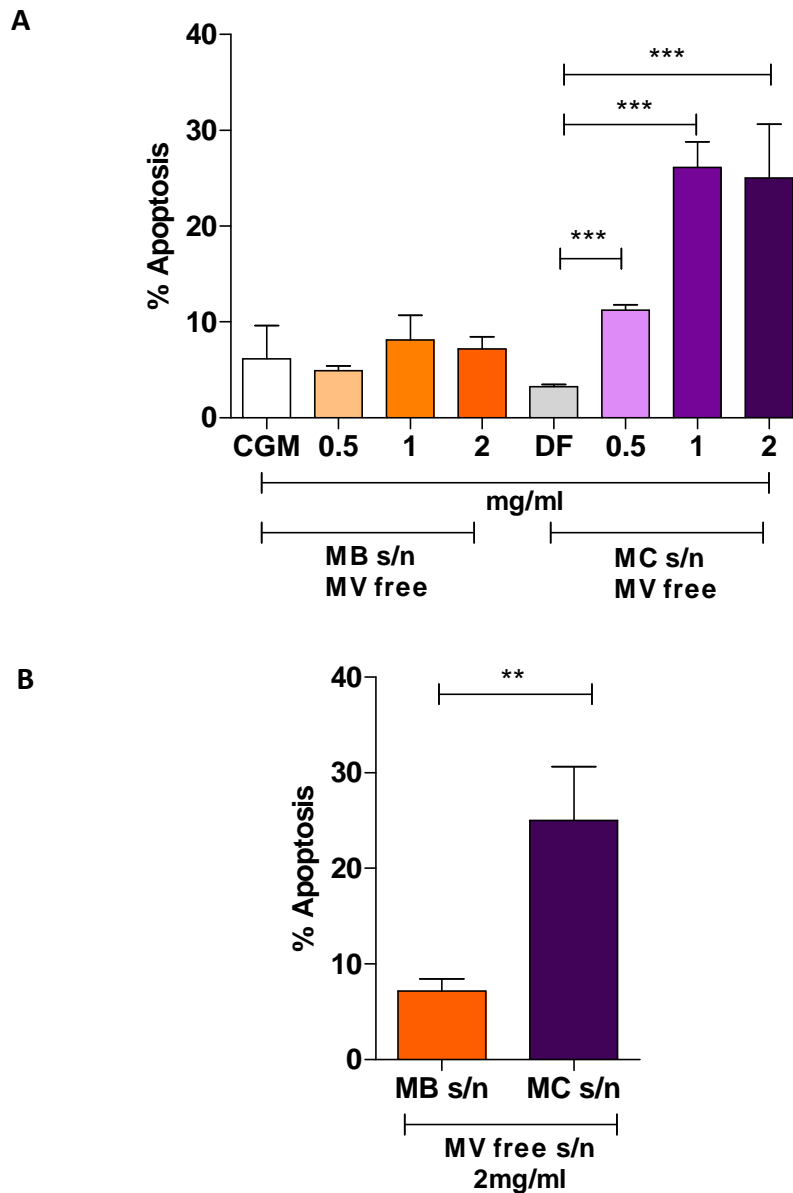


Fig 3.6: Comparison between the apoptotic effect of Human Skeletal muscle cell MV free supernatant on highly metastatic prostate cancer cells. A) PC3M cells were treated with either complete growth medium (CGM), skeletal muscle differentiation medium (DF-DMEM + 15% HS), various protein concentrations of MV free supernatant (s/n) from myoblast (MB) or myocytes (MC) and incubated at 37°C for 72 hrs. The cells were then stained with Guava ViaCount reagent and analysed by flow cytometry. **B)** Comparison of the apoptotic effect elicited by MV free MB s/n and MC s/n at high protein concentration (2mg/ml) on PC3M cells. The data represents the mean ± standard deviation of one of two experiments performed in triplicate. **: P < 0.005, ***: P < 0.0001 was considered statistically significant.

3.3.2.3 HSkMC MVs inhibits the migration of PC3M cells

Following the observation of an apoptotic effect of HSkMC supernatant on prostate cancer cells, the next step was to determine the effect of skeletal muscle cell MVs on the proliferation and growth of PC3M cells. Briefly, PC3M cells seeded overnight were scratched and treated with or without 30µg of HSkMC MVs (or PC3M MVs) and then incubated at 37°C (5% CO₂ conditions) for 24 h. Post incubation, the cells were analysed by microscopy.

The migration index was calculated for each well using the migration index formula shown below, where G_0 is the width of the scratch before incubation and G_1 is the width of the scratch after a 24 h incubation period.

$$\text{Migration index} = \left(\frac{G_0 - G_1}{G_0} \right) \times 100$$

The migration index is the measure of the percentage movement of cells from one region to another in a given time period. In this case the distance the cells moved across the path created by the scratch was measured as the migration index. This was then considered to be directly proportional to cell growth.

On calculating the migration index after 24 h, the control treatment had an index of about 25% hence confirming that the cells were viable and there was cell growth and proliferation (**Fig 3.7 A & B**). Moreover, 24 h incubation of PC3M cells with PC3M MVs had no effect on the proliferation or growth of the cells whatsoever as indicated by the migration index of about 23% which was similar to the control.

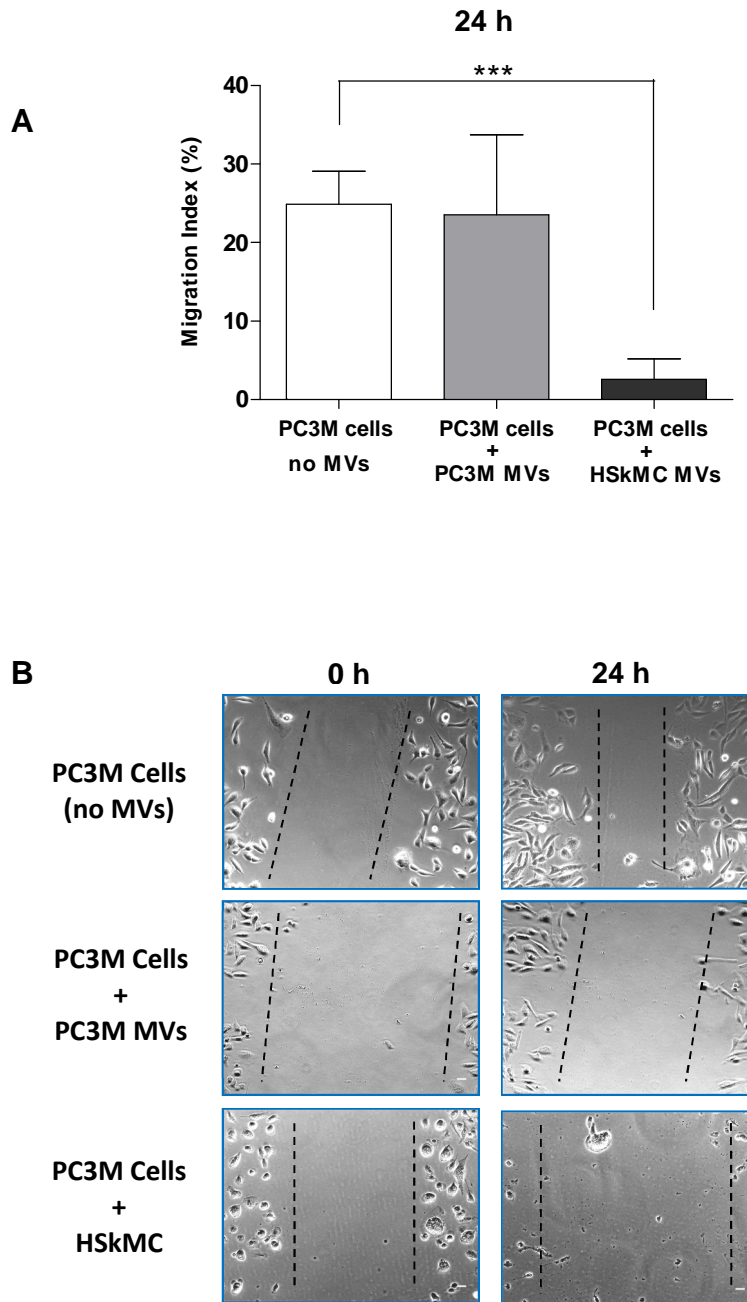


Fig 3.7: HSkMC MVs inhibits the migration and growth of highly metastatic PC3M cells. A & B. PC3M cells were treated with or without PC3M MVs or HSkMC MVs and incubated for 24 h. The Migration index was calculated after 24 h. The data represents the mean \pm standard deviation of one of two experiments performed in triplicate. $*P < 0.05$ was considered statistically significant. The dotted lines represent the migration distance covered by cells during the experiment. Scale bar - 100 μ m.

On the other hand, observation of PC3M cells incubated with 30µg/ml of HSkMC MVs for 24hrs, through microscopy showed a further widening of the scratch made initially (**Fig 3.6 B**). The majority of the cells had detached and all that was left in the well were cells that were stressed and cell debris. On calculating the migration index, there was a significant 10-fold reduction to about 2.6% compared to the control (25%) (**Fig 3.6 A**) or the treatment with PC3M microvesicles (24%). This therefore indicates that Human skeletal muscle cell derived MVs carry an active factor/factors that is not only attenuating proliferation and growth but also inducing apoptosis in PC3M cells.

3.3.2.4 HSkMC MV mass spectrometry analysis

After the observation of cell toxicity and anti-proliferation effects of HSkMC MVs on PC3M cells, we sought to investigate the protein cargo carried by these MVs that could potentially be the reason for the effect observed above by mass spectrometry. Briefly, MVs isolated from myoblast and myocytes were subjected to differential centrifugation (sec 2.2.3) and the MVs isolated were lysed with RIPA buffer (sec 2.2.6) and then analysed on Waters nano UPLC-Q/TOF premier platform mass spectrometer (UCL-ICH) as per section 2.2.12.

<u>OK</u>	<u>Accession</u>	<u>Entry</u>	<u>Description</u>	<u>mW (Da)</u>	<u>pI (pH)</u>
2	ENO1_YEAST	P00924	Enolase 1 OS Saccharomyces cerevisiae strain ATCC 204508 S288c GN ENO1 PE 1 SV 3	46787	6.1538
2	UBC_HUMAN	P0CG48	Polyubiquitin C OS Homo sapiens GN UBC PE 1 SV 3	76991	7.7578
2	HBA_HUMAN	P69905	Hemoglobin subunit alpha OS Homo sapiens GN HBA1 PE 1 SV 2	15247	9.1787
2	HBB_HUMAN	P68871	Hemoglobin subunit beta OS Homo sapiens GN HBB PE 1 SV 2	15988	6.8804
2	ACTG_HUMAN	P63261	Actin cytoplasmic 2 OS Homo sapiens GN ACTG1 PE 1 SV 1	41765	5.1606
2	TRYP_PIG	P00761	Trypsin OS Suscrofa PE 1 SV 1	24393	6.9141
2	RAP1B_HUMAN	P61224	Ras related protein Rap 1b OS Homo sapiens GN RAP1B PE 1 SV 1	20811	5.4653
2	MFGM_HUMAN	Q08431	Lactadherin OS Homo sapiens GN MFGE8 PE 1 SV 2	43095	8.0596
2	APOE_HUMAN	P02649	Apolipoprotein E OS Homo sapiens GN APOE PE 1 SV 1	36131	5.4829
1	IKBP1_HUMAN	Q5VVH5	Interleukin 1 receptor associated kinase 1 binding protein 1 OS Homo sapiens GN IRAK1BP1 PE 2 SV 1	29088	9.2065
2	KCRM_HUMAN	P06732	Creatine kinase M type OS Homo sapiens GN CKM PE 1 SV 2	43073	6.8364
1	HSP7C_HUMAN	P11142	Heat shock cognate 71 kDa protein OS Homo sapiens GN HSPA8 PE 1 SV 1	70854	5.2002
1	SYC1L_HUMAN	A8MT33	Synaptonemal complex central element protein 1 like OS Homo sapiens GN SYCE1L PE 2 SV 3	27380	4.7988
2	ALBU_HUMAN	P02768	Serum albumin OS Homo sapiens GN ALB PE 1 SV 2	69321	5.8608
2	C2CD5_HUMAN	Q86YS7	C2 domain containing protein 5 OS Homo sapiens GN C2CD5 PE 1 SV 1	110376	5.3467

Table 3.1: Identities of proteins from myoblast MVs. Briefly, MVs isolated from healthy myoblast cells *in-vitro* were lysed, prepared and analysed by the MSe Label-free quantitation UPLC-Q/TOF mass spectrometry. The “OK” column provides simplified information about the data quality and confidence score (2 = 95%; 1 = 50% confidence level). Enolase 1 OS from yeast served as an internal control.

OK	Accession	Entry	Description	mW (Da)	pI (pH)
2	ENO1_YEAST	P00924	Enolase 1 OS Saccharomyces cerevisiae strain ATCC 204508 S288c GN ENO1 PE 1 SV 3	46787	6.1538
2	ALBU_HUMAN	P02768	Serum albumin OS Homo sapiens GN ALB PE 1 SV 2	69321	5.8608
2	GPX3_HUMAN	P22352	Glutathione peroxidase 3 OS Homo sapiens GN GPX3 PE 1 SV 2	25385	8.2222
2	CI170_HUMAN	A2RU37	Uncharacterized protein C9orf170 OS Homo sapiens GN C9orf170 PE 2 SV 1	13360	11.0376
2	SYAP1_HUMAN	Q96A49	Synapse associated protein 1 OS Homo sapiens GN SYAP1 PE 1 SV 1	39908	4.2539
2	GELS_HUMAN	P06396	Gelsolin OS Homo sapiens GN GSN PE 1 SV 1	85644	5.8418
2	A2MG_HUMAN	P01023	Alpha 2 macroglobulin OS Homo sapiens GN A2M PE 1 SV 3	163187	6.0029
1	NHLC2_HUMAN	Q8NBF2	NHL repeat containing protein 2 OS Homo sapiens GN NHLRC2 PE 1 SV 1	79393	5.1914

Table 3.2: Identities of proteins from myocyte MVs. Briefly, MVs isolated from healthy myocyte cells *in-vitro* were lysed, prepared and analysed by the MSe Label-free quantitation UPLC-Q/TOF mass spectrometry. The “OK” column provides simplified information about the data quality and confidence score (2 = 95%; 1 = 50% confidence level). Enolase 1 OS from yeast served as an internal control.

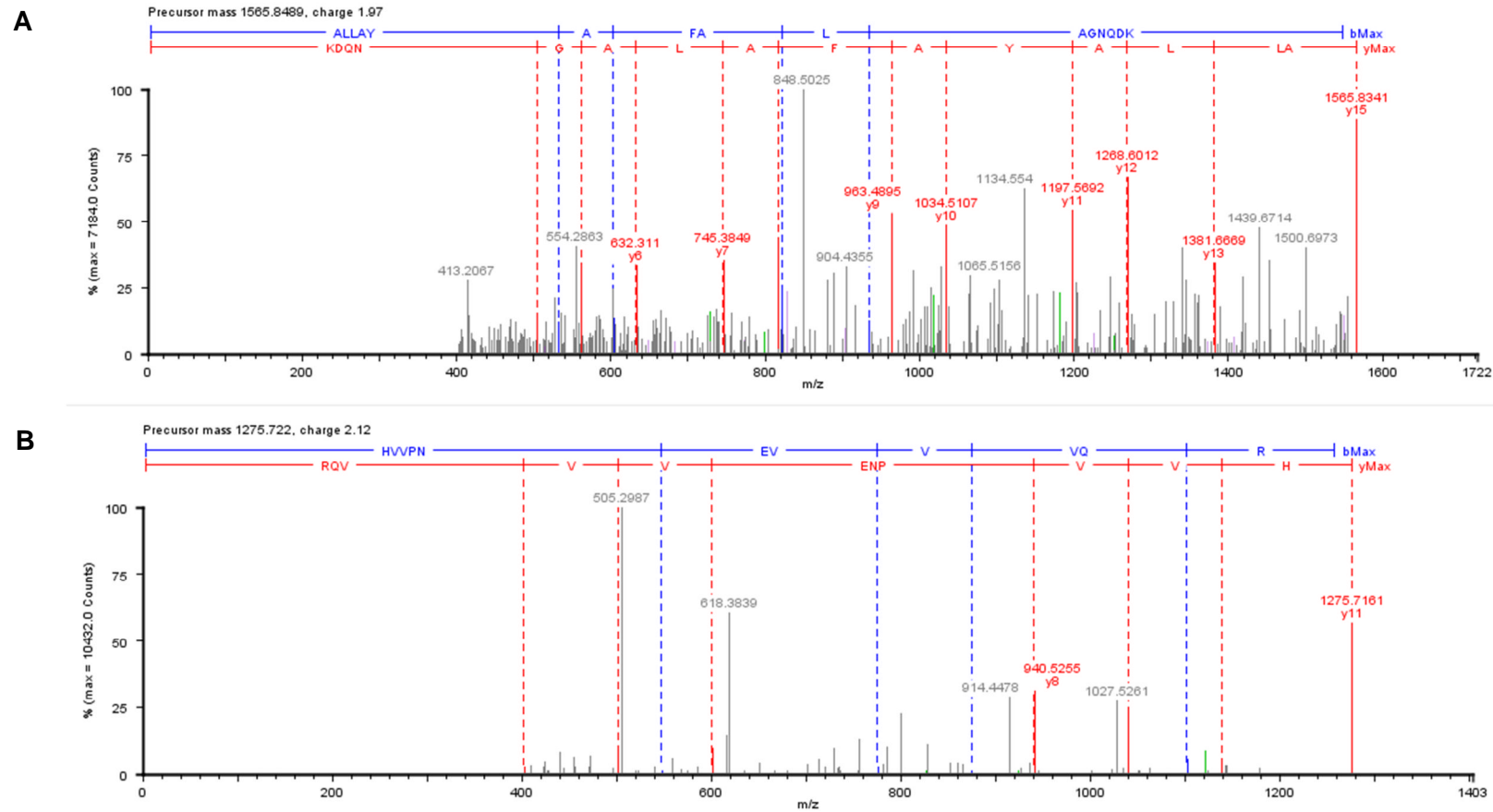


Fig 3.8: UPLC-Q/TOF Spectra shot of proteins Identified from analysis of myocyte MVs. A) Alpha 2 macroglobulin - a 163 kDa protein that acts as a protein inhibitor as well as a carrier molecule for cytokines and growth factors. **B)** Gelsolin is a 86kDa protein that has been shown to play a role in microvesiculation through actin reorganization (ref (1)). It has also been implicated in caspase 3 mediated apoptosis and has been shown to be down-regulated in tumour cells during carcinogenesis of various cancers (ref (2)).

3.3.2.4.1 Proteins identified from myoblast MV analysis

ProteinLynx GlobalServer version 2.4 (Waters, UK) was used to process the data obtained from the sample analysis. Protein identifications were obtained by searching a human proteome UniProt database. Altogether, 15 proteins were identified out of which Yeast Enolase 1 OS (P00924) (loading control) and Porcine Trypsin OS (P00761) (for trypsin digestion) are proteins that are not part of the sample and were added manually as part of the analysis process, therefore a total of 13 proteins were detected to be present in myoblast MVs (**Table 3.1**). Out of these proteins, 10 proteins had a confidence score of 2 (95%) (OK column) which means that the probability of that protein being part of the sample is 95% and therefore is not a false positive. On the other hand 3 proteins that were detected had a confidence level of 1 (50%) which means the probability of the proteins being part of the sample is 50% hence increasing the chances of them being false positives. All of the proteins identified below apart from creatine kinase M and C2 domain containing protein 5 have been reported to have been present in MVs and/or exosomes from other sources such as urine, saliva, cells and malignant ascites (179).

Polyubiquitin-C is a polymer chain of ubiquitin linked by different lysine (Lys) residues. The function of Polyubiquitin-C when attached to a target protein depends on the lysine residue that is linked with the target protein. For instance Lys-6 linkage is involved in DNA repair; Lys-29 linkage is also

involved in lysosomal degradation. In its unbound state Polyubiquitin-C is involved in protein kinase activation and cell signalling (180,181).

Haemoglobin subunit alpha and *subunit beta* are involved in the transport of oxygen from the lungs to the peripheral tissues (182).

Actin cytoplasmic 2 (gamma 1 actin) is an unusual form of actin to be present in skeletal muscle, however it has been shown to be expressed at very low levels in the costamere (cytoskeletal networks that couple peripheral myofibrils to the sarcolemma) of the skeletal muscle (183). On the other hand this form of actin has been reported by various researchers to be present in microvesicles and exosomes from various other types of cells (184-186).

Ras-related protein Rap-1bis a small GTPase that plays a role in the establishment of basal endothelial barrier function through endothelial junction control (187).

Lactadherin plays a role in VEGF dependent neovascularization and also contributes to the removal of apoptotic cells in many tissues. It has also been shown to have an affinity towards PS enriched surfaces in a receptor independent manner (188).

Apolipoprotein E is a transporter protein that carries fat soluble vitamins, cholesterol, and lipoproteins to the blood via the lymphatic system. It is an important protein for the metabolism of lipoproteins and has been shown to have other functions such as regulation of the immune system (189).

Creatine kinase M - an enzyme primarily present in the cytoplasm of skeletal muscle and is important for energy transduction in tissues with augmented, sporadic energy demands like skeletal muscle, brain, and heart (190).

C2 domain containing protein 5 is a protein required for the translocation of glucose transporter GLUT4 to the plasma membrane. It has also been shown to bind phospholipid rich membranes in a calcium dependent manner (191).

3.3.2.4.2 Proteins identified from myocyte MV analysis

Altogether 7 proteins were identified (excluding Enolase) out of which 6 proteins had a confidence level of 95% (OK value - 2) and one had a confidence level of 50% (OK value - 1) (**Table 3.2**). Compared to myoblast microvesicles, myocyte MVs carry fewer proteins that are not common apart from serum albumin protein which was present in both the microvesicles. All of the proteins identified below been reported to have been present in MVs and/or exosomes from other sources such as urine, saliva, cells and malignant ascites (179)

Glutathione peroxidase 3 is a protein that was identified in MVs from myocytes. It is a selenium-dependent enzyme that is secreted to scavenge hydrogen peroxide and free radicals to reduce systemic oxidative stress (192).

Synapse associated protein 1 - not much information is available on this protein, however a proline-rich synapse associated protein 1 (ProSAP1) has

been reported to play a role in synaptic transmission in peripheral nervous system as well the neuromuscular junction (193).

Alpha-2-macroglobulin is a protease inhibitor that is able to inactivate multiple classes of proteinases such as cysteine proteinases, serine proteinases, and metalloproteinases. It also acts as a carrier molecule for various growth factors and cytokines such as TGF- β , insulin, and IL-1 β (194,195).

Gelsolin (**Fig 3.8**) is the most potent Ca^{2+} and polyphosphoinositide 4,5-bisphosphate (PIP₂) dependent actin filament severing and capping protein that is implicated in actin remodelling in both viable and apoptotic cells as well as microvesiculation (196). Other than this it has also been implicated as a pro-apoptotic agent through a caspase dependent mechanism (197) therefore making it a prime protein of interest since MVs and supernatant from myocytes induced apoptosis in PC3M cells as shown above.

3.3.3 Summary of the apoptotic effect of HSkMC MVs on PC3M cells

The data obtained on investigating the effect of HSkMC MVs on the PC3M prostate cancer cell line was very interesting. As mentioned above the prominence of cancer occurring in or spreading to skeletal muscle is very low. When incubating PC3M cells with supernatant from myoblast and myocyte healthy cells, there was a significant increase in apoptosis of PC3M cells incubated with myocyte supernatant in a dose-dependent manner. This effect was further enhanced when filtering the supernatant to exclude MVs.

Further investigation showed that on treating PC3M cells with MVs from myocytes this reduced proliferation and increased apoptosis compared to MVs from PC3M cells therefore indicating that MVs from myocytes exhibit cytotoxic effects on PC3M cells. Through mass spectrometry analysis of MVs from myoblast and myocytes a candidate protein gelsolin present in myocyte MVs was identified that could be one of the proteins behind the observed cytotoxic properties of HSkMC MVs. Fig 3.9 therefore summarises the overall mechanism of the apoptotic effect of HSkMC MVs observed in the experiments above on PC3M cells.

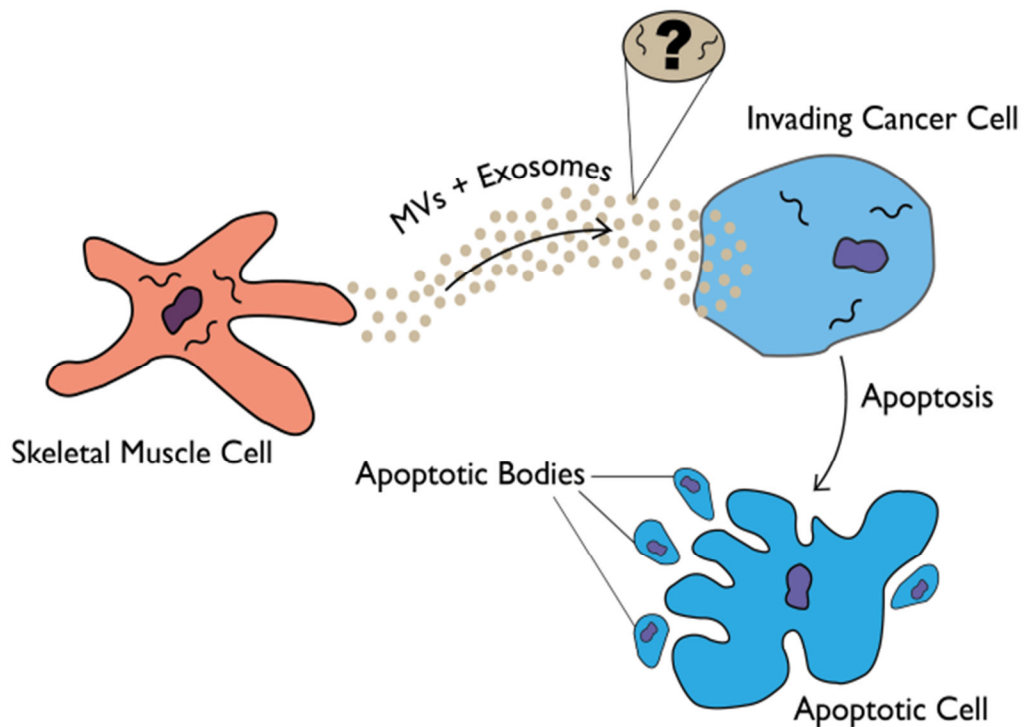


Fig 3.9: The effect of HSkMC MVs on PC3M prostate cancer cells. In this study, we postulate that HSkMC MVs and possibly exosomes, upon release participate(s) in eliciting some, if not all of the cytotoxic effects observed on target tumour cells.

4. The role of Peptidylarginine deiminase on microvesiculation

4.1 Introduction

Peptidylarginine deiminase is a Ca^{2+} -dependent post-translational modification enzyme that replaces protein bound arginine and methylarginine residues with citrulline causing structural and functional changes in target proteins in an irreversible manner (70). To date, five isoforms have been identified in humans that are tissue-specific expressions apart from PAD2 that has been found to be expressed in multiple tissues such as cells from the haematopoietic lineage as well as secretory glands (69). As aforementioned, PAD enzymes have been shown to regulate various physiological functions (91) as well as being implemented in various diseases such as autoimmune diseases, neurodegenerative diseases and cancer (67,76,198).

PAD2 and PAD4 are the two isotypes that have recently been linked with cancer with the latter shown to have elevated levels in cancer patients. Out of the two isotypes, PAD4 has been shown to play a regulatory role on p53 and its target genes, activation of proto-oncogenes such as *c-fos*, as well as dysfunctioning various cytokeratin isoforms that are involved in mediating apoptosis in cancer cells through protein deimination (also known as citrullination) (107,109,110). PAD2 on the other hand has been shown to play a role in gene regulation in breast cancer cells (85,199).

Given that both the activation of PAD enzymes and of other enzymes involved in the biogenesis of MVs are dependent on calcium and that there

are elevated levels of both PAD and MVs in cancer and other human diseases, I sought to investigate the interplay between the two.

4.2 Methodologies

4.2.1 PAD isotype expression in cancer and non-cancerous cells

To determine the isotype of PAD expressed in cancer and non-cancer cells, K562, PC3, and PNT2 cells were labelled with PAD2 and PAD4 antibody and analysed by flow cytometry, microscopy and Western blot.

4.2.1.1 Flow cytometry

K562, PC3, or PNT2 cells were washed and viability measured using the Guava Viacount assay. 5×10^5 cells were seeded in 1.5ml Eppendorf tubes in triplicate and fixed with 4% paraformaldehyde for 10 min at room temperature. The cells were then washed three times with cold PBS at 400 g for 5 min and resuspended in permeabilisation buffer (PBB) (0.5% Triton-X 100 in PBS) for 5 min at room temperature. Permeabilised cells were washed three times as mentioned above and incubated with mouse anti-human PAD4 or rabbit anti-human PAD2 primary antibody (1:500 in 3% BSA/PBS) at 4°C for 1 h with shaking. Post incubation cells were washed three times and incubated with anti-mouse (PAD4) or anti-rabbit (PAD2) IgG-FITC conjugated secondary antibody (1:350 dilutions, at 4°C for 1 h on shaker). The samples were then washed three times with cold 1% BSA/PBS again and resuspended in 200 µl of PBS containing 3% BSA, 1% NaN₃ and analysed by flow cytometry.

4.2.1.2 Fluorescence Microscopy

PC3 and PNT2 cells (5×10^5 cells/well) were seeded on a coverslip in a 24-well plate in triplicate, 24 h before the experiment. After 24 h, the cells were washed gently with prewarmed PBS and fixed with 4% paraformaldehyde for 10 min at room temperature. The cells were then washed three times with cold PBS and resuspended in PBB for a further 5 min at room temperature. Post incubation, the buffer was removed and cells washed three times as mentioned above.

The cells were then incubated with mouse anti-human PAD4 or rabbit anti-human PAD2 primary antibody (1:500 dilutions in 3% BSA/PBS) for 1 hr at 4°C on a shaker. After incubation the cells were washed three times with cold PBS and further incubated with anti-mouse (for PAD4) and anti-rabbit (for PAD2) AlexaFluor 488 conjugated IgG secondary antibody (5µg/ml in 3% BSA/PBS) at 4°C for 1 h on a shaker in the dark. The cells were then washed three times with cold 1% BSA/PBS and the cover slips mounted on to slides with DAPI-VECTASHIELD medium (Vector Laboratories Inc. Burlingame, CA). Images were collected using a fluorescence microscope (1X81 motorized inverted fluorescence microscope, Olympus Corporation).

4.2.1.3 Western Blotting

In order to identify PAD isotypes via Western blotting, K562, PC3 and PNT2 cells were lysed as per section 2.2.6 and immunoblotted as mentioned in sections 2.2.7 - 2.2.11. The dilution of PAD4 and PAD2 primary antibodies

used was 1:500, HRP conjugated IgG secondary antibody was 1:1000 and anti- β -actin used as loading controls was 1:500.

4.2.2 The Effect of PAD inhibition on MV release

To determine the effect of PAD enzyme on the release of MVs by cells, the function of the enzyme was blocked by chloramidine (an irreversible pan-PAD enzyme inhibitor (89)).

K562, PC3 and PNT2 (the latter two first trypsinised), were washed, quantified and checked for viability (Guava Viacount assay). Cells were then resuspended in prewarmed, serum-free RPMI 1640 and seeded in triplicate at 5×10^5 cells/microcentrifuge tube. Various concentrations of chloramidine (from 2.5 μ M to 50 μ M) were added and the cell preparations incubated at 37°C (5% CO₂ humidified conditions) for 30 min.

Post incubation, the cell preparations were washed once with prewarmed PBS and resuspended in prewarmed serum-free RPMI 1640 supplemented with 2mM CaCl₂ followed by addition of 10% NHS (MV free) and further incubated at 37°C (5% CO₂, humidified conditions) for 30 min with shaking.

The tubes were then removed and placed on ice for 1 minute to stop any further reactions and then centrifuged at 200 *g* for 5 min to remove any cell debris. The resultant supernatant was transferred to sterile 1.5 ml Eppendorf tubes, and treated as mentioned in section 2.2.3 for isolation of MVs. The resulting pellet of MVs was suspended in 200 μ l of sterile PBS and analysed using flow cytometry (Guava express plus, Guava technologies).

In some experiments BzATP (300 μ M) was used instead of NHS as a microvesicle inducing agent and the concentration of chloramidine was maintained at 25 μ M instead of a range of concentrations as mentioned above.

4.2.3 F95 Immunoprecipitation (IP)

To determine the proteins that had been citrullinated by the PAD enzyme when stimulated for microvesiculation, cell lysates from K562 and PC3 cells treated with or without chloramidine were immunoprecipitated (Catch and Release v2.0 IP kit, Millipore) with the pan-citrulline F95 antibody that specially recognizes protein bound citrullines (200) (kindly gifted by Dr Anthony Nicholas, University of Alabama, Birmingham, USA).

4.2.3.1 Materials and Reagents

- 1x Wash buffer - Diluted from 10X catch release buffer (provided in kit)
- Spin columns
- Capture tubes
- 1.5 ml microcentrifuge tubes (Eppendorf)
- Antibody affinity ligand - provided in the kit
- F95 antibody
- Denaturing elution buffer with β -Mercaptoethanol (5% v/v) added immediately before use.

Throughout - Wash and Elution Buffers were diluted with Milli-Q water.

4.2.3.2 IP Protocol

Spin columns, capture tubes and 1.5 ml microcentrifuge tubes to be used were labelled. Caps and snap-off plugs located at the bottom of the spin

columns were removed and stored for later use. Individual spin columns were then inserted into individual capture tubes and centrifuged at 2000 *g* for 30 sec to remove the resin slurry buffer. The columns were then washed twice with 400 μ l of 1x wash buffer (provided in kit) at 2000 *g* for 30 sec. The snap-off plugs removed earlier were then plugged back in the spin columns.

As per the manufacturers' directions a volume of combined reagents had to be determined to add to the spin columns as follows: 500 μ g of cell lysate, 4 μ g of F95 antibody, affinity ligand (10 μ l - fixed volume) and 1x wash buffer (the volume of which was adjusted to 500 μ l final volume). After determining the volumes required for each of the reagents mentioned above, they were added in the respective spin columns in the following order: 1x wash buffer, cell lysate, F95 primary antibody, and the antibody capture affinity ligand. The spin columns were then capped and incubated at 4°C on a rotator overnight.

Post incubation, the spin columns were inserted in capture tubes with the snap-off plugs removed and centrifuged at 2000 *g* for 30 sec. The flow-through was transferred to 1.5 ml microcentrifuge tubes and stored at -20°C for later analysis. The columns were then washed three times with 400 μ l of 1x wash buffer spinning at 2000 *g* for 30 sec. Each of the washes were collected in one tube and stored at -20°C for later analysis if required.

The columns were then placed in fresh capture tubes and the protein eluted by adding 70 μ l of 1x denaturing elution buffer containing 5% β -Mercaptoethanol and centrifuging at 2000 *g* for 30 sec. For maximum

recovery of the protein a successive elution step was carried out with 4x denaturing buffer instead. The eluate was then stored at -20°C for Western blot analysis.

For some experiments 1×10^7 K562 cells were treated with or without 10 μ M chloramidine and stimulated with or without 10% NHS (MV free) (as per section 4.2.2). The cells were then washed three times with cold PBS at 200 *g* for 5 min and lysed with RIPA buffer (as per section 2.2.6). 500 μ g of cell lysate from each of the treatments was then immunoprecipitated with F95 antibody and the eluate analysed for citrullinated β -actin by immunoblotting.

4.2.4 Western blot analysis of citrullinated proteins from PC3M cells stimulated for microvesiculation

In order to compare protein profiles of citrullinated proteins between PC3M cells that were not stimulated or stimulated for microvesiculation or PAD inhibited prior to stimulation, cell lysates from healthy PC3 cells only, or PC3 cells pre-treated with or without 50 μ M chloramidine and then stimulated with 300 μ M BzATP was subjected to Western blot analysis.

Briefly, 50 μ g of cell lysates were separated by SDS-PAGE (10% gel) and transferred to a nitrocellulose membrane as per section 2.2.5 - 2.2.9. The membrane was then incubated with blocking buffer (5% BSA/TBS-T) for 1 hr on a shaker at room temperature. This was followed by an overnight incubation with F95 antibody (1:3000 in 5% BSA/TBS-T) on a shaker at 4°C. On the following day six 10 min washing steps were performed with TBS-T followed by a 1 hr incubation with secondary isotype matched HRP

conjugated antibody (α -mouse IgM 1:5000 in 5% BSA/TBS-T) at room temperature on a shaker. The membrane was then washed as before and visualised via ECL as mentioned before (sec 2.2.10)

4.2.5 Mass Spectrometry analysis of citrullinated proteins from PC3M cells stimulated for microvesiculation

In order to identify proteins that were citrullinated during microvesicle stimulation of PC3M cells, 2000 μ g of cell lysates from healthy PC3 cells only, or PC3 cells pre-treated with or without 50 μ M chloramidine and then stimulated with 300 μ M BzATP was immunoprecipitated with F95 antibody and eluted with 70 μ l of non-denaturing buffer four times successively for maximum recovery of protein. The eluate was then subjected to mass spectrometry analysis as per section 2.2.12.

4.2.6 Role of chloramidine on the cytotoxic effect of methotrexate on cancer cells

In order to understand whether chloramidine would enhance the cytotoxic effect of methotrexate, K562 cells were washed and resuspended in prewarmed RPMI 1640. 5×10^4 cells were then seeded into 1.5 ml microcentrifuge tubes and treated with or without 100 μ M chloramidine and incubated at 37°C (5% CO₂, humidified conditions) for 30 min. Post incubation the cells were washed three times with prewarmed PBS at 200 g for 5 min. The cells were then resuspended in 450 μ l of prewarmed CGM supplemented with 2mM CaCl₂ and seeded to a 24-well plate. Cells were then treated with 100 μ M chloramidine, 100 μ M methotrexate or both in

combination. Treatments without any of the chemicals served as controls. The 24-well plate was then incubated at 37°C (5% CO₂ humidified conditions) for 24 h and 48 h.

Post incubation the cells were transferred to 1.5 ml microcentrifuge tubes and centrifuged at 500 *g* for 5 min. The wells were then washed once with prewarmed PBS which was then transferred to the individual tubes containing the cells. The cells were then centrifuged once more at 500 *g* for 5 min and resuspended in prewarmed RPMI 1640 and analysed for apoptosis in flow cytometry using the Guava Nexin Assay (Guava Millipore).

The experiment was then repeated with PC3 cells for a 48 h period; however the cells were seeded in 24-well plates 24 h before the experiment to allow the cells to attach and settle. After the experiment, the supernatant was collected, washed once at 500 *g* for 5 min, and the cells resuspended in prewarmed RPMI 1640 and analysed for apoptosis as described above.

4.3 Results

4.3.1 PAD 2 and 4 are expressed in K562, PC3 and PNT2 cells

In order to investigate the role of PAD in normal and cancer cells, it was important to evaluate the expression of PAD isozymes in the cells under analysis. To achieve this, in brief, K562, PC3, and PNT2 cells were washed and fixed with 4% paraformaldehyde for 10 min at room temperature (RT) and then permeabilised with permeabilisation Buffer. Cells were then washed and labelled with anti-PAD2 or anti-PAD4 antibody in 3% BSA/PBS and incubated at 4°C on shaker for 1 h. Post incubation, the cells were washed and labelled with FITC conjugated anti-rabbit IgG in 3% BSA/PBS and incubated for a further 1 hr at 4°C on a shaker. Cells were then washed and resuspended in PBS containing 3% BSA, 1% NaN₃ and analysed by flow cytometry for PAD expression.

For microscopy experiments, 5×10^5 PC3 and PNT2 cells were pre-seeded on a cover slip in 12-well plates 24 hrs before the experiment. On the day of the experiment the cells were washed, fixed and permeabilised as described above. The cells were then labelled with anti-PAD2 and anti-PAD4 antibody (1:500 dilutions) and incubated at 4°C for 1 hr. Cells were washed three times with cold PBS and labelled with AlexaFluor 488 conjugated anti-rabbit IgG secondary antibody (5 µg/ml) and incubated for 1 hr at 4°C. Post incubation, cells were washed and cover slips mounted on microscope slides with DAPI-Vectashield medium.

The results showed that K562, PC3 and PNT2 cells express both PAD2 and PAD4 isozymes (**Fig 4.1, and 4.2**). Microscopy images of both PNT2 and PC3 cells showed that both PAD isozymes were present intracellularly, localized primarily in the nucleus as well as the cytoplasm (**Fig 4.1 A**). This was further ascertained by Western blotting whereby 30 µg of healthy cell lysates obtained from K562, PC3 and PNT2 cells were resolved by 10% SDS-PAGE. The proteins were transferred to nitrocellulose membrane and immunoblotted with anti-PAD4, anti-PAD2 and anti-β-actin antibodies (**Fig 4.1 B**).

As the presence of both PAD2 and 4 isozymes was established in K562, PC3 and PNT2 cells the next step was to analyse the expression levels of these enzymes in the various cell lines through flow cytometry. Overall, the expression of PAD4 was higher in all cell lines compared to PAD2. Even though K562 cells did not show a significant difference in expression between both the isotypes, the mean PAD4 expression was higher at 80% compared to PAD2 (57%) (**Fig 4.2 A, C**). PC3 cells on the other hand had a significantly higher expression of PAD4 (83%) compared to PAD2 (38%) (**Fig 4.2 A, D**). PNT2 cells also followed a similar trend of higher PAD4 expression (70%) and a low PAD2 expression (30%) (**Fig 4.2 A, E**).

Comparing PAD4 expression between the cell lines, there was no significant difference between K562 and PC3 cells or PNT2 cells. However between PNT2 (non-cancerous) and PC3 cell (cancerous), there was a significance difference (**Fig 4.2 A**) with the cancerous expressing higher levels. The same

trend was observed with PAD2 expression whereby the cancer variant (PC3) of the normal prostate cell line (PNT2) expressed significantly more PAD2 protein (**Fig 4.2 B**). Similar trends were also observed when comparing the Median Fluorescence Intensity (indicating the expression of PAD/cell) between the cell lines (**Fig 4.2 B**).

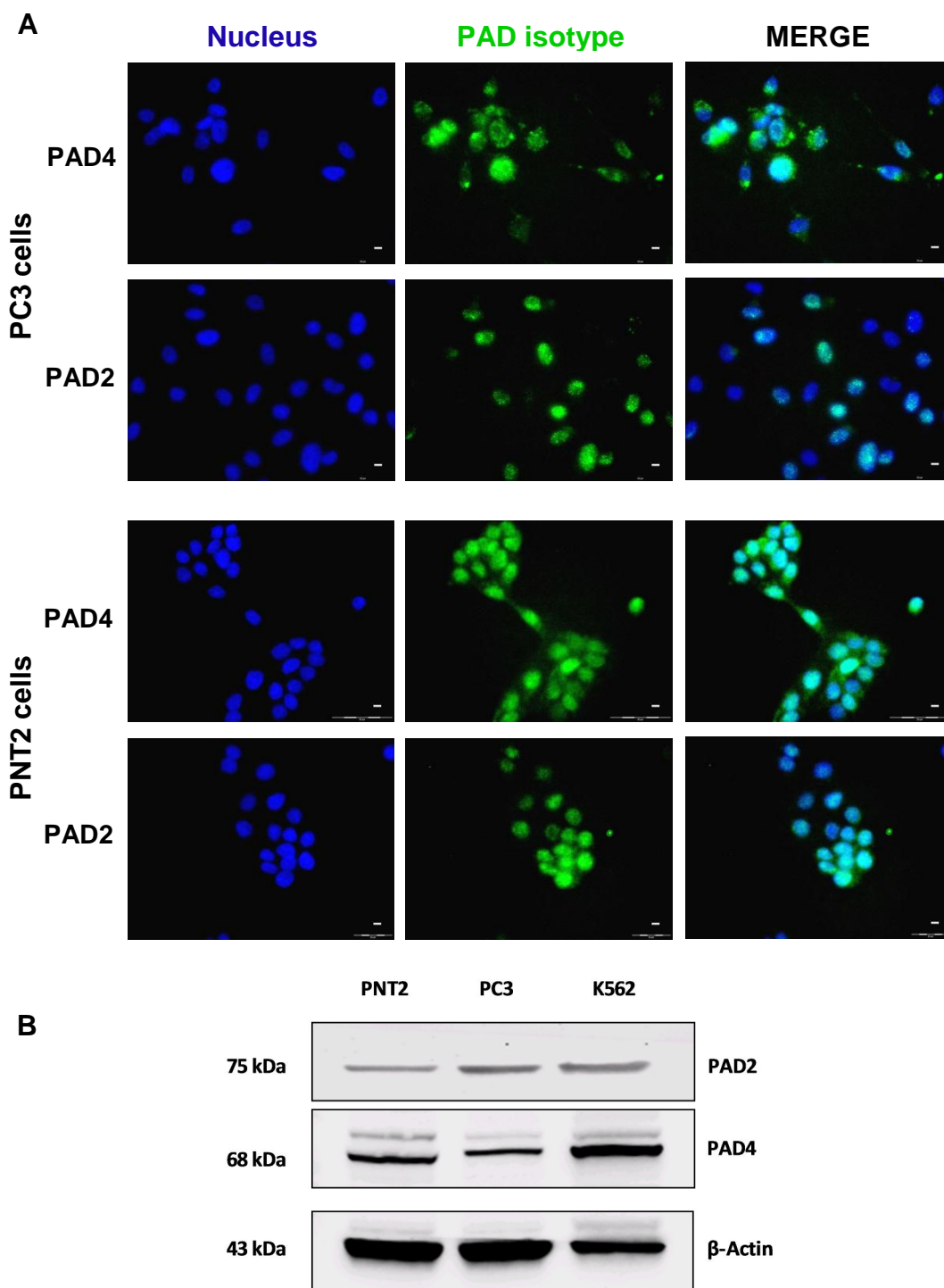


Fig 4.1: Cellular expression of PAD isotypes. (A) Immunofluorescence images of PC3 and PNT2 cells expressing PAD4 and PAD2 isotypes (40X Magnification). (B) Western blot analysis of healthy K562, PC3 and PNT2 cells expressing PAD4 enzyme. Proteins were resolved on a 10% SDS-gel, and western blot carried out with anti-PAD2, anti-PAD4 and anti- β -actin (loading control).

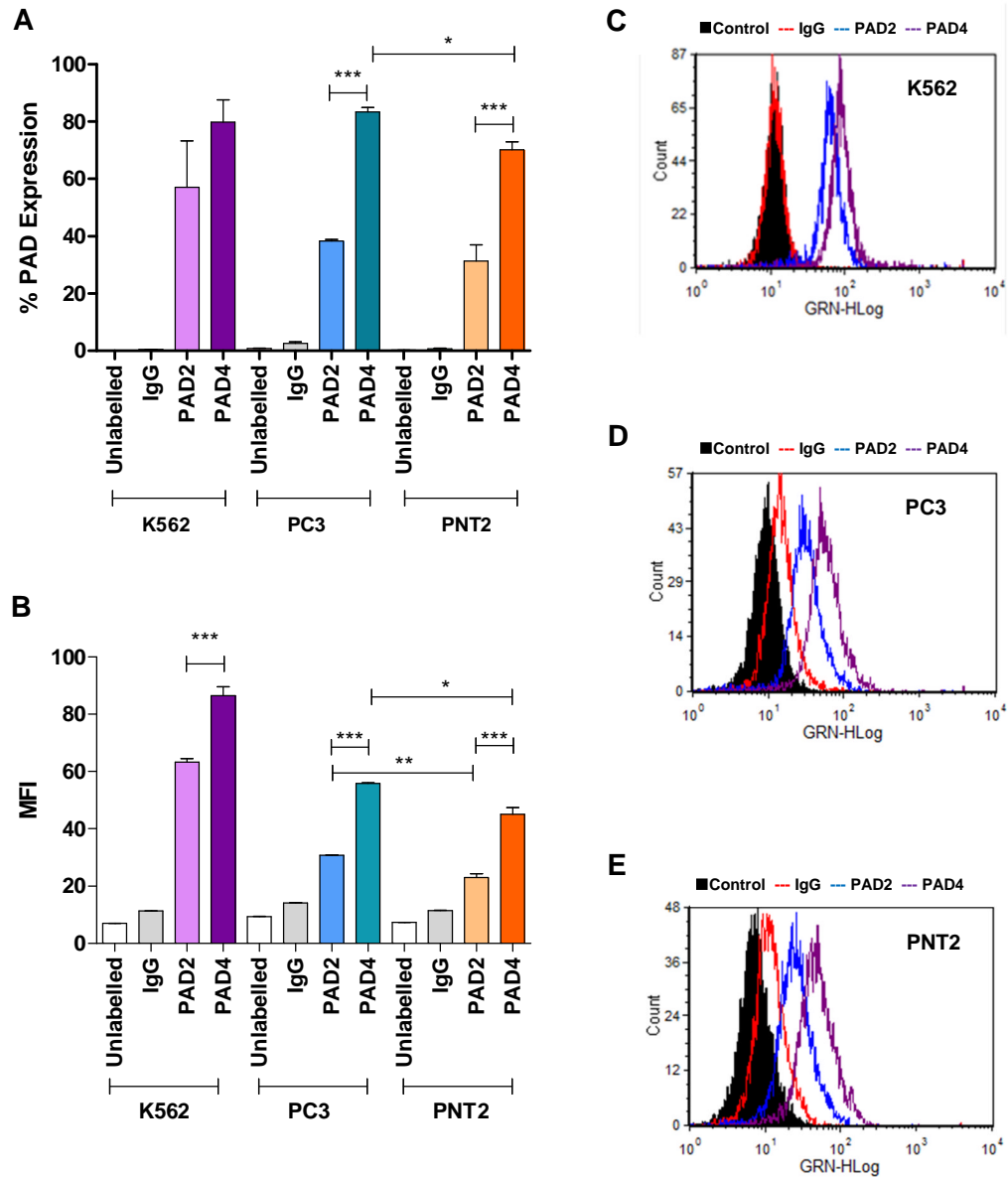


Fig 4.2: Flow cytometry analysis of cellular expression of PAD isotypes in cancer and non-cancerous cells. K562 (A, C), PC3 (A, D) and PNT2 (A, E) cells were fixed, permeabilised and labelled with anti-PAD2 and anti-PAD4 antibody followed by FITC-IgG secondary antibody and analysed for PAD expression via flow cytometry. (B) Median Fluorescence Intensity (MFI), indicative of expression levels of PAD/cell. Data represents the mean±SEM of two independent experiments performed in triplicate. * $P < 0.05$, ** $P < 0.005$, *** $P < 0.001$ was considered statistically significant.

4.3.2 PAD activation is needed for microvesiculation of cancer and non-cancer cells

As it was established that cancerous and non-cancerous cell lines express PAD isotypes intracellularly, the next step was to evaluate the function of the enzymes in microvesiculation by blocking them with the irreversible inhibitor chloramidine in a dose-dependent manner.

Briefly, 5×10^5 cells were washed and preincubated with or without various concentrations of chloramidine for 30 min at 37°C, 5% CO₂, under humidified conditions. The cells were then washed once with PBS and incubated with or without 10% NHS and further incubated for 30 min at 37°C to induce microvesiculation.

For some experiments, cells were preincubated with 25 µM chloramidine for 30 min at 37°C, washed once with PBS and then further incubated in the presence or absence of 300 µM BzATP instead of 10% NHS to induce microvesiculation. Post incubation, the cells were centrifuged. Microvesicles were then isolated via differential centrifugation of the resulting supernatant and analysed by flow cytometry.

4.3.2.1 Chloramidine inhibits microvesiculation in K562 cells

Flow cytometry analysis of MVs showed a significant increase in MV production when treated with 10% NHS (MV-free) compared to control. Pre-incubating cells with a low concentration, 2.5 µM of chloramidine, had no inhibitory effect on microvesiculation (**Fig 4.3 A**) whatsoever. However, on

doubling the concentration to 5 μM , microvesiculation was significantly reduced by 36% from 7×10^4 MVs/ml to 4.5×10^4 MVs/ml and doubling the concentration further to $10 \mu\text{M}$ reduced the release of microvesicles by 74% to 1.8×10^4 MVs/ml. A further increase in concentration of chloramidine to 25 μM and 50 μM did significantly reduce microvesiculation from 4.8×10^5 MVs/ml (stimulated with NHS) to 2×10^5 MVs/ml, the margin of inhibition between 10 μM and 25 μM concentration being about 8% (**Fig 4.3 B**). This therefore indicates that although the inhibitory effect of chloramidine increases in a dose dependent manner there is a saturation concentration level after which no further significant inhibitory effect in microvesiculation is noticed.

On stimulating the cells with 300 μM BzATP (a well established stimulant of microvesiculation in cells (201)), there was a significant 5-fold increase in the release of microvesicles from 4.2×10^4 MVs/ml (control) to 2.2×10^5 MVs/ml. This was considerably reduced by 50% to 1.2×10^5 MVs/ml on treating the cells with 25 μM chloramidine (**Fig 4.3 C**). This therefore signifies that the inhibitory effect of chloramidine on microvesiculation is not a coincidence of a reaction with NHS and that the PAD enzymes somehow play a role in microvesiculation of K562 cells.

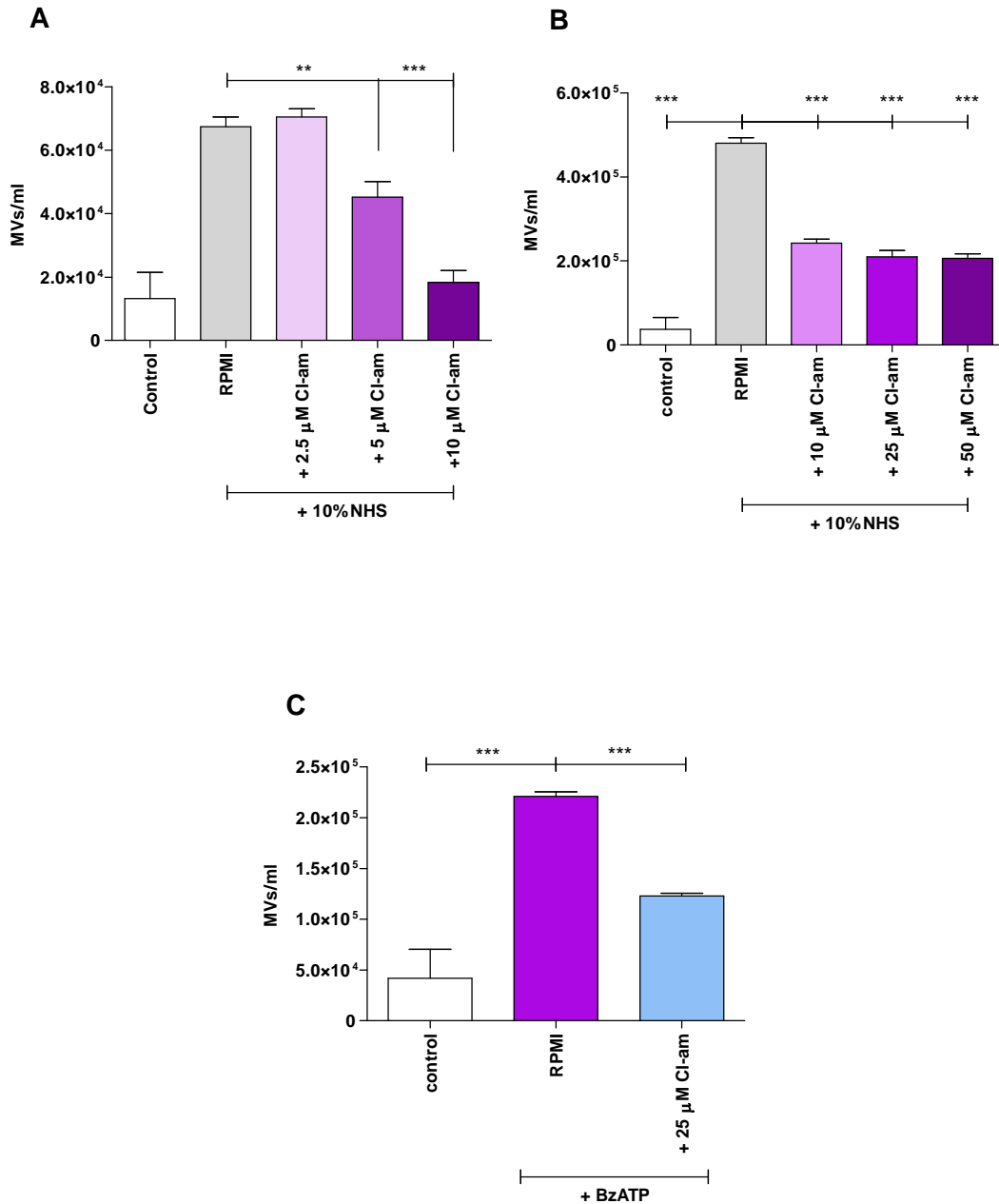


Fig 4.3: Chloramidine inhibits microvesiculation in K562 cells. (A-B) K562 cells pre-incubated with or without various concentrations of chloramidine (Cl-am) were treated with 10% NHS (MV-free) and incubated at 37°C for 30 minutes. MVs were then isolated from the experiment and analysed by flow cytometry. (C) K562 cells pre-incubated with or without 25 μM chloramidine (Cl-am) were treated with 300 μM BzATP and incubated at 37°C for 30 minutes. MVs were then isolated from the experiment and analysed by flow cytometry. The data represents the mean ± standard deviation of one of two experiments performed in triplicates. **P*<0.05, ***P*<0.005, ****P*<0.001 was considered statistically significant.

4.3.2.2 Chloramide inhibits microvesiculation in PC3 cells and the translocation of PAD4 and partially PAD2 to the nucleus during MV release

In order to investigate the effect of chloramide on microvesiculation in another cancer cell line, PC3 cells were pre-treated with various concentrations of chloramide and microvesiculation induced either with 10% NHS or 300 μ M BzATP. Microvesicles were then isolated and analysed by flow cytometry.

On analysing the results, a similar trend to K562 cells was observed. Incubating cells with 10% NHS for 30 min, increased the number of MVs released 2.5 times from 4.8×10^4 MVs/ml (control) to 12×10^4 MVs/ml (**Fig 4.4 A**). However, pre-incubating the cells with 2.5 μ M and 5 μ M chloramide did abrogate the stimulatory effect of NHS by reducing microvesiculation significantly from 1.2×10^5 MVs/ml to 0.94×10^5 MVs/ml (2.5 μ M) and 1.0×10^5 MVs/ml (5 μ M) respectively (**Fig 4.4 A**). The inhibitory effect was more profound on increasing the concentration to 10 μ M whereby there was a reduction of microvesiculation from 12×10^4 MVs/ml (without chloramide) to 3×10^4 MVs/ml (with 10 μ M chloramide) (**Fig 4.4 A**). Increasing the concentration of chloramide further to 25 μ M and 50 μ M did show a reduction in microvesicle release in a dose dependent manner (**Fig 4.4 B**), therefore asserting the role of PAD enzymes in microvesiculation in the cell lines investigated.

Pre-incubating cells with chloramidine and replacing the microvesicle stimulating agent with BzATP instead of NHS also had the same effect as observed on K562 cells whereby the release of microvesicles was reduced by 50% from 2.8×10^4 MVs/ml (without chloramidine) to 1.4×10^4 MVs/ml on inhibition.

This therefore indicates that it is not the stimulus of microvesiculation but the cellular release mechanism that is affected by chloramidine and that the PAD enzyme that is inhibited as a result could play a role in the shedding of microvesicles.

To further understand the localization of PAD4 and PAD2 enzymes during stimulation and inhibition by NHS and chloramidine, pre-seeded PC3 cells were treated with or without $10 \mu\text{M}$ chloramidine for 30 min at 37°C , followed by stimulation with or without 10% NHS for 30 min at 37°C . The cells were then fixed with 4% paraformaldehyde and permeabilised with 0.5% triton x. The cells were then labelled with PAD4 or PAD2 antibody followed by isotype matched AlexaFluor 488 antibody and mounted onto slides for microscopy analysis.

Fluorescence microscopy revealed the translocation of PAD4 as reflected by the increase in fluorescence intensity from the cytoplasm (**Fig 4.5 i, C-white arrows**) to the nucleus (**Fig 4.5 ii, C-white arrows**) when treated with NHS for 30 min. This increase in fluorescence intensity was however reduced on pre-incubating cells with chloramidine prior to treatment with NHS (**Fig 4.5 iii**), also there was a reduction in the population of cells expressing PAD4

compared to control or cells treated with NHS (**Fig 4.5 B iii**). Further analysis showed that chloramidine was most likely preventing the translocation of the enzyme to the nucleus (**Fig 4.5 C iii**) as the fluorescence is mainly observed around the nucleus as pointed out by the white arrows in the magnified image in *Fig 4.5 C iii*. This data therefore indicates that translocation of PAD4 to the nucleus plays a likely role in the release of microvesicles when stimulated with NHS.

A similar result was obtained when labelling cells with PAD2. Untreated cells had PAD2 fluorescence in the perinuclear region as marked by the white arrows in *Fig 4.6 C i*. This therefore meant that PAD2 is primarily localised in the cytoplasm at a resting state. However, on stimulating the cells with NHS for 30 min, the fluorescence intensity was increased in the nuclear region of the cell (**Fig 4.6 ii**) as marked by the white arrows in *Fig 4.6 C ii*. This therefore shows that like PAD4, PAD2 also translocates to the nucleus when the cell is stimulated. However it was also noticed that fluorescence was also fairly high around the nucleus therefore suggesting that there is only partial transfer of the enzyme to the nucleus. On pre-incubating the cells with PAD inhibitor chloramidine prior to stimulating with NHS, less enzyme is translocated to the nucleus as reflected by the reduction in fluorescence (**Fig 4.6 iii**) compared to applying the stimulation without inhibition (**Fig 4.6 ii**). This therefore suggests that PAD2 plays a partial role in the nucleus together with the cytoplasm during microvesiculation when stimulated with NHS.

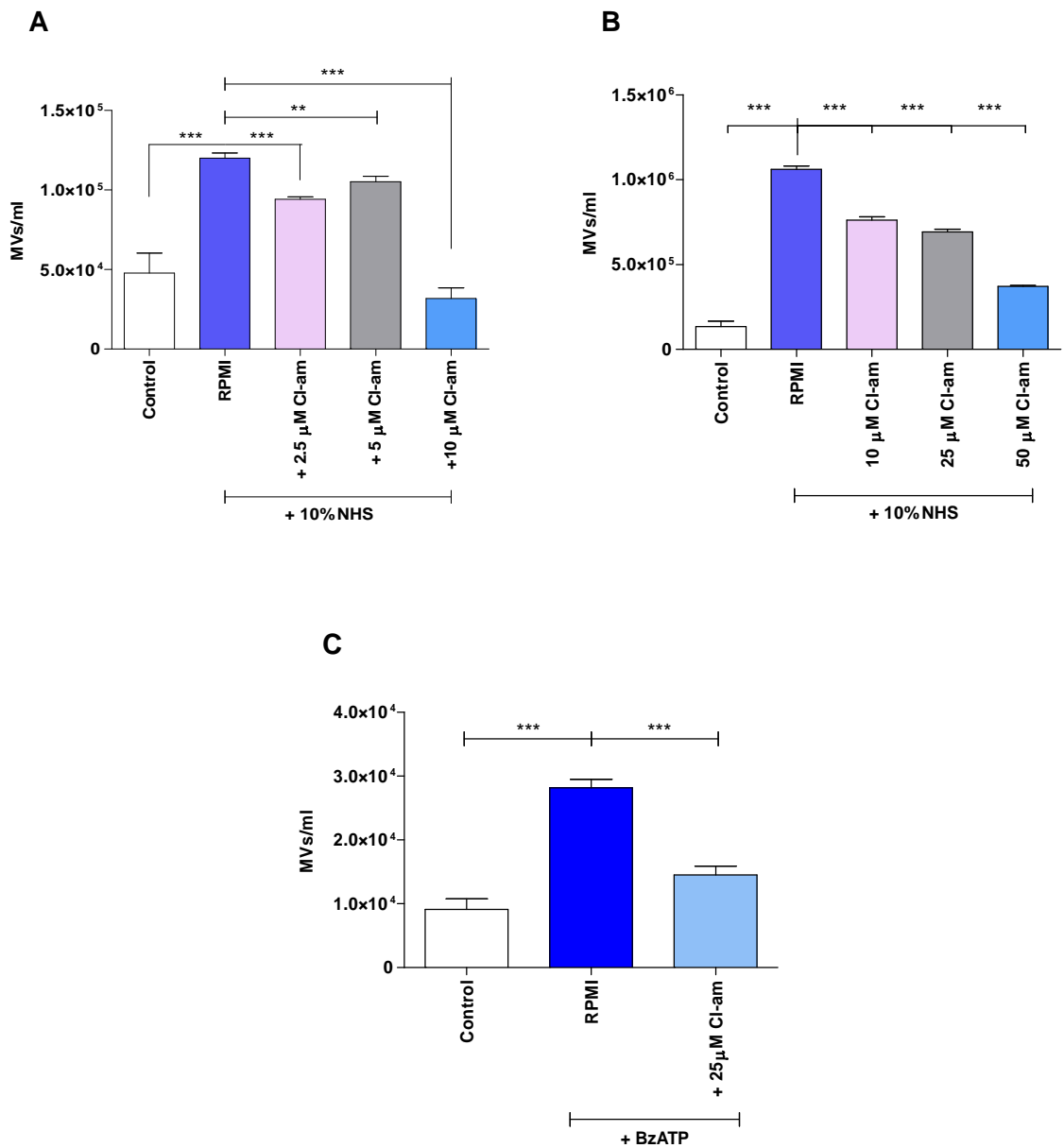


Fig 4.4: Chloramidine inhibits microvesiculation in PC3 cells. (A-B) PC3 cells pre-treated with or without various concentrations of chloramidine (Cl-am) were stimulated with 10% NHS (MV-free) and incubated at 37°C for 30 minutes. MVs were then isolated from the experiment and analysed by flow cytometry. (C) PC3 cells pre-treated with or without 25 μM Cl-am were stimulated with 300 μM BzATP and incubated at 37°C for 30 minutes. MVs were then isolated and analysed by flow cytometry. The data represents the mean ± standard deviation of one of two experiments performed in triplicates. * $P < 0.05$, ** $P < 0.005$, *** $P < 0.001$ was considered statistically significant.

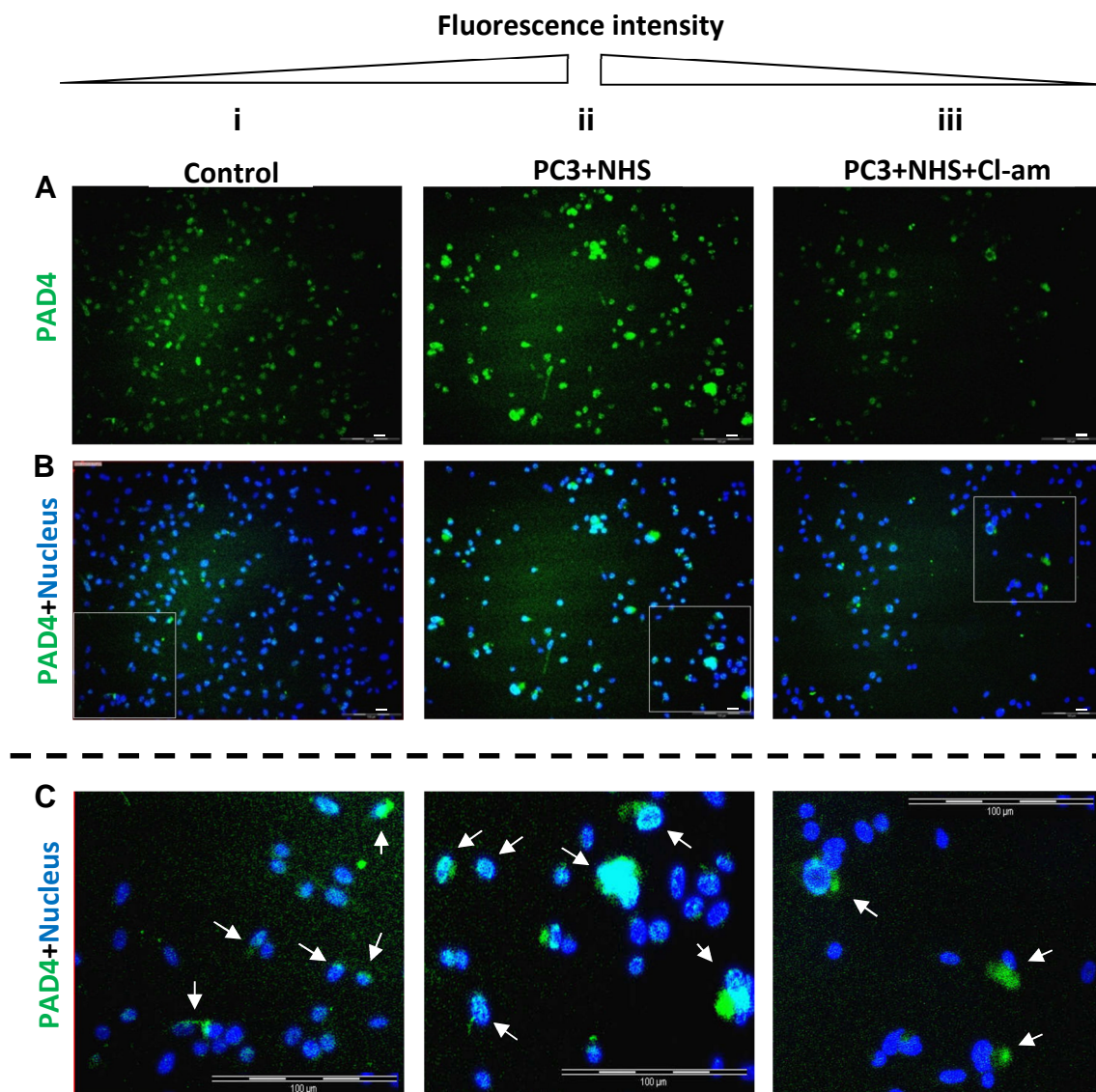


Fig 4.5: The effect of chloramidine on the localization and expression of PAD4 in PC3 cells. PC3 cells pre-seeded on coverslips were pre-treated with 10μM chloramidine (iii) or without (i, ii) for 30min at 37°C. The cells were then washed and incubated at 37°C for 30 min in the presence (ii, iii) or absence (i) of NHS and fixed with 4% paraformaldehyde, labelled for PAD4 expression, and analysed by fluorescence microscopy. **(A)** PAD4 (green) expression in PC3 cells, **(B)** localization of PAD4 in relation to the nucleus (DAPI-blue) of the cell. **(C)** Magnified (white rectangle (B)) images showing the localization (white arrows) of PAD4 expression relative to the nucleus of the PC3 cells from (B). Scale bar - 100μm.

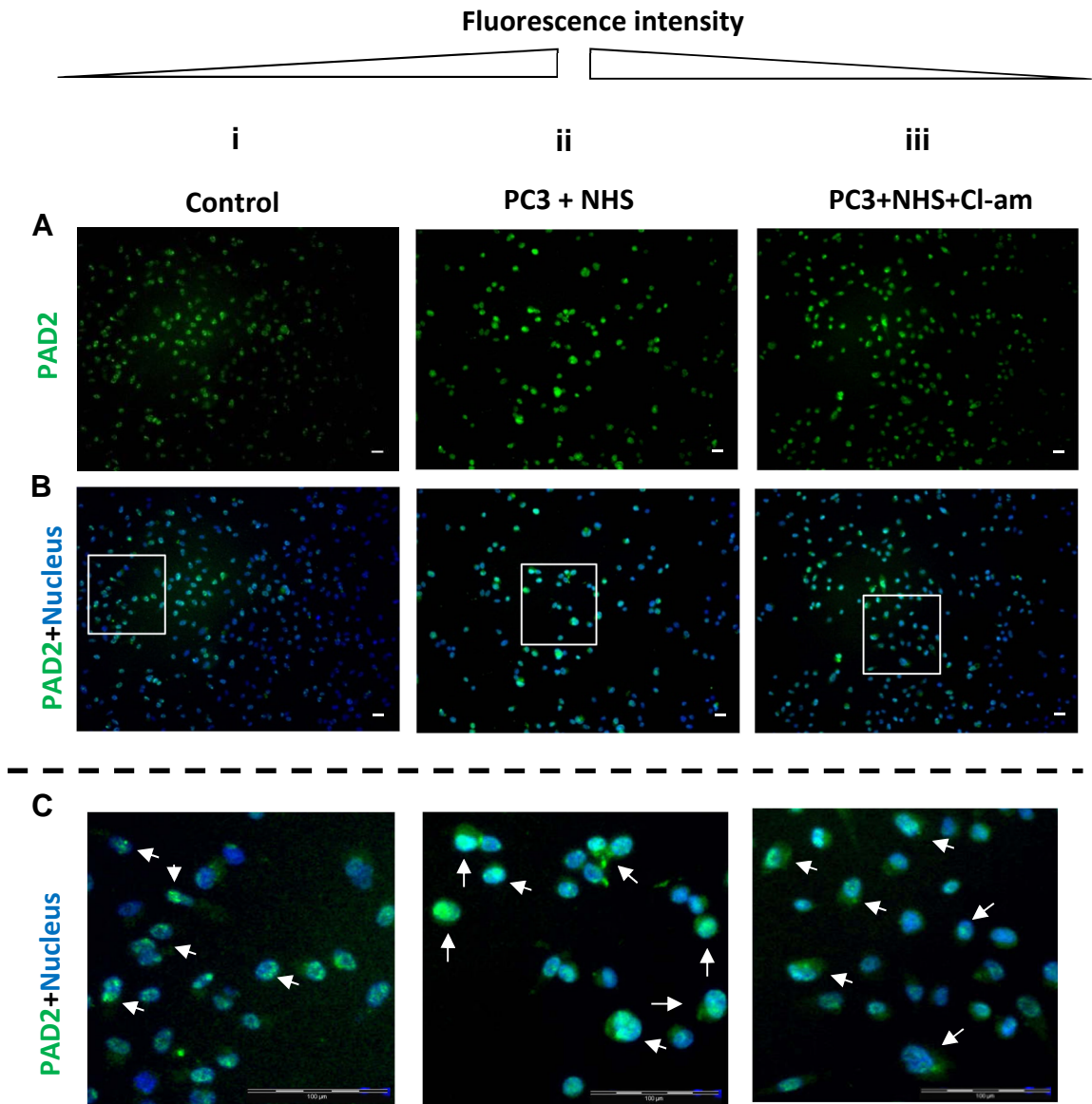


Fig 4.6: The effect of chloramidine on the localization and expression of PAD2 in PC3 cells. PC3 cells pre-seeded on coverslips were pre-treated with 10 μ M chloramidine (iii) or without (i, ii) for 30min at 37°C. The cells were then washed and incubated at 37°C for 30 min in the presence or absence of NHS. The cells were then fixed with 4% paraformaldehyde, labelled for PAD2 expression, and analysed by fluorescence microscopy. **(A)** PAD2 (green) expression in PC3 cells, **(B)** localization of PAD2 in relation to the nucleus (DAPI-blue) of the cell. **(C)** Magnified (white rectangle (B)) images showing the localization (white arrows) of PAD2 expression relative to the nucleus of the PC3 cells from **(B)**. Scale bar - 100 μ m

4.3.2.3 Chloramide inhibits microvesiculation in PNT2 cells

After observing the inhibitory effect of chloramide on microvesiculation of cancer cells, we sought to investigate if this effect could be observed in non-cancerous cells. PNT2 cells were chosen as they are the non-cancerous (benign) variant of the PC3 cells.

On analysing the result, it was clearly evident that chloramide did have an inhibitory effect on microvesiculation of PNT2 cells. Although a 10 μM concentration of chloramide was sufficient to have a reducing effect on the release of microvesicles for PC3 and K562 cells, this was not the case for this cell line (**Fig 4.7 A**). Nevertheless, increasing the concentration of chloramide to 25 μM and 50 μM subsequently did have a dose-dependent inhibitory effect as the concentration of microvesicles released was reduced significantly from 1.2×10^4 MVs/ml (NHS stimulated) to 2.6×10^3 (25 μM chloramide) and 4×10^3 MVs/ml (50 μM chloramide) (**Fig 4.7 A**). On treating the cells with BzATP as a stimulant for microvesiculation the release of microvesicles was significantly inhibited by about 70% from 5.6×10^5 (BzATP stimulated) to 1.6×10^5 MVs/ml (chloramide treated) (**Fig 4.7 B**).

This data therefore suggests the effect of chloramide in inhibiting microvesicle release to be similar amongst various cell lines. This therefore means that PAD enzyme, which is inhibited by chloramide, could have a significant role in the release of MV, across a wide array of cancerous and non-cancerous cell lines.

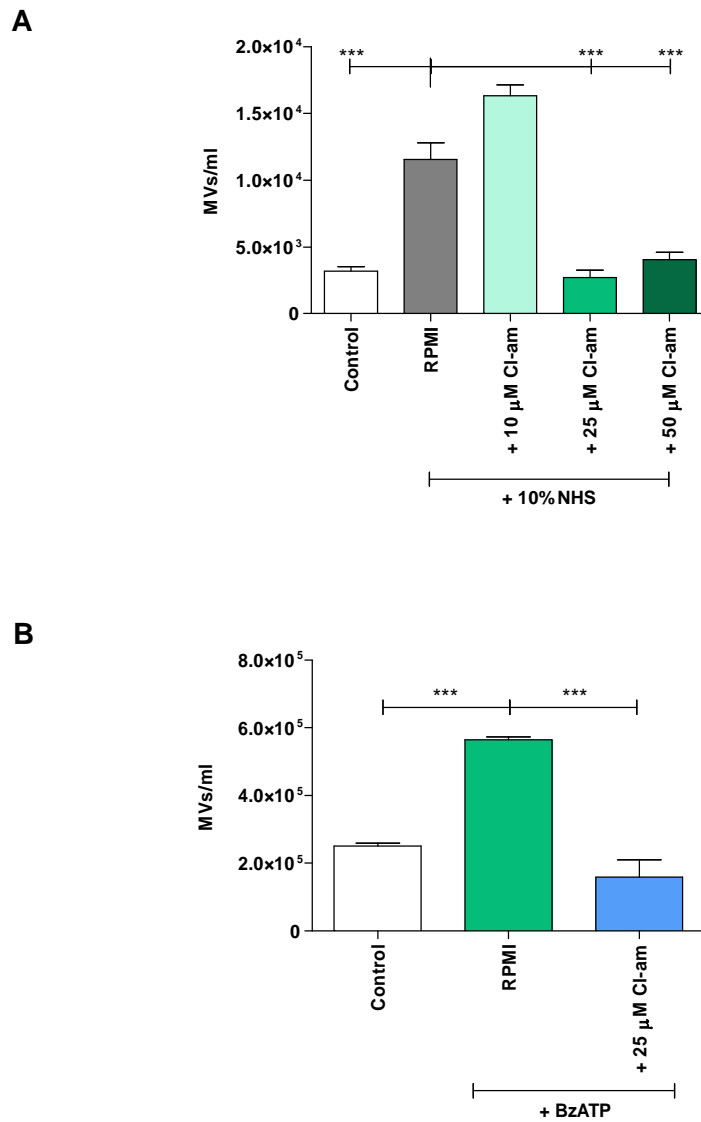


Fig 4.7: Chloramidine inhibits microvesiculation in PNT2 cells. (A) PNT2 cells pre-incubated with or without increasing concentrations of chloramidine (Cl-am) were stimulated with 10% NHS (MV free) and incubated at 37°C for 30 minutes. MVs were then isolated and analysed by flow cytometry. (B) PNT2 cells pre-treated with or without 25 μM Cl-am were stimulated with 300 μM BzATP and incubated at 37°C for 30 minutes. MVs were then isolated and analysed by flow cytometry. The data represents the mean ± standard deviation of one of two experiments performed in triplicates. **P*<0.05, ***P*< 0.005, ****P*< 0.001 was considered statistically significant.

4.3.3 During MV release from K562 cells the cytoskeletal protein β -Actin is deiminated by PAD enzyme

Given that inhibiting PAD with chloramidine significantly reduced microvesiculation in both cancer and normal cells we sought to investigate the mechanism by which this was happening. During microvesiculation the actin filaments that are part of the cytoskeleton undergo considerable rearrangement that allows the shedding of microvesicles (6). Further to this, Combes *et al* also reported that β -actin plays a significant role in the formation of agonist-induced microvesicles by interacting mechanically with other actin-rich structures (202) and a study by Andrade *et al* revealed that β and γ -actins are citrullinated by PAD isotypes in the sera of patients with rheumatoid arthritis (69). On the basis of this information we sought to investigate the citrullination of β -actin when stimulating microvesiculation in K562 cells with NHS.

Briefly, 1×10^7 K562 cells were washed and pre-treated with or without $10 \mu\text{M}$ chloramidine at 37°C for 30 min. The cells were then washed once and further incubated with 10% NHS at 37°C for 30 min to stimulate microvesiculation. Healthy K562 cells without any treatment served as control. Post incubation the cells were washed, lysed with RIPA buffer (as per section 2.2.6) and the total protein concentration determined.

500 μg of protein lysates from each of the treatments was then immunoprecipitated with anti-citrulline F95 antibody overnight at 4°C with shaking using the Catch and Release V2.0 kit (see section 4.2.3). The

immunoprecipitated protein fractions were then subjected to 10% SDS-PAGE and Western blotting, the blot being labelled with mouse monoclonal anti- β -actin (1:500) and subsequently HRP conjugated goat anti-mouse IgG (1:1000). The blot was analysed via chemiluminescence and the band intensities analysed through Image J software as per the manufacturer's instructions.

Untreated K562 cells had a very low expression of citrullinated β -actin with a very low peak (**Fig 4.8 B L1**) and band intensity of 2255.5 units (**Fig 4.8 A, B, C lane 1**). However, cells treated with NHS to stimulate microvesiculation had a more distinct band with a significantly high peak (**Fig 4.8 B L3**) and a band intensity (8979.6 units) about 4 times greater than untreated cells (**Fig 4.8 A, B, C lane 3**). Cells that were pre-incubated with chloramidine and then stimulated with NHS had a band intensity of 4313.5 units which was twice as high as the control but almost twice as low as NHS stimulated cells untreated with the PAD inhibitor (**Fig 4.8 A, B, C lane 2**). This data therefore indicates that deimination of β -actin is increased when stimulating cells with NHS, and is markedly reduced by almost 50% on pre-treating the cells with chloramidine before stimulation with NHS. As microvesiculation is also reduced on pre-treating the cells with chloramidine there is a possibility that citrullination of β -actin could play an important role in the shedding process of microvesicles.

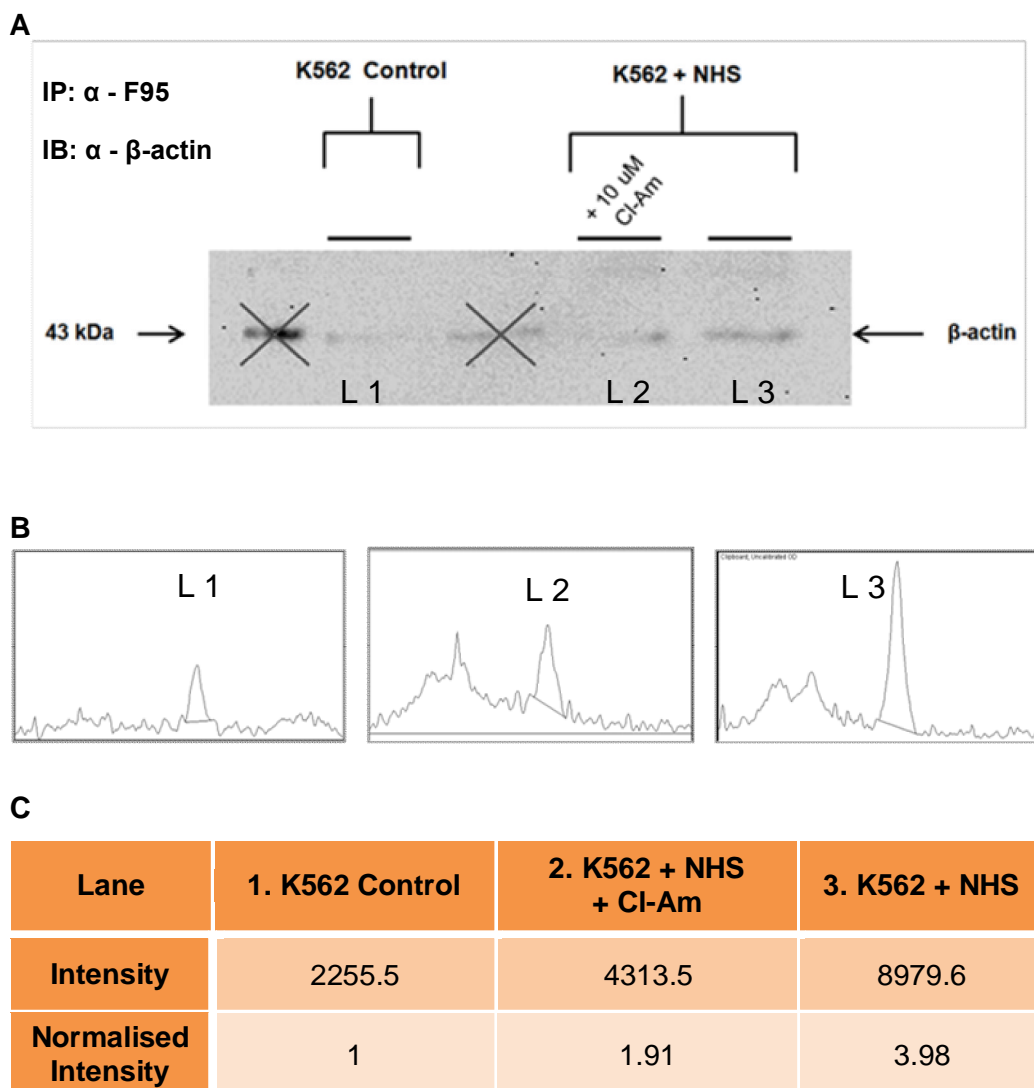


Fig 4.8: Citrullination of β -actin by PAD enzymes. (A) Western blot detecting citrullinated β -actin in immunoprecipitated (IP) deiminated protein lysates from healthy K562 cells (Lane 1), or K562 cells pre-treated with (Lane 2) or without (Lane 3) 10 μ M Chloramidine and stimulated with 10% NHS. (B) Profiles representing the β -actin band intensity from each of the treatment mentioned in the immunoblot in A. The peaks labelled L1, L2, and L3 are a direct representation of the bands observed in A. (C) Tabular representation of the β -actin band intensity and normalised intensity from each of the treatments immunoblotted above. Bands marked with X should be ignored as they are not part of the experiment.

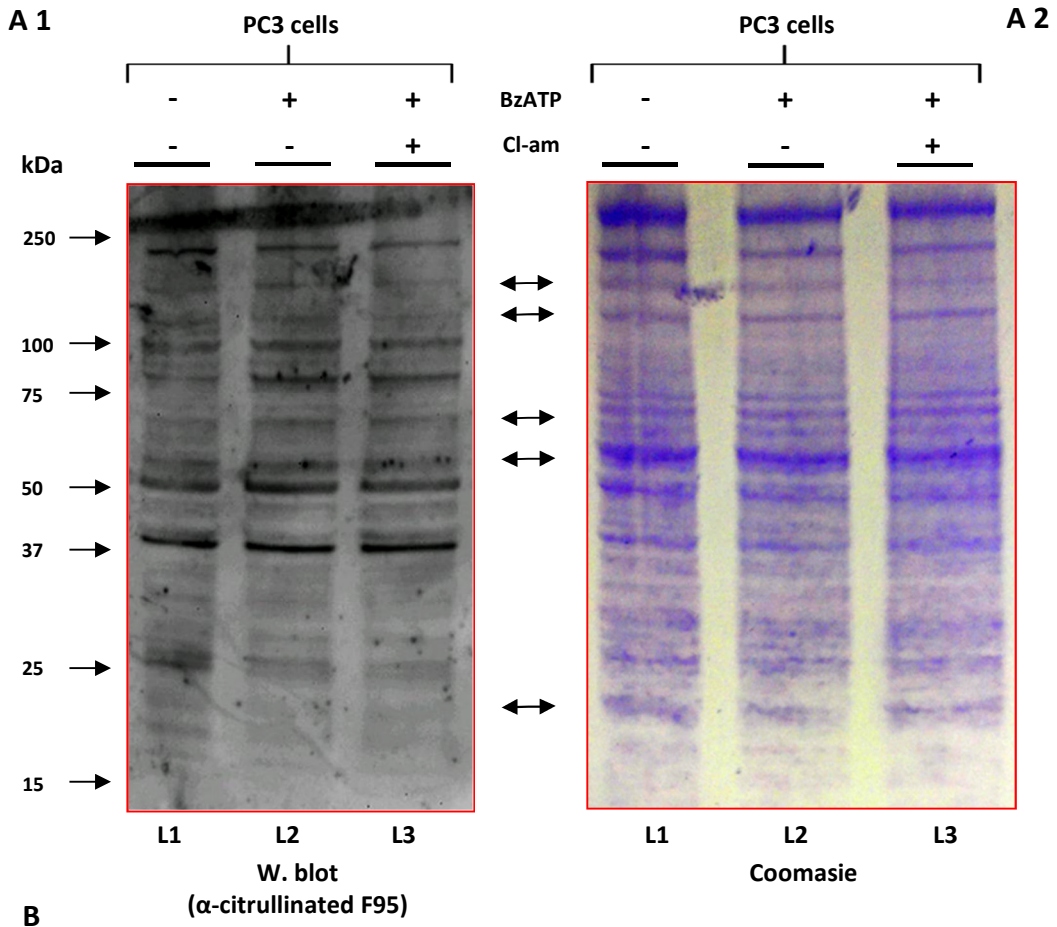
4.3.4 PAD inhibition reduces deimination levels of proteins in PC3 cells stimulated to microvesiculate with BzATP

After observing an increase in the deimination of β -actin when stimulating cells to release microvesicles we decided to establish if other proteins were deiminated together with β -actin during stimulation and if they actually played a role in microvesiculation. Briefly, lysates from healthy PC3 cells, PC3 cells stimulated with BzATP, and PC3 cells preincubated with chloramidine prior to BzATP stimulation were separated on 10% SDS-PAGE and stained with Coomassie blue or transferred on a nitrocellulose membrane, blocked for 1 hr at room temperature with 5% BSA/TBS-T and labelled with anti-citrulline F95 antibody overnight at 4°C to detect deiminated proteins. The membrane was then washed six times for 10 min with TBS-T and labelled with anti-mouse anti-IgM HRP conjugated secondary antibody for 1 hr at room temperature. The membrane was then washed as before and analysed by chemiluminescence.

The analysis showed a broad range of bands of citrullinated proteins of various sizes in all three treatments (**Fig 4.9 A1 L1, L2, L3**). Furthermore, the pattern of bands observed on the Coomassie blue stained gel were similar to the pattern of bands observed on the membrane, however there were some bands which were more prominent on the gel that were not present on the membrane and vice versa (**Fig 4.9 A1, A2, and double arrows**). This therefore indicated that although the pattern was similar not all the proteins observed on the gel were citrullinated. Further analysis on the

band intensities observed on the membrane and the gel by ImageJ software as per manufacturer's protocol revealed a very interesting result. Comparing the overall band intensities between treatments on the membrane probed with anti-citrulline F95 and therefore indicating deiminated proteins, lysates from healthy PC3 had a higher overall band intensity (39149.5) compared to the other two treatments. However the difference was not much between PC3 cells and PC3 cells stimulated with BzATP (37547.09). Interestingly a reduction in band intensity was observed from lysates of PC3 cells pretreated with chloramidine (29032.51) compared to the other treatments (**Fig 4.9 B**). This therefore indicates that either fewer proteins were citrullinated or proteins were citrullinated to a lesser extent even after stimulation due to the inhibition of the PAD enzymes by chloramidine.

The overall data therefore indicates that although a broad range of citrullinated proteins were observed in all the three treatments there was a reduction of band intensities (deiminated proteins) comparing PC3 cells stimulated to microvesiculate and those in which PAD enzymes were simultaneously inhibited. Hence further analysis would be required to identify the individual proteins that have been deiminated in each of the three treatments to understand the involvement of PAD mediated citrullination in microvesiculation.



lane no.	Treatment	Band Intensity	
		Western blot (Deiminated proteins)	Coomassie (Total proteins)
1	PC3	39149.46	90638.13
2	PC3 + BzATP	37547.09	84316.27
3	PC3 + Cl-am + BzATP	29032.51	75169.86

Fig 4.9: Immunoblot and gel of citrullinated proteins from PC3 cells stimulated for microvesiculation. (A) Lysates from healthy PC3 cells (L1), or PC3 cells pre-treated with (L3) or without (L2) 50µM Chloramidine (Cl-am) and stimulated with 300µM BzATP were either separated on SDS-PAGE (stained with Coomassie blue (A2)) and/or transferred on a nitrocellulose membrane (A1) and immunoblotted with anti-citrulline F95 antibody and analysed via chemiluminescence. Double arrows represent proteins visible in the gel that are either not citrullinated or less citrullinated. (B) Tabular representation of band intensity of total proteins (on gel) or citrullinated proteins (on membrane) from each of the treatments immunoblotted above.

4.3.5 Mass Spectrometry analysis of deiminated proteins from PC3 cells stimulated for microvesiculation

After observing multiple proteins that were deiminated during stimulation with BzATP we sought out to identify these proteins by mass spectrometry analysis. Briefly, cell lysates from PC3 cells, PC3 cells stimulated with BzATP and PC3 cells treated with the PAD inhibitor chloramidine prior to BzATP stimulation were immunoprecipitated with F95 antibody for citrullinated proteins. The eluate was then subjected to mass spectrometry analysis to identify deiminated proteins present in each of the three samples.

As mentioned earlier ProteinLynx GlobalServer version 2.4 was used to process the data obtained from the analysis. Citrullinated proteins were identified through the human proteome UniProt database. Altogether, 6 proteins were identified out of which Yeast Enolase 1 (P00924) is a protein that was not part of the sample and was added manually as part of the analysis process. Therefore a total of 5 proteins were detected to be deiminated in PC3 cells without any stimulation or PAD inhibition (**Table 4.1 A**). Out of the five proteins, 4 had a confidence score of 2 (95% - low probability of false positive) (OK column) and 1 had a confidence score of 1 (50% - high probability of false positive).

Nucleoside diphosphate kinase B is one of the protein that was identified only in PC3 healthy cells. It is involved in the synthesis of nucleoside triphosphates apart from ATP. It has been identified as a candidate tumour metastasis suppressor, has histidine protein kinase activity and is a

transcriptional activator of the regulatory *myc* gene that has been associated with cancer formation (203,204).

Putative elongation factor 1 alpha like 3 is another protein that was identified to be deiminated. This protein has been reported to promote GTP-dependant binding of aminoacyl-tRNA to the A-site of ribosomes during protein synthesis (205).

Glyceraldehyde-3-phosphate dehydrogenase (**Fig 4.10**) is a multifunctional enzyme that plays a role in glycolysis as well as nuclear functions such as transcription, DNA replication as well as apoptosis to name a few (206). It has also been implicated to play a role in the organization and assembly of the cytoskeleton (207).

Actin alpha skeletal muscle (**Fig 4.11**) is a protein that is highly conserved and plays a role in cell motility and microvesiculation as mentioned above. The fact that this protein was present at high confidence level of 95% (OK score = 2) in healthy PC3 cells (**Table 4.1 A, Fig 4.11 A**), PC3 cells stimulated with BzATP (**Table 4.1 B, Fig 4.11 B**), but at a lower OK score of 1 (50% confidence score) in cells treated with chloramidine (**Table 4.1 C, Fig 4.11 C**) therefore suggests that actin does get deiminated by the PAD enzymes with or without stimulation for microvesiculation and the deiminated protein is reduced when blocking the enzyme with chloramidine. This result matches with the result obtained above by Western blotting (Fig 4.8) whereby deimination of β -actin was reduced when inhibiting K562 cells with chloramidine prior to stimulation with BzATP for microvesiculation.

OK	Accession	Entry	Description	mW (Da)	pI (pH)
(A) PC3 cells only					
2	ENO1_YEAST	P00924	Enolase 1 OS Saccharomyces cerevisiae strain ATCC 204508 S288c GN ENO1 PE 1 SV 3	46787	6.1538
2	NDKB_HUMAN	P22392	Nucleoside diphosphate kinase B OS Homo sapiens GN NME2 PE 1 SV 1	17286	8.7568
2	EF1A3_HUMAN	Q5VTE0	Putative elongation factor 1 alpha like 3 OS Homo sapiens GN EEF1A1P5 PE 5 SV 1	50153	9.4131
2	G3P_HUMAN	P04406	Glyceraldehyde 3 phosphate dehydrogenase OS Homo sapiens GN GAPDH PE 1 SV 3	36030	8.6968
1	C170L_HUMAN	Q96L14	Cep170 like protein OS Homo sapiens GN CEP170P1 PE 5 SV 2	32628	5.3335
2	ACTS_HUMAN	P68133	Actin alpha skeletal muscle OS Homo sapiens GN ACTA1 PE 1 SV 1	42023	5.0713
(B) PC3 cells + BzATP					
2	ENO1_YEAST	P00924	Enolase 1 OS Saccharomyces cerevisiae strain ATCC 204508 S288c GN ENO1 PE 1 SV 3	46787	6.1538
2	SREK1_HUMAN	Q8WXA9	Splicing regulatory glutamine lysine rich protein 1 OS Homo sapiens GN SREK1 PE 1 SV 1	59345	10.8721
2	ACTS_HUMAN	P68133	Actin alpha skeletal muscle OS Homo sapiens GN ACTA1 PE 1 SV 1	42023	5.0713
1	G3P_HUMAN	P04406	Glyceraldehyde 3 phosphate dehydrogenase OS Homo sapiens GN GAPDH PE 1 SV 3	36030	8.6968
1	TBA1B_HUMAN	P68363	Tubulin alpha 1B chain OS Homo sapiens GN TUBA1B PE 1 SV 1	50119	4.7622
1	TNNT3_HUMAN	P45378	Troponin T fast skeletal muscle OS Homo sapiens GN TNNT3 PE 1 SV 3	31805	5.5869
(C) PC3 cells + chloramidine + BzATP					
2	ENO1_YEAST	P00924	Enolase 1 OS Saccharomyces cerevisiae strain ATCC 204508 S288c GN ENO1 PE 1 SV 3	46787	6.1538
1	ACTS_HUMAN	P68133	Actin alpha skeletal muscle OS Homo sapiens GN ACTA1 PE 1 SV 1	42023	5.0713
1	NDKA_HUMAN	P15531	Nucleoside diphosphate kinase A OS Homo sapiens GN NME1 PE 1 SV 1	17137	5.7671
1	TNNT3_HUMAN	P45378	Troponin T fast skeletal muscle OS Homo sapiens GN TNNT3 PE 1 SV 3	31805	5.5869

Table 4.1: Identities of citrullinated proteins from PC3 cell lysates stimulated for microvesiculation. Cell lysates from Healthy PC3 cells (A), PC3 cells stimulated with BzATP (B) or PC3 cells treated with chloramidine prior to BzATP stimulation (C) were immunoprecipitated for citrullinated proteins and the eluate analysed by MSe Label-free quantitation UPLC-Q/TOF mass spectrometry. The “OK” column simplifies information about data quality and confidence score (2 = 95%; 1 = 50%).

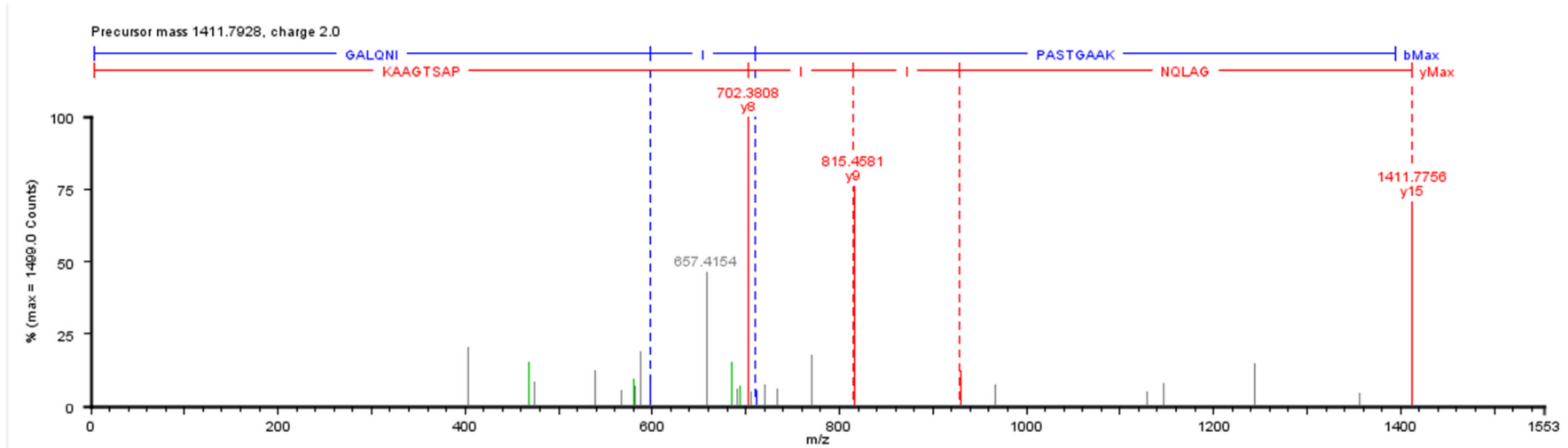


Fig 4.10: UPLC-Q/TOF Spectra shot of deiminated glyceraldehyde-3-phosphate dehydrogenase identified from the analysis of healthy PC3 cell lysates. Healthy PC3 cell lysates were immunoprecipitated with F95 antibody for citrullinated proteins. The eluate was then analysed by MSE Label-free quantitation mass spectrometry to identify proteins that were deiminated by PAD enzyme.

Splicing regulatory glutamine lysine rich protein 1 is one of the two proteins that were identified with high confidence level in PC3 cells when stimulated with BzATP. Its function is to regulate alternative splicing by modulating the activity of other splice factors during RNA splicing (205).

Although citrullinated proteins were identified in the sample of PC3 cells pre-treated with chloramidine, none of the proteins had a confidence score of 95% (OK score 2) (**Table 4.1 C**). However one interesting observation was that actin that was present in the other two samples (PC3 healthy, and PC3 + BzATP stimulation) with a high confidence score was only present with a low confidence level (**Table 4.1 C**) in this sample. The overall result therefore shows that similar proteins such as glyceraldehyde-3-phosphate dehydrogenase and actin (both of which are involved with the cell cytoskeleton) were deiminated in both PC3 cells with or without stimulation and the overall number of deiminated proteins is reduced significantly when inhibiting the cells with chloramidine therefore suggesting the involvement of PAD indirectly during cytoskeletal rearrangement, an essential process during microvesiculation.

4.3.6 The PAD and microvesiculation inhibitor chloramidine sensitizes erythroleukaemic K562 cells to cancer drug mediated cytotoxicity

One mechanism that contributes to cancer drug resistance is the ability of cancer cells to evade chemotherapeutic agents by increasing active drug efflux through microvesicle shedding (208,209). Previous work from our

laboratory (209) has shown that on inhibition of microvesiculation through other inhibitory agents, reduces the resistance of the cancer cell to for example the anticancer drug methotrexate (MTX).

As chloramidine inhibits microvesiculation in K562 cells, we sought to investigate whether treating cells with chloramidine in combination with the anticancer drug methotrexate has any effect on cell survival. Briefly, K562 cells were washed and resuspended in prewarmed RPMI 1640. The cells were treated with or without 100 μ M chloramidine (the concentration of chloramidine to have the most potent effect on reducing cell viability (210)) and incubated at 37°C, 5% CO₂, humidified conditions for 30 minutes. Post incubation the cells were washed and resuspended in prewarmed CGM supplemented with 2mM CaCl₂ and seeded in a 24-well plate. Cells were then treated with 100 μ M chloramidine or 100 μ M MTX or in combination with both the agents. Treatments without any of the chemicals served as controls. The 24-well plate was then incubated at 37°C for 24 hr and 48 hrs. Post incubation the cells were analysed for viability via flow cytometry.

Over the span of 24 hr, K562 cells treated with MTX did have a significant reduction in viability by 10% compared to untreated cells (**Fig 4.12 A**). Similar results were also observed when combining MTX with chloramidine with a significant reduction in viability of only 7% compared to untreated cells (**Fig 4.12 A**). Treating the cells with chloramidine alone had no effect whatsoever on the viability. However, on increasing the incubation period to

48 h the % viability of the cells treated with chloramidine alone dropped significantly by 34% compared to control (**Fig 4.12 B**).

Moreover, chloramidine was found to be more effective than MTX alone as the former reduced viability of cells by 23% more than the latter over a 48 h period. This effect was further enhanced by combining the PAD inhibitor with MTX whereby viability was significantly reduced to 39% compared to chloramidine (61%) and MTX (84%) alone (**Fig 4.12 B**).

The trends observed above were further reflected by analysing the apoptosis levels. Cells treated with chloramidine alone had an apoptotic population of 31%, whereas with MTX alone the population was halved to about 16.7% (**Fig 4.12 C**). However, the combination therapy proved to be most effective as the apoptosis levels were the highest at 60% compared to the control or any other treatment (**Fig 4.12 C**). This data therefore indicates that chloramidine on its own is an effective inducer of cytotoxicity compared to MTX but that a combination of both the agents had a synergistic effect, proving to be even more effective in reducing K562 cell survival.

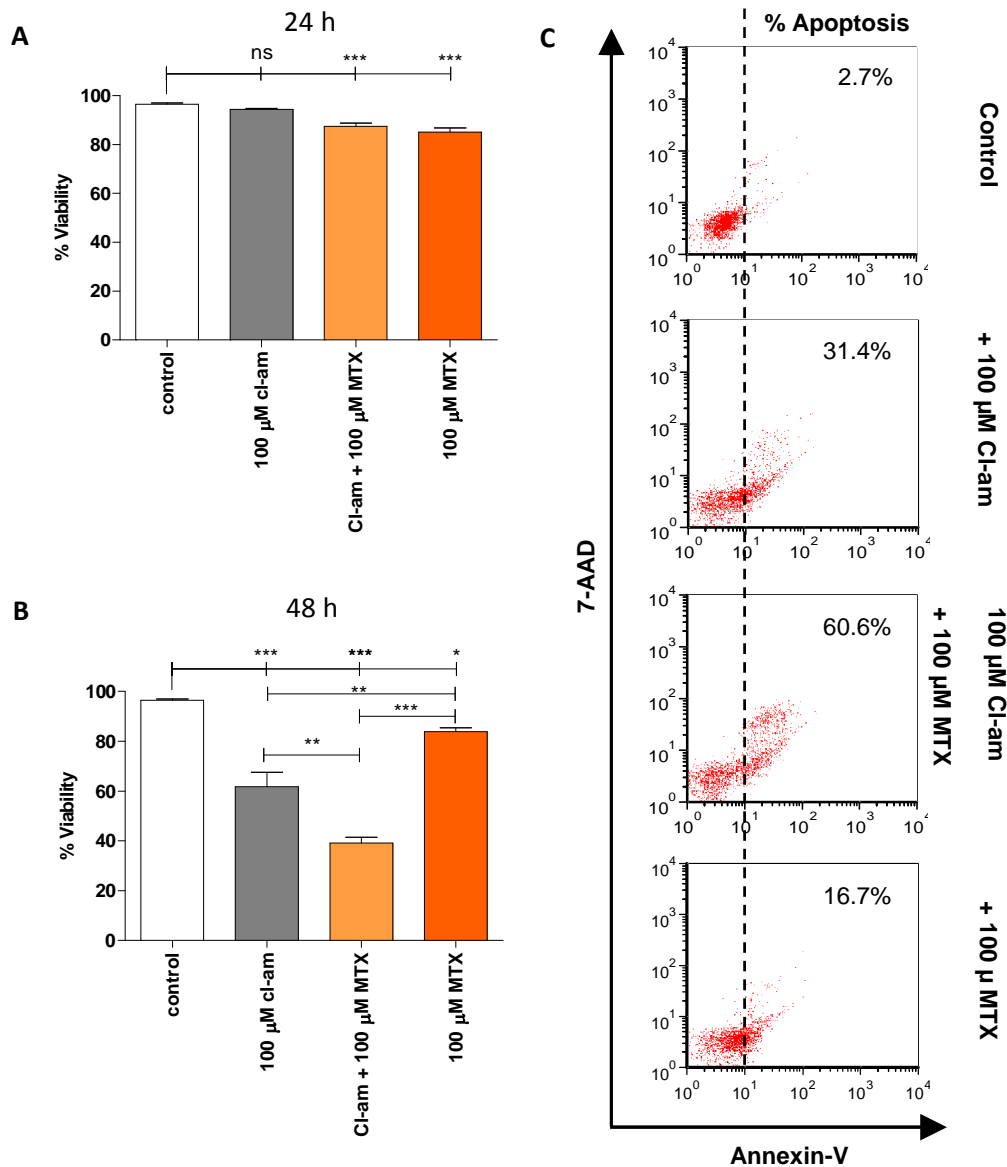


Fig 4.12: Chloramidine synergistically enhances the cytotoxic effects of methotrexate on K562 cells. Cells were pre-treated with or without chloramidine (Cl-am) for 30 min and then incubated with or without 100 μ M Methotrexate (MTX) or in combination with 100 μ M Cl-am or with 100 μ M Cl-am only for 24 h (A) or 48 h (B) and then analysed for cell viability via flow cytometry. (C) Dot plot presentation of apoptosis of K562 cells after the 48 h incubation period (from B). The data represents the mean \pm standard deviation of one of two experiments performed in triplicate. * P <0.05, ** P <0.005, *** P <0.001 was considered statistically significant.

4.3.7 The PAD and microvesiculation inhibitor chloramidine renders PC3 cells more sensitive to cancer drug mediated cytotoxicity

Given the significant cytotoxic effect of chloramidine alone and in combination with MTX on K562 cells, we sought to investigate if this effect could be replicated on the prostate cancer cell line, PC3. The same protocol was applied as mentioned before (sec 4.3.6)

As there was not much difference between the treatments over a 24 h period for K562 cells (**Fig 4.12 A**), PC3 cells were incubated over a 48 h period instead. However, the cells were observed under the microscope after 24 h and the cells looked healthy, morphologically (data not shown). However, over a 48 h period similar trends were observed as with K562 cells such that cells treated with chloramidine only were significantly less viable (54%) and more apoptotic (27.4%) compared to untreated cells (90% viability and 4.3% apoptosis) (**Fig 4.13 A, B**).

PC3 cells treated with only MTX also showed a significant reduction in viability by 8% and increase in apoptosis by 12.3% compared to control (**Fig 4.13 A, B**). Nevertheless, the effectiveness of MTX was not as significant as chloramidine. However, on combining both the agents together the effectiveness was increased further significantly. Viability was reduced to 35.4% and apoptosis increased to 50.2% (**Fig 4.13 A, B**). This data therefore indicates that although chloramidine and methotrexate reduce the cell survival ability of PC3 cells significantly on their own, a synergistic effect can be noticed on combining the agents together over a 48 hr period.

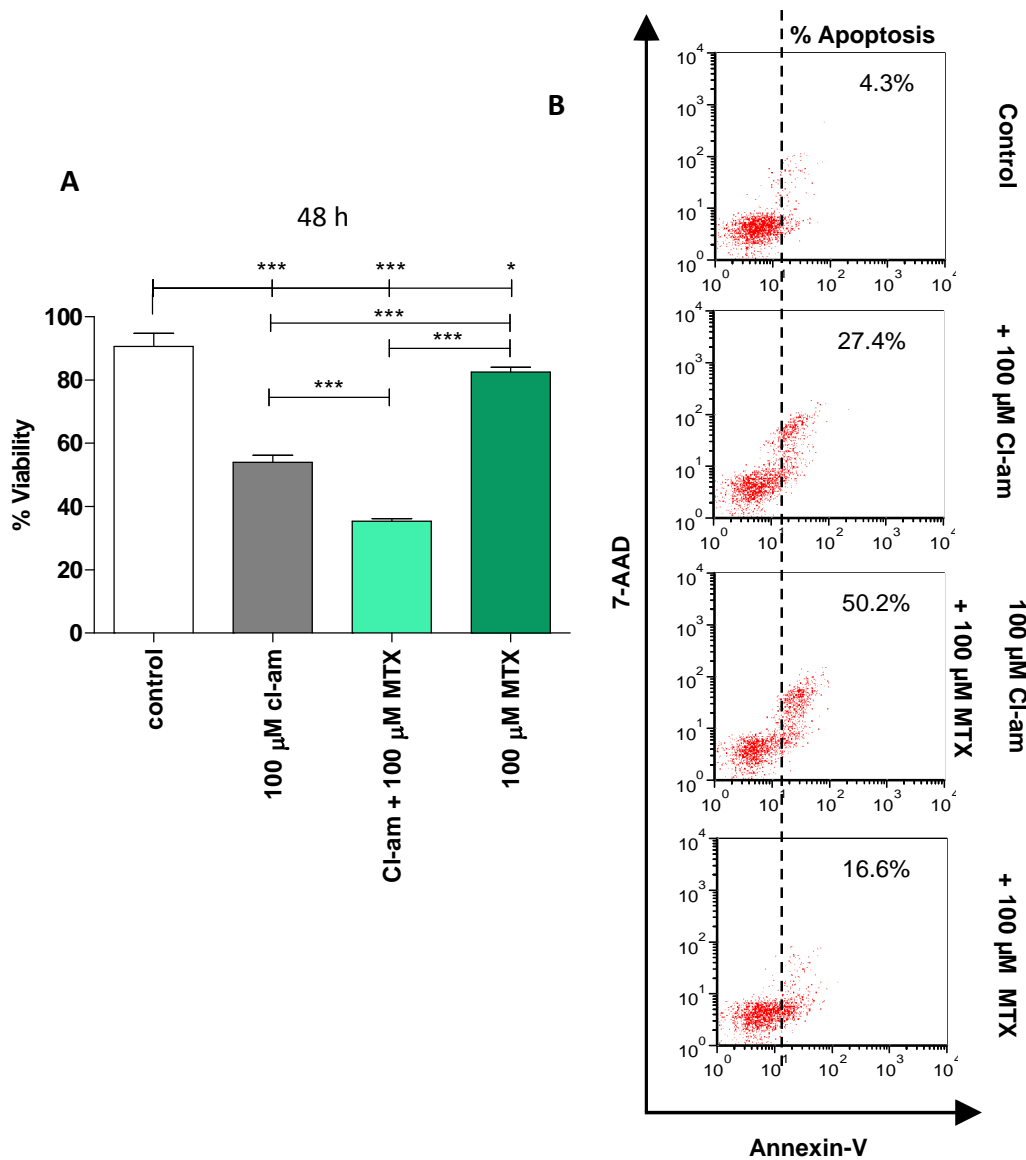


Fig 4.13: Chloramidine synergistically increases the cytotoxic effects of methotrexate on PC3 cells. (A) Cells were pre-treated with or without chloramidine (Cl-am) for 30 min and then incubated with or without 100 μ M Cl-am or 100 μ M Methotrexate (MTX) or in combination with 100 μ M Cl-am for 48 h and then analysed for cell viability via flow cytometry. (B) Dot plot presentation of apoptosis of PC3 cells after the 48 h incubation period (from A). The data represents the mean \pm standard deviation of one of two experiments performed in triplicate. * P <0.05, ** P <0.005, *** P <0.001 was considered statistically significant.

4.3.8 Summary of the role of PAD on microvesiculation and PAD inhibitors on the viability of cancer cells

PADs are posttranscriptional regulatory enzymes that have been shown to play an important role in cell physiology as well as pathology such as autoimmune diseases and cancer. The data obtained so far has shown the presence of PAD4 and PAD2 in cancerous and non-cancerous cells at a cytosolic and nuclear level. PAD4 has been shown to be elevated in both K562 and PC3 cells compared to PNT2 cells. Furthermore, stimulating K562, PC3 and PNT2 cells with NHS initiated the translocation of PAD4 and a partial translocation of PAD2 to the nucleus. Inhibiting the PAD enzymes with the pan-PAD inhibitor chloramidine abrogated the nuclear translocation of the enzymes as well as reduced the release of MVs in a dose dependent manner. Western blot analysis of deiminated β -actin levels in K562 cells stimulated with NHS showed an increase in deimination of β -actin which was reduced in cells pre-treated with chloramidine prior to stimulation. Mass spectrometry analysis further confirmed this when deiminated actin alpha-1 was identified from PC3 cells stimulated for microvesiculation and abrogated as reflected by a low confidence score from PC3 cells treated with chloramidine prior to stimulation. This data therefore suggest that PADs play a role in the biogenesis of MVs through the deimination of β -actin and actin alpha-1 (**Fig 4.14**).

As aforementioned, PAD has also been implicated in various diseases particularly cancer. Here we report that on treating both K562 and PC3 cells

with PAD inhibitor chloramidine there is a significant reduction in cell viability compared to treatment with methotrexate alone. However on combining both the drugs a synergistic effect was observed (**Fig 4.14**). This data therefore suggests chloramidine as a potential candidate as an anticancer drug that could be used in combination with other therapies.

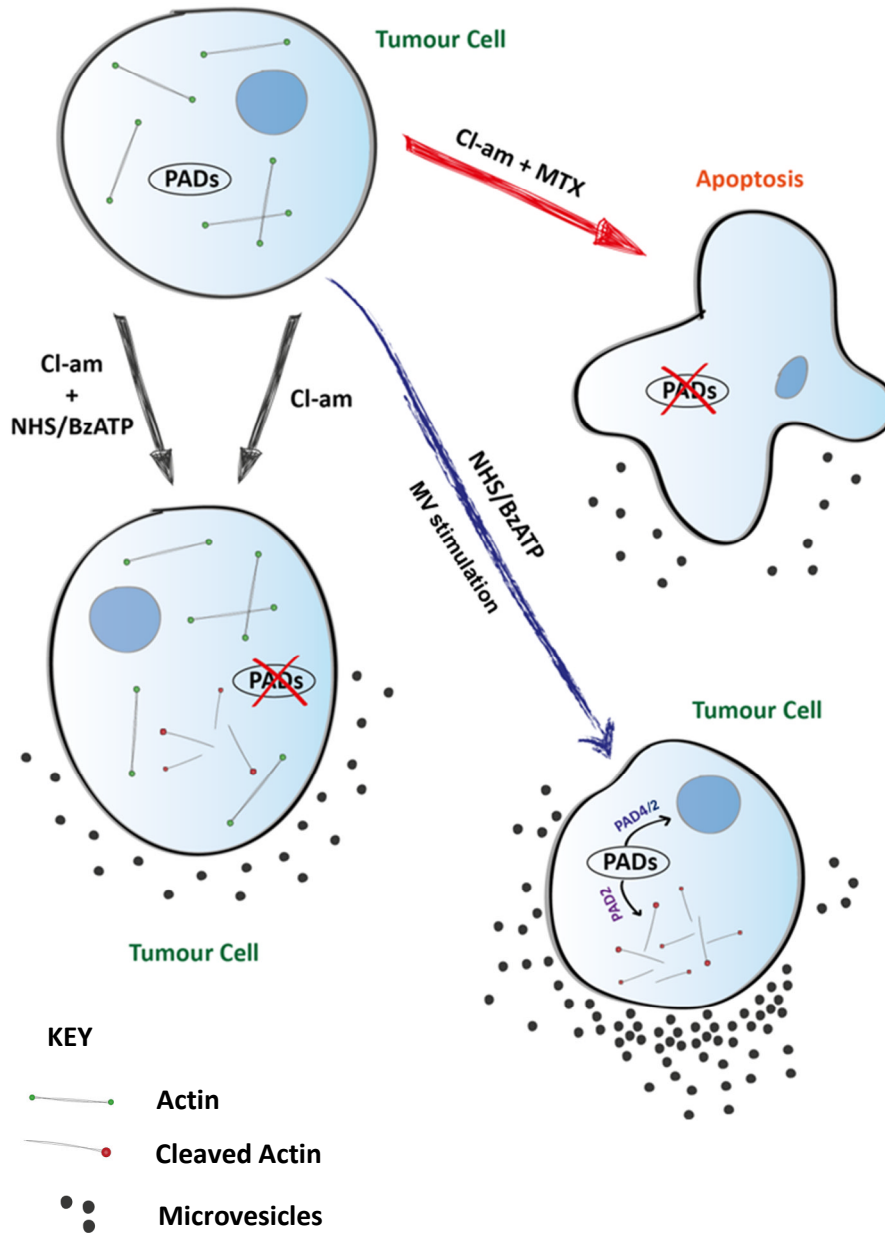


Fig 4.14: The proposed role of PAD in microvesiculation and the potential therapeutic application of PAD inhibitors in anti-cancer therapy. PAD4 and PAD2 are cytosolic enzymes which when stimulating (NHS/BzATP) the cell to microvesiculate, translocate to the nucleus (PAD4 and PAD2) or remain partially in the cytosol (PAD2) and play a role in the biogenesis of MV release either by influencing actin-cytoskeleton cleavage (PAD2) and/or by deimination of genes in the nucleus (PAD4/PAD2) that are involved in microvesiculation. The blocking of PAD isozymes with pan-PAD inhibitor chloramidine (Cl-am) abrogates the release of MVs and when combined with the anti-cancer drug methotrexate (MTX) works synergistically to induce cytotoxic effects.

5. The role of iC3b deposition on apoptotic cancer cells and their MVs in inhibiting DC maturation with the aim of developing novel immunotherapeutic strategies to inhibit tolerance of tumour cells

5.1 Introduction

Dendritic cells (DCs) are cells of the immune system that are involved in antigen processing and presentation, expression of co-stimulatory molecules and secretion of mediators to initiate T-cell mediated immune responses (123). It is due to these properties that these natural adjuvants have become an essential target in the efforts to develop a form of cancer immunotherapy (211). Various approaches have been adapted such as presenting DCs with tumour peptides or lysates, transfection with tumour genetic material as well as the use of apoptotic tumour cells and fragments (160,212-214). On the other hand, there is also evidence of tumour mediated dysfunction or apoptosis of DC cells. For instance, Chaux *et al* reported that DCs associated with tumours expressed low levels of co-stimulatory molecules (215) and Pinzon-Charry *et al* reported abnormal apoptosis of blood DCs in patients with breast cancer (147). Others have also reported the ability of tumour cells to render classical immature DCs tolerant and therefore inhibit any anti-tumour response by the immune system towards the cancer (151).

Further to this, it is a well-established fact that the uptake of apoptotic cells by DCs induces self-tolerance (216). In addition, the activation of the complement system in the apoptotic environment leads to the deposition of iC3b on the apoptotic cell surface therefore acting as an opsonin for DCs. iC3b interacts with the DC CR3 receptor (CD11b/CD18) and to a lesser extent the CR4 receptor (CD11c/CD18) thereby aiding with the

internalisation of apoptotic cells. Furthermore, this interaction between iC3b and DCs has been reported to induce tolerance (166).

Cancer therapies such as chemotherapy and radiotherapy induce apoptosis in tumour cells (217,218). Furthermore, the release of microvesicles is increased not only in cancer cells but also by cells undergoing apoptosis (219). On the basis of this information I proposed to investigate whether iC3b opsonised apoptotic tumour cells release MVs rich in iC3b, and whether these MVs have the ability to render DC cells tolerant. I also propose to investigate the effects of MVs from tumour cells on DC cell function.

5.2 Methodologies

5.2.1 Heat Induced Apoptosis assay

In order to investigate the effects of iC3b on MVs from cancer apoptotic cells, K562 and PC3 cells had to be made apoptotic. Heat-stress was chosen as an inducer of apoptosis since using chemical agents would result in the chemical agent being incorporated within the MVs which would mask any effect of iC3b on the target cell.

K562 and PC3 cells were washed twice with pre-warmed PBS, quantified and checked for viability. 5×10^5 cells were resuspended in prewarmed RPMI 1640 and transferred to individual Eppendorf tubes with a final volume of 100 μ l. The tubes were then placed in a hot plate at 60°C for 2 min and then incubated at 37°C for up to 60 min with 15 min time intervals.

Post incubation the cells were placed on ice for 1 min to stop the reaction. 100 μ l of Guava Nexin reagent was added to all the treatments and incubated for 20 min at RT on a shaker. The cells were then analysed for apoptosis by flow cytometry.

5.2.2 iC3b deposition assay

The assay was performed to investigate the deposition of iC3b on apoptotic cancer cells. To induce apoptosis K562 and PC3 cells were washed twice with PBS and resuspended in prewarmed complete growth medium. The cells were then stained with ViaCount reagent and quantified by Flow cytometry. 5×10^5 cells were then resuspended in 100 μ l of RPMI 1640 in

twelve individual Eppendorf tubes. Nine out of twelve tubes were placed in a hot plate at 60°C for 2 min and transferred to an incubator at 37°C for 45 min for K562 cells and 60 min for PC3 cells. The remaining three tubes served as control and were not placed in a hot plate.

Post incubation the cells were resuspended in 500µl of Veronal buffer and incubated at 37°C either with or without 50% NHS (or Heat Inactivated NHS for 45 min (For Western blot and microscopy analysis only). The cells were then washed twice with prewarmed PBS at 500 g for 5 min and fixed with 4% paraformaldehyde for 10 min at RT. Post fixation the cells were washed three times with cold PBS at 500 g for 5 min 4°C and labelled with mouse monoclonal human (neoantigen) anti-iC3b antibody (10µg/ml) (Quidel, USA) at 4°C for 1 hr on a shaker. Following incubation, cells were washed twice at 500 g for 5 min 4°C and labelled with FITC conjugated mouse anti-IgG antibody (1:350) for 1hr at 4°C on a shaker.

After labelling the cells were washed twice with PBS and resuspended in flow cytometry analysis buffer and the relative fluorescence determined by flow cytometry.

For some experiments cells were also treated with 50% NHS pre-treated with 80 µM CRIT-H17 peptide for 30 min at room temperature. For other experiments cells were also pre-treated with 10 µg/ml Annexin V for 30 min at 37°C before treating with 50% NHS. For both conditions, cells were fixed and labelled with primary and secondary antibody as mentioned above and analysed by flow cytometry.

5.2.3 Fluorescence microscopy analysis of iC3b deposition on cells

Healthy or apoptotic K562 cells were resuspended in 500µl of Veronal buffer and incubated at 37°C with or without 50% NHS or HI NHS for 45 min. The cells were then washed twice with prewarmed PBS at 500 g for 5 min and fixed with 4% paraformaldehyde for 10 min at room temperature. Post fixation the cells were washed three times with cold PBS at 500 g for 5 min at 4°C and labelled with mouse monoclonal anti-iC3b antibody (10µg/ml) at 4°C for 1hr with shaking. Following incubation, cells were washed twice at 500 g for 5 min 4°C and labelled with AlexaFluor 488 mouse anti-IgG (5µg/ml) for 1hr at 4°C with shaking.

Post labelling the cells were washed twice with PBS and transferred into 12-well plates containing L-polylysine coated coverslips. The plate was then centrifuged to allow the cells to adhere to the coverslips. After centrifugation the coverslips were mounted onto slides for microscopy analysis.

5.2.4 Western blot analysis of iC3b deposition on cells

After treating the cells with either HI NHS or NHS (sec 5.2.2) the cells were lysed and analysed by Western blotting (as per sections 2.2.7 - 2.2.11). Primary antibody used was mouse monoclonal antibody to human iC3b (1:500 diluted in 3% Milk/PBS-T), and secondary was goat anti-mouse HRP conjugated IgG (1:1000 diluted in 3% Milk/PBS-T).

5.2.5 Detection of iC3b on MVs from apoptotic cells

To determine the presence of iC3b on MVs from apoptotic cells, K562 apoptotic cells were treated with or without 50% NHS as per section 5.2.2. However the cells were not fixed with paraformaldehyde but labelled directly with anti-iC3b antibody followed by FITC conjugated mouse anti-IgG antibody for 1h at 4°C on a shaker as per section 5.2.2.

Post labelling, the cells were resuspended in Veronal buffer supplemented with 2mM CaCl₂ and stimulated with 300 µM BzATP for 30 min at 37°C for 45 min to induce microvesiculation. The cells were then centrifuged at 500 g for 5 min and the resulting supernatant was transferred to fresh 1.5 ml Eppendorf tubes and processed (as per section 2.2.3) for the isolation of MVs. The MVs were then analysed by flow cytometry (Guava Express plus) for the expression of iC3b.

5.2.6 Isolation of MVs with or without iC3b from cancer cells

K562 and PC3 cells were washed and checked for viability using Guava ViaCount assay. 1×10^7 cells were then resuspended in 1.8 ml of prewarmed RPMI 1640, and 300 µl of the cell suspension was transferred into fresh 1.5 ml microcentrifuge tubes (15×10^5 cells/tube) and heated in a hot plate at 60°C for 2 min (K562) or 3 min (PC3). The tubes were then incubated at 37°C for 45 min (K562 cells) and 60 min (PC3 cells) on a shaker. Post incubation, the cells were transferred into a single 15 ml centrifuge tube and washed once with prewarmed PBS at 500 g for 5 min. The cells were then resuspended in 2.5 ml Veronal buffer supplemented with 2mM CaCl₂ (or 5 ml

Veronal buffer with 2mM CaCl₂ for cells not treated with NHS) and 50% NHS and incubated at 37°C for 45 min on a shaker.

Following incubation, cells treated with 50% NHS were further diluted with Veronal buffer with CaCl₂ to reduce the concentration of NHS to 12.5%. For cells without NHS a further 5 ml of CaCl₂ supplemented Veronal buffer was added together with 10 µM calcium ionophore and 3 mM ATP, a combination that has been shown to stimulate MV release in cells. Both the treatments were then further incubated at 37°C, 5% CO₂ humidified conditions for 2 hrs on a shaker. Post incubation the cells were centrifuged at 500 g for 5 min and the resulting supernatant processed for MV isolation (as per section 2.2.3). The MVs obtained were then stored at -80°C for later use.

5.2.7 Western blot analysis of iC3b expression on MVs from apoptotic cells

MVs isolated from apoptotic K562 and PC3 cells (as per section 6.1.6) were lysed and analysed by Western blotting (as per section 2.2.7 - 2.2.11) for iC3b expression. Primary antibody used was mouse monoclonal antibody to human iC3b (1:500 diluted in 3% Milk/PBS-T), and secondary was goat anti-mouse HRP conjugated IgG (1:1000 diluted in 3% Milk/PBS-T).

5.2.8 Isolation of peripheral blood mononuclear cells from whole blood

Human blood peripheral mononuclear cells (PBMC) were purified from whole blood of healthy donors (ethical approval and informed consent obtained) by centrifugation through a Histopaque 1077 (Sigma Aldrich) gradient. Venous

blood was collected into EDTA-containing tubes and each 7 ml of blood sample was layered over a 7 ml solution of Histopaque 1077. Sample was centrifuged at 400 g for 30 min and the mononuclear cell layer (buffy coat) was removed by aspiration using a plastic Pasteur pipette into a 15 ml conical tube. The cells were then washed with 10 ml of PBS/Citrate Buffer three times by centrifugation at 200 g for 10 min. After the washes the cells were resuspended in 1 ml of complete RPMI growth medium supplemented with 10% heat inactivated FBS and quantified by flow cytometry using the Guava ViaCount assay.

5.2.9 Isolation of CD14⁺ monocytes from PBMC

CD14⁺ monocytes were isolated from PBMC using the MACS CD14 positive selection kit (Miltenyi Biotech). Briefly, PBMC with >95% viability were resuspended in 80µl of pre-cooled isolation Buffer (PBS supplemented with 0.5% BSA and 2 mM EDTA) together with 20 µl of CD14 microbeads per 1×10^7 cells. The cells were mixed well and incubated at 4°C for 15 min. For some experiments the cells were labelled with fluorochrome-labelled antibody to CD14 and incubated at 4°C for a further 5 min in the dark. Post incubation the cells were washed once with 2 ml of isolation buffer at 300 g for 10 min and resuspended in 500 µl of isolation buffer.

The monocytes labelled with the CD14 Microbeads were separated using the MS columns provided with the kit (Miltenyi Biotech). The column was first placed in the separator (Miltenyi Biotech) and primed by rinsing through 500 µl of isolation buffer. The cells were then placed in the column and allowed to

pass through into a fresh 2 ml Eppendorf tube. The column was then washed three times by passing through 500 µl of isolation buffer which was also collected together with the eluate.

After washing, the column was transferred to a 15 ml conical tube, filled with 2 ml of isolation buffer and flushed immediately with the plunger provided. The resulting cells were then analysed by flowcytometry for viability, quantity and purity. The purity of monocytes exceeded 95%, as determined by flow cytometry after staining the cells with fluorochrome-labelled antibody to CD14, and viability was greater than 97% as determined following staining with Viacount assay dye (Guava ViaCount, Guava Technologies, UK)

5.2.10 Differentiation of CD14⁺ monocytes to immature DC (iDC)

Monocytes isolated from PBMC were seeded in a 12-well plate at 1×10^6 cells/ml in CGM supplemented with 10% heat inactivated FBS, 800 IU/ml of Granulocyte-Macrophage- Colony stimulating factor (GM-CSF) and 500 IU/ml of Interleukin-4 (IL-4) (Immunotools UK). The cells were incubated for 6 days at 37°C with half of the media from each well replenished on day 3 with fresh cytokines at the same concentration. On day 6 the cells were detached and analysed by flowcytometry for iDC phenotype.

5.2.11 The effect of iC3b opsonised apoptotic cells on iDC maturation

In order to investigate the effect of apoptotic cells opsonised by iC3b on the maturation of iDCs, 1×10^5 iDCs were seeded in CGM in a 96 well plate in triplicate. Healthy K562 cells were rendered apoptotic by exposing them to a

hot plate at 60°C for 2 min followed by incubation at 37°C for 45 min. The apoptotic cells were then added to iDC cells at a ratio of 1:3 (iDC:apoptotic cells) in the presence or absence of 25% NHS. For some experiments the CR3 (CD11b/CD18) iC3b receptor on iDCs was blocked by treating with anti-CD11b for 30 min at 37°C prior to adding apoptotic cells in the presence of 25% NHS. The plate was then incubated at 37°C for 2 hr after which 1 µg/ml of lipopolysaccharide (LPS) was added for 24 hr to induce maturation. Treatment without apoptotic cells and LPS served as a negative control whereas treatment with LPS only served as a positive control.

Post incubation the cells were washed twice with PBS at 300 g for 10 min and then fixed with 2% paraformaldehyde for 5 min. The cells were then washed twice as above, labelled with DC maturation markers (FITC-CD83, and FITC-CD86 (Immunotools) at a dilution of 1:100 in 3% BSA/PBS) and incubated for 1 hr at 4°C with shaking. Post incubation the cells were washed three times with ice cold PBS at 300 g for 10 min, resuspended in 6% BSA/PBS and analysed by flow cytometry.

5.2.12 The effect of iC3b rich apoptotic cell MVs on DC maturation

In order to investigate the effect of apoptotic cell MVs carrying iC3b on the maturation of iDCs, 1×10^5 iDCs were seeded in CGM in a 96-well plate in triplicate. Apoptotic cell MVs with or without iC3b or MVs from PC3 or K562 cells were added to the wells at a ratio of 1:10 (iDC: MVs) and incubated for 24 hr at 37°C. For some experiments the CR3 (CD11b/CD18) iC3b receptor on iDCs was blocked by treating them with anti-CD11b antibody for 30 min at

37°C prior to adding the MVs. After 24 hr, 1 µg/ml of LPS was added for a further 24 hr to induce maturation. Treatment without MVs and LPS served as a negative control whereas treatment with LPS only served as a positive control.

Post incubation the cells were washed twice with PBS at 300 *g* for 10 min and then fixed with 2% paraformaldehyde for 5 min. The cells were then washed twice as above, labelled with DC maturation markers (FITC-CD83, and FITC-CD86 (Immunotools, Germany) at a dilution of 1:100 in 3% BSA/PBS) and incubated for 1 hr at 4°C with shaking. Post incubation the cells were washed three times with ice cold PBS at 300 *g* for 10 min, resuspended in 6% BSA/PBS and analysed by flow cytometry.

5.3 Results

5.3.1 Cancer cell apoptosis assay

5.3.1.1 Induction of apoptosis of K562 by heat stress

To study the effects of iC3b on apoptotic cancer cells, the erythroleukaemic K562 cell line was made apoptotic by heat stress induction. In order to achieve the optimal incubation period to achieve the maximum number of early apoptotic cells, K562 cells were incubated for different time intervals at 37°C after heat exposure.

Briefly, K562 cells were resuspended in RPMI and exposed to heat at 60°C on a hot plate for 2 min. The cells were then incubated at 37°C for up to 60 min with increasing cumulative time intervals of 15 min. Post incubation the cells were analysed for apoptosis by flow cytometry.

On comparing the control with the cell treatments exposed to heat shock, there was a significant decrease in viability by at least 32% collectively (average of all treatments) (**Fig 5.1 A**). Furthermore, a significant increase in apoptosis (collective mean apoptosis - 68%) in all the treatments was also observed compared to control (5.3% apoptosis) (**Fig 5.1 B**). This therefore confirmed that exposing K562 cells to high temperatures for a short time was inducing apoptosis. Further analysis of the overall apoptosis showed that the treatment left for 15 min had a significantly high level of apoptotic cells (80%) compared to treatments incubated for 60 and 45 min (57.6% and 63.2%) (**Fig 5.1 B**). However, on comparing the levels of early apoptosis, treatments

incubated for 45 min had significantly more cells in early apoptosis (19.25%) and less in late stage apoptosis (43.9%) compared to the 30 min time interval which had 11.5% (**Fig 5.1 C**) in early apoptosis and 68.2% in late apoptosis (**Fig 5.1 D**).

Although, cells incubated for 15 min had similar numbers of apoptotic cells in the early stage (18.9%) to the 45 min time interval, the results obtained were inconclusive due to the erratic nature of the values obtained as can be seen from the error bars (**Fig 5.1 C, D**).

Therefore, the optimal time interval for the induction of apoptosis was considered to be 45 min as the time interval was less than 60 min, and it generated fairly high numbers of apoptotic cells with the majority of the population in early apoptosis compared to late apoptosis, out of all the applied time intervals.

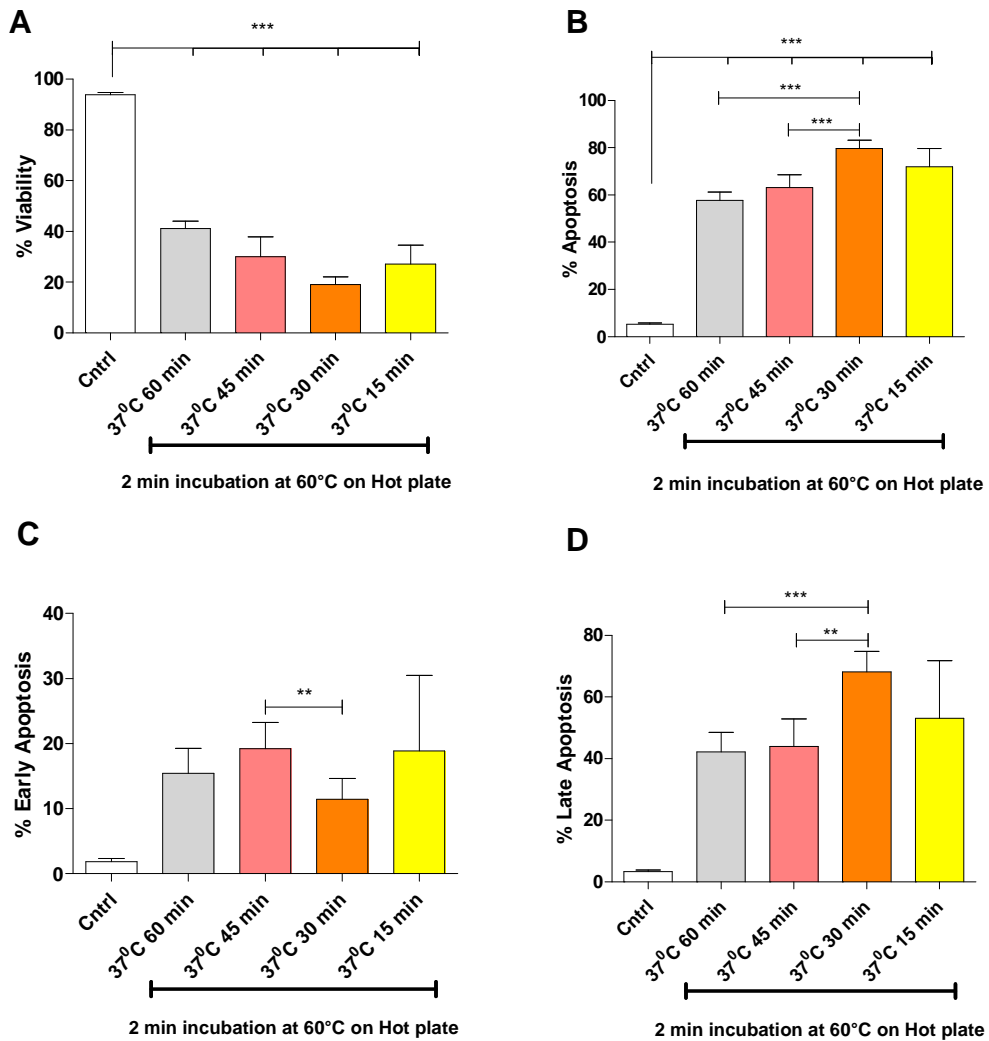


Fig 5.1: Heat stress induced apoptosis of K562 cells. K562 cells were made apoptotic by exposure to heat stress for 2 min followed by incubation at 37°C. Apoptosis was determined immediately after treatment by Guava Nexin Assay using flow cytometry. **A)** % of cells viable after heat treatment, **B)** % of cells apoptotic after heat treatment, **C)** % of cells in early apoptosis after heat treatment, **D)** % of cells in late apoptosis after heat treatment. The data represents the mean \pm standard deviation of two independent experiments performed in triplicate. * $P < 0.05$, ** $P < 0.005$, *** $P < 0.001$ was considered statistically significant.

5.3.1.2 Induction of apoptosis of PC3 cells by heat stress

After establishing the optimal incubation time and temperature to achieve a maximum number of apoptotic K562 cells, the next step was to achieve the same for the PC3 prostate cancer cell line.

Briefly, PC3 cells were resuspended in RPMI and exposed to heat at 60°C on a hot plate for 2 min. The cells were then incubated at 37°C for up to 60 min with increasing cumulative time intervals of 15 min. Post incubation the cells were analysed for apoptosis by flow cytometry.

PC3 cells exposed to heat shock had a significant reduction in viability from 96% (untreated) to 35% (mean of all heat treated treatments) (**Fig 5.2 A**) and an increase in apoptosis from 4% (untreated) to 50% (average of all the heat shock exposed treatments). Furthermore, incubating cells for 45 min and 60 min after heat shock exposure had significantly more apoptotic cells compared to incubating cells for 15 min or less (**Fig 5.2 B**). This therefore confirmed that just as for K562 cells, exposure of PC3 cells to heat shock for a short time (2 min) was also inducing apoptosis.

Further analysis of the data to understand the stage of apoptosis the cells were at after heat shock treatment revealed that, the treatment incubated for 60 min after heat shock had the significantly highest percentage of cells in early apoptosis (12.5%) compared to the rest of the treatments. Although there was no significant difference in early apoptotic levels between the 60 min treatment and the 0-15 min treatments the former had a high population of apoptotic cells overall compared to the latter (**Fig 5.2 B**). Furthermore,

incubating cells for 45 min resulted in a significantly lower percentage of cells in early apoptosis (9.2%) compared to the 60 min incubation time (12.5%), (**Fig 5.2 C**) and no significant difference between the levels of late apoptosis between the two treatments was observed (**Fig 5.2 D**). The 30 min time interval had the lowest population of early apoptotic cells (5%) (**Fig 5.2 C**) and a high amount of late apoptotic cells (47%) (**Fig 5.2 D**), therefore this incubation time was not considered to be optimal for inducing apoptosis.

Hence, the optimal time interval for the induction of apoptosis was considered to be 60 min as it generated a significantly high population of apoptotic cells overall in early stage apoptosis out of all the applied time intervals.

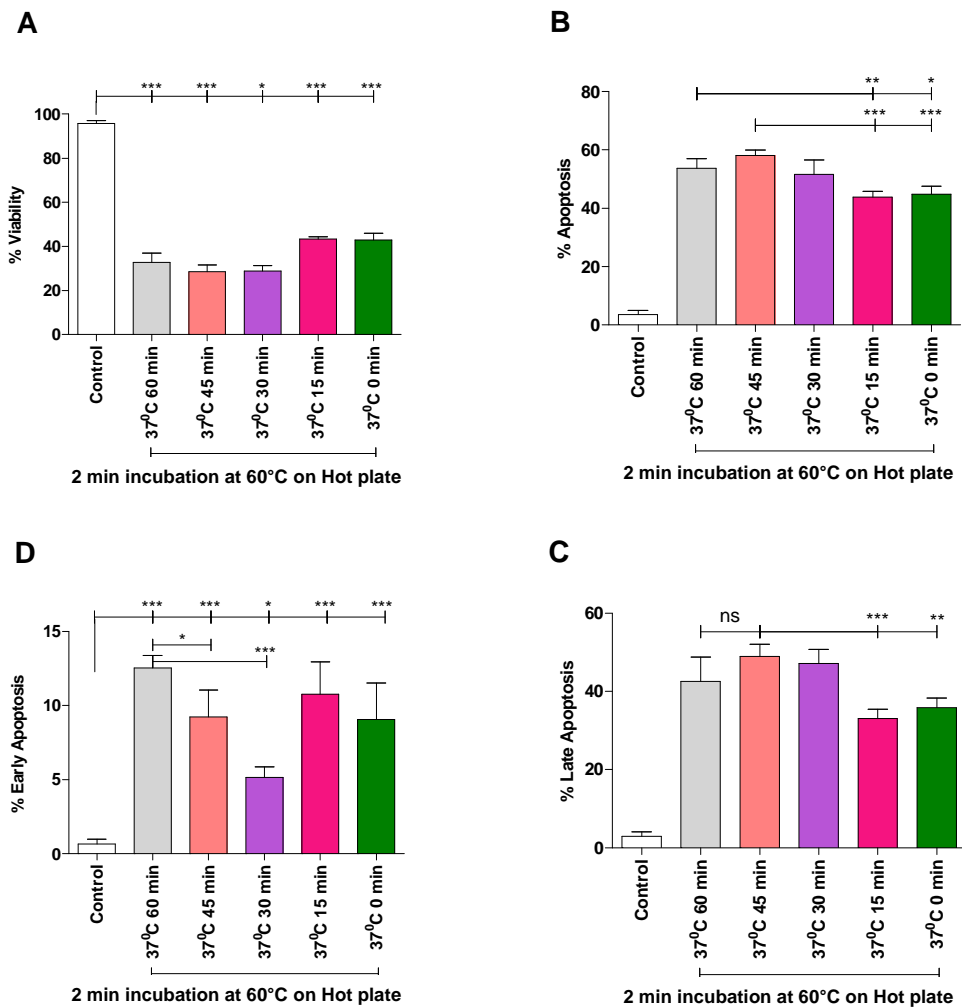


Fig 5.2: Heat stress induced apoptosis of PC3 cells. PC3 cells were made apoptotic by exposure to heat stress for 2 min followed by incubation at 37°C. Apoptosis was determined immediately after treatment by Guava Nexin Assay using flow cytometry. **A)** % of cells viable after heat treatment, **B)** % of cells apoptotic after heat treatment, **C)** % of cells in early apoptosis after heat treatment, **D)** % of cells in late apoptosis after heat treatment. The data represents the mean \pm standard deviation of two independent experiments performed in triplicate. * $P < 0.05$, ** $P < 0.005$, *** $P < 0.001$ was considered statistically significant.

5.3.2 Deposition of iC3b on cancerous apoptotic cells

5.3.2.1 iC3b is deposited on apoptotic K562 cells

Before the effect of iC3b carried by MVs could be studied it was important to first investigate the deposition of iC3b on cancerous apoptotic cells. Briefly, K562 cells were made apoptotic by exposing them to heat at 60°C in a hot plate for 2 min. The cells were then incubated at 37°C, 5% CO₂ conditions for 60 minutes. Immediately after incubation, the cells were resuspended in veronal buffer and treated with or without 50% NHS as a source of iC3b for 45 min at 37°C. Healthy cells treated with 50% NHS served as controls.

Post incubation, the cells were washed twice with PBS at 500 g for 5 min and fixed with 4% paraformaldehyde. The cells were then labelled with iC3b antibody, followed by FITC conjugated secondary antibody and subsequently analysed for expression via flow cytometry.

As described earlier, iC3b or inactivated C3b protein is a component of the complement system, present in serum whose role it is to opsonise apoptotic and foreign debris thereby rendering it visible to the immune system. Treating apoptotic cells with 50% NHS significantly increased the deposition of iC3b to 19% compared to that achieved (10%) on untreated apoptotic cells (**Fig 5.3 A, E**). Furthermore, healthy cells treated with 50% NHS only expressed 4% iC3b (**Fig 5.3 A, D**) compared to apoptotic cells therefore confirming the high affinity of iC3b towards the latter.

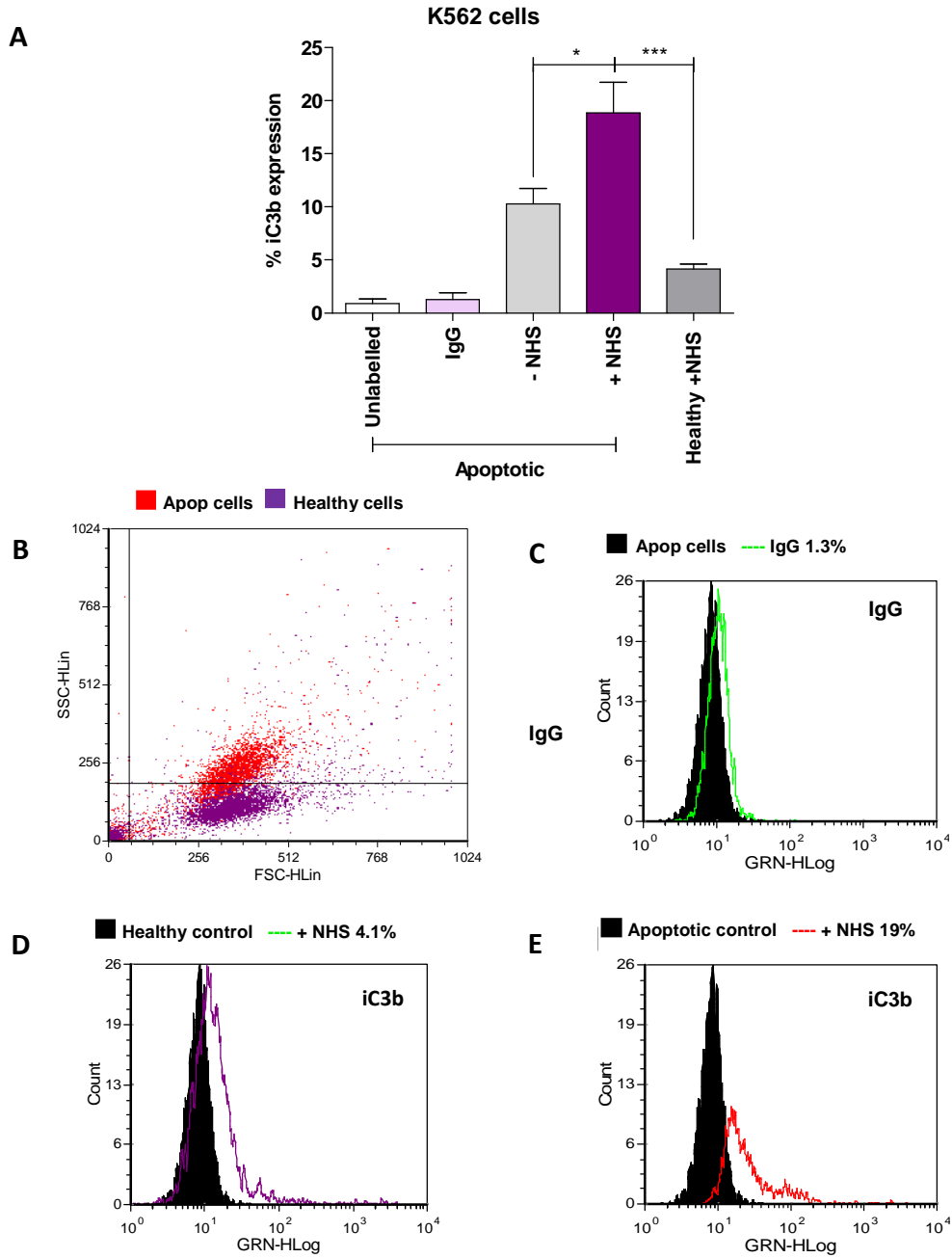


Fig 5.3: Deposition of iC3b on K562 apoptotic cells. A) Determination of membrane bound iC3b on healthy and apoptotic cells opsonised in the presence or absence of 50% NHS. iC3b expression was analysed by flow cytometry. The data represents the mean \pm SEM from two independent experiments performed in triplicate. * $P < 0.05$, ** $P < 0.005$, *** $P < 0.001$ was considered statistically significant. **(B)** Dot plot representation of the gated population of apoptotic cells (Red) positive for iC3b deposition when treated with or without 50% NHS. The population in purple represents healthy cells. **(C-E)** Histogram representing the relative fluorescence of cells labelled for iC3b deposition.

To further complement the results obtained by flow cytometry, K562 cells were treated in the same manner as described for the flow cytometry experiment. However, the secondary antibody was replaced with AlexaFluor 488 conjugated anti-mouse IgG (5µg/ml). The treatments were then washed and transferred on to L-Polylysine coated coverslips and subsequently onto slides for microscopy analysis (See sec 5.2.3).

Analysis of the images revealed a similar result to that obtained through flow cytometry. iC3b expression on apoptotic cells incubated without NHS or with heat treated NHS (HI NHS) was less compared to apoptotic cells treated with NHS, thus confirming the result obtained by flow cytometry and also verifying NHS as a source of iC3b (**Fig 5.4 A, B**). Furthermore, healthy K562 cells treated with NHS did not express iC3b on their surface (**Fig 5.4 A**) therefore validating that iC3b only binds to apoptotic cells as an opsonin. Higher magnification images of apoptotic cells treated with NHS revealed that the deposition of iC3b is in a more punctate formation rather than an even all round deposition on the surface (**Fig 5.4 B**). This data overall therefore further confirmed the specificity of iC3b to apoptotic cells as well as normal human serum as a likely source.

Western blotting also revealed a similar trend as observed with flow cytometry and microscopy. Factor I mediated cleavage of C3b to iC3b generates two α -chain fragments (α_1 – 67 kDa, and α_2 - 45 kDa) which are linked with the 75 kDa β -chain from the initial C3b chain through disulphide bonds (220) (**Fig 5.5 A**).

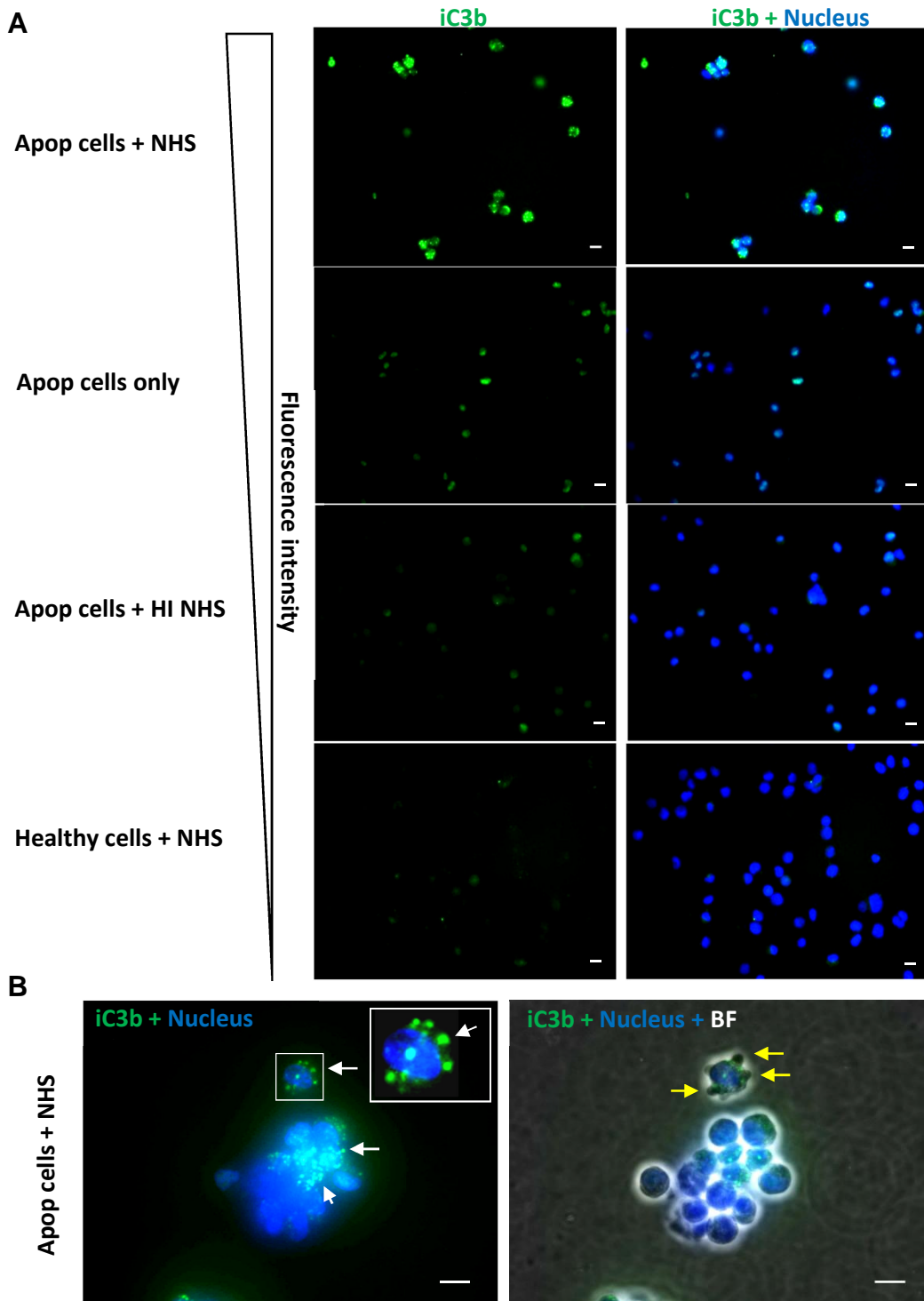


Fig 5.4: Immunofluorescence microscopy showing iC3b deposition on K562 apoptotic cells. (A) K562 healthy or apoptotic cells (Apop) were incubated in the presence or absence of 50% NHS or Heat inactivated NHS (HI NHS) at 37° for 45 min. The cells were then immunolabelled with anti-iC3b (green) and mounted onto slides for microscopy analysis. Nuclei were labelled with DAPI (blue). (B) Higher magnification (40X magnification) image of apoptotic K562 cells treated with NHS opsonised by iC3b (White arrows). Bright field (BF) image shows apoptotic blebs (Yellow arrows) on apoptotic K562 cells. Scale bar - 50µm

The presence of these three bands therefore forms the basis of identification of iC3b on a Western blot. Healthy cells treated with or without NHS did not reveal iC3b bands therefore confirming data obtained through flow cytometry. On the other hand, apoptotic cells treated with NHS revealed iC3b bands (at 75 kDa - β chain, 67 kDa - α_1 chain, and 45 kDa - α_2 chain) (**Fig 5.5 B**) thereby confirming the deposition of iC3b as shown by flow cytometry and microscopy analysis earlier. Nonetheless, bands at 75 and 67 kDa (weaker band) were also revealed by apoptotic cells exposed to HI NHS, but the band at 45 kDa was absent therefore indicating the presence of C3b rather than iC3b (220) (**Fig 5.5 A**) compared to apoptotic cells treated with NHS (**Fig 5.5 B**).

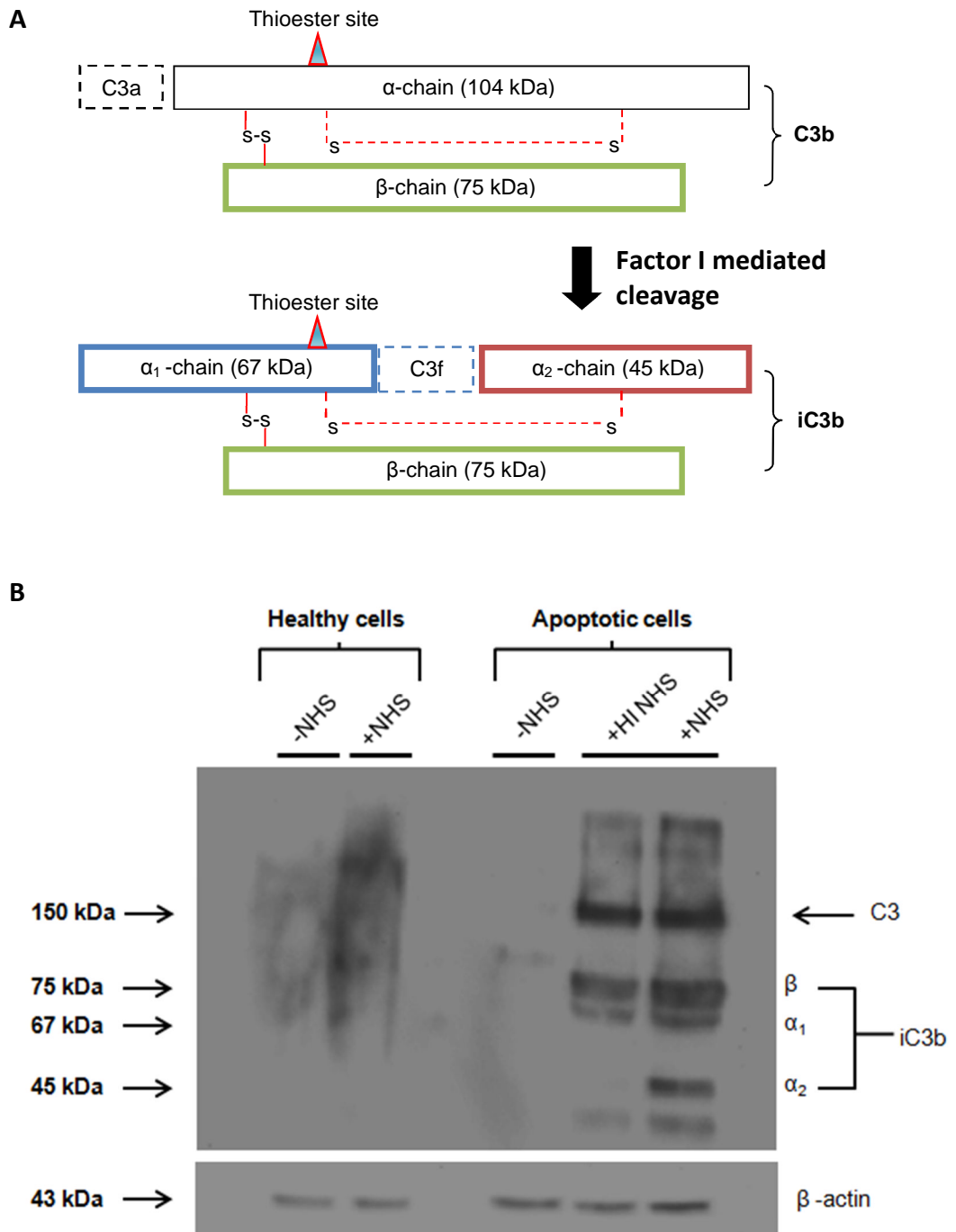


Fig 5.5: Immunoblot detection of iC3b on K562 apoptotic cells. (A) Schematic diagram representing the cleavage of C3b to iC3b. C3b interacts with regulatory protein factor H to promote inactivation by protease factor I, leading to the loss of a small fragment from the α' chain, C3f, and the formation of the inactive fragment iC3b. (B) Healthy and apoptotic K562 cells were incubated at 37°C with or without 50% NHS or HI NHS for 45 min. After washing, cells were lysed and immunoblotted with anti-iC3b antibody followed by ECL development. iC3b is represented by three bands at 75 kDa (β chain), 67 kDa (α_1 chain), and 45 kDa (α_2 chain). Lower panel shows β -actin as a representation of equal loading.

5.3.2.2 iC3b is deposited on apoptotic PC3 cells

After observing the deposition of iC3b on apoptotic K562 cells, we sought to confirm whether iC3b would be deposited on apoptotic PC3 cells. The experiment was conducted in exactly the same manner as with K562 cells (sec 5.3.2.1) and analysed by flow cytometry.

As before, treating apoptotic PC3 cells (**Fig 5.6 B**) with 50% NHS significantly increased the deposition of iC3b to 52% compared to that achieved (7%) on cells not treated with NHS (**Fig 5.6 A, E**). Moreover, healthy cells (**Fig 5.6 B**) treated with NHS expressed less than 1% of iC3b (**Fig 5.6 A, D**) on its surface compared to apoptotic cells therefore further confirming the high affinity of iC3b towards apoptotic cells.

This result was further ascertained by Western blotting whereby healthy cell lysates treated with or without NHS revealed no bands whatsoever when labelled for iC3b expression (**Fig 5.7**). Similarly, apoptotic PC3 cells that were not treated with NHS or treated with heat inactivated NHS also did not reveal any iC3b bands although a very weak band at 100 kDa (**Fig 5.7**) was observed with the HI NHS treatment corresponding to the α chain of C3b (**Fig 5.5 A**). On the other hand, PC3 apoptotic cell lysates that were treated with NHS revealed two bands at 67 kDa and 45 kDa corresponding to the iC3b α_1 and α_2 fragments (**Fig 5.5 A**) therefore validating results obtained with flow cytometry.

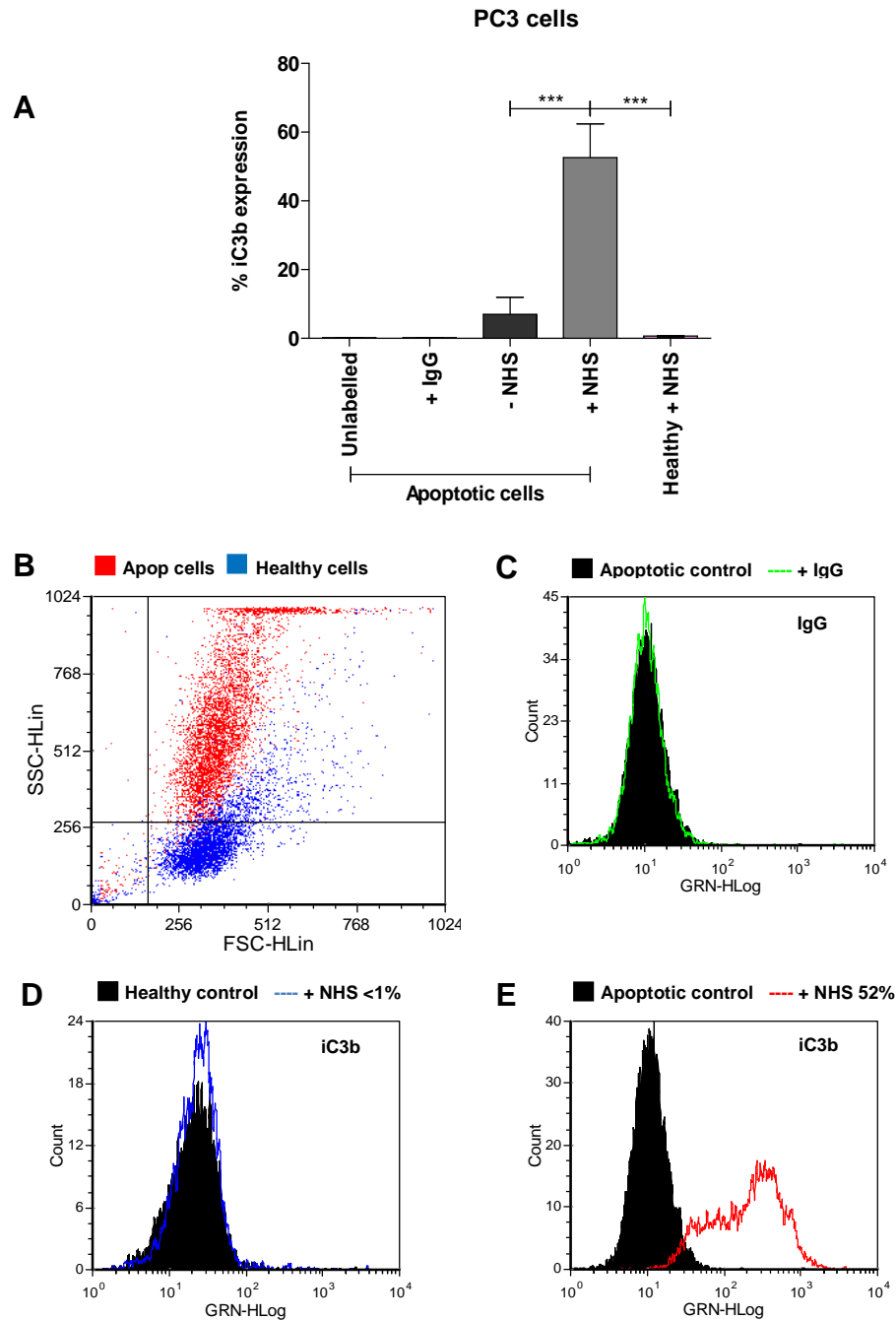


Fig 5.6: Deposition of iC3b on apoptotic PC3 cells. A) Determination of membrane bound iC3b on healthy and apoptotic cells opsonised in the presence or absence of 50% NHS. iC3b expression was verified via flow cytometry. The data represents the mean \pm SEM from two independent experiments performed in triplicate. $***P < 0.001$ was considered statistically significant. **(B)** Dot plot representation of the gated population of apoptotic cells (Red) positive for iC3b expression when treated with or without 50% NHS. The population in blue represents healthy cells. **(C-E)** Histogram representing the relative fluorescence of cells labelled for iC3b deposition.

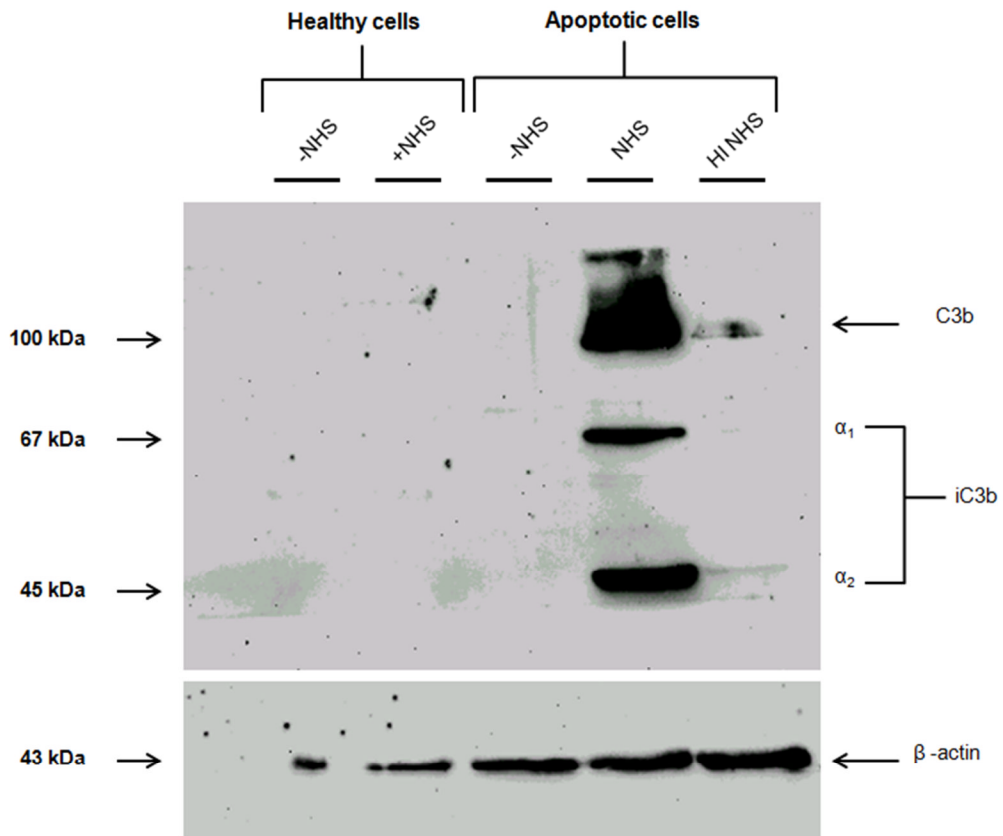


Fig 5.7: Immunoblot representing iC3b deposition on apoptotic PC3 cells. Healthy and apoptotic PC3 cells were incubated at 37°C with or without 50% NHS or HI NHS for 45 min. After washing, cells were lysed and immunoblotted with anti-iC3b antibody followed by ECL development. Lower panel shows β -actin, as a representation of equal loading.

5.3.3 The complement inhibitory peptide Complement C2 receptor trispanning (CRIT) and its role in inhibiting the deposition of iC3b on cancer cells

Complement C2 receptor trispanning (CRIT) is a three transmembrane receptor that has affinity for the human complement protein C2. CRIT-H17 is an 11 amino acid derivative from the C-terminal part of the first extracellular domain of CRIT and has been shown to regulate the complement system (221). As the CRIT-H17 peptide blocks C2 cleavage, subsequently preventing C3 convertase (essential for C3 cleavage to C3a and b) formation (221,222) and therefore inhibition of the classical pathway, and also blocks the factor I-mediated cleavage of C3b thus preventing formation of iC3b (**Fig A1 - appendix**), I sought to investigate whether the CRIT-H17 peptide would have an effect on iC3b deposition on apoptotic cells.

5.3.3.1 The complement inhibitory peptide CRIT-H17 inhibits the deposition of iC3b on K562 cells

Briefly, apoptotic K562 cells were treated with or without 50% NHS (pre-treated with or without 80 μ M CRIT-H17 for 30 min at 37°C) for 45 min at 37°C. Post incubation the cells were washed once, fixed with 4% paraformaldehyde and labelled with mouse monoclonal anti human-iC3b antibody (10 μ g/ml), followed by anti-mouse FITC conjugated IgG secondary antibody (1:350 dilution) and subsequently analysed for expression by flow cytometry.

As observed before, incubating K562 apoptotic cells (**Fig 5.8 B**) with NHS showed a significantly increased deposition of iC3b (55%) on the cell surface compared to control (**Fig 5.8 A, E**). However, on pre-treating the cells with CRIT-H17 prior to NHS stimulation significantly reduced iC3b expression to 35% (**Fig 5.8 A, D**). Although this drop in deposition was only by 20% and not a total inhibition of deposition, the result was considered to be highly significant. This data therefore indicates that CRIT-H17 plays a partial role in regulating iC3b deposition on apoptotic cells. Apoptotic cells labelled with only FITC-conjugated anti-IgG (**Fig 5.8 A, C**) only expressed iC3b at 1.6% compared to the high levels observed with NHS treatment therefore confirming the specificity of the primary antibody (anti-iC3b antibody).

5.3.3.2 CRIT-H17 inhibits the deposition of iC3b on PC3 cells

After observing the inhibitory effect of CRIT-H17 on the deposition of iC3b on K562 cells, we sought to investigate whether this effect could be replicated on PC3 cells. Apoptotic PC3 cells were treated in the same manner as K562 mentioned above (sec 5.3.3.1). Post treatment the cells were labelled for iC3b expression and analysed through flow cytometry.

The results observed were similar to those observed with K562 cells (**Fig 5.8**). PC3 apoptotic cells (**Fig 5.9 B**) treated with NHS had a significant rise in surface expression of iC3b by 41% compared to control (**Fig 5.9 A, E**). However, on treating apoptotic cells with CRIT-H17 prior to treatment with NHS, the deposition of iC3b reduced significantly to 31% (**Fig 5.9 A, D**). This inhibition of iC3b by 10% using CRIT-H17 and the results obtained from

K562 cells indicates that CRIT-H17 plays a partial role either directly or indirectly in inhibiting the deposition of iC3b on apoptotic cells.

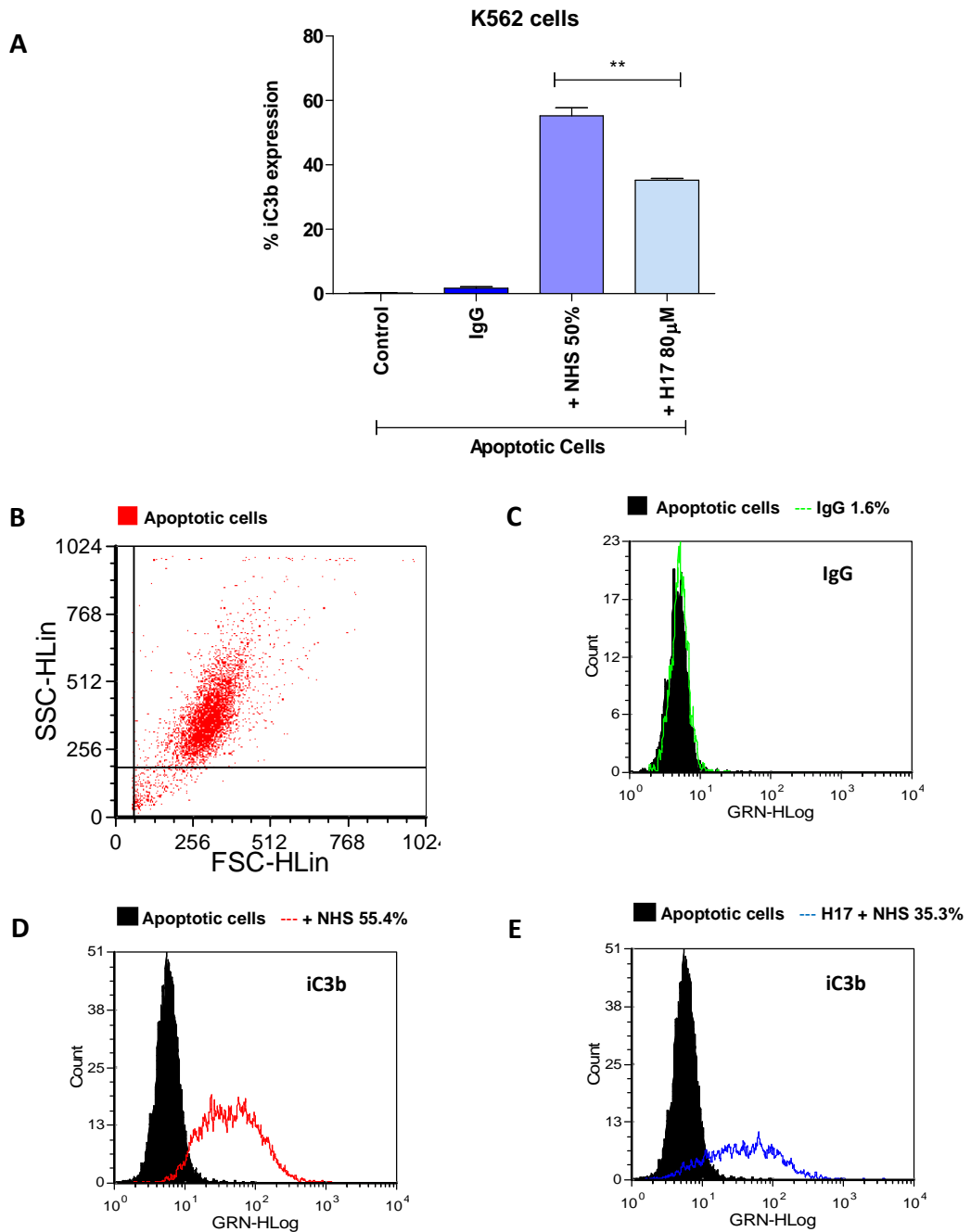


Fig 5.8: CRIT-H17 mediated inhibition of iC3b deposition on apoptotic K562 cells. A) Determination of membrane bound iC3b on apoptotic cells pre-treated with or without 80 μM CRIT-H17 (H17) in the presence or absence of 50% NHS. iC3b expression was verified by flow cytometry. The data represents the mean ± SEM from two independent experiments performed in triplicate. ****P < 0.005** was considered statistically significant. **(B)** Dot plot representation of the population of apoptotic cells (Red) to which all the results were gated. **(C-E)** Histograms representing the relative fluorescence of apoptotic cells labelled with FITC anti-mouse IgG (control) or anti human-iC3b from the experiment performed in **A**.

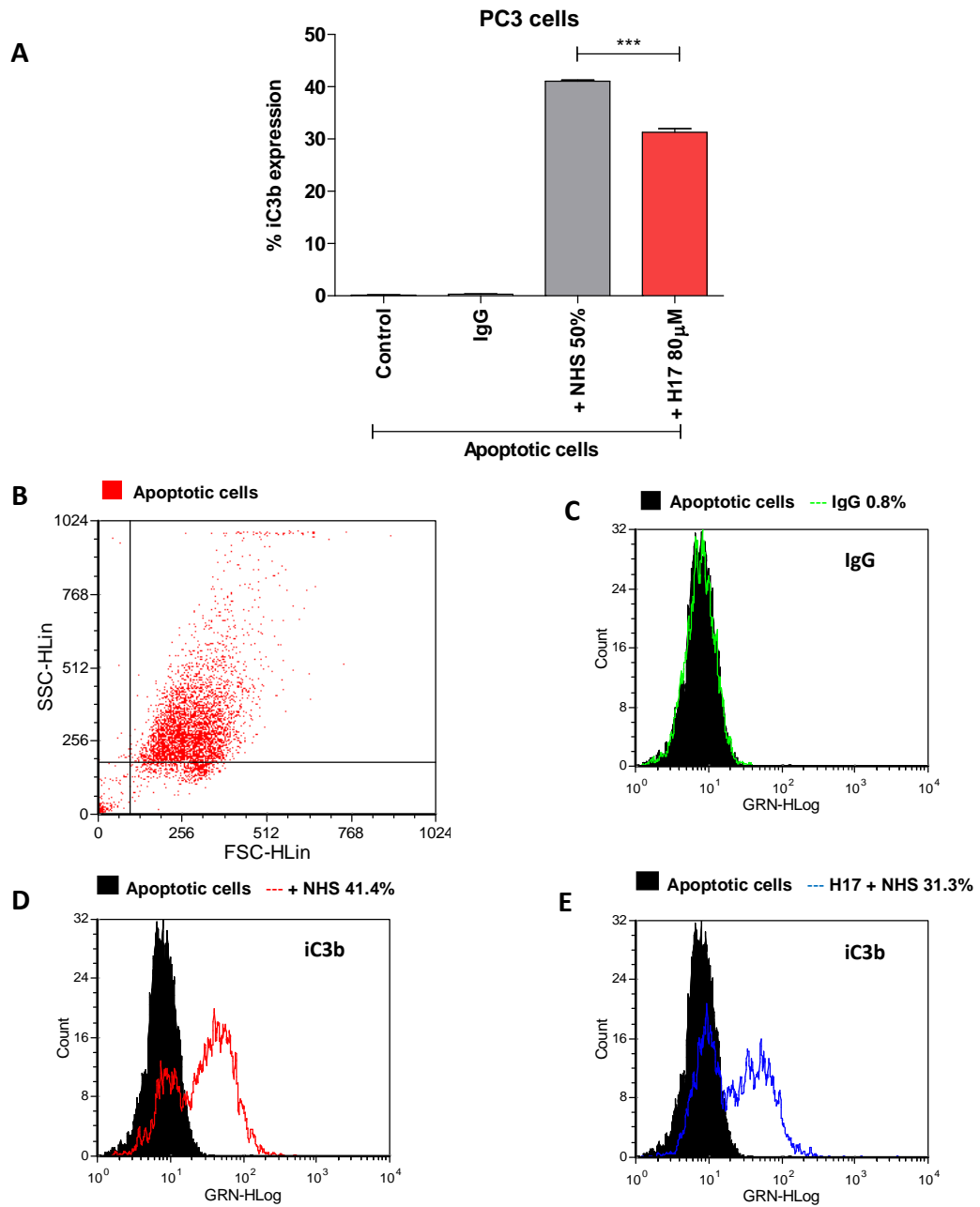


Fig 5.9: CRIT-H17 mediated inhibition of iC3b deposition on apoptotic PC3 cells. A) Determination of membrane bound iC3b on apoptotic cells pre-treated with or without 80 µM CRIT-H17 (H17) in the presence or absence of 50% NHS. iC3b expression was verified via flow cytometry. The data represents the mean ± SEM from two independent experiments performed in triplicate. *** $P < 0.001$ was considered statistically significant. **(B)** Dot plot representation of apoptotic cells (red) to which the results were gated. **(C-E)** Histograms representing the relative fluorescence of apoptotic cells labelled with FITC anti-mouse IgG (control) or anti human-iC3b from the experiment performed in **A**.

5.3.4 Blocking exposed phosphatidylserine inhibits the deposition of iC3b on apoptotic cancer cells

During apoptosis there is an imbalance between the cell membrane phospholipids, and phosphatidylserine (PS) is translocated to the outer leaflet of the cell membrane (223). PS therefore acts as a ligand for the recognition and engulfment of apoptotic cells by phagocytes and antigen presenting cells (223). As PS plays an important role in apoptosis we sought to investigate whether it was involved in the deposition of iC3b on apoptotic cells.

5.3.4.1 Blocking PS with annexin-V inhibits the deposition of iC3b on K562 cells

Briefly, apoptotic K562 cells were pre-treated with or without 10 µg/ml Annexin-V for 30 min at 37°C. Post incubation the cells were washed once and treated with or without 50% NHS for 45 min at 37°C. The cells were then fixed with 4% paraformaldehyde and labelled with mouse monoclonal anti human-iC3b antibody (10 µg/ml), followed by isotype matched FITC conjugated secondary antibody (1:350 dilutions) (some cells were only labelled with the secondary IgG antibody as a control) and subsequently analysed for expression via flow cytometry.

Incubating apoptotic K562 cells (**Fig 5.10 B**) with 50% NHS increased the deposition of iC3b by 45% compared to control (**Fig 5.10 A, E**). This increase in deposition was however significantly reduced by approximately 50% when pre-treating the cells with annexin-V (**Fig 5.10 A, D**).

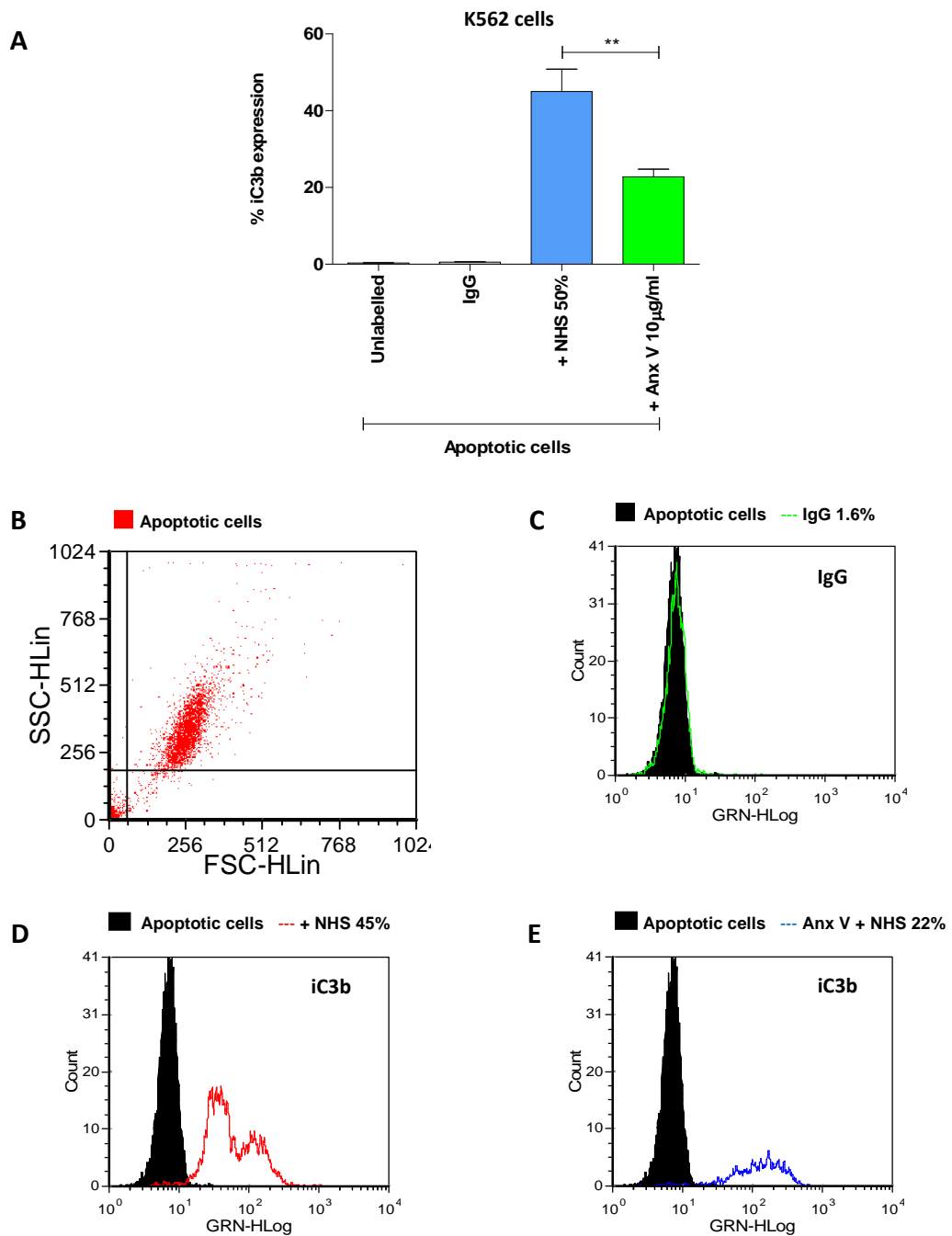


Fig 5.10: Blocking of PS inhibits the deposition of iC3b on apoptotic K562 cells. **A)** Determination of membrane bound iC3b on apoptotic cells pre-treated with or without 10 µg/ml of Annexin-V (Anx V) in the presence or absence of 50% NHS. iC3b expression was verified by flow cytometry. The data represents the mean ± SEM from two independent experiments performed in triplicate. ** $P < 0.005$ was considered statistically significant. **(B)** Dot plot representation of apoptotic cells (red) to which the results were gated. **(C-E)** Histograms representing the relative fluorescence of apoptotic cells labelled with FITC anti-mouse IgG (isotype control) or anti human-iC3b from the experiment performed in **A**.

This reduction was considered to be highly significant and therefore indicates that the exposure of PS either directly or indirectly plays a role in iC3b deposition.

5.3.4.2 Blocking PS with annexin-V inhibits the deposition of iC3b on PC3 cells

After observing a significant effect of annexin-V mediated PS inhibition on the deposition of iC3b on K562 apoptotic cells, we tried the same with the prostate cancer cell line PC3.

Analysis of the results demonstrated a similar trend as observed with K562 cells (**Fig 5.10**). PC3 apoptotic cells (**Fig 5.11 B**) when treated with NHS had a high expression of iC3b (41%) (**Fig 5.11 A, E**) on its surface which was significantly reduced by approximately 50% when pre-treating the cells with annexin-V (**Fig 5.11 A, D**). These findings therefore suggest that PS on apoptotic cells together with its role as a ligand has a partial but significant function either directly or indirectly on the deposition of iC3b on apoptotic cells from the two cell lines tested.

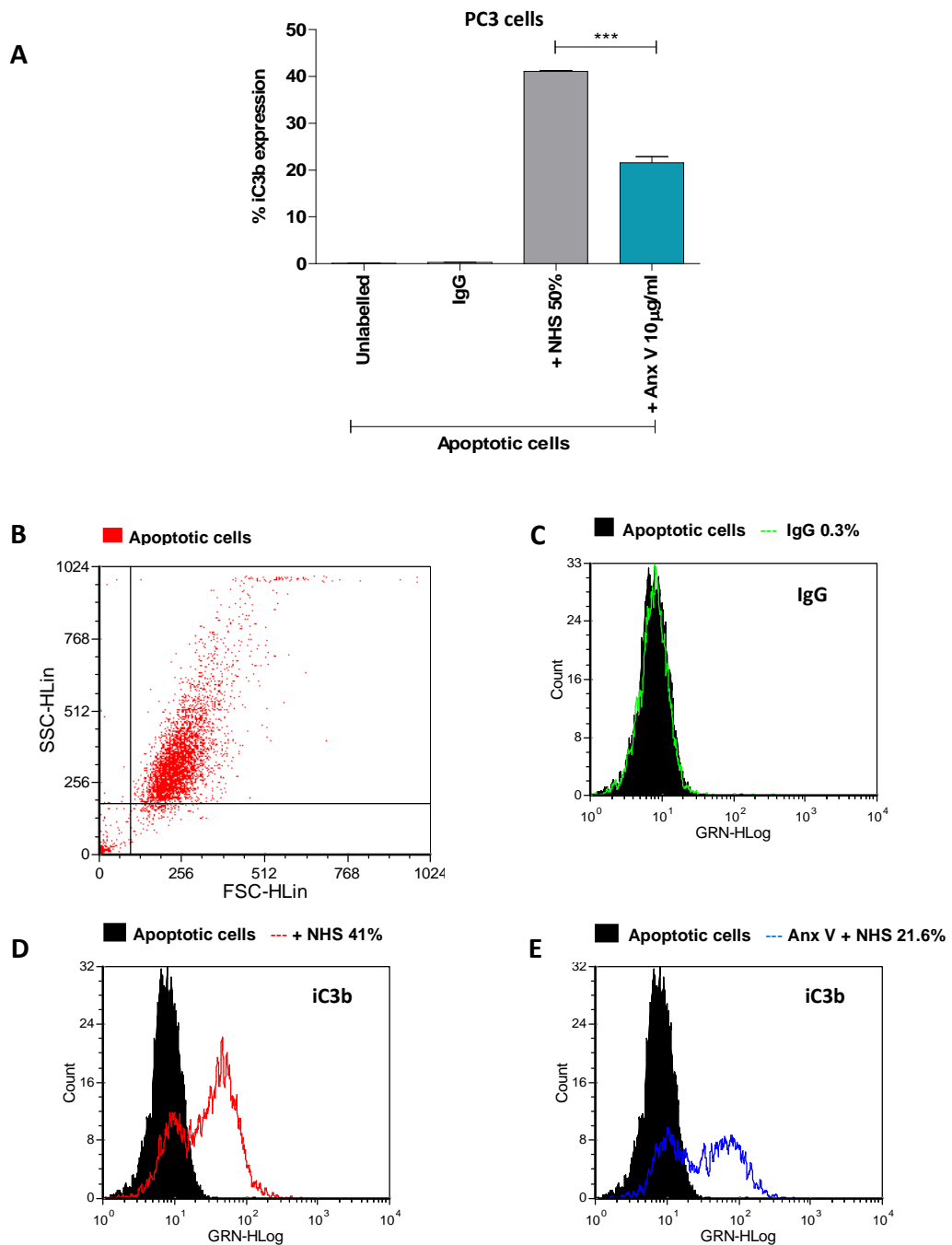


Fig 5.11: Blocking of PS inhibits the deposition of iC3b on apoptotic PC3 cells. A) Determination of membrane bound iC3b on apoptotic cells pre-treated with or without 10 µg/ml of Annexin-V (Anx V) in the presence or absence of 50% NHS. iC3b expression was verified by flow cytometry. The data represents the mean ± SEM from two independent experiments performed in triplicate. *** $P < 0.001$ was considered statistically significant. **(B)** Dot plot representation of apoptotic cells (red) to which the results were gated. **(C-E)** Histograms representing the relative fluorescence of apoptotic cells labelled with FITC anti-mouse IgG (isotype control) or anti human-iC3b from the experiment performed in **A**.

5.3.5 iC3b is also deposited on MVs released from apoptotic cancer cells

As mentioned earlier in this thesis, cancer cells tend to release more microvesicles than non-cancerous cells. Furthermore, apoptotic cells release microvesicles at a higher concentration than healthy cells. As MVs act as cellular vehicles carrying parent cell cargo we sought to investigate whether microvesicles from apoptotic cancer cells exposed to complement would express iC3b deposited on the parent cell.

5.3.5.1 iC3b is carried on MVs released from apoptotic K562 and PC3 cells

Briefly, apoptotic K562 cells were incubated with or without 50% NHS for 45 min at 37°C. Post incubation the cells were washed once and labelled with anti-human iC3b (10 µg/ml) for 1 hr at 4°C on a shaker followed by isotype matched FITC conjugated secondary antibody (1:350 dilution) for 1 hr at 4°C, also with shaking. Post incubation, the cells were resuspended in veronal buffer supplemented with 2mM CaCl₂ and microvesiculation stimulated by the addition of 300 µM BzATP for 30 min at 37°C. The cells were then centrifuged and supernatant collected for microvesicle isolation (as per section 2.2.3). The MVs collected were analysed by flow cytometry for iC3b expression.

On analysing the results it was observed that microvesicles from apoptotic cells treated with 50% NHS significantly expressed more iC3b on their surface (24%) compared to cells not treated with NHS (10%) (**Fig 5.12 A**).

This data was further validated by Western blot which showed that lysates from MVs isolated from apoptotic K562 and PC3 cells treated with NHS revealed bands at 75 kDa, 67 kDa and 45 kDa which corresponds to the β , α_1 and α_2 fragments of iC3b (**Fig 5.12 B**). A band at ~120 kDa was also observed that is likely to be C3b (**Fig 5.12 B**). No iC3b bands were observed from lysates of MVs isolated from apoptotic cells without NHS treatment. Importantly therefore this data demonstrates for the first time that iC3b that is deposited on apoptotic cancer cells can be expelled through microvesiculation.

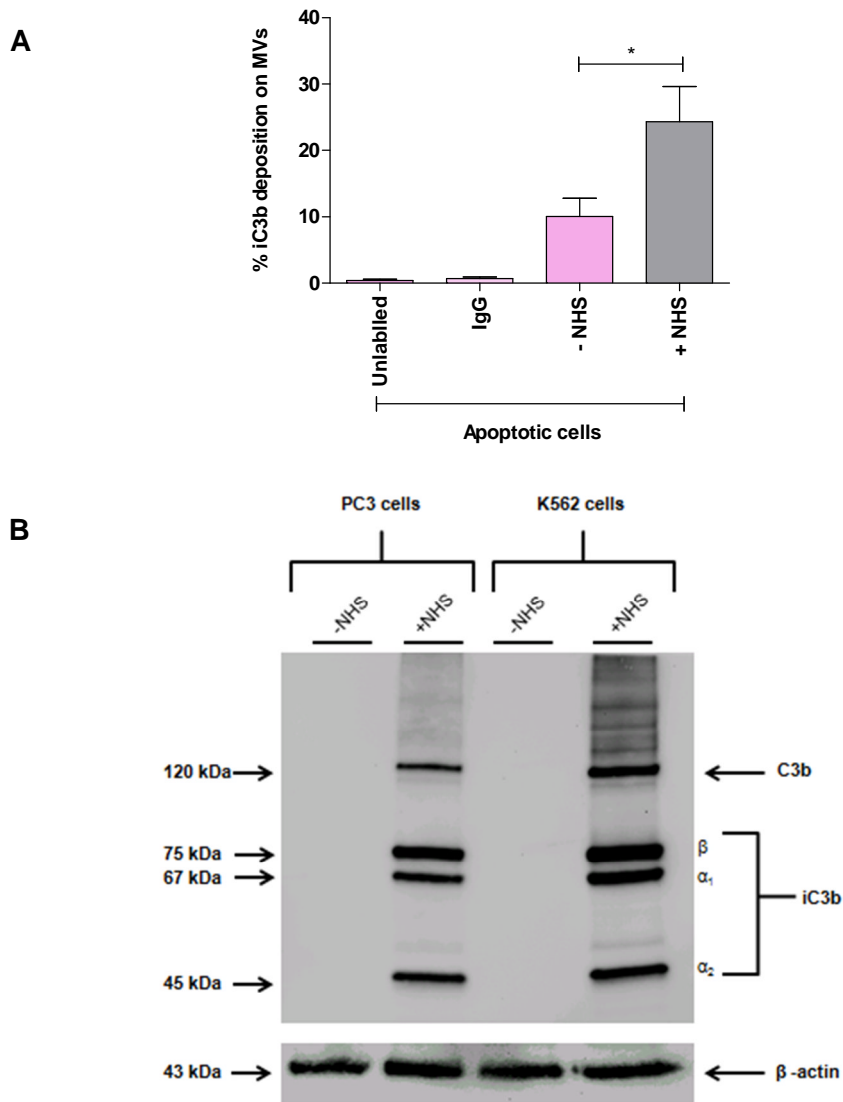


Fig 5.12 Expression of iC3b on apoptotic cancer cell MVs. (A) Apoptotic K562 cells incubated in the presence or absence of 50% NHS were labelled for iC3b expression. The cells were washed and stimulated for microvesiculation with 300 μ M BzATP for 30 min at 37°C. Post incubation the supernatant was collected and microvesicles isolated and analysed by flow cytometry for iC3b expression. MVs from cells treated with NHS had significantly more expression of iC3b on their surface compared to cells not treated with NHS. The data represents the mean \pm SEM from two independent experiments performed in triplicate. * P <0.05 was considered statistically significant. **(B)** Western blot representing the deposition of iC3b on MVs (50 μ g/ml) isolated from apoptotic K562 and PC3 cells treated with or without NHS. Bands at 67 kDa and 45 kDa correspond to the iC3b α_1 and α_2 fragments therefore confirming the presence of iC3b on MVs from apoptotic cells.

5.3.6 Isolation of CD14⁺ monocytes from healthy blood donors

In order to investigate the effects of iC3b opsonised apoptotic cells and MVs on iDCs, CD14⁺ monocytes (which are precursor cells for iDCs) were isolated from Buffy coats obtained from healthy blood donors using CD14⁺ microbeads (Miltenyi Biotech). Briefly, peripheral blood mononuclear cells (PBMC) present in the Buffy coat are washed and labelled with CD14 magnetic microbeads (Miltenyi Biotech) as per the manufacturer's protocol. The PBMCs are then washed again and passed through a MACS column (Miltenyi Biotech) placed in a magnetic field. The column is washed three times with MACS buffer and the effluent collected. The column is then flushed with MACS buffer in a separate tube to collect CD14⁺ cells that were held back due to the magnetic field. A small sample is then collected and labelled with FITC conjugated anti-CD14 antibody together with a sample from PBMCs prior to separation and the effluent left after the separation. All three samples are then analysed by flow cytometry for CD14 positivity and purity.

Analysis of the results showed that prior to separation, the PBMC population (a mixture of lymphocytes, monocytes, macrophages and dendritic cells) had only 12.6% of cells expressing CD14 (**Fig 5.13 A**). However after passing the sample through the MACS column, the percentage of cells expressing CD14⁺ that was retained in the column increased to 93.4% (**Fig 5.13 B**). Furthermore, labelling cells from the effluent for CD14 revealed only 0.32% expression (**Fig 5.13 C**) therefore confirming that the majority of the CD14⁺ population of cells was retained in the column. This therefore showed that

using the MACS bead technology for separating CD14⁺ monocytes worked effectively and that the population of monocytes obtained for differentiation into iDCs was of high purity.

5.3.7 Differentiation of CD14⁺ monocytes to iDCs

The monocytes isolated from PBMCs as described above were seeded in 12-well plates at 1×10^6 cells/ml/well and cultured in RPMI 1640 with 10% heat inactivated FBS, 800 IU/ml human GM-CSF and 500 IU/ml human IL-4 (Immunotools, Germany) for 6 days. On day 6 the cells were washed and fixed with 2% paraformaldehyde. Post fixation the cells were labelled with iDC markers (HLA-DR, CD14, CD83 and CD86 (Immunotools, Germany)) and analysed by flow cytometry.

When monocytes differentiate to immature dendritic cells, the CD14 marker is lost and other markers such as HLA-DR, and CD86 are expressed which are absent on monocytes. Flow cytometry analysis of the cells on day 6 revealed that the cells had significantly reduced CD14 expression to 1.1% (**Fig 5.14 A**) and were positive for other DC markers such as HLA-DR (24.3%) and CD86 (11.6%) (**Fig 5.14 A**). However, CD83 expression was very low (3.3%) (**Fig 5.14 A**) therefore confirming that the monocytes had differentiated to iDC and not mature DC as CD83 is only expressed in DCs in their mature state.

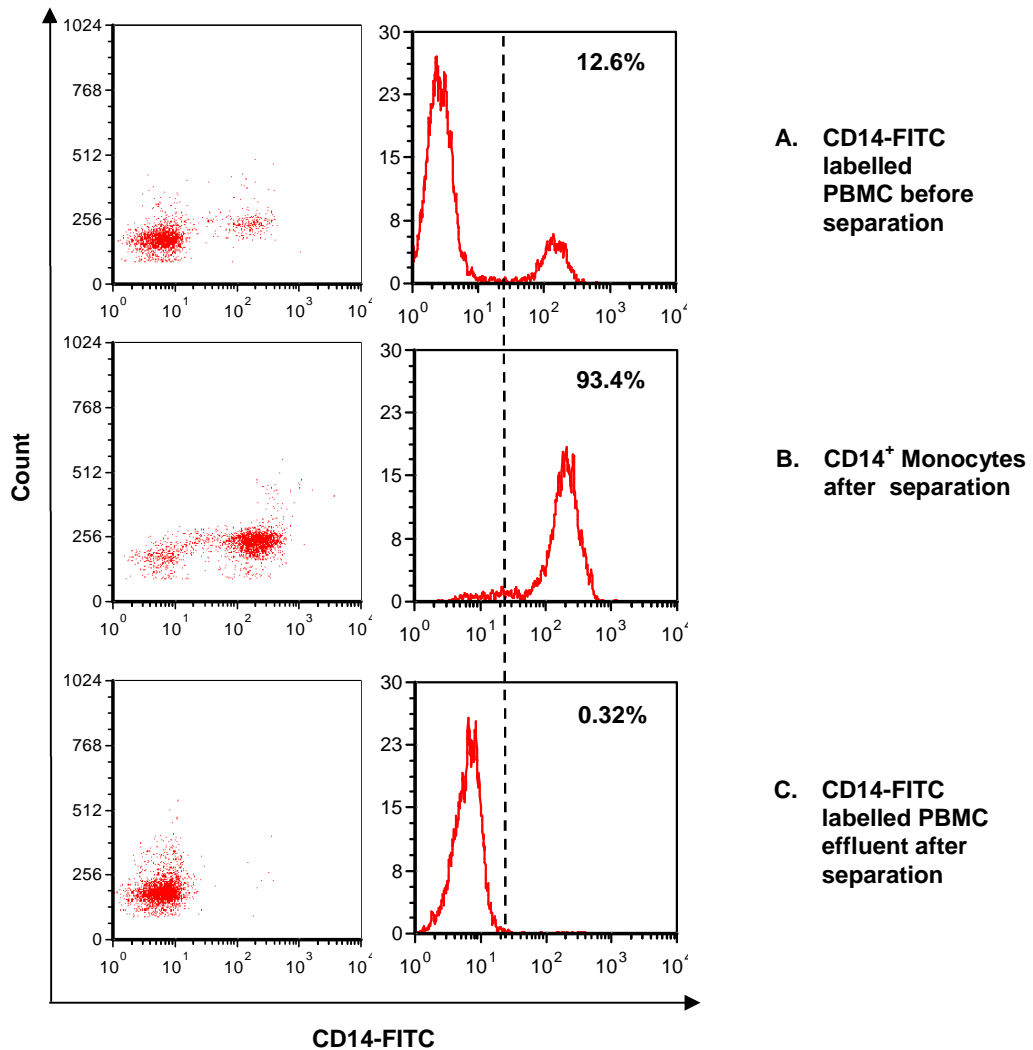


Fig 5.13: CD14⁺ Monocytes isolated from Healthy blood donors. Peripheral blood mononuclear cells (PBMC) were isolated from buffy coats from healthy blood donors. The PBMCs were then incubated with CD14⁺ magnetic microbeads and FITC-CD14 antibody **(A)** and then separated using MACS column and magnet. CD14⁺ monocytes **(B)** would stick to the column due to the magnetic beads while the CD14⁻ cells are passed through in the effluent **(C)**. The three populations of cells were then analysed by flow cytometry for CD14 positivity. The data represented is from one of three independent experiments.

Microscopy analysis further confirmed the differentiation of monocytes to iDCs as the cells were much larger than monocytes and had developed spear like process on the cell membrane (Yellow arrows - **Fig 5.14 B**) which are characteristic for immature dendritic cells. This data therefore suggests that CD14⁺ monocytes had successfully differentiated to iDCs in the presence of GM-CSF and IL-4 after 6 days of culture.

5.3.8 iC3b opsonised apoptotic cells inhibit iDC maturation

In order to investigate the effect of iC3b opsonised apoptotic cells on the maturation of DC cells, immature DC cells (1×10^5 cells/well) were seeded in a 96 well plate and either treated with K562 apoptotic cells (ratio of 1 DC:3 apoptotic cells) in the presence or absence of NHS (source of iC3b) or pre-treated with anti CD11b (iC3b receptor CR3 inhibitor on DC cells) for 30 min followed by apoptotic cells in the presence of NHS for 2 hr at 37°C. After 2 hr, 1 µg/ml LPS was added to all the treatments and incubated for 24 hr at 37°C to induce maturation of DC cells. iDCs without any treatment served as control. Post incubation the supernatant was collected for IL-10 analysis and the cells fixed, labelled with DC maturation markers (CD86 and CD83) and analysed by flow cytometry.

When DCs mature in the presence of LPS there is an increase in the expression of maturation markers such as CD86 and CD83. Flow cytometry analysis revealed that on treating iDC with LPS for 24 hr, the expression of CD86 increased significantly from 44% (iDC without LPS) to 63% and CD83 was increased from 21% (iDC without LPS) to 39% (**Fig 5.15 A**).

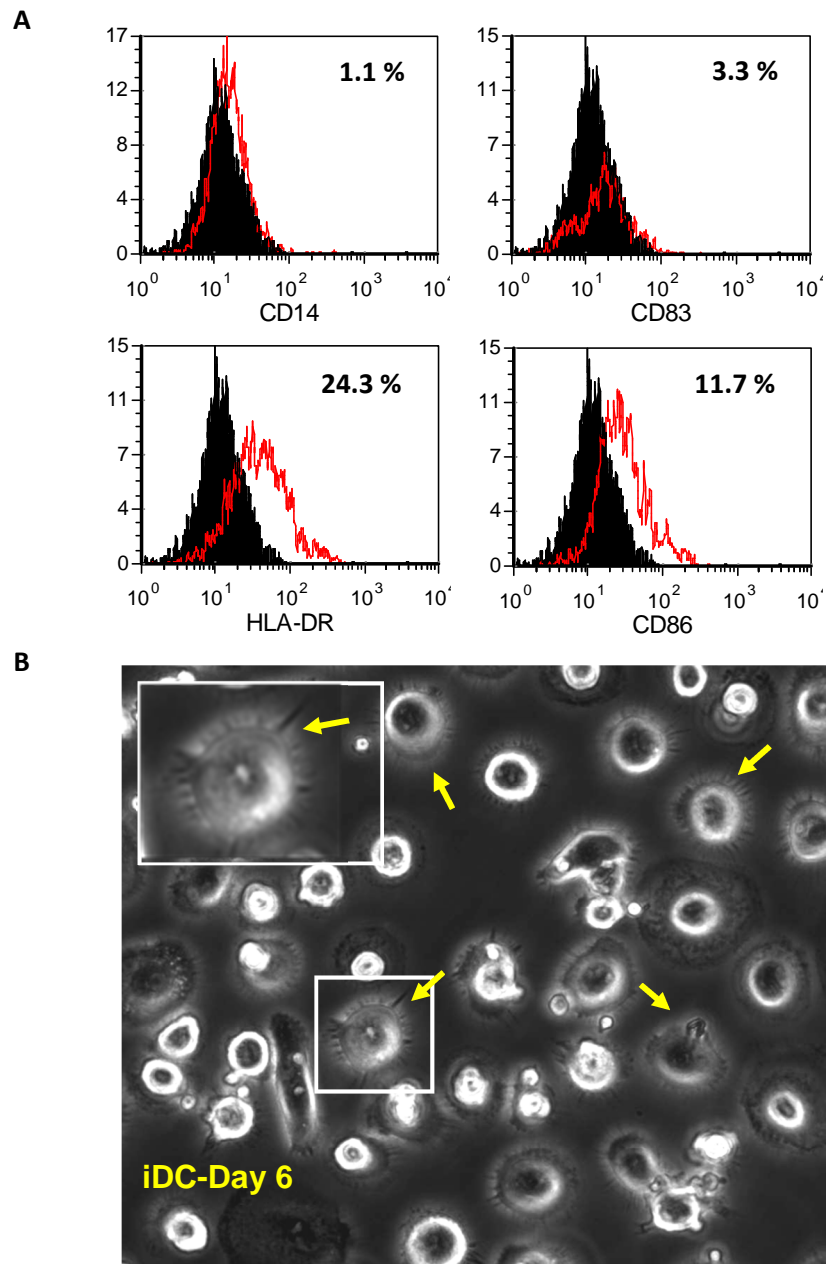


Fig 5.14: Differentiation of CD14⁺ monocytes to immature DC cells. CD14⁺ monocytes were cultured in CGM supplemented with 10% heat inactivated FBS, 800 IU/ml human GM-CSF and 500 IU/ml human IL-4 for 6 days at 37°C. On day 6 the cells were fixed with 2% paraformaldehyde, labelled with FITC conjugated CD14, HLA-DR, CD83, and CD86 and analysed by flow cytometry (**A**). The data represents one of two independent experiments performed in triplicate. (**B**) Microscopy analysis of iDC cell morphology. The yellow arrows represent iDC cells with spear like processes extending from the cell membrane.

Furthermore, treating iDCs with apoptotic cells in the absence of NHS also resulted in a significant increase in CD86 (71.2%) and CD83 (76.5%) expression therefore confirming a mature phenotype (**Fig 5.15 A**). However on treating iDC with apoptotic cells in the presence of NHS, there was a significant reduction in the expression of CD86 (23.1%) and CD83 (60.5%) compared to pulsing iDC with apoptotic cells in the absence of NHS. This therefore suggests the presence of a component in NHS that was preventing the maturation of iDCs. To further investigate this effect, iDCs were preincubated with anti-CD11b (which blocks the CR3 receptor on DC cells that binds to iC3b) for 30 min prior to treating with apoptotic cells in the presence of NHS. The results showed a reversal of the inhibitory effect. There was a significant increase in the expression of CD86 (42.3%) and CD83 (88.2%) compared to iDC treated with apoptotic cells in the presence of NHS (**Fig 5.15 A**). The peptide CRIT-H17 which can reduce the level of iC3b available for deposition on apoptotic erythroleukaemia cells (K562) and prostate cancer cells (sec 5.3.3.1 and 5.3.3.2, respectively) (**Fig A1 - Appendix**) was able to abrogate the block on iDC maturation imposed by iC3b-opsonised apoptotic cells for both the maturation markers (CD83 – 76% and CD86 – 38% compared to iDCs without CRIT-H17 - 60.6% for CD83 and 21% for CD86) significantly (**Fig 5.15 B**). This data therefore suggests that apoptotic cells when opsonised with iC3b have an inhibitory effect on the maturation of immature DCs which is reversed to a certain level by inhibiting the interaction between opsonised iC3b and CR3 through blocking the iC3b receptor (CR3) on DC cells.

5.3.9 iC3b-rich apoptotic MVs inhibit the maturation of iDCs

After observing the inhibitory effect of iC3b opsonised apoptotic cells on DC maturation, we sought out to investigate whether iC3b rich MVs from these apoptotic cells would have a similar effect on DC maturation.

Briefly, immature DC cells were seeded (1×10^5 cells/well) in a 96 well plate and either treated with K562 apoptotic cell MVs (ratio of 1 DC:10 MVs) with or without iC3b or pre-treated with anti-CD11b for 30 min followed by iC3b rich K562 apoptotic cell MVs for 24 hr at 37°C. After incubation, 1 µg/ml LPS was added to all the treatments and incubated for a further 24 hr at 37°C. iDCs without any treatment served as control. Post incubation the supernatant was collected for IL-10 analysis and the cells fixed, labelled with DC maturation markers (CD86 and CD83) and analysed by flow cytometry.

The results obtained from the analysis were unexpected. Treatment of iDCs with LPS for 24 hrs increased the expression of CD86 significantly from 35.7% (iDCs without LPS) to 67.6% and CD83 was increased from 16.1% to 35.4% (**Fig 5.15 C**). Furthermore, treating iDCs with apoptotic MVs without iC3b prior to maturation with LPS also increased the expression of CD86 (58.5%) and CD83 (37.3%) compared to iDCs without MVs (**Fig 5.15 C**). Treating iDCs with iC3b-rich apoptotic MVs increased CD86 expression to 75% and CD83 expression to 51.8% compared to iDCs without any treatment (67.6% for CD86 and 35.4% for CD83). Furthermore, there was no significant difference in expression levels of CD86 between iDCs treated with LPS in the presence or absence of apoptotic cell MVs without iC3b (**Fig 5.15**

C). Nonetheless, an interesting observation was the expression of CD83. iDCs treated with iC3b-rich apoptotic cell MVs had CD83 expression levels (51.8%) significantly higher compared to iDCs treated with apoptotic cell MVs without iC3b (37.3%), however on blocking the iC3b receptor on iDC cells with anti-CD11b prior to iC3b rich MV treatment, further increased the expression of CD83 to 64.5% (**Fig 5.15 C**). There was no significant effect on CD86 expression levels in the presence of anti-CD11b. This data therefore suggests that MVs rich in iC3b have no effect on the maturation of iDCs in the presence of LPS in this model.

As mentioned above after treating iDCs with both apoptotic cells and apoptotic cell MVs the supernatant was collected and analysed for IL-10 by ELISA (enzyme-linked immunosorbent assay) (eBioscience, USA) as per manufacturer's protocol. IL-10 is an anti-inflammatory cytokine released by immunoregulatory DC cells (224).

Analysis of the results showed no significant difference in IL-10 production by iDCs treated with or without apoptotic cells with or without iC3b or anti-CD11b (**Fig 5.16 A**). However a marked increase in IL-10 production was observed in iDCs treated with MVs compared to iDCs treated with apoptotic cells (**Fig 5.16 A**). Furthermore, IL-10 production was increased significantly from 27.4 pg/ml (iDC with apop MVs) to 63.9 pg/ml when treating iDCs with iC3b rich MVs from apoptotic cells (**Fig 5.16 A**). This increase in IL-10 production was significantly reduced to 26 pg/ml when pre-incubating the cells with anti-CD11b (**Fig 5.16 A**).

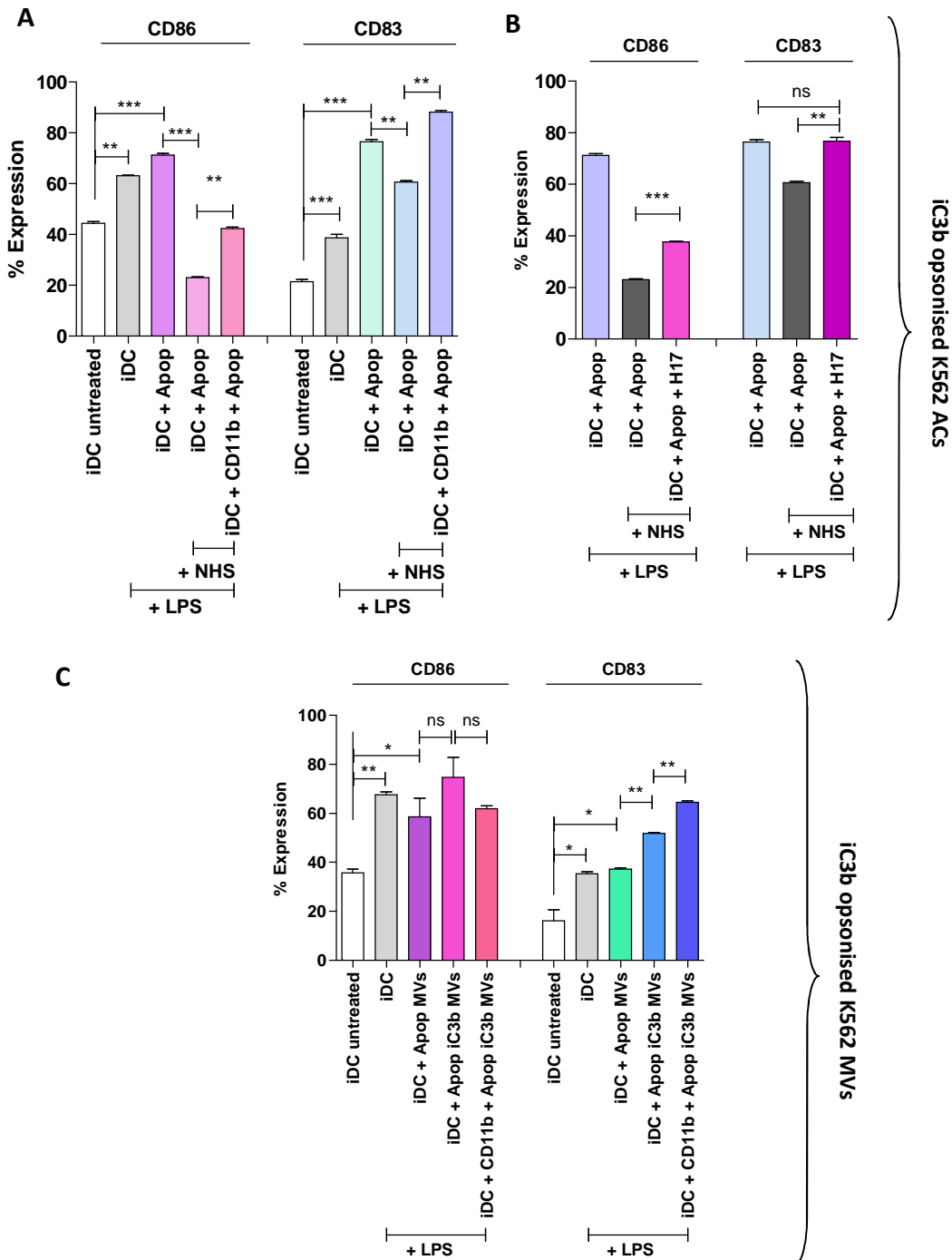


Fig 5.15: The effect of iC3b opsonised apoptotic K562 cells and MVs on DC maturation. (A) iDCs were treated with apoptotic cells in the presence or absence of NHS (source of iC3b) for 2 hrs followed by LPS to induce maturation. For some treatments, iDCs were pretreated with anti-CD11b antibody (iC3b receptor inhibitor) followed by apoptotic cells with NHS and LPS maturation. **(B)** iDCs were also treated with apoptotic cells in the presence of NHS pretreated with complement inhibitor H17 followed by LPS maturation. **(C)** iDC cells were treated with or without apoptotic cell MVs with or without iC3b for 24 hrs followed by LPS to induce maturation. For some treatments, iDCs were pretreated with anti-CD11b antibody followed by iC3b rich MV treatment and LPS maturation. The cells were then labelled with DC maturation markers CD86 and CD83 and analysed by flow cytometry. Data represents the mean \pm standard error of the mean from two independent experiments performed in triplicate. * $P < 0.05$, ** $P < 0.005$, or *** $P < 0.001$ was considered statistically significant.

This data therefore suggests that although iC3b on apoptotic cell MVs had no inhibitory effect on the maturation of DC cells (as seen phenotypically with the maturation markers - **Fig 5.15 B**), there was an effect on the functional aspect of the DCs as a marked increase in the release of the anti-inflammatory cytokine IL-10 was observed which was effectively inhibited in the presence of DC iC3b receptor (CR3) inhibitor anti-CD11b.

5.3.10 The effect of cancer cell MVs on DC maturation

After observing the effect of apoptotic cell MVs on the maturation of DC cells we sought out to investigate whether MVs from healthy cancer cells had any effect on DC maturation. Briefly, immature DC cells (1×10^5 cells/well) were seeded in a 96 well plate and either treated with PC3 or K562 cell MVs (ratio of 1 DC:10 MVs) for 24 hrs at 37°C. After incubation, 1 µg/ml LPS was added to all the treatments and incubated for a further 24 hrs at 37°C to induce maturation. iDCs without any treatment served as negative control. Post incubation the supernatant was collected for IL-10 analysis and the cells fixed, labelled with DC maturation markers (CD86 and CD83) and analysed by flow cytometry.

Flow cytometry analysis revealed an interesting result. Treating iDCs with PC3 cell MVs significantly prevented the maturation of DC cells as there was no significant difference in the expression of CD86 (42.2%) and CD83 (19.7%) compared to immature DCs without any treatment (negative control) (CD86-35.7%; CD83-16.1%) (**Fig 5.16 B**). On the other hand, treating iDCs with K562 cell MVs had no inhibitory effect on the maturation of DCs

phenotypically as expression of CD86 (61.1%) and CD83 (50.2%) was significantly higher than iDCs without any treatment and similar or significantly higher than iDCs treated with only LPS (positive control) (CD86-67.6%; CD83-35.4%) (**Fig 5.16 B**).

IL-10 ELISA analysis revealed a similar result to that observed with apoptotic MVs. IL-10 production by iDCs treated with PC3 cell MVs (56.1 pg/ml) and K562 cell MVs (49 pg/ml) was significantly higher than iDCs treated without any MVs (**Fig 5.16 A**). This data therefore suggests that PC3 cell MVs have a significant effect on the phenotype and function of DC cells, whereas K562 cell MVs has a more prominent effect on the function (through increased IL-10 release) as opposed to the phenotype of DC cells.

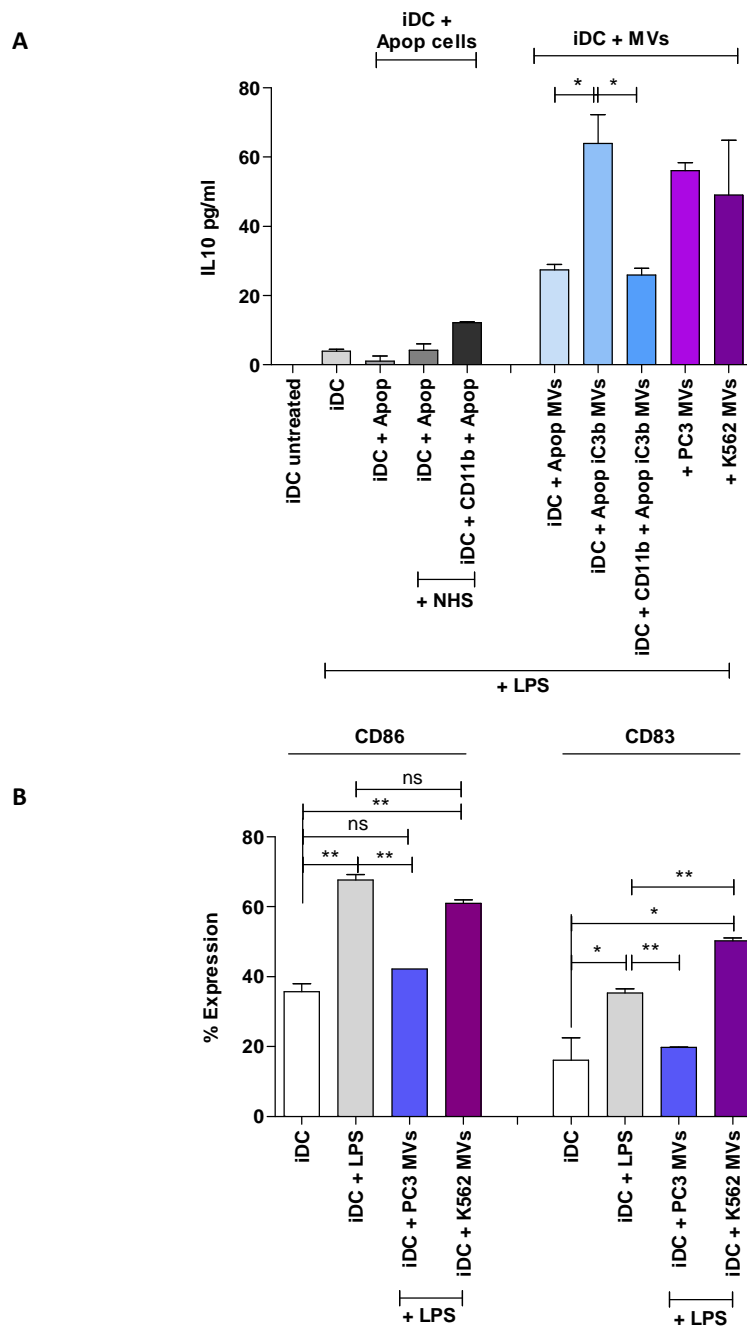


Fig 5.16: A) DCs treated with apoptotic MVs with or without iC3b release elevated levels of IL-10. IL-10 concentrations present in supernatants from iDCs treated either with or without apoptotic cells in the presence or absence of NHS or apoptotic cell MVs with or without iC3b or cancer cell derived MVs. **B) The effect of cancer cell MVs on DC maturation.** iDCs were treated with or without PC3 or K562 MVs for 24 hrs followed by maturation by LPS for a further 24 hrs. The cells were then labelled with DC maturation markers CD86 and CD83 and analysed by flow cytometry. Data represents the mean \pm standard error of the mean from two independent experiments performed in triplicate. * $P < 0.05$, and ** $P < 0.005$ was considered statistically significant.

5.3.11 Summary of the effect of iC3b and cancer cell derived MVs on DC cell maturation

iC3b is a complement protein that acts as an opsonin on apoptotic cells to allow their rapid clearance and uptake by antigen presenting cells such as DCs. iC3b on apoptotic cells has been shown to have a regulatory effect on DCs. The data obtained so far has shown that apoptotic cells in the presence of NHS do get opsonised by iC3b and that the iC3b can be carried by MVs released by these apoptotic cells as shown by Western blot. Furthermore, pulsing immature dendritic cells with apoptotic cells in the presence of NHS did inhibit LPS induced maturation of DC cells which was reversed up to a certain level on blocking the iC3b receptor (CR3) present on DC cells with anti-CD11b.

As microvesiculation is increased during apoptosis and iC3b was found to be deposited on MVs of apoptotic cells, we sought to investigate whether MVs rich in iC3b had a similar effect to apoptotic cells opsonised with iC3b on DC cells. The result obtained was inconclusive because phenotypically (considering DC markers CD86 and CD83) there was no inhibition of DC maturation observed when treating iDCs with apoptotic MVs rich in iC3b. However, there was a marked increase in the levels of IL-10 present in the supernatant of iDC cells when cultured with apoptotic MVs or cancer cell MVs compared to apoptotic cells. Furthermore, supernatant from iDC culture with apoptotic cell MVs rich in iC3b had a highly significant increased amount of IL-10 compared to the treatment with apoptotic MVs without iC3b. Fascinatingly, the levels of IL-10 were reduced significantly when blocking

the CR3 receptor on iDC cells prior to treating them with MVs rich in iC3b. This therefore confirmed that MVs rich in iC3b has some sort of a regulatory effect on DC cells as IL-10 is an anti-inflammatory cytokine. A similar effect of increased IL-10 levels in iDC supernatants was also observed when treating iDCs with PC3 and K562 MVs. Although K562 MVs did not have much of an inhibitory effect on the DC maturation markers, IL-10 levels were markedly increased. PC3 MVs on the other hand showed both an inhibitory effect on DC maturation markers as well as an increase in IL-10 production when incubating them with iDCs.

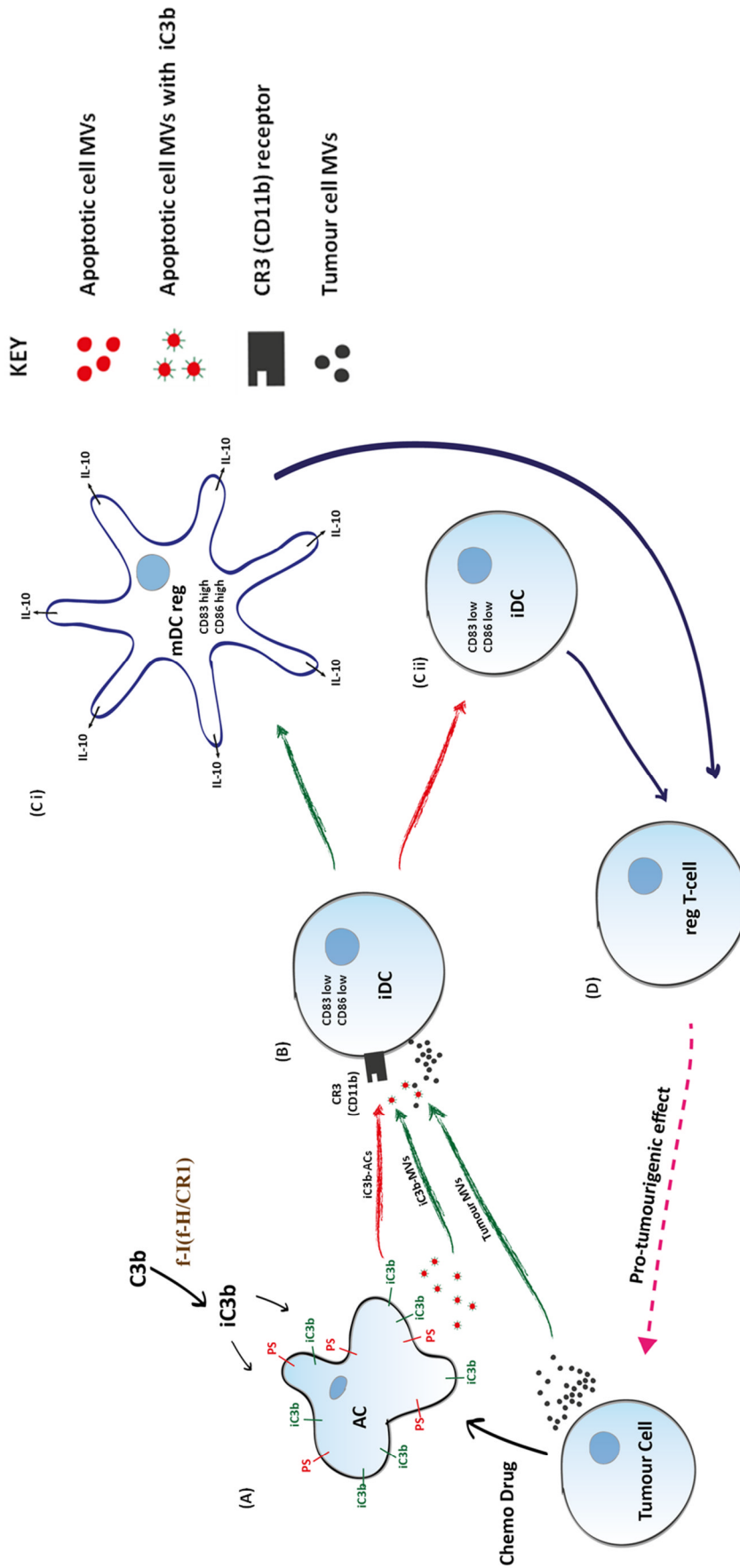


Fig 5.17: The role of iC3b deposited on apoptotic cancer cells and their MVs on the maturation and function of DC cells. Apoptotic tumour cells opsonised by iC3b (A) inhibit the maturation of iDC cells (B) which could render them tolerogenic (C i) and therefore up-regulate regulatory T cells (reg-T-cell) (D) that exhibit pro-tumourigenic properties. iC3b rich MVs from apoptotic tumour cells (B) or MVs from healthy tumour cells do not inhibit maturation of DC but activate them to produce anti-inflammatory cytokine IL-10 which is a property of regulatory DCs (mDC reg) (C ii) that also activate regulatory T-cells which exhibit pro-tumourigenic properties (D).

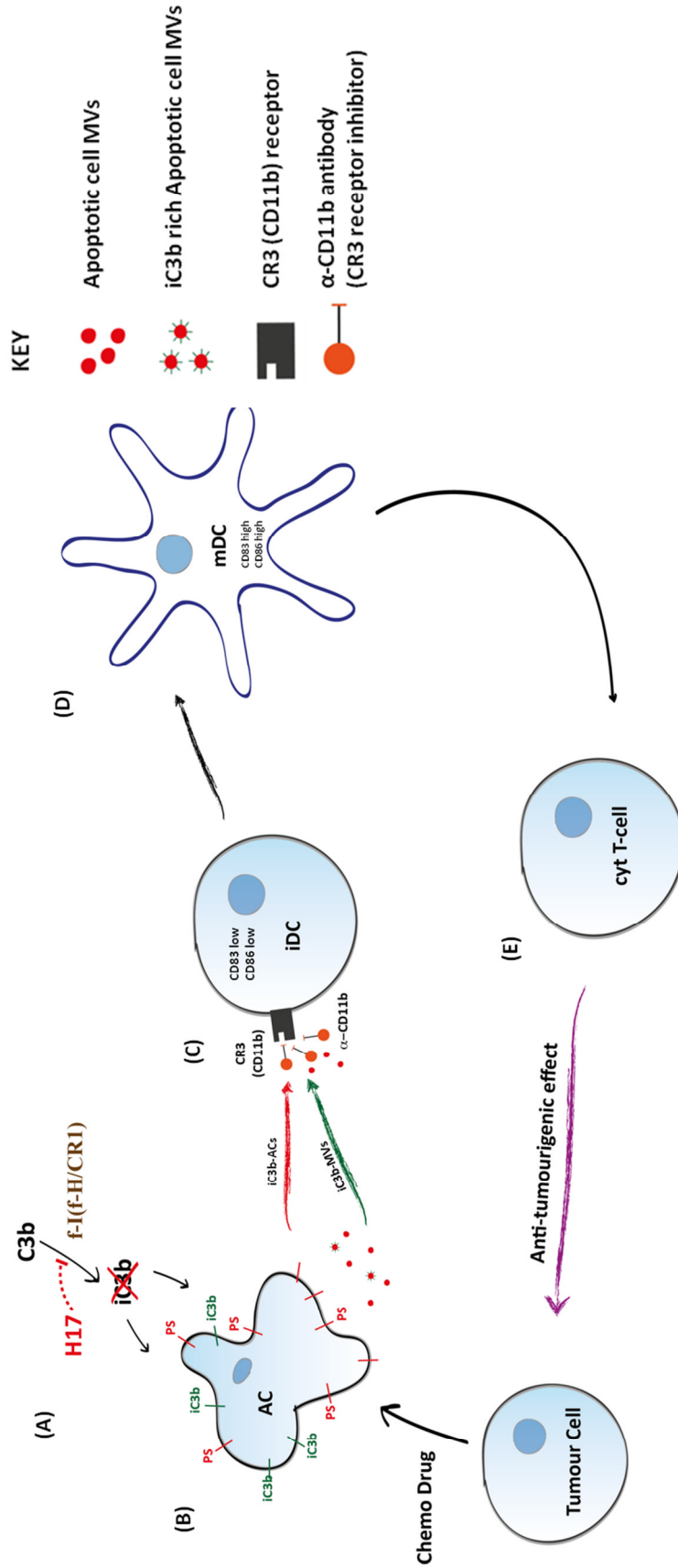


Fig 5.18: The proposed effect of H17 and blocking the iC3b (CR3) receptor on DCs on the maturation and function of DCs. CRIT-H17 inhibits factor H/CR1 mediated cleavage of C3b to iC3b therefore depleting iC3b levels (A). This in turn prevents the deposition of iC3b on apoptotic tumour cells (AC) and their MVs (B) therefore inhibiting their effect on immature DCs (iDC) (D). Furthermore, blocking the iC3b receptor on iDCs (C) abrogates the iC3b mediated inhibition of DC maturation, therefore allowing the DCs to mature (D) and have a pro-tumourigenic effect by activating cytotoxic T-cells (E).

6. Discussion

Over the past few years the scientific community in areas allied to immunology and medicine has taken a great interest in the role of MVs in helping maintain the delicate balance between health and disease. Apart from playing a role in various physiological functions such as thrombosis, inflammation, angiogenesis, cellular cross talk and vasoconstriction (167,225-227), they have been linked with a wide range of clinical conditions such as diabetes, cardiovascular diseases, inflammatory diseases, autoimmune diseases, and cancer (169,228-230).

It has been well established by various studies that cells tend to release more MVs when stimulated by physiological factors such as sheer stress and sub-lytic complement (6,231). In addition to this, exogenous stimulants such as adenosine diphosphate, epinephrine, collagen, thrombin and PMA have also been reported to increase cellular MV production (232). Our study further established this fact, as stimulating cells with 5% NHS (an exogenous mimicry of sub-lytic complement) showed an increase in the release of MVs. Further to this, our findings also showed that MCF7 and PC3M a highly metastatic cancer cell line produced more MVs than the noncancerous PNT2 and HSkMC cell lines, hence suggesting that cancerous cells produce more MVs, which is in accordance with the findings of others (57,59,169). A possible explanation for this finding could be a mechanism suggested by Sims *et al.* in 1988 known as "complement resistance" whereby on exposure to complement, cells simply release MVs rich in C5b-9 (Membrane Attack Complex) as a form of protection from external stress (47). The same

mechanism has been shown in past studies to have been adopted by cancer cells (48,49) and we postulate the same mechanism in our findings.

6.1 MVs and/or exosomes released from human myocytes induce apoptosis of highly metastatic PC3M cells

Human Skeletal muscle is one of the tissues in the human body that exhibits resistance towards cancer metastasis (233). A study conducted by Parlakian *et al* also reported that mice myogenic cells when co-cultured with melanoma cells lead to inhibition of melanin pigment formation. In addition GFP labelled melanoma and carcinoma cells fuse to form myotubes during co-culture with myoblasts. Furthermore, serum-free muscle-conditioned media exhibited cytotoxic and cytostatic effects on metastatic cells that was not observed on non-metastatic cells (234). In line with this our current findings showed that myocyte supernatant whether filtered or not had a significant apoptotic effect on highly metastatic prostate cancer cells. This effect was not replicated by supernatant from myoblasts, complete growth medium or skeletal muscle differentiation medium (DMEM 15% HS).

In the past, Djaldetti *et al* have reported in their study, low molecular weight factors released by differentiated skeletal muscle cells that have inhibitory effects on tumour cell growth (119). They then further went on to identify one such factor as adenosine, although other factors were also identified in the skeletal muscle conditioned medium that exerted similar cytotoxic effects to adenosine (120). On the basis of this information and our findings we propose the presence of a factor released by myocytes that could be causing

the observed effect on cancer cells. This apoptotic effect of the supernatant was then further enhanced after filtration through a 0.22 μm pore membrane. A possible explanation for this would be that filtration has removed entities larger than ~ 200 nm in diameter. As exosomes constitute a homogenous population of extracellular vesicles of 100 nm in diameter and since the filtrate obtained was added in the same protein concentration as the supernatant pre-filtering, one can speculate that the enhanced level of apoptosis induced in the highly metastatic PC3M cells is due to the exosomes being present in higher concentration (larger MVs having been removed). Nevertheless, there is still a possibility that very small microvesicles (100--150 nm in diameter) could be involved as the existence of MVs in this size range has been suggested recently (personal communication, Inal, J.). Various researchers in the past have reported the apoptotic effect of MVs on cells. Andreola *et al* reported that MVs from melanoma cells induced Fas-mediated apoptosis in Jurkat cells (51). In addition, Sarkar *et al* also reported the apoptotic effect of caspase-1 encapsulated MVs from activated monocytes on vascular smooth muscle cells (235). Further to this, as reported in this thesis addition of MVs from skeletal muscle cells reduced proliferation and growth of PC3M prostate cancer cells. There may also have been a concentration of soluble proteins which would have passed through a 0.22 μm pore filter causing the observed effect due to the same protein concentration of myocyte supernatant being added to PC3M cells in the case of unfiltered (still carrying MVs) and in filtered supernatants (having no MVs) but, SDS-PAGE could not confirm this.

MVs have long been regarded as "cellular debris", however this view has changed over the past few years. They have been implicated to play important roles in both physiological and pathological systems (236-239). In cancer, MVs have been shown to act as carriers of various soluble proteins, growth factor receptors such as Endothelial Cell Growth Factor receptor (EGFR), micro RNAs, etc. that have been shown to aid in tumour survival and spread (239). Physiologically, MVs have been identified as mediators of intercellular communication by transferring growth factors, micro RNAs, enzymes for example between cells and therefore influence processes as diverse as differentiation, migration and angiogenesis to mention a few (168,239). Various studies have also shown MVs to play a role in cell repair and homeostasis. For instance, MVs derived from platelets had the capability of repairing myocardial injury after an infarction (240).

Proteins lacking a signal peptide are exported in MVs

Further to this, it has also been reported that a heterogeneous group of unconventional extracellular secretory proteins that are either lacking or do not make use of signal peptide-dependent secretory transport (conventional means of transport of proteins in the cell through the endoplasmic reticulum/golgi-dependent secretory pathway) are capable of translocating through the cytoplasm to the plasma membrane and out of the cell through vesicular or non-vesicular pathways with microvesiculation being one pathway (241). An example of such a protein is the proinflammatory cytokine interleukin-1 β which lacks a signal peptide and has been reported by Mackenzie *et al* to be secreted by human THP-1 monocytes by microvesicle

shedding upon monocyte activation (242). Other proteins such as fibroblast growth factor (FGF)-1, FGF-2, galectin (Gal)-3, and macrophage migration inhibitory factor (MIF) have all been reported to be transported to the plasma membrane through the adenosine triphosphate cassette transport channel (ABCA1) needed for the release of MVs or by exocytosis of exosomes (241,243,244). Furthermore, it was found that addition of MVs from skeletal muscle cells reduced proliferation and growth of tumour cells as reflected by the migration index and induced apoptosis. On the basis of this information and the results obtained from current experiments, we postulate that the active protein factor(s) may be released by myocytes through exosomes or MVs that are smaller than 0.22 μ m, the majority ranging from 0.1 μ m to 1 μ m (7,17,168,245).

Gelsolin is found in MVs released from human myocytes

In order to further investigate this effect, MVs from myoblast and myocytes were analysed by mass spectrometry to identify any active protein(s) that have the potential of causing the cytotoxic effects observed on PC3M cells. Various proteins were identified from the mass spectrometry analysis with more from myoblast MVs compared to myocyte MVs. However, interestingly, the majority of the proteins identified have been reported to be carried by MVs from other sources such as cells, urine, saliva, and malignant ascites as reported in vesiclepedia a database containing a collection of data at a molecular level (lipid, RNA, and protein) identified from different classes of extracellular vesicles (MV, exosomes and ectosomes) from over 300 independent studies published over the past several years (179).

Out of all the proteins identified one protein was considered as a candidate active protein - gelsolin. As aforementioned gelsolin is a Ca^{2+} -regulated multifunctional and ubiquitous protein mainly involved in actin filament severing and capping during actin remodelling in processes such as cell motility and microvesiculation, in both viable and apoptotic cells (196).

Gelsolin has also been reported to act either as an effector or inhibitor of apoptosis depending on the pathological condition, cell type and specific tissues that are involved (246-248). As a pro-apoptotic agent, gelsolin has been shown to mediate apoptosis by acting as a substrate for caspase-3 during apoptosis. Kothakota *et al* reported the cleavage of gelsolin by caspase-3 in multiple cell types and the resulting N-terminal half of gelsolin not only exhibited actin severing activity that was independent of Ca^{2+} but also contributed to morphological changes observed during apoptosis. Moreover, neutrophils isolated from gelsolin knockout mice had delayed signs of apoptosis such as membrane blebbing and DNA fragmentation compared to wild-type neutrophils (246). A similar result was reported by Geng *et al* whereby treating vascular smooth muscle cells with proinflammatory cytokines lead to caspase-3 induced gelsolin fragmentation which in turn contributed towards actin cytoskeletal collapse, nuclear fragmentation and apoptosis. Furthermore, adenovirus mediated transfection of the N-terminal gelsolin fragment into smooth muscle cell also exhibited a similar apoptotic effect. This effect was however abrogated in gelsolin knockout smooth muscle cell or when a caspase-3 inhibitor was applied (247). The enzyme deoxyribonuclease (DNase I) is an enzyme that is

responsible for DNA fragmentation during apoptosis and is in an inactive state when bound to cytoplasmic actin (249). However, the N-terminal gelsolin has been reported to disrupt the actin-DNase I interaction therefore activating the enzyme leading to an enhanced apoptotic activity (249). Other than caspase-3, caspase-7, 8 and 9 have also been shown to cleave gelsolin (250).

Role of gelsolin in cancer

Gelsolin also plays an important regulatory role in cancer. The expression of gelsolin has been shown to be downregulated in more than 60% of a wide variety of cancers including breast (251), prostate (252), colorectal (253) and oral cancers (254) to name a few. Interestingly, Sagawa *et al* reported that on overexpressing gelsolin in the PC10 lung cancer cell line known to have downregulated gelsolin levels, tumourigenecity was significantly reduced together with cell proliferation by inhibiting protein kinase C (PKC) activation (255). Furthermore, when Tanaka *et al* knocked down gelsolin via silent RNA (siRNA) in the non-tumourigenic mammary epithelial cell line MCF10a, typical hallmark signs of epithelial-mesenchymal transition were observed such as loss of contact inhibition, fibroblastic conversion, and increased motility and invasiveness and a switch from E to N-cadherin expression (256).

On the basis of this information and our findings we postulate that gelsolin present in MVs/exosomes of myocytes act as a substrate for caspases present in cancer cells that would lead to the generation of the N-terminal

gelsolin fragment which in turn would have an apoptotic effect on the PC3M cells. Secondly, the gelsolin present in MVs from myocytes would replace gelsolin already downregulated in cancer cells and thereby have an anti-proliferative and anti-tumourigenic effect. Even though this is just a postulation, much work needs to be done to prove this hypothesis, which if substantiated would not only increase our understanding on the role and function of microvesicles and exosomes but also open a new avenue for cancer research and therapy.

6.2 The potential role of PADs in MV biogenesis

More recently the involvement of peptidylarginine deiminase (PADs), a group of enzymes that in calcium dependent manner catalyse post-translational citrullination of various proteins, has also come to light in the biology of cancer (105). Chang *et al* (2006) reported a significant expression of PAD4 in many tumour tissues particularly in various forms of adenocarcinomas (107). They further reported an increased expression of PAD4 in malignant tumours as well as in the blood of patients suffering from cancer (105). In addition, various functions of PAD4 in cancer survival and progression have also been postulated. It has been reported that cytokeratin (CK), a protein which is part of the intra-cytoplasmic cytoskeleton, which plays a role in caspase mediated apoptosis and a potential tumour marker is citrullinated by PAD4. The citrullination prevents caspase cleavage of cytokeratin resulting in inhibition of apoptosis in tumour cells (107) and MV release is a feature of cells in early apoptosis. Similarly, another protein that has been identified

which is modified by PAD4 is antithrombin. On citrullination the antithrombin can no longer inhibit thrombin which has various pro-cancer functions such as cell proliferation, angiogenesis and fibrin formation (107).

PAD4 has also been shown to play a role in the epigenetics of cancer. Translational modification of histone proteins has been shown to play a role in the regulation of various genes, particularly in the regulation of the tumour suppressor gene *p53*. Physiologically, PAD4 serves as a co-repressor of the *p53* gene (by modifying various histone proteins), which codes for the tumour suppressor protein p53. It is also a well established fact that the p53 protein is either damaged or virtually absent in cancer cells. Hence an over-expression of PAD4 would explain one way by which this protein is inactive in tumours, as it would repress the gene that codes for p53 (198).

Both MVs and PADs have been shown to depend on an influx of calcium ions in order to be activated (6,105). In addition, PS has been reported to act as a catalyst by reducing the threshold of Ca^{2+} ions required to activate PAD (257). However, no link has been established as of yet of MVs and PAD playing a role synergistically in cancer. On the basis of this information we decided to investigate the role of PAD in MV release by cancerous and non-cancerous cells.

PAD4 and PAD2 play a role in microvesiculation in cancer cells

As aforementioned, PAD4 levels have been shown to be elevated in various tumours including breast carcinoma and prostate adenocarcinoma (107). In support of this we also report similar findings whereby PAD isotypes 4 and 2

were shown to be present with significantly elevated levels in K562 erythroleukaemia cells and PC3 prostate cancer cells compared to normal prostate cells (control). Furthermore, the PAD isotypes were localised partially in the cytoplasm and the nucleus of both normal and cancerous prostate cells.

This thesis also report for the first time that upon stimulating cells with normal human serum to induce microvesiculation, translocation of PAD4 and a partial translocation of PAD2 to the nucleus was observed in PC3 cells. Interestingly, inhibiting the PAD isotypes with the pan-PAD inhibitor chloramidine (210) prior to NHS stimulation prevented the translocation of the enzymes to the nucleus. Furthermore, analysis of MVs released during PAD inhibition prior to stimulation with multiple microvesiculation stimulants revealed a dose-dependent inhibitory effect of chloramidine on the release of MVs in both tumourigenic and non-tumourigenic cell lines, therefore suggesting that PAD may play a role in the biogenesis mechanism of MVs not only in cancer cells but also in normal cells. As chloramidine is known to be a pan-PAD inhibitor, which particular isoform(s) of PAD were inhibited cannot be stipulated at this stage.

Deimination of the cytoskeletal actins may be involved in MV release

Actins have been shown to play an important role during microvesiculation. For instance the redistribution of the actin-cytoskeleton during MV formation through the activation of Rho/Rho-associated kinase (ROCK) pathways during apoptosis and thrombin stimulation involves f-actin stress fibres (19).

Furthermore, Latham *et al* recently reported in their paper the role of β -actin in the regulation of MV formation. They observed that on stimulating endothelial cells to microvesiculate there was a redistribution of β -actin into stress fibres which in turn correlated with membrane protrusions and microvesiculation. On inhibiting Rho-kinase with Y-27632 this abolished the β -actin stress fibres and abrogated the release of MVs to near basal levels thereby confirming the role of β -actin in microvesiculation (202). In addition to this, a mass spectrometry analysis by Van Beer *et al* of synovial fluid from patients with rheumatoid arthritis identified β -actin as a deiminated protein (258). Furthermore, a study carried out by Darrah *et al* reported the deimination of β and γ actins in the sera of patients with rheumatoid arthritis by the PAD2 isotype (69). On the basis of this information a link between β -actin deimination and microvesiculation was investigated.

Data obtained from the investigation shows for the first time that the deimination of β -actin increased upon stimulating K562 cells with NHS, and decreased markedly when pre-treating the cells with chloramidine prior to stimulation with NHS. Furthermore, mass spectrometry analysis of deiminated proteins from PC3 cells stimulated for microvesiculation with BzATP in the presence or absence of chloramidine revealed actin alpha 1 as a deiminated protein. In addition, the confidence level of the protein was reduced to 50% in PC3 cells pre-treated with chloramidine prior to stimulation. On the basis of this information it can be postulated that deimination of β -actin and possibly actin alpha-1 could play an important role in the shedding process of MVs.

Pan-PAD inhibitor chloramidine works synergistically on combining with methotrexate

There are several recent studies that have reported the cytotoxic effect of PAD inhibitors on cancer cells without affecting normal cells (89,259,260). For instance Slack *et al* reported that potent PAD4 inhibitors fluoramidine and chloramidine exhibited cytotoxic effects at micro-molar concentrations on several cancer cell lines such as HL60, MCF-7, HT-29 whereas no effect was observed on non-cancerous cells. Furthermore, other than reducing cell viability, an ability to cause differentiation of HL60 and HT29 cells was also observed (210). Slack *et al* have also shown a synergistic effect whereby cell cytotoxicity was increased when combining the inhibitors with the cancer drug doxorubicin (210). A similar finding from this study has also been reported whereby K562 and PC3 cells treated with chloramidine exerted a significant cytotoxic effect compared to methotrexate alone which was further enhanced on combining chloramidine with methotrexate.

This data therefore is in agreement to what has been reported before and further confirms the cytotoxic effect of chloramidine over a wide range of cancers as well a synergistic effect with multiple cancer drugs. However we can now postulate a mechanism for the synergistic effect of chloramidine/fluoramidine with doxorubicin reported by Slack *et al* and of chloramidine with methotrexate (this thesis) which is that chloramidine's role in inhibiting MV release (likely through inhibiting the deimination of cellular actins) sensitizes the cells to the chemotherapeutic drug(s). The mechanism for this in turn has been reported by colleagues in CMIRC and others ((209)

and PhD thesis - The role of microvesicles in cancer and viral infection) whereby cells are rendered more sensitive to cancer drugs when they are inhibited from removing them from the cell by microvesiculation.

Various studies have shown that MVs play a role in cellular cross talk whereby multiple proteins, receptors, mRNAs and other cellular molecules are exchanged between cells through the paracrine function of cells. For instance, the transfer of CD41 antigen to endothelial cells has been reported in earlier studies (261). Similarly MVs have also been shown to act as carriers whereby active molecules can be carried to have an effect at a distal site from the origin of MV release. Our group has recently reported that TGF- β carried by MVs significantly reduced proliferation of THP1 monocytes (20) and reduced the infection of Hela cells and *in vivo* in mice with the parasite *Trypanosoma cruzi* (262). As mentioned earlier, Chang *et al* did report the presence of PAD4 in the plasma, however the mechanism by which this happens is still unknown (107). On the basis of this information and the findings from our study we postulate that tumour cells may increase the production of MVs through a mechanism involving PAD4, which in turn would allow the PAD enzyme to be packaged in these MVs through which it could be carried in the plasma where the enzyme would modify various proteins such as antithrombin and aid in tumourigenesis indirectly.

Taken together, these findings suggest that PAD enzymes may play a potential role in the microvesiculation of cancer and non-cancerous cells directly through the deimination of cellular actins involved in actin-cytoskeletal rearrangement or indirectly through the deimination of histone

proteins in the nucleus - a mechanism that still needs to be investigated. We also suggest PAD inhibitors as novel therapeutic agents that could be applied in the current regime of therapy in combination with other forms of cancer treatment.

6.3 iC3b from apoptotic cancer cells and MVs have an effect on DC phenotype and function

DCs are professional antigen presenting cells that act as nature's adjuvants (123). They have the ability to process and present antigens and therefore activate T cells locally and in the lymphatic system. DCs also have the ability to regulate the immune system by promoting immunotolerance to avoid an autoimmune response, particularly during apoptosis where self-antigens may be generated (156). However, over the years, research has shown the ability of tumours to manipulate this ability of DCs to avoid an anti-tumour immune response (158). Three main mechanisms have been identified through which tumour cells can regulate DC mediated immunity; tumour-mediated apoptosis of DCs, dysfunction of DCs, and converting DCs into regulatory cells that promote immunotolerance.

The complement system has also been shown to be activated during apoptosis. Various researchers have reported complement mediated cleavage of C3b to iC3b which is then deposited on apoptotic cells thereby enhancing their uptake by phagocytes (164,263). In addition, recently a group have reported the ability of apoptotic tumour cells to induce DC tolerance by releasing iC3b that can bind to CR3 receptors on DC cells and

render them immature (160). Further to this, Chen *et al.* also reported the involvement of PS in the inhibition of DC maturation. They observed that PS liposomes inhibited up-regulation of DC maturation markers such as CD80, CD86, CD40, CD83, HLA-DR etc as well as release of interleukin 12p70 in response to lipopolysaccharide (LPS). They also noticed that PS treated DCs had diminished their ability to stimulate allogeneic T cells as well as interferon γ producing CD4⁺ T cells (264). As MVs are rich in PS and have the ability to transport cargo from the parent cells we sought to investigate the role of MVs from healthy or iC3b opsonised apoptotic tumour cells on DC biology.

CRIT-H17 and Annexin V inhibit iC3b deposition on apoptotic cancer cells

Heat stress was opted as an apoptotic stimulant as previous work from our group has shown MVs from tumour cells exposed to chemotherapeutic drugs have the ability to carry these drugs and cause apoptosis when exposed to healthy cells (209). Hence using chemotherapeutic agents to induce apoptosis would enrich MVs with the drug which when exposed to DCs might mask the effect of PS and/or iC3b that we were investigating.

On exposing apoptotic tumour cells to NHS, deposition of iC3b was detected both by flow cytometry and Western blotting therefore confirming data from other researchers who have shown iC3b deposition on apoptotic cells (160,164,265). Furthermore, it has also been reported for the first time that the complement inhibitor peptide CRIT-H17 significantly abrogates the

deposition of iC3b on apoptotic tumour cells. CRIT-H17 is a more potent variant of CRIT peptide that inhibits complement C2 which in turn limits the extent of the classical pathway C3 convertase formation that is required for the cleavage of C3 to C3a and C3b (222). C3b is then further cleaved by complement factor H and factor I to form a proteolytic inactive iC3b which serves as an opsonin for apoptotic cells (266). A further way CRIT-H17 may inhibit formation of iC3b (unpublished, personal communication, Inal, J.) is via inhibition of another serine protease, factor I, which together with its cofactors, CR1/factor H, prevents the cleavage of C3b thus further limiting iC3b formation.

On the basis of this information it can be postulated that CRIT-H17 by limiting the formation of iC3b as mentioned thereby reduces the availability of the opsonin to bind to the apoptotic tumour cells. However the inhibitory effect was not abrogated completely and a possible explanation for this can be the presence of iC3b in the NHS before the addition of CRIT-H17.

Interestingly, this thesis also reports that on blocking PS on apoptotic K562 and PC3 cells with annexin V this abrogated the deposition of iC3b by almost 50%. Further to this, a study by Mevorach *et al* also reported a similar finding whereby only 40% of apoptotic murine thymocytes preincubated with annexin V had iC3b deposited on their surface (267). On the basis of this information together with the findings reported it can strongly be suggested that exposure of PS on apoptotic cells plays a partial role in complement activation as well as iC3b opsonisation in an apoptotic environment.

iC3b on apoptotic tumour cells inhibit the maturation of iDCs

There has been a growing body of evidence suggesting tumour induced dysfunction and tolerance of DCs (146,150,151). In addition, there have also been reports of impaired DC maturation and tolerance mediated by apoptotic cells (268,269). For instance, Verbovetski *et al* have shown in their study that iC3b opsonisation of apoptotic cells did facilitate their uptake by iDCs but in turn prevented the maturation of iDCs by down regulating CD86 and other maturation markers (263). A study by Morelli *et al* also showed reduced amounts of proinflammatory cytokine RNAs in splenic marginal zone DC after uptake of apoptotic cells in the presence of serum (216). Furthermore, Schmidt *et al* reported that iC3b released by apoptotic tumour cells prevented maturation and induced tolerance by binding to iDC both *in vitro* and *in vivo*.

Here we report that iDCs pulsed with apoptotic K562 cells in the absence of iC3b led to a more mature status as reflected by high DC maturation markers (CD86 high and CD83 high). This effect was however abrogated in the presence of iC3b, nevertheless on blocking the iC3b receptor (CR3 receptor) on iDCs prior to treatment with apoptotic cells in the presence of iC3b the mature status of DCs was restored but not to the full extent as reflected by some maturation markers such as CD86. Interestingly, the inhibition of iDC maturation induced by iC3b apoptotic cells was partially reversed (CD83 high, CD86 low) when treating iDCs with apoptotic cells in the presence of serum pretreated with CRIT-H17 peptide. An explanation for this could be the presence of preformed iC3b already present in the serum that the CRIT-

H17 cannot inhibit. The data is therefore in accordance with what has been reported previously, however at this stage the data only confirms the inhibitory effect of iC3b on the maturation status. Whether or not the DCs are tolerant is still under investigation.

MVs from apoptotic and non-apoptotic cancer cells have a regulatory effect on DC cells

Numerous studies have confirmed that MVs secreted by cancer cells play a role in immune suppression and other pro-cancer activities. For instance, Andreola *et al* have reported Fas ligand mediated apoptosis of lymphocytes by melanoma cell derived MVs (51). Liu *et al* have reported that murine mammary carcinoma cell exosomes promote tumour growth by suppression of natural killer cell activity (270). MVs from tumour cells have also been reported to induce, expand and up-regulate T regulatory functions (271,272). Furthermore, Yu *et al* have also reported tumour derived exosomes to inhibit the differentiation of bone marrow derived DCs (273). In addition, Stahl *et al* in their study detected the presence of iC3b on MVs isolated from whole blood (274).

In accordance with this information I report for the first time that MVs isolated from iC3b opsonised apoptotic cancer cells have iC3b deposited on them. Furthermore, incubating these iC3b-rich MVs with iDCs did not inhibit DC maturation but increased the production of the anti-inflammatory cytokine IL-10 which was abrogated on blocking the iC3b receptor (CR3) on iDCs. This therefore suggests that iC3b carrying MVs have some sort of a regulatory

effect on DC cells. Furthermore, a similar effect was also observed when treating iDCs with healthy K562 cell MVs whereby maturation was not inhibited but IL-10 production was increased significantly. On the other hand, treating iDCs with MVs from PC3 cells we observed that maturation of iDCs was inhibited and IL-10 production was increased significantly. Furthermore, iDCs that were treated with MVs (apoptotic or healthy) produced significantly more IL-10 compared to iDCs treated with apoptotic cells. A similar result was also observed by Gasser *et al* who observed that MVs from neutrophils phagocytosed by macrophages caused them to release anti-inflammatory cytokines such as transforming growth factor β 1 (TGF- β 1) (275). This data therefore suggests that MVs from different cancer cells may have separate effects on the phenotype of DC cells however a more immunosuppressive effect towards their function.

In addition, Sohn *et al* have reported in their study that the binding of iC3b to the CR3 receptor on antigen presenting cells resulted in the production of TGF- β 2 and IL-10 both of which have immunosuppressive properties (166). Furthermore, DCs that have regulatory properties have been described to have increased expression of CD86 and CD80 markers with the ability of producing IL-10 and supporting the development of regulatory T cells (276).

On the basis of this information and the current findings of this study, It can be postulated that iC3b from apoptotic tumour cells have the ability to inhibit DC maturation thereby rendering them immuno-tolerogenic. On the other hand, iC3b-rich MVs from apoptotic cancer cells convert iDCs to regulatory mature DCs (regDC) that produce anti-inflammatory cytokines such as IL-10.

Both iDCs and regDCs would have an immunosuppressive effect on T-cell mediated cytotoxicity against cancers (a theory that is currently under investigation).

Furthermore on observing the blocking effect of CRIT-H17 towards iC3b deposition on apoptotic cancer cells as well as a reversing effect of iC3b-apoptotic cell mediated DC maturation inhibition, there is a possibility of developing CRIT-H17 into a therapeutic anti-cancer agent in combination with other cancer therapies.

6.4 Summary and concluding remarks

In conclusion MVs are now widely accepted as biological entities that participate in important biological functions at a physiological and pathological level. They have been implicated in various diseases including diabetes mellitus, autoimmune diseases, thrombosis and cancer. This thesis provides further evidence to support MVs as biological entities that can play both a therapeutic as well as a pathological role in disease states such as cancer.

This thesis illuminates a therapeutic potential of myocyte MVs and their cargo through the observation of cytotoxic and anti-proliferative effects of myocyte MVs/exosomes on prostate cancer cells. It also reports a novel role of PADs in the biogenesis of MVs in both cancer and non-cancer cells, whereby the inhibition of PADs by the pan-PAD inhibitor chloramidine reduced the expression of PADs which in turn abrogated the release of MVs from cells. Moreover, on combining chloramidine with the anti-cancer drug

methotrexate this significantly increased its cytotoxic effect on cancer cells in a synergistic manner therefore highlighting a therapeutic use of chloramidine in cancer. Furthermore, this work identified the role of iC3b on apoptotic cells and the MVs they release. iC3b opsonised apoptotic cells prevented the maturation of DC cells and MVs from apoptotic cancer cells induced the production of the anti-inflammatory cytokine IL-10 from mature DCs, both of which were abrogated on blocking the iC3b receptor on DCs.

This thesis therefore expands on the current function and role of MVs in both a physiological and pathological environment with a potential of developing into a future therapeutic strategy against cancer and other diseases.

7. Appendix

7.1 Additional figures

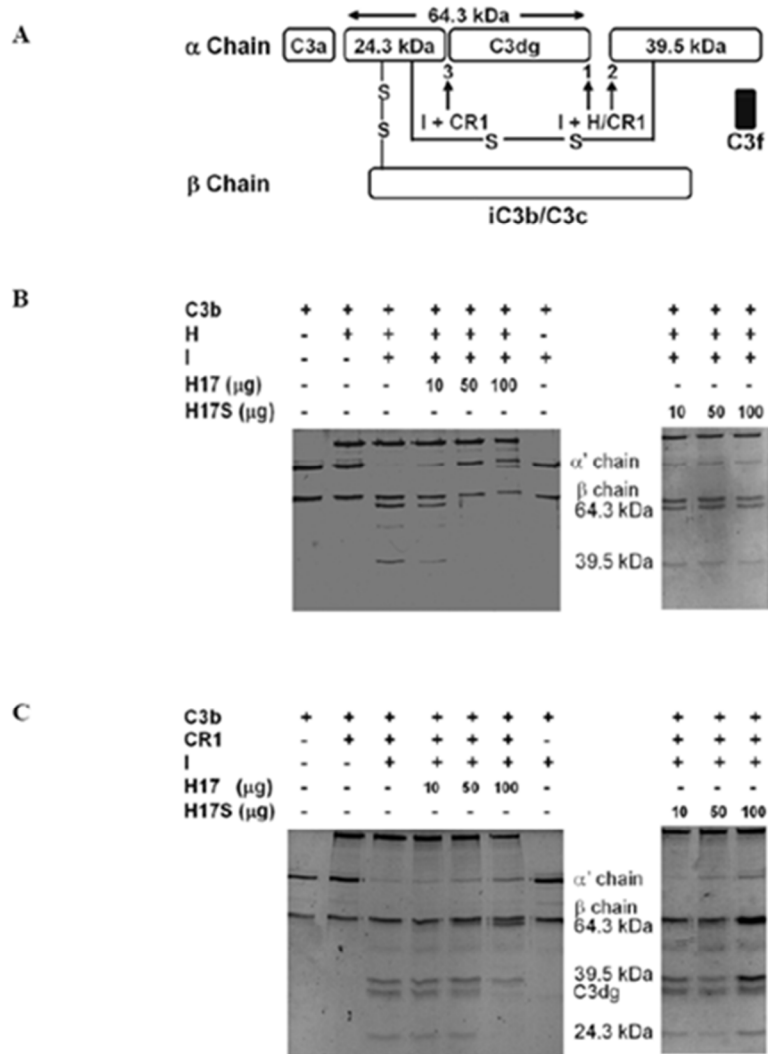


Fig A1: Inhibition of FH and CR1 cofactor activities by CRIT-H17. **A)** Schematic representation of C3b showing the Factor I (FI) (arrows 1,2 and 3) cleavage sites in the presence of Factor H (FH) and CR1. Different amounts of either CRIT-H17 or CRIT-H17S peptides (10-100 µg) were pre-incubated with 500 ng C3b for 30 min at RT. After pre-incubation, 100 ng FI and either 500 ng FH (B) or 500 ng CR1 (C) were added for additional 2 hr incubation at 37°C. The inhibition effect of CRIT-H17 and CRIT-H17S peptides on the cleavage of C3b by FI were analysed by 10% SDS-PAGE (reducing conditions) and the gel was stained with ProteoBlue staining solution. (Figure from PhD thesis: Biochemical and functional studies of a novel complement inhibitor, CRIT with its interaction partners, Hui, K.- M. , 2005)

7.2 Materials

7.2.1 Chemicals

Acrylamide/Bisacrylamide	Sigma-Aldrich
Annexin V Alexa Fluor 488	Invitrogen
Annexin V reagent	R&D Systems
APS (Ammonium persulphate)	Sigma-Aldrich
Barbituric acid	Sigma-Aldrich
BCA protein assay kit	Pierce Biosciences
BSA (Bovine serum albumin)	Sigma-Aldrich
Bromophenol blue	Fisher Scientific
Calcium chloride	Sigma-Aldrich
Calpeptin	Merck Biosciences
Chloramidine (PAD Inhibitor)	Kind gift from Dr Sigrun Lange
Coomassie brilliant blue	BDH Limited, Poole, England
DAPI VectaShield mounting medium	Vector Labs
DMSO (Dimethyl sulfoxide)	Sigma-Aldrich
DTT (Dithiothreitol)	Fisher Scientific
ECL WB Detection Reagent	SignaGen Laboratories
Ethanol	Fisher Scientific
FBS (Foetal Bovine Serum)	Fisher Scientific
Glacial acetic acid	Fisher Scientific
Glycerol	Sigma-Aldrich
Glycine	Sigma-Aldrich
Guava ViaCount reagent	Guava Technologies, UK
Guava Nexin reagent	Guava Technologies, UK
HSkMC growth medium	Promocell
HSkMC differentiation medium	Promocell
Halt Protease Cocktail	Pierce, Thermo-Scientific
HCl (Hydrochloric acid)	Fisher Scientific
HEPES	Sigma-Aldrich
Hybrid nitrocellulose membrane	Amersham Biosciences
Isopropanol	Sigma-Aldrich
Kanamycin	Sigma-Aldrich
Methanol	Fisher Scientific
Milk powder	Marvel Original, Dublin
NHS (Normal Human Serum)	Sigma-Aldrich
Paraformaldehyde	Sigma-Aldrich
PBS (Phosphate Buffered Saline)	Fisher Scientific
Penicillin / Streptomycin	Fisher Scientific

PMA (Phorbol-12-myristate-13-acetate)	Pierce, Thermo-Scientific
PMSF	Sigma-Aldrich
Propidium iodide	Sigma-Aldrich
Protein molecular weight marker	BioRad
R-18 (OctadecylRhodamine B Cl)	Invitrogen Molecular Probes
RPMI	Sigma-Aldrich
SDS (Sodium dodecyl sulphate)	Sigma-Aldrich
Sodium azide	Avocado Research Chemicals
Sodium barbital	Sigma-Aldrich
Sodium chloride	Sigma-Aldrich
Sodium hydroxide	Sigma-Aldrich
Sucrose	Sigma-Aldrich
TEMED	Sigma-Aldrich
Tris base	Sigma-Aldrich
Trichloroacetic acid	Fisher Scientific
Triton X-100	Sigma-Aldrich
Trypsin/EDTA solution	Sigma-Aldrich
Tween 20	Sigma-Aldrich

7.3 Equipment

Cell culture flasks (75 cm ²)	Fisher Scientific
Centrifuge 5804 R	Eppendorf
Centrifuge 5810 R	Eppendorf
Cover glass (18 mm)	Fisher Scientific
Gel loading tips	Corning
Guava EasyCyte flow cytometer	Guava Technologies, UK
Fluorescence microscope (1X81)	Olympus Corporation, Germany
FLUOstar Omega plate reader	BMG Labtech, UK
Incubator Heraeus CO ₂ -Auto-Zero	Thermo Electron Corporation
Mini-PROTEAN 3-gel system	BioRad
Microcentrifuge 5417R	Eppendorf
Microplate (12-well)	Sigma-Aldrich
Microplate (24-well)	Sigma-Aldrich
Microplate (96-well)	Sigma-Aldrich
Nikon Inverted Microscope,	Nikon Eclipse, Japan
pH-Meter 766 Calimatic	Jenway
Roto-Shake Genie	Denley
Semi-dry transfer system	BioRad
Small volume tips	Sigma-Aldrich

Sorvall ultracentrifuge RC6	Thermo Electron Corporation
Sorvall T-865 rotor	Sorvall
F-20 micron rotor	Sorvall
Sonicating waterbath	Townson& Mercer Ltd, Croydon
UVP Chemiluminescence	UVP Bioimaging Systems, UK

7.4 Antibodies

Anti-Annexin V AlexaFluor 488	eBiosciences
Mouse anti-PAD4	Abcam
Rabbit anti-PAD2	Abcam
Mouse F95 antibody	Kind gift Dr Anthony Nichols
Mouse anti-CD1a-FITC	Immunotools
Mouse anti-CD14-PE	Immunotools
Mouse anti-CD83-FITC	Immunotools
Mouse anti-CD86-FITC	Immunotools
Mouse anti- β -Actin	Santacruz biotech
Mouse anti-IgM-HRP	Kind gift Dr Sigrun Lange
Mouse anti-IgG-HRP	Sigma-Aldrich
Rabbit anti-IgG-HRP	Sigma-Aldrich
Mouse anti-IgG-FITC	Sigma-Aldrich
Rabbit anti-IgG-FITC	Sigma-Aldrich
Mouse anti-IgG AlexaFluor 488	Invitrogen
Mouse anti-IgG AlexaFluor 488	Invitrogen

7.5 Experimental Solutions

N/B - pH was either adjusted with 4 M HCl or 4 M NaOH

7.5.1 Mammalian cell freeze medium

60%	FBS (v/v)
5%	DMSO (v/v)
1%	Penicillin/Streptomycin
34%	Cell Growth Medium

7.5.2 HSkMC cell freezing medium

90%	HSkMC CGM (v/v)
10%	DMSO (v/v)
1%	Penicillin/Streptomycin

7.5.3 Lysis Buffer pH 7.4

100 mM	HEPES-KOH
2 mM	CaCl ₂
0.2%	Triton X-100 (v/v)
1:100	HALT Protease inhibitor
	Millipore water

Made up to 50 ml and stored as 1 ml aliquots at -20°C. pH was adjusted with 4 M HCl.

7.5.4 SDS PAGE Solutions

7.5.4.1 (4X) SDS Sample buffer- pH 6.8

200 mM	Tris-HCl
40%	Glycerol
2%	SDS (w/v)
0.2%	Bromophenol blue (w/v)
20 mM	DTT (added fresh on the day)
	Millipore water
	pH was adjusted using 4 M HCl solution

7.5.4.2 (0.5 M) Stacking buffer- pH 6.8

18.17 g Tris base

Dissolved in 100 ml deionised water and pH adjusted to 8.8

7.5.4.3 Resolving gel solution (10%)

2 ml ddH₂O
1.25 ml 1.5 M Tris-HCl, pH 8.8
0.050 ml 10% SDS (w/v)
1.66 ml Acrylamide/Bis30% (w/v)
0.025 ml 10% APS (w/v)
0.0025 ml TEMED

7.5.4.4 Stacking gel solution

1.53 ml ddH₂O
0.625 ml 0.5 M Tris-HCl, pH 6.8
0.025 ml 10% SDS (w/v)
0.335 ml Acrylamide/Bis 30% (w/v)
0.0125 ml 10 % APS (w/v)
0.0025 ml TEMED

7.5.4.5 10X Electrophoresis running buffer (1L)

250 mM Tris-HCl, pH 8.3
1925 mM Glycine
50 ml 20% SDS (w/v)
950 ml ddH₂O

7.5.4.6 Coomassie Brilliant Blue G-250

0.025% Coomassie blue (w/v)
10% Acetic acid (v/v)
90% ddH₂O (v/v)

Mixed and filtered (Whatman number 1 paper)

7.5.4.7 Destaining solution (500 ml)

35 ml	Acetic acid
25 ml	Methanol
440 ml	ddH ₂ O

7.5.4.8 Transfer buffer (10X)

250 mM	Tris base
1925 mM	Glycine
500 ml	ddH ₂ O

7.5.4.9 Phosphate Buffered Saline (PBS) solution - 1L

140 mM	NaCl
2.7 mM	KCl
10 mM	Na ₂ HPO ₄
1.8 mM	KH ₂ PO ₄
	ddH ₂ O

7.5.4.10 Phosphate Buffered Saline – Tween 20 (PBS-T)

1 L	PBS
1 ml	Tween 20

7.5.4.11 Tris-Buffered Saline – Tween 20 (TBS-T)

50 mM	Tris base
150 mM	NaCl
0.05%	Tween 20

Dissolved in 500 ml of deionized water pH adjusted to 7.6

7.5.4.12 Blocking buffer

6%	Milk powder (w/v)
100 ml	PBS-T

7.5.4.13 Antibody dilution buffer (WB)

3%	Milk powder (w/v)
100 ml	PBS-T

7.5.4.14 Permeabilisation Buffer (PBB)

0.5%	Tween 20 (v/v)
	PBS

7.5.5 Immunofluorescence antibody dilution buffers**7.5.5.1 Cell Dilution Medium**

10%	FBS
1%	NaN ₃ (w/v)
	PBS solution

7.5.5.2 Primary and secondary antibody dilution buffer

3%	BSA (w/v)
	PBS

7.5.5.3 Flow cytometry analysis buffer

3%	BSA (w/v)
1%	NaN ₃ (w/v)
	PBS

7.5.5.4 Veronal buffer – pH 7.4

0.15 mM	CaCl ₂
141 mM	NaCl
0.5 mM	MgCl ₂
1.8 mM	Na Barbitol
3.1 mM	Barbituric acid

All components dissolved in 500 ml of deionised water

7.5.6 Annexin V binding buffer – pH 7.4

10 mM	HEPES/ NaOH
140 mM	NaCl
2.5 mM	CaCl ₂

All components dissolved in 100 ml of deionised water

8. References

1. McLaughlin, P. J., J. T. Gooch, H. G. Mannherz, and A. G. Weeds. 1993. Structure of gelsolin segment 1-actin complex and the mechanism of filament severing. *Nature* 364: 685-692.
2. Kwiatkowski, D. J. 1999. Functions of gelsolin: motility, signaling, apoptosis, cancer. *Curr. Opin. Cell Biol.* 11: 103-108.
3. Raposo, G., and W. Stoorvogel. 2013. Extracellular vesicles: exosomes, microvesicles, and friends. *J. Cell Biol.* 200: 373-383.
4. Vader, P., X. O. Breakefield, and M. J. Wood. 2014. Extracellular vesicles: emerging targets for cancer therapy. *Trends Mol. Med.*
5. Ratajczak, J., M. Wysoczynski, F. Hayek, A. Janowska-Wieczorek, and M. Z. Ratajczak. 2006. Membrane-derived microvesicles: important and underappreciated mediators of cell-to-cell communication. *Leukemia* 20: 1487-1495.
6. Piccin, A., W. G. Murphy, and O. P. Smith. 2007. Circulating microparticles: pathophysiology and clinical implications. *Blood Rev.* 21: 157-171.
7. Diamant, M., M. E. Tushuizen, A. Sturk, and R. Nieuwland. 2004. Cellular microparticles: new players in the field of vascular disease? *Eur. J. Clin. Invest* 34: 392-401.
8. Chargaff E, W. R. 1946. The biological significance of the thromboplastic protein of blood. *J Biol Chem* 166: 189-197.
9. Wolf, P. 1967. The nature and significance of platelet products in human plasma. *Br. J Haematol.* 13: 269-288.
10. Ardoin, S. P., J. C. Shanahan, and D. S. Pisetsky. 2007. The role of microparticles in inflammation and thrombosis. *Scand. J. Immunol.* 66: 159-165.
11. Li, G. H., P. D. Arora, Y. Chen, C. A. McCulloch, and P. Liu. 2012. Multifunctional roles of gelsolin in health and diseases. *Med. Res. Rev.* 32: 999-1025.
12. Beleznyay, Z., A. Zachowski, P. F. Devaux, M. P. Navazo, and P. Ott. 1993. ATP-dependent aminophospholipid translocation in erythrocyte vesicles: stoichiometry of transport. *Biochemistry* 32: 3146-3152.
13. Zwaal, R. F., P. Comfurius, and E. M. Bevers. 1993. Mechanism and function of changes in membrane-phospholipid asymmetry in platelets and erythrocytes. *Biochem. Soc. Trans.* 21: 248-253.

14. Zwaal, R. F., P. Comfurius, and E. M. Bevers. 2004. Scott syndrome, a bleeding disorder caused by defective scrambling of membrane phospholipids. *Biochim. Biophys. Acta* 1636: 119-128.
15. Kelton, J. G., T. E. Warkentin, C. P. Hayward, W. G. Murphy, and J. C. Moore. 1992. Calpain activity in patients with thrombotic thrombocytopenic purpura is associated with platelet microparticles. *Blood* 80: 2246-2251.
16. Miyoshi, H., K. Umeshita, M. Sakon, S. Imajoh-Ohmi, K. Fujitani, M. Gotoh, E. Oiki, J. Kambayashi, and M. Monden. 1996. Calpain activation in plasma membrane bleb formation during tert-butyl hydroperoxide-induced rat hepatocyte injury. *Gastroenterology* 110: 1897-1904.
17. Lynch, S. F., and C. A. Ludlam. 2007. Plasma microparticles and vascular disorders. *Br. J. Haematol.* 137: 36-48.
18. Distler, J. H., L. C. Huber, S. Gay, O. Distler, and D. S. Pisetsky. 2006. Microparticles as mediators of cellular cross-talk in inflammatory disease. *Autoimmunity* 39: 683-690.
19. Coleman, M. L., E. A. Sahai, M. Yeo, M. Bosch, A. Dewar, and M. F. Olson. 2001. Membrane blebbing during apoptosis results from caspase-mediated activation of ROCK I. *Nat. Cell Biol* 3: 339-345.
20. Ansa-Addo, E. A., S. Lange, D. Stratton, S. ntwi-Baffour, I. Cestari, M. I. Ramirez, M. V. McCrossan, and J. M. Inal. 2010. Human plasma membrane-derived vesicles halt proliferation and induce differentiation of THP-1 acute monocytic leukemia cells. *J Immunol.* 185: 5236-5246.
21. Kerr, J. F., A. H. Wyllie, and A. R. Currie. 1972. Apoptosis: a basic biological phenomenon with wide-ranging implications in tissue kinetics. *Br. J. Cancer* 26: 239-257.
22. Hristov, M., W. Erl, S. Linder, and P. C. Weber. 2004. Apoptotic bodies from endothelial cells enhance the number and initiate the differentiation of human endothelial progenitor cells in vitro. *Blood* 104: 2761-2766.
23. Simak, J., and M. P. Gelderman. 2006. Cell membrane microparticles in blood and blood products: potentially pathogenic agents and diagnostic markers. *Transfus. Med. Rev.* 20: 1-26.
24. Simak, J., K. Holada, and J. G. Vostal. 2002. Release of annexin V-binding membrane microparticles from cultured human umbilical vein endothelial cells after treatment with camptothecin. *BMC. Cell Biol.* 3: 11.
25. Mills, J. C., N. L. Stone, J. Erhardt, and R. N. Pittman. 1998. Apoptotic membrane blebbing is regulated by myosin light chain phosphorylation. *J. Cell Biol.* 140: 627-636.
26. Pan, B. T., and R. M. Johnstone. 1983. Fate of the transferrin receptor during maturation of sheep reticulocytes in vitro: selective externalization of the receptor. *Cell* 33: 967-978.

27. Trajkovic, K., C. Hsu, S. Chiantia, L. Rajendran, D. Wenzel, F. Wieland, P. Schwille, B. Brugger, and M. Simons. 2008. Ceramide triggers budding of exosome vesicles into multivesicular endosomes. *Science* 319: 1244-1247.
28. van Dommelen, S. M., P. Vader, S. Lakhal, S. A. Kooijmans, W. W. van Solinge, M. J. Wood, and R. M. Schiffelers. 2012. Microvesicles and exosomes: opportunities for cell-derived membrane vesicles in drug delivery. *J. Control Release* 161: 635-644.
29. Hurley, J. H., E. Boura, L. A. Carlson, and B. Rozycki. 2010. Membrane budding. *Cell* 143: 875-887.
30. Conde-Vancells, J., E. Rodriguez-Suarez, N. Embade, D. Gil, R. Matthiesen, M. Valle, F. Elortza, S. C. Lu, J. M. Mato, and J. M. Falcon-Perez. 2008. Characterization and comprehensive proteome profiling of exosomes secreted by hepatocytes. *J. Proteome. Res.* 7: 5157-5166.
31. Subra, C., D. Grand, K. Laulagnier, A. Stella, G. Lambeau, M. Paillasse, M. P. De, B. Monsarrat, B. Perret, S. Silvente-Poirot, M. Poirot, and M. Record. 2010. Exosomes account for vesicle-mediated transcellular transport of activatable phospholipases and prostaglandins. *J. Lipid Res.* 51: 2105-2120.
32. Vlassov, A. V., S. Magdaleno, R. Setterquist, and R. Conrad. 2012. Exosomes: current knowledge of their composition, biological functions, and diagnostic and therapeutic potentials. *Biochim. Biophys. Acta* 1820: 940-948.
33. Vader, P., X. O. Breakefield, and M. J. Wood. 2014. Extracellular vesicles: emerging targets for cancer therapy. *Trends Mol. Med.*
34. Jemal, A., F. Bray, M. M. Center, J. Ferlay, E. Ward, and D. Forman. 2011. Global cancer statistics. *CA Cancer J Clin.* 61: 69-90.
35. Hsu, H. H., and N. P. Camacho. 1999. Isolation of calcifiable vesicles from human atherosclerotic aortas. *Atherosclerosis* 143: 353-362.
36. Chironi, G. N., C. M. Boulanger, A. Simon, F. gnat-George, J. M. Freyssinet, and A. Tedgui. 2009. Endothelial microparticles in diseases. *Cell Tissue Res.* 335: 143-151.
37. Amabile, N., C. Heiss, W. M. Real, P. Minasi, D. McGlothlin, E. J. Rame, W. Grossman, M. T. De, and Y. Yeghiazarians. 2008. Circulating endothelial microparticle levels predict hemodynamic severity of pulmonary hypertension. *Am. J Respir. Crit Care Med.* 177: 1268-1275.
38. Friend, C., W. Marovitz, G. Henie, W. Henie, D. Tsuei, K. Hirschhorn, J. G. Holland, and J. Cuttner. 1978. Observations on cell lines derived from a patient with Hodgkin's disease. *Cancer Res.* 38: 2581-2591.
39. Ginestra, A., P. La, F. Saladino, D. Cassara, H. Nagase, and M. L. Vittorelli. 1998. The amount and proteolytic content of vesicles shed by human cancer cell lines correlates with their in vitro invasiveness. *Anticancer Res.* 18: 3433-3437.

40. Kim, H. K., K. S. Song, Y. S. Park, Y. H. Kang, Y. J. Lee, K. R. Lee, H. K. Kim, K. W. Ryu, J. M. Bae, and S. Kim. 2003. Elevated levels of circulating platelet microparticles, VEGF, IL-6 and RANTES in patients with gastric cancer: possible role of a metastasis predictor. *Eur. J Cancer* 39: 184-191.
41. Zwicker, J. I., H. A. Liebman, D. Neuberg, R. Lacroix, K. A. Bauer, B. C. Furie, and B. Furie. 2009. Tumor-derived tissue factor-bearing microparticles are associated with venous thromboembolic events in malignancy. *Clin. Cancer Res.* 15: 6830-6840.
42. Boing, A. N., C. M. Hau, A. Sturk, and R. Nieuwland. 2008. Platelet microparticles contain active caspase 3. *Platelets.* 19: 96-103.
43. Sapet, C., S. Simoncini, B. Lloriod, D. Puthier, J. Sampol, C. Nguyen, F. gnat-George, and F. Anfosso. 2006. Thrombin-induced endothelial microparticle generation: identification of a novel pathway involving ROCK-II activation by caspase-2. *Blood* 108: 1868-1876.
44. bid Hussein, M. N., A. N. Boing, A. Sturk, C. M. Hau, and R. Nieuwland. 2007. Inhibition of microparticle release triggers endothelial cell apoptosis and detachment. *Thromb. Haemost.* 98: 1096-1107.
45. Shedden, K., X. T. Xie, P. Chandaroy, Y. T. Chang, and G. R. Rosania. 2003. Expulsion of small molecules in vesicles shed by cancer cells: association with gene expression and chemosensitivity profiles. *Cancer Res.* 63: 4331-4337.
46. Safaei, R., B. J. Larson, T. C. Cheng, M. A. Gibson, S. Otani, W. Naerdemann, and S. B. Howell. 2005. Abnormal lysosomal trafficking and enhanced exosomal export of cisplatin in drug-resistant human ovarian carcinoma cells. *Mol. Cancer Ther.* 4: 1595-1604.
47. Sims, P. J., E. M. Faioni, T. Wiedmer, and S. J. Shattil. 1988. Complement proteins C5b-9 cause release of membrane vesicles from the platelet surface that are enriched in the membrane receptor for coagulation factor Va and express prothrombinase activity. *J Biol Chem* 263: 18205-18212.
48. Whitlow, M. B., and L. M. Klein. 1997. Response of SCC-12F, a human squamous cell carcinoma cell line, to complement attack. *J Invest Dermatol.* 109: 39-45.
49. Carney, D. F., C. H. Hammer, and M. L. Shin. 1986. Elimination of terminal complement complexes in the plasma membrane of nucleated cells: influence of extracellular Ca²⁺ and association with cellular Ca²⁺. *J Immunol.* 137: 263-270.
50. Hakulinen, J., S. Junnikkala, T. Sorsa, and S. Meri. 2004. Complement inhibitor membrane cofactor protein (MCP; CD46) is constitutively shed from cancer cell membranes in vesicles and converted by a metalloproteinase to a functionally active soluble form. *Eur. J Immunol.* 34: 2620-2629.
51. Andreola, G., L. Rivoltini, C. Castelli, V. Huber, P. Perego, P. Deho, P. Squarcina, P. Accornero, F. Lozupone, L. Lugini, A. Stringaro, A. Molinari,

- G. Arancia, M. Gentile, G. Parmiani, and S. Fais. 2002. Induction of lymphocyte apoptosis by tumor cell secretion of FasL-bearing microvesicles. *J Exp. Med.* 195: 1303-1316.
52. Huber, V., S. Fais, M. Iero, L. Lugini, P. Canese, P. Squarcina, A. Zaccheddu, M. Colone, G. Arancia, M. Gentile, E. Seregni, R. Valenti, G. Ballabio, F. Belli, E. Leo, G. Parmiani, and L. Rivoltini. 2005. Human colorectal cancer cells induce T-cell death through release of proapoptotic microvesicles: role in immune escape. *Gastroenterology* 128: 1796-1804.
53. Keryer-Bibens, C., C. Pioche-Durieu, C. Villemant, S. Souquere, N. Nishi, M. Hirashima, J. Middeldorp, and P. Busson. 2006. Exosomes released by EBV-infected nasopharyngeal carcinoma cells convey the viral latent membrane protein 1 and the immunomodulatory protein galectin 9. *BMC Cancer* 6: 283.
54. Valenti, R., V. Huber, P. Filipazzi, L. Pilla, G. Sovena, A. Villa, A. Corbelli, S. Fais, G. Parmiani, and L. Rivoltini. 2006. Human tumor-released microvesicles promote the differentiation of myeloid cells with transforming growth factor-beta-mediated suppressive activity on T lymphocytes. *Cancer Res.* 66: 9290-9298.
55. Janowska-Wieczorek, A., M. Wysoczynski, J. Kijowski, L. Marquez-Curtis, B. Machalinski, J. Ratajczak, and M. Z. Ratajczak. 2005. Microvesicles derived from activated platelets induce metastasis and angiogenesis in lung cancer. *Int. J Cancer* 113: 752-760.
56. Janowska-Wieczorek, A., L. A. Marquez-Curtis, M. Wysoczynski, and M. Z. Ratajczak. 2006. Enhancing effect of platelet-derived microvesicles on the invasive potential of breast cancer cells. *Transfusion* 46: 1199-1209.
57. Graves, L. E., E. V. Ariztia, J. R. Navari, H. J. Matzel, M. S. Stack, and D. A. Fishman. 2004. Proinvasive properties of ovarian cancer ascites-derived membrane vesicles. *Cancer Res.* 64: 7045-7049.
58. Rauch, U., and S. Antoniak. 2007. Tissue factor-positive microparticles in blood associated with coagulopathy in cancer. *Thromb. Haemost.* 97: 9-10.
59. Hron, G., M. Kollars, H. Weber, V. Sagaster, P. Quehenberger, S. Eichinger, P. A. Kyrle, and A. Weltermann. 2007. Tissue factor-positive microparticles: cellular origin and association with coagulation activation in patients with colorectal cancer. *Thromb. Haemost.* 97: 119-123.
60. Baj-Krzyworzeka, M., R. Szatanek, K. Weglarczyk, J. Baran, B. Urbanowicz, P. Branski, M. Z. Ratajczak, and M. Zembala. 2006. Tumour-derived microvesicles carry several surface determinants and mRNA of tumour cells and transfer some of these determinants to monocytes. *Cancer Immunol. Immunother.* 55: 808-818.
61. Baj-Krzyworzeka, M., R. Szatanek, K. Weglarczyk, J. Baran, and M. Zembala. 2007. Tumour-derived microvesicles modulate biological activity of human monocytes. *Immunol. Lett.* 113: 76-82.

62. ROGERS, G. E. 1962. Occurrence of citrulline in proteins. *Nature* 194: 1149-1151.
63. Shirai, H., T. L. Blundell, and K. Mizuguchi. 2001. A novel superfamily of enzymes that catalyze the modification of guanidino groups. *Trends Biochem. Sci.* 26: 465-468.
64. Tarcsa, E., L. N. Marekov, G. Mei, G. Melino, S. C. Lee, and P. M. Steinert. 1996. Protein unfolding by peptidylarginine deiminase. Substrate specificity and structural relationships of the natural substrates trichohyalin and filaggrin. *J Biol Chem* 271: 30709-30716.
65. ROGERS, G. E., H. W. Harding, and I. J. Llewellyn-Smith. 1977. The origin of citrulline-containing proteins in the hair follicle and the chemical nature of trichohyalin, an intracellular precursor. *Biochim. Biophys. Acta* 495: 159-175.
66. Chavanas, S., M. C. Mechin, H. Takahara, A. Kawada, R. Nachat, G. Serre, and M. Simon. 2004. Comparative analysis of the mouse and human peptidylarginine deiminase gene clusters reveals highly conserved non-coding segments and a new human gene, PADI6. *Gene* 330: 19-27.
67. Vossenaar, E. R., S. Nijenhuis, M. M. Helsen, A. van der Heijden, T. Senshu, W. B. van den Berg, W. J. van Venrooij, and L. A. Joosten. 2003. Citrullination of synovial proteins in murine models of rheumatoid arthritis. *Arthritis Rheum.* 48: 2489-2500.
68. Ellsworth, R. E., A. Vertrees, B. Love, J. A. Hooke, D. L. Ellsworth, and C. D. Shriver. 2008. Chromosomal alterations associated with the transition from in situ to invasive breast cancer. *Ann. Surg. Oncol.* 15: 2519-2525.
69. Darrah, E., A. Rosen, J. T. Giles, and F. Andrade. 2012. Peptidylarginine deiminase 2, 3 and 4 have distinct specificities against cellular substrates: novel insights into autoantigen selection in rheumatoid arthritis. *Ann. Rheum. Dis.* 71: 92-98.
70. Knuckley, B., C. P. Causey, J. E. Jones, M. Bhatia, C. J. Dreyton, T. C. Osborne, H. Takahara, and P. R. Thompson. 2010. Substrate specificity and kinetic studies of PADs 1, 3, and 4 identify potent and selective inhibitors of protein arginine deiminase 3. *Biochemistry* 49: 4852-4863.
71. Terakawa, H., H. Takahara, and K. Sugawara. 1991. Three types of mouse peptidylarginine deiminase: characterization and tissue distribution. *J. Biochem.* 110: 661-666.
72. Senshu, T., K. Akiyama, A. Ishigami, and K. Nomura. 1999. Studies on specificity of peptidylarginine deiminase reactions using an immunochemical probe that recognizes an enzymatically deiminated partial sequence of mouse keratin K1. *J Dermatol. Sci.* 21: 113-126.
73. Watanabe, K., K. Akiyama, K. Hikichi, R. Ohtsuka, A. Okuyama, and T. Senshu. 1988. Combined biochemical and immunochemical comparison of peptidylarginine deiminases present in various tissues. *Biochim. Biophys. Acta* 966: 375-383.

74. Urano, Y., K. Watanabe, A. Sakaki, S. Arase, Y. Watanabe, F. Shigemi, K. Takeda, K. Akiyama, and T. Senshu. 1990. Immunohistochemical demonstration of peptidylarginine deiminase in human sweat glands. *Am. J Dermatopathol.* 12: 249-255.
75. Vossenaar, E. R., T. R. Radstake, H. A. van der, M. A. van Mansum, C. Dieteren, D. J. de Rooij, P. Barrera, A. J. Zendman, and W. J. van Venrooij. 2004. Expression and activity of citrullinating peptidylarginine deiminase enzymes in monocytes and macrophages. *Ann. Rheum. Dis.* 63: 373-381.
76. Pritzker, L. B., S. Joshi, G. Harauz, and M. A. Moscarello. 2000. Deimination of myelin basic protein. 2. Effect of methylation of MBP on its deimination by peptidylarginine deiminase. *Biochemistry* 39: 5382-5388.
77. Inagaki, M., Y. Nishi, K. Nishizawa, M. Matsuyama, and C. Sato. 1987. Site-specific phosphorylation induces disassembly of vimentin filaments in vitro. *Nature* 328: 649-652.
78. Moscarello, M. A., D. D. Wood, C. Ackerley, and C. Boulias. 1994. Myelin in multiple sclerosis is developmentally immature. *J. Clin. Invest* 94: 146-154.
79. Rogers, G., B. Winter, C. McLaughlan, B. Powell, and T. Nesci. 1997. Peptidylarginine Deiminase of the Hair Follicle: Characterization, Localization, and Function in Keratinizing Tissues. *J Investig Dermatol* 108: 700-707.
80. Wright, P. W., L. C. Bolling, M. E. Calvert, O. F. Sarmiento, E. V. Berkeley, M. C. Shea, Z. Hao, F. C. Jayes, L. A. Bush, J. Shetty, A. N. Shore, P. P. Reddi, K. S. Tung, E. Samy, M. M. Allietta, N. E. Sherman, J. C. Herr, and S. A. Coonrod. 2003. ePAD, an oocyte and early embryo-abundant peptidylarginine deiminase-like protein that localizes to egg cytoplasmic sheets. *Dev. Biol* 256: 73-88.
81. Esposito, G., A. M. Vitale, F. P. Leijten, A. M. Strik, A. M. Koonen-Reemst, P. Yurttas, T. J. Robben, S. Coonrod, and J. A. Gossen. 2007. Peptidylarginine deiminase (PAD) 6 is essential for oocyte cytoskeletal sheet formation and female fertility. *Mol. Cell Endocrinol.* 273: 25-31.
82. Nakashima, K., T. Hagiwara, and M. Yamada. 2002. Nuclear localization of peptidylarginine deiminase V and histone deimination in granulocytes. *J Biol Chem* 277: 49562-49568.
83. Asaga, H., K. Nakashima, T. Senshu, A. Ishigami, and M. Yamada. 2001. Immunocytochemical localization of peptidylarginine deiminase in human eosinophils and neutrophils. *J Leukoc. Biol* 70: 46-51.
84. Nakashima, K., T. Hagiwara, A. Ishigami, S. Nagata, H. Asaga, M. Kuramoto, T. Senshu, and M. Yamada. 1999. Molecular characterization of peptidylarginine deiminase in HL-60 cells induced by retinoic acid and 1 α ,25-dihydroxyvitamin D(3). *J Biol Chem* 274: 27786-27792.

85. Cherrington, B. D., X. Zhang, J. L. McElwee, E. Morency, L. J. Anguish, and S. A. Coonrod. 2012. Potential role for PAD2 in gene regulation in breast cancer cells. *PLoS. One.* 7: e41242.
86. KP, U., V. Subramanian, A. P. Nicholas, P. R. Thompson, and P. Ferretti. 2014. Modulation of calcium-induced cell death in human neural stem cells by the novel peptidylarginine deiminase-AIF pathway. *Biochim. Biophys. Acta* 1843: 1162-1171.
87. Lange, S., S. Gogel, K. Y. Leung, B. Vernay, A. P. Nicholas, C. P. Causey, P. R. Thompson, N. D. Greene, and P. Ferretti. 2011. Protein deiminases: new players in the developmentally regulated loss of neural regenerative ability. *Dev. Biol.* 355: 205-214.
88. Mastronardi, F. G., D. D. Wood, J. Mei, R. Raijmakers, V. Tseveleki, H. M. Dosch, L. Probert, P. Casaccia-Bonnel, and M. A. Moscarello. 2006. Increased citrullination of histone H3 in multiple sclerosis brain and animal models of demyelination: a role for tumor necrosis factor-induced peptidylarginine deiminase 4 translocation. *J. Neurosci.* 26: 11387-11396.
89. Luo, Y., K. Arita, M. Bhatia, B. Knuckley, Y. H. Lee, M. R. Stallcup, M. Sato, and P. R. Thompson. 2006. Inhibitors and inactivators of protein arginine deiminase 4: functional and structural characterization. *Biochemistry* 45: 11727-11736.
90. Cuthbert, G. L., S. Daujat, A. W. Snowden, H. Erdjument-Bromage, T. Hagihara, M. Yamada, R. Schneider, P. D. Gregory, P. Tempst, A. J. Bannister, and T. Kouzarides. 2004. Histone deimination antagonizes arginine methylation. *Cell* 118: 545-553.
91. Anzilotti, C., F. Pratesi, C. Tommasi, and P. Migliorini. 2010. Peptidylarginine deiminase 4 and citrullination in health and disease. *Autoimmun. Rev.* 9: 158-160.
92. Anzilotti, C., G. Merlini, F. Pratesi, C. Tommasi, D. Chimenti, and P. Migliorini. 2006. Antibodies to viral citrullinated peptide in rheumatoid arthritis. *J Rheumatol.* 33: 647-651.
93. Migliorini, P., F. Pratesi, C. Tommasi, and C. Anzilotti. 2005. The immune response to citrullinated antigens in autoimmune diseases. *Autoimmun. Rev.* 4: 561-564.
94. Ishida-Yamamoto, A., T. Senshu, H. Takahashi, K. Akiyama, K. Nomura, and H. Iizuka. 2000. Decreased deiminated keratin K1 in psoriatic hyperproliferative epidermis. *J Invest Dermatol* 114: 701-705.
95. van Boekel, M. A., E. R. Vossenaar, F. H. van den Hoogen, and W. J. van Venrooij. 2002. Autoantibody systems in rheumatoid arthritis: specificity, sensitivity and diagnostic value. *Arthritis Res.* 4: 87-93.
96. van Venrooij, W. J., J. M. Hazes, and H. Visser. 2002. Anticitrullinated protein/peptide antibody and its role in the diagnosis and prognosis of early rheumatoid arthritis. *Neth. J Med.* 60: 383-388.

97. Meyer, O., C. Labarre, M. Dougados, P. Goupille, A. Cantagrel, A. Dubois, P. Nicaise-Roland, J. Sibilia, and B. Combe. 2003. Anticitrullinated protein/peptide antibody assays in early rheumatoid arthritis for predicting five year radiographic damage. *Ann. Rheum. Dis.* 62: 120-126.
98. Smeets, T. J., E. R. Vossenaar, W. J. van Venrooij, and P. P. Tak. 2002. Is expression of intracellular citrullinated proteins in synovial tissue specific for rheumatoid arthritis? Comment on the article by Baeten et al. *Arthritis Rheum.* 46: 2824-2826.
99. Masson-Bessiere, C., M. Sebbag, E. Girbal-Neuhausser, L. Nogueira, C. Vincent, T. Senshu, and G. Serre. 2001. The major synovial targets of the rheumatoid arthritis-specific anti-flaggrin autoantibodies are deiminated forms of the alpha- and beta-chains of fibrin. *J Immunol.* 166: 4177-4184.
100. Boggs, J. M., G. Rangaraj, K. M. Koshy, C. Ackerley, D. D. Wood, and M. A. Moscarello. 1999. Highly deiminated isoform of myelin basic protein from multiple sclerosis brain causes fragmentation of lipid vesicles. *J Neurosci. Res.* 57: 529-535.
101. Pritzker, L. B., S. Joshi, J. J. Gowan, G. Harauz, and M. A. Moscarello. 2000. Deimination of myelin basic protein. 1. Effect of deimination of arginyl residues of myelin basic protein on its structure and susceptibility to digestion by cathepsin D. *Biochemistry* 39: 5374-5381.
102. Cao, L., R. Goodin, D. Wood, M. A. Moscarello, and J. N. Whitaker. 1999. Rapid release and unusual stability of immunodominant peptide 45-89 from citrullinated myelin basic protein. *Biochemistry* 38: 6157-6163.
103. Pritzker, L. B., and M. A. Moscarello. 1998. A novel microtubule independent effect of paclitaxel: the inhibition of peptidylarginine deiminase from bovine brain. *Biochim. Biophys. Acta* 1388: 154-160.
104. Moscarello, M. A., B. Mak, T. A. Nguyen, D. D. Wood, F. Mastronardi, and S. K. Ludwin. 2002. Paclitaxel (Taxol) attenuates clinical disease in a spontaneously demyelinating transgenic mouse and induces remyelination. *Mult. Scler.* 8: 130-138.
105. Chang, X., J. Han, L. Pang, Y. Zhao, Y. Yang, and Z. Shen. 2009. Increased PADI4 expression in blood and tissues of patients with malignant tumors. *BMC. Cancer* 9: 40.
106. Wang, L., X. Chang, G. Yuan, Y. Zhao, and P. Wang. 2010. Expression of peptidylarginine deiminase type 4 in ovarian tumors. *Int. J Biol Sci.* 6: 454-464.
107. Chang, X., and J. Han. 2006. Expression of peptidylarginine deiminase type 4 (PAD4) in various tumors. *Mol. Carcinog.* 45: 183-196.
108. Wang, Y., J. Wysocka, J. Sayegh, Y. H. Lee, J. R. Perlin, L. Leonelli, L. S. Sonbuchner, C. H. McDonald, R. G. Cook, Y. Dou, R. G. Roeder, S. Clarke, M. R. Stallcup, C. D. Allis, and S. A. Coonrod. 2004. Human PAD4 regulates

- histone arginine methylation levels via demethylination. *Science* 306: 279-283.
109. Zhang, X., M. J. Gamble, S. Stadler, B. D. Cherrington, C. P. Causey, P. R. Thompson, M. S. Roberson, W. L. Kraus, and S. A. Coonrod. 2011. Genome-wide analysis reveals PADI4 cooperates with Elk-1 to activate c-Fos expression in breast cancer cells. *PLoS. Genet.* 7: e1002112.
 110. Tanikawa, C., K. Ueda, H. Nakagawa, N. Yoshida, Y. Nakamura, and K. Matsuda. 2009. Regulation of protein Citrullination through p53/PADI4 network in DNA damage response. *Cancer Res.* 69: 8761-8769.
 111. Guo, Q., and W. Fast. 2011. Citrullination of inhibitor of growth 4 (ING4) by peptidylarginine deminase 4 (PAD4) disrupts the interaction between ING4 and p53. *J Biol. Chem.* 286: 17069-17078.
 112. Yao, H., P. Li, B. J. Venters, S. Zheng, P. R. Thompson, B. F. Pugh, and Y. Wang. 2008. Histone Arg modifications and p53 regulate the expression of OKL38, a mediator of apoptosis. *J Biol. Chem.* 283: 20060-20068.
 113. Li, P., H. Yao, Z. Zhang, M. Li, Y. Luo, P. R. Thompson, D. S. Gilmour, and Y. Wang. 2008. Regulation of p53 target gene expression by peptidylarginine deiminase 4. *Mol. Cell Biol.* 28: 4745-4758.
 114. Razak, A. R., R. Chhabra, A. Hughes, S. England, P. Dildey, and R. McMenemin. 2007. Muscular metastasis, a rare presentation of non-small-cell lung cancer. *MedGenMed.* 9: 20.
 115. Herring, C. L., Jr., J. M. Harrelson, and S. P. Scully. 1998. Metastatic carcinoma to skeletal muscle. A report of 15 patients. *Clin. Orthop. Relat Res.* 272-281.
 116. Plaza, J. A., D. Perez-Montiel, J. Mayerson, C. Morrison, and S. Suster. 2008. Metastases to soft tissue: a review of 118 cases over a 30-year period. *Cancer* 112: 193-203.
 117. Seely, S. 1980. Possible reasons for the high resistance of muscle to cancer. *Med. Hypotheses* 6: 133-137.
 118. Pouyssegur, J., A. Franchi, and G. Pages. 2001. pHi, aerobic glycolysis and vascular endothelial growth factor in tumour growth. *Novartis. Found. Symp.* 240: 186-196.
 119. Djaldetti, M., B. Sredni, R. Zigelman, M. Verber, and P. Fishman. 1996. Muscle cells produce a low molecular weight factor with anti-cancer activity. *Clin. Exp. Metastasis* 14: 189-196.
 120. Fishman, P., S. Bar-Yehuda, and L. Vagman. 1998. Adenosine and other low molecular weight factors released by muscle cells inhibit tumor cell growth. *Cancer Res.* 58: 3181-3187.

121. Luo, C., Y. Jiang, Y. Liu, and X. Li. 2002. Experimental study on mechanism and rarity of metastases in skeletal muscle. *Chin Med. J. (Engl.)* 115: 1645-1649.
122. Shurin, M. R. 1996. Dendritic cells presenting tumor antigen. *Cancer Immunol. Immunother.* 43: 158-164.
123. Steinman, R. M. 1991. The dendritic cell system and its role in immunogenicity. *Annu. Rev. Immunol.* 9: 271-296.
124. Satpathy, A. T., X. Wu, J. C. Albring, and K. M. Murphy. 2013. Re(de)fining the dendritic cell lineage. *Nat. Immunol.* 14: 413.
125. Lutz, M. B., and G. Schuler. 2002. Immature, semi-mature and fully mature dendritic cells: which signals induce tolerance or immunity? *Trends Immunol.* 23: 445-449.
126. Mahnke, K., E. Schmitt, L. Bonifaz, A. H. Enk, and H. Jonuleit. 2002. Immature, but not inactive: the tolerogenic function of immature dendritic cells. *Immunol. Cell Biol.* 80: 477-483.
127. Manicassamy, S., and B. Pulendran. 2011. Dendritic cell control of tolerogenic responses. *Immunol. Rev.* 241: 206-227.
128. Bjorck, P., H. X. Leong, and E. G. Engleman. 2011. Plasmacytoid dendritic cell dichotomy: identification of IFN-alpha producing cells as a phenotypically and functionally distinct subset. *J. Immunol.* 186: 1477-1485.
129. Reizis, B., M. Colonna, G. Trinchieri, F. Barrat, and M. Gilliet. 2011. Plasmacytoid dendritic cells: one-trick ponies or workhorses of the immune system? *Nat. Rev. Immunol.* 11: 558-565.
130. Vermi, W., M. Soncini, L. Melocchi, S. Sozzani, and F. Facchetti. 2011. Plasmacytoid dendritic cells and cancer. *J. Leukoc. Biol.* 90: 681-690.
131. Lin, A., A. Schildknecht, L. T. Nguyen, and P. S. Ohashi. 2010. Dendritic cells integrate signals from the tumor microenvironment to modulate immunity and tumor growth. *Immunology Letters* 127: 77-84.
132. Shurin, M. R., G. V. Shurin, A. Lokshin, Z. R. Yurkovetsky, D. W. Gutkin, G. Chatta, H. Zhong, B. Han, and R. L. Ferris. 2006. Intratumoral cytokines/chemokines/growth factors and tumor infiltrating dendritic cells: friends or enemies? *Cancer Metastasis Rev.* 25: 333-356.
133. Lotze, M. T. 1997. Getting to the source: dendritic cells as therapeutic reagents for the treatment of patients with cancer. *Ann. Surg.* 226: 1-5.
134. Lijun, Z., Z. Xin, S. Danhua, L. Xiaoping, W. Jianliu, W. Huilan, and W. Lihui. 2012. Tumor-infiltrating dendritic cells may be used as clinicopathologic prognostic factors in endometrial carcinoma. *Int. J. Gynecol. Cancer* 22: 836-841.

135. Nestor, M. S., and A. J. Cochran. 1987. Identification and quantification of subsets of mononuclear inflammatory cells in melanocytic and other human tumors. *Pigment Cell Res.* 1: 22-27.
136. Reichert, T. E., C. Scheuer, R. Day, W. Wagner, and T. L. Whiteside. 2001. The number of intratumoral dendritic cells and zeta-chain expression in T cells as prognostic and survival biomarkers in patients with oral carcinoma. *Cancer* 91: 2136-2147.
137. Poppema, S., E. B. Brocker, L. L. de, D. Terbrack, T. Visscher, H. A. Ter, E. Macher, T. H. The, and C. Sorg. 1983. In situ analysis of the mononuclear cell infiltrate in primary malignant melanoma of the skin. *Clin. Exp. Immunol.* 51: 77-82.
138. Schrama, D., S. P. Thor, W. H. Fischer, A. D. McLellan, E. B. Brocker, R. A. Reisfeld, and J. C. Becker. 2001. Targeting of lymphotoxin-alpha to the tumor elicits an efficient immune response associated with induction of peripheral lymphoid-like tissue. *Immunity.* 14: 111-121.
139. Thompson, E. D., H. L. Enriquez, Y. X. Fu, and V. H. Engelhard. 2010. Tumor masses support naive T cell infiltration, activation, and differentiation into effectors. *J. Exp. Med.* 207: 1791-1804.
140. Gatter, K. C., H. B. Morris, B. Roach, P. Mortimer, K. A. Fleming, and D. Y. Mason. 1984. Langerhans' cells and T cells in human skin tumours: an immunohistological study. *Histopathology* 8: 229-244.
141. Toriyama, K., D. R. Wen, E. Paul, and A. J. Cochran. 1993. Variations in the distribution, frequency, and phenotype of Langerhans cells during the evolution of malignant melanoma of the skin. *J. Invest Dermatol.* 100: 269S-273S.
142. Esche, C., A. Lokshin, G. V. Shurin, B. R. Gastman, H. Rabinowich, S. C. Watkins, M. T. Lotze, and M. R. Shurin. 1999. Tumor's other immune targets: dendritic cells. *J. Leukoc. Biol.* 66: 336-344.
143. Peguet-Navarro, J., M. Sportouch, I. Popa, O. Berthier, D. Schmitt, and J. Portoukalian. 2003. Gangliosides from human melanoma tumors impair dendritic cell differentiation from monocytes and induce their apoptosis. *J. Immunol.* 170: 3488-3494.
144. Kiertscher, S. M., J. Luo, S. M. Dubinett, and M. D. Roth. 2000. Tumors promote altered maturation and early apoptosis of monocyte-derived dendritic cells. *J. Immunol.* 164: 1269-1276.
145. Yang, T., T. F. Witham, L. Villa, M. Erff, J. Attanucci, S. Watkins, D. Kondziolka, H. Okada, I. F. Pollack, and W. H. Chambers. 2002. Glioma-associated hyaluronan induces apoptosis in dendritic cells via inducible nitric oxide synthase: implications for the use of dendritic cells for therapy of gliomas. *Cancer Res.* 62: 2583-2591.

146. Katsenelson, N. S., G. V. Shurin, S. N. Bykovskaia, J. Shogan, and M. R. Shurin. 2001. Human small cell lung carcinoma and carcinoid tumor regulate dendritic cell maturation and function. *Mod. Pathol.* 14: 40-45.
147. Pinzon-Charry, A., T. Maxwell, M. A. McGuckin, C. Schmidt, C. Furnival, and J. A. Lopez. 2006. Spontaneous apoptosis of blood dendritic cells in patients with breast cancer. *Breast Cancer Res.* 8: R5.
148. Banchereau, J., F. Briere, C. Caux, J. Davoust, S. Lebecque, Y. J. Liu, B. Pulendran, and K. Palucka. 2000. Immunobiology of dendritic cells. *Annu. Rev. Immunol.* 18: 767-811.
149. Chaux, P., M. Moutet, J. Faivre, F. Martin, and M. Martin. 1996. Inflammatory cells infiltrating human colorectal carcinomas express HLA class II but not B7-1 and B7-2 costimulatory molecules of the T-cell activation. *Lab Invest* 74: 975-983.
150. Makarenkova, V. P., G. V. Shurin, I. L. Tourkova, L. Balkir, G. Pirtskhalaishvili, L. Perez, V. Gerein, J. M. Siegfried, and M. R. Shurin. 2003. Lung cancer-derived bombesin-like peptides down-regulate the generation and function of human dendritic cells. *J. Neuroimmunol.* 145: 55-67.
151. Shurin, M. R., Z. R. Yurkovetsky, I. L. Tourkova, L. Balkir, and G. V. Shurin. 2002. Inhibition of CD40 expression and CD40-mediated dendritic cell function by tumor-derived IL-10. *Int. J. Cancer* 101: 61-68.
152. Tourkova, I. L., G. V. Shurin, S. Wei, and M. R. Shurin. 2007. Small rho GTPases mediate tumor-induced inhibition of endocytic activity of dendritic cells. *J. Immunol.* 178: 7787-7793.
153. Tourkova, I. L., G. V. Shurin, G. S. Chatta, L. Perez, J. Finke, T. L. Whiteside, S. Ferrone, and M. R. Shurin. 2005. Restoration by IL-15 of MHC class I antigen-processing machinery in human dendritic cells inhibited by tumor-derived gangliosides. *J. Immunol.* 175: 3045-3052.
154. Enk, A. H., H. Jonuleit, J. Saloga, and J. Knop. 1997. Dendritic cells as mediators of tumor-induced tolerance in metastatic melanoma. *Int. J. Cancer* 73: 309-316.
155. Lizee, G., L. G. Radvanyi, W. W. Overwijk, and P. Hwu. 2006. Improving antitumor immune responses by circumventing immunoregulatory cells and mechanisms. *Clin. Cancer Res.* 12: 4794-4803.
156. Hawiger, D., K. Inaba, Y. Dorsett, M. Guo, K. Mahnke, M. Rivera, J. V. Ravetch, R. M. Steinman, and M. C. Nussenzweig. 2001. Dendritic cells induce peripheral T cell unresponsiveness under steady state conditions in vivo. *J. Exp. Med.* 194: 769-779.
157. Jonuleit, H., E. Schmitt, G. Schuler, J. Knop, and A. H. Enk. 2000. Induction of interleukin 10-producing, nonproliferating CD4(+) T cells with regulatory properties by repetitive stimulation with allogeneic immature human dendritic cells. *J. Exp. Med.* 192: 1213-1222.

158. Ma, Y., G. V. Shurin, D. W. Gutkin, and M. R. Shurin. 2012. Tumor associated regulatory dendritic cells. *Semin. Cancer Biol.* 22: 298-306.
159. Ghiringhelli, F., P. E. Puig, S. Roux, A. Parcellier, E. Schmitt, E. Solary, G. Kroemer, F. Martin, B. Chauffert, and L. Zitvogel. 2005. Tumor cells convert immature myeloid dendritic cells into TGF-beta-secreting cells inducing CD4+CD25+ regulatory T cell proliferation. *J. Exp. Med.* 202: 919-929.
160. Schmidt, J., C. Klempf, M. W. Buchler, and A. Marten. 2006. Release of iC3b from apoptotic tumor cells induces tolerance by binding to immature dendritic cells in vitro and in vivo. *Cancer Immunol. Immunother.* 55: 31-38.
161. Paidassi, H., P. Tacnet-Delorme, G. J. Arlaud, and P. Frchet. 2009. How phagocytes track down and respond to apoptotic cells. *Crit Rev. Immunol.* 29: 111-130.
162. Demaria, S., N. Bhardwaj, W. H. McBride, and S. C. Formenti. 2005. Combining radiotherapy and immunotherapy: a revived partnership. *Int. J. Radiat. Oncol. Biol. Phys.* 63: 655-666.
163. Steinman, R. M., and M. Pope. 2002. Exploiting dendritic cells to improve vaccine efficacy. *J. Clin. Invest* 109: 1519-1526.
164. Takizawa, F., S. Tsuji, and S. Nagasawa. 1996. Enhancement of macrophage phagocytosis upon iC3b deposition on apoptotic cells. *FEBS Lett.* 397: 269-272.
165. Pittoni, V., and G. Valesini. 2002. The clearance of apoptotic cells: implications for autoimmunity. *Autoimmun. Rev.* 1: 154-161.
166. Sohn, J. H., P. S. Bora, H. J. Suk, H. Molina, H. J. Kaplan, and N. S. Bora. 2003. Tolerance is dependent on complement C3 fragment iC3b binding to antigen-presenting cells. *Nat. Med.* 9: 206-212.
167. Kim, H. K., K. S. Song, J. H. Chung, K. R. Lee, and S. N. Lee. 2004. Platelet microparticles induce angiogenesis in vitro. *Br. J Haematol.* 124: 376-384.
168. Roos, M. A., L. Gennero, T. Denysenko, S. Reguzzi, G. Cavallo, G. P. Pescarmona, and A. Ponzetto. 2010. Microparticles in physiological and in pathological conditions. *Cell Biochem. Funct.* 28: 539-548.
169. Castellana, D., F. Toti, and J. M. Freyssinet. 2010. Membrane microvesicles: macromessengers in cancer disease and progression. *Thromb. Res.* 125 Suppl 2: S84-S88.
170. Kuhlmann, I. 1995. The prophylactic use of antibiotics in cell culture. *Cytotechnology* 19: 95-105.
171. Lozzio, B. B., C. B. Lozzio, E. G. Bamberger, and A. S. Feliu. 1981. A Multipotential Leukemia Cell Line (K-562) of Human Origin. *Proceedings of the Society for Experimental Biology and Medicine. Society for Experimental Biology and Medicine (New York, N. Y.)* 166: 546-550.

172. Heywood, W. E., P. Mills, S. Grunewald, V. Worthington, J. Jaeken, G. Carreno, H. Lemonde, P. T. Clayton, and K. Mills. 2013. A new method for the rapid diagnosis of protein N-linked congenital disorders of glycosylation. *J. Proteome. Res.* 12: 3471-3479.
173. Manwaring, V., W. E. Heywood, R. Clayton, R. H. Lachmann, J. Keutzer, P. Hindmarsh, B. Winchester, S. Heales, and K. Mills. 2013. The identification of new biomarkers for identifying and monitoring kidney disease and their translation into a rapid mass spectrometry-based test: evidence of presymptomatic kidney disease in pediatric Fabry and type-I diabetic patients. *J. Proteome. Res.* 12: 2013-2021.
174. Antwi-Baffour, S., S. Kholia, Y. K. Aryee, E. A. Ansa-Addo, D. Stratton, S. Lange, and J. M. Inal. 2010. Human plasma membrane-derived vesicles inhibit the phagocytosis of apoptotic cells--possible role in SLE. *Biochem. Biophys. Res. Commun.* 398: 278-283.
175. Biancone, L., S. Bruno, M. C. Deregibus, C. Tetta, and G. Camussi. 2012. Therapeutic potential of mesenchymal stem cell-derived microvesicles. *Nephrol. Dial. Transplant.* 27: 3037-3042.
176. Lee, Y., A. S. El, and M. J. Wood. 2012. Exosomes and microvesicles: extracellular vesicles for genetic information transfer and gene therapy. *Hum. Mol. Genet.* 21: R125-R134.
177. Reynolds, E. S. 1963. The use of lead citrate at high pH as an electron-opaque stain in electron microscopy. *J. Cell Biol.* 17: 208-212.
178. Cestari, I. d. S., E. Ansa-Addo, P. Pathak, M. Ramirez, and J. Inal. 2008. The intracellular Trypanosoma cruzi induces the release from monocytes of plasma membrane-derived microvesicles which protect the parasite from host complement. *Molecular Immunology* 45: 4173.
179. Kalra, H., R. J. Simpson, H. Ji, E. Aikawa, P. Altevogt, P. Askenase, V. C. Bond, F. E. Borrás, X. Breakefield, V. Budnik, E. Buzas, G. Camussi, A. Clayton, E. Cocucci, J. M. Falcon-Perez, S. Gabrielsson, Y. S. Gho, D. Gupta, H. C. Harsha, A. Hendrix, A. F. Hill, J. M. Inal, G. Jenster, E. M. Kramer-Albers, S. K. Lim, A. Llorente, J. Lotvall, A. Marcilla, L. Mincheva-Nilsson, I. Nazarenko, R. Nieuwland, E. N. Nolte-'t Hoen, A. Pandey, T. Patel, M. G. Piper, S. Pluchino, T. S. Prasad, L. Rajendran, G. Raposo, M. Record, G. E. Reid, F. Sanchez-Madrid, R. M. Schiffelers, P. Siljander, A. Stensballe, W. Stoorvogel, D. Taylor, C. Thery, H. Valadi, B. W. van Balkom, J. Vazquez, M. Vidal, M. H. Wauben, M. Yanez-Mo, M. Zoeller, and S. Mathivanan. 2012. Vesiclepedia: a compendium for extracellular vesicles with continuous community annotation. *PLoS. Biol.* 10: e1001450.
180. Huang, F., D. Kirkpatrick, X. Jiang, S. Gygi, and A. Sorkin. 2006. Differential regulation of EGF receptor internalization and degradation by multiubiquitination within the kinase domain. *Mol. Cell* 21: 737-748.
181. Komander, D. 2009. The emerging complexity of protein ubiquitination. *Biochem. Soc. Trans.* 37: 937-953.

182. Ascenzi, P., L. Leboffe, and F. Polticelli. 2013. Reactivity of the human hemoglobin "dark side". *IUBMB. Life* 65: 121-126.
183. Sonnemann, K. J., D. P. Fitzsimons, J. R. Patel, Y. Liu, M. F. Schneider, R. L. Moss, and J. M. Ervasti. 2006. Cytoplasmic gamma-actin is not required for skeletal muscle development but its absence leads to a progressive myopathy. *Dev. Cell* 11: 387-397.
184. Hong, B. S., J. H. Cho, H. Kim, E. J. Choi, S. Rho, J. Kim, J. H. Kim, D. S. Choi, Y. K. Kim, D. Hwang, and Y. S. Gho. 2009. Colorectal cancer cell-derived microvesicles are enriched in cell cycle-related mRNAs that promote proliferation of endothelial cells. *BMC. Genomics* 10: 556.
185. Miguet, L., K. Pacaud, C. Felden, B. Hugel, M. C. Martinez, J. M. Freyssinet, R. Herbrecht, N. Potier, D. A. van, and L. Mauvieux. 2006. Proteomic analysis of malignant lymphocyte membrane microparticles using double ionization coverage optimization. *Proteomics*. 6: 153-171.
186. Koga, K., K. Matsumoto, T. Akiyoshi, M. Kubo, N. Yamanaka, A. Tasaki, H. Nakashima, M. Nakamura, S. Kuroki, M. Tanaka, and M. Katano. 2005. Purification, characterization and biological significance of tumor-derived exosomes. *Anticancer Res.* 25: 3703-3707.
187. Pannekoek, W. J., J. R. Linnemann, P. M. Brouwer, J. L. Bos, and H. Rehmann. 2013. Rap1 and Rap2 antagonistically control endothelial barrier resistance. *PLoS. One.* 8: e57903.
188. Raymond, A., M. A. Ensslin, and B. D. Shur. 2009. SED1/MFG-E8: a bi-motif protein that orchestrates diverse cellular interactions. *J. Cell Biochem.* 106: 957-966.
189. Zhang, H. L., J. Wu, and J. Zhu. 2010. The role of apolipoprotein E in Guillain-Barre syndrome and experimental autoimmune neuritis. *J. Biomed. Biotechnol.* 2010: 357412.
190. Guimaraes-Ferreira, L. 2014. Role of the phosphocreatine system on energetic homeostasis in skeletal and cardiac muscles. *Einstein. (Sao Paulo)* 12: 126-131.
191. Xie, X., Z. Gong, V. Mansuy-Aubert, Q. L. Zhou, S. A. Tatulian, D. Sehart, F. Gnad, L. M. Brill, K. Motamedchaboki, Y. Chen, M. P. Czech, M. Mann, M. Kruger, and Z. Y. Jiang. 2011. C2 domain-containing phosphoprotein CDP138 regulates GLUT4 insertion into the plasma membrane. *Cell Metab* 14: 378-389.
192. El, H. M., E. Jean, A. Turki, G. Hugon, B. Vernus, A. Bonnieu, E. Passerieux, A. Hamade, J. Mercier, D. Laoudj-Chenivresse, and G. Carnac. 2012. Glutathione peroxidase 3, a new retinoid target gene, is crucial for human skeletal muscle precursor cell survival. *J. Cell Sci.* 125: 6147-6156.
193. Raab, M., T. M. Boeckers, and W. L. Neuhuber. 2010. Proline-rich synapse-associated protein-1 and 2 (ProSAP1/Shank2 and ProSAP2/Shank3)-

- scaffolding proteins are also present in postsynaptic specializations of the peripheral nervous system. *Neuroscience* 171: 421-433.
194. Sottrup-Jensen, L. 1989. Alpha-macroglobulins: structure, shape, and mechanism of proteinase complex formation. *J. Biol. Chem.* 264: 11539-11542.
 195. Feige, J. J., A. Negoescu, M. Keramidas, S. Souchelnitskiy, and E. M. Chambaz. 1996. Alpha 2-macroglobulin: a binding protein for transforming growth factor-beta and various cytokines. *Horm. Res.* 45: 227-232.
 196. Sun, H. Q., M. Yamamoto, M. Mejillano, and H. L. Yin. 1999. Gelsolin, a multifunctional actin regulatory protein. *J. Biol. Chem.* 274: 33179-33182.
 197. Mazumdar, B., K. Meyer, and R. Ray. 2012. N-terminal region of gelsolin induces apoptosis of activated hepatic stellate cells by a caspase-dependent mechanism. *PLoS. One.* 7: e44461.
 198. Li, P., D. Wang, H. Yao, P. Doret, G. Hao, Q. Shen, H. Qiu, X. Zhang, Y. Wang, G. Chen, and Y. Wang. 2010. Coordination of PAD4 and HDAC2 in the regulation of p53-target gene expression. *Oncogene* 29: 3153-3162.
 199. McElwee, J. L., S. Mohanan, O. L. Griffith, H. C. Breuer, L. J. Anguish, B. D. Cherrington, A. M. Palmer, L. R. Howe, V. Subramanian, C. P. Causey, P. R. Thompson, J. W. Gray, and S. A. Coonrod. 2012. Identification of PADI2 as a potential breast cancer biomarker and therapeutic target. *BMC. Cancer* 12: 500.
 200. Nicholas, A. P., and J. N. Whitaker. 2002. Preparation of a monoclonal antibody to citrullinated epitopes: its characterization and some applications to immunohistochemistry in human brain. *Glia* 37: 328-336.
 201. Pizzirani, C., D. Ferrari, P. Chiozzi, E. Adinolfi, D. Sandona, E. Savaglio, and V. F. Di. 2007. Stimulation of P2 receptors causes release of IL-1beta-loaded microvesicles from human dendritic cells. *Blood* 109: 3856-3864.
 202. Latham, S. L., C. Chaponnier, V. Dugina, P. O. Couraud, G. E. Grau, and V. Combes. 2013. Cooperation between beta- and gamma-cytoplasmic actins in the mechanical regulation of endothelial microparticle formation. *FASEB J.* 27: 672-683.
 203. Wieland, T., H. J. Hippe, K. Ludwig, X. B. Zhou, M. Korth, and S. Klumpp. 2010. Reversible histidine phosphorylation in mammalian cells: a teeter-totter formed by nucleoside diphosphate kinase and protein histidine phosphatase 1. *Methods Enzymol.* 471: 379-402.
 204. Postel, E. H., S. J. Berberich, S. J. Flint, and C. A. Ferrone. 1993. Human c-myc transcription factor PuF identified as nm23-H2 nucleoside diphosphate kinase, a candidate suppressor of tumor metastasis. *Science* 261: 478-480.
 205. Uniprot. 2014. UniProt.

206. Ercolani, L., B. Florence, M. Denaro, and M. Alexander. 1988. Isolation and complete sequence of a functional human glyceraldehyde-3-phosphate dehydrogenase gene. *J. Biol. Chem.* 263: 15335-15341.
207. Tisdale, E. J. 2001. Glyceraldehyde-3-phosphate dehydrogenase is required for vesicular transport in the early secretory pathway. *J. Biol. Chem.* 276: 2480-2486.
208. Bebawy, M., V. Combes, E. Lee, R. Jaiswal, J. Gong, A. Bonhoure, and G. E. Grau. 2009. Membrane microparticles mediate transfer of P-glycoprotein to drug sensitive cancer cells. *Leukemia* 23: 1643-1649.
209. Jorfi, S., and J. M. Inal. 2013. The role of microvesicles in cancer progression and drug resistance. *Biochem. Soc. Trans.* 41: 293-298.
210. Slack, J. L., C. P. Causey, and P. R. Thompson. 2011. Protein arginine deiminase 4: a target for an epigenetic cancer therapy. *Cell Mol. Life Sci.* 68: 709-720.
211. Palucka, K., and J. Banchereau. 2012. Cancer immunotherapy via dendritic cells. *Nat. Rev. Cancer* 12: 265-277.
212. Reinhard, G., A. Marten, S. M. Kiske, F. Feil, T. Bieber, and I. G. Schmidt-Wolf. 2002. Generation of dendritic cell-based vaccines for cancer therapy. *Br. J. Cancer* 86: 1529-1533.
213. Asada, H., T. Kishida, H. Hirai, J. Imanishi, and O. Mazda. 2004. 262. Dendritic Cell (DC) Vaccine Loaded with Apoptotic Tumor Fragments Effectively Suppress Preestablished Malignant Melanoma in Mice. *Mol Ther* 9: S100-S101.
214. Kokhaei, P., M. R. Rezvany, L. Virving, A. Choudhury, H. Rabbani, A. Osterborg, and H. Mellstedt. 2003. Dendritic cells loaded with apoptotic tumour cells induce a stronger T-cell response than dendritic cell-tumour hybrids in B-CLL. *Leukemia* 17: 894-899.
215. Chaux, P., N. Favre, B. Bonnotte, M. Moutet, M. Martin, and F. Martin. 1997. Tumor-infiltrating dendritic cells are defective in their antigen-presenting function and inducible B7 expression. A role in the immune tolerance to antigenic tumors. *Adv. Exp. Med. Biol.* 417: 525-528.
216. Morelli, A. E., A. T. Larregina, W. J. Shufesky, A. F. Zahorchak, A. J. Logar, G. D. Papworth, Z. Wang, S. C. Watkins, L. D. Falo, Jr., and A. W. Thomson. 2003. Internalization of circulating apoptotic cells by splenic marginal zone dendritic cells: dependence on complement receptors and effect on cytokine production. *Blood* 101: 611-620.
217. Makin, G., and J. A. Hickman. 2000. Apoptosis and cancer chemotherapy. *Cell Tissue Res.* 301: 143-152.
218. Balcer-Kubiczek, E. K. 2012. Apoptosis in radiation therapy: a double-edged sword. *Exp. Oncol.* 34: 277-285.

-
219. Hugel, B., M. C. Martinez, C. Kunzelmann, and J. M. Freyssinet. 2005. Membrane microparticles: two sides of the coin. *Physiology. (Bethesda.)* 20: 22-27.
220. Nilsson, U. R., L. Funke, B. Nilsson, and K. N. Ekdahl. 2011. Two conformational forms of target-bound iC3b that distinctively bind complement receptors 1 and 2 and two specific monoclonal antibodies. *Ups. J. Med. Sci.* 116: 26-33.
221. Inal, J. M., and J. A. Schifferli. 2002. Complement C2 receptor inhibitor trispanning and the beta-chain of C4 share a binding site for complement C2. *J. Immunol.* 168: 5213-5221.
222. Inal, J. M., K. M. Hui, S. Miot, S. Lange, M. I. Ramirez, B. Schneider, G. Krueger, and J. A. Schifferli. 2005. Complement C2 receptor inhibitor trispanning: a novel human complement inhibitory receptor. *J. Immunol.* 174: 356-366.
223. Fadok, V. A., D. R. Voelker, P. A. Campbell, J. J. Cohen, D. L. Bratton, and P. M. Henson. 1992. Exposure of phosphatidylserine on the surface of apoptotic lymphocytes triggers specific recognition and removal by macrophages. *J. Immunol.* 148: 2207-2216.
224. Kassianos, A. J., M. Y. Hardy, X. Ju, D. Vijayan, Y. Ding, A. J. Vulink, K. J. McDonald, S. L. Jongbloed, R. B. Wadley, C. Wells, D. N. Hart, and K. J. Radford. 2012. Human CD1c (BDCA-1)+ myeloid dendritic cells secrete IL-10 and display an immuno-regulatory phenotype and function in response to *Escherichia coli*. *Eur. J. Immunol.* 42: 1512-1522.
225. Toth, B., C. A. Lok, A. Boing, M. Diamant, J. A. van der Post, K. Friese, and R. Nieuwland. 2007. Microparticles and exosomes: impact on normal and complicated pregnancy. *Am. J. Reprod. Immunol.* 58: 389-402.
226. Berckmans, R. J., R. Nieuwland, M. C. Kraan, M. C. Schaap, D. Pots, T. J. Smeets, A. Sturk, and P. P. Tak. 2005. Synovial microparticles from arthritic patients modulate chemokine and cytokine release by synoviocytes. *Arthritis Res. Ther.* 7: R536-R544.
227. Boulanger, C. M., A. Scoazec, T. Ebrahimian, P. Henry, E. Mathieu, A. Tedgui, and Z. Mallat. 2001. Circulating microparticles from patients with myocardial infarction cause endothelial dysfunction. *Circulation* 104: 2649-2652.
228. Nomura, S., Y. Ozaki, and Y. Ikeda. 2008. Function and role of microparticles in various clinical settings. *Thromb. Res.* 123: 8-23.
229. Chironi, G., A. Simon, B. Hugel, P. M. Del, J. Gariepy, J. M. Freyssinet, and A. Tedgui. 2006. Circulating leukocyte-derived microparticles predict subclinical atherosclerosis burden in asymptomatic subjects. *Arterioscler. Thromb. Vasc. Biol* 26: 2775-2780.
230. Mallat, Z., B. Hugel, J. Ohan, G. Leseche, J. M. Freyssinet, and A. Tedgui. 1999. Shed membrane microparticles with procoagulant potential in human

- atherosclerotic plaques: a role for apoptosis in plaque thrombogenicity. *Circulation* 99: 348-353.
231. Morgan, B. P., and A. K. Campbell. 1985. The recovery of human polymorphonuclear leucocytes from sublytic complement attack is mediated by changes in intracellular free calcium. *Biochem. J* 231: 205-208.
232. Horstman, L. L., and Y. S. Ahn. 1999. Platelet microparticles: a wide-angle perspective. *Crit Rev. Oncol. Hematol.* 30: 111-142.
233. Bar-Yehuda, S., F. Barer, L. Volfsson, and P. Fishman. 2001. Resistance of muscle to tumor metastases: a role for α_3 adenosine receptor agonists. *Neoplasia*. 3: 125-131.
234. Parlakian, A., I. Gooma, S. Solly, L. Arandel, A. Mahale, G. Born, G. Marazzi, and D. Sassoon. 2010. Skeletal muscle phenotypically converts and selectively inhibits metastatic cells in mice. *PLoS. One.* 5: e9299.
235. Sarkar, A., S. Mitra, S. Mehta, R. Raices, and M. D. Wewers. 2009. Monocyte derived microvesicles deliver a cell death message via encapsulated caspase-1. *PLoS. One.* 4: e7140.
236. Grange, C., M. Tapparo, F. Collino, L. Vitillo, C. Damasco, M. C. Deregibus, C. Tetta, B. Bussolati, and G. Camussi. 2011. Microvesicles released from human renal cancer stem cells stimulate angiogenesis and formation of lung premetastatic niche. *Cancer Res.* 71: 5346-5356.
237. Camussi, G., M. C. Deregibus, S. Bruno, V. Cantaluppi, and L. Biancone. 2010. Exosomes/microvesicles as a mechanism of cell-to-cell communication. *Kidney Int.* 78: 838-848.
238. Bruno, S., C. Grange, M. C. Deregibus, R. A. Calogero, S. Saviozzi, F. Collino, L. Morando, A. Busca, M. Falda, B. Bussolati, C. Tetta, and G. Camussi. 2009. Mesenchymal stem cell-derived microvesicles protect against acute tubular injury. *J. Am. Soc. Nephrol.* 20: 1053-1067.
239. Muralidharan-Chari, V., J. W. Clancy, A. Sedgwick, and C. D'Souza-Schorey. 2010. Microvesicles: mediators of extracellular communication during cancer progression. *J. Cell Sci.* 123: 1603-1611.
240. Benameur, T., R. Andriantsitohaina, and M. C. Martinez. 2009. Therapeutic potential of plasma membrane-derived microparticles. *Pharmacol. Rep.* 61: 49-57.
241. Nickel, W., and M. Seedorf. 2008. Unconventional mechanisms of protein transport to the cell surface of eukaryotic cells. *Annu. Rev. Cell Dev. Biol.* 24: 287-308.
242. Mackenzie, A., H. L. Wilson, E. Kiss-Toth, S. K. Dower, R. A. North, and A. Surprenant. 2001. Rapid secretion of interleukin-1beta by microvesicle shedding. *Immunity.* 15: 825-835.

243. Combes, V., N. Coltel, M. Alibert, E. M. van, C. Raymond, I. Juhan-Vague, G. E. Grau, and G. Chimini. 2005. ABCA1 gene deletion protects against cerebral malaria: potential pathogenic role of microparticles in neuropathology. *Am. J. Pathol.* 166: 295-302.
244. Flieger, O., A. Engling, R. Bucala, H. Lue, W. Nickel, and J. Bernhagen. 2003. Regulated secretion of macrophage migration inhibitory factor is mediated by a non-classical pathway involving an ABC transporter. *FEBS Lett.* 551: 78-86.
245. Zahra, S., J. A. Anderson, D. Stirling, and C. A. Ludlam. 2011. Microparticles, malignancy and thrombosis. *Br. J. Haematol.* 152: 688-700.
246. Kothakota, S., T. Azuma, C. Reinhard, A. Klippel, J. Tang, K. Chu, T. J. McGarry, M. W. Kirschner, K. Koths, D. J. Kwiatkowski, and L. T. Williams. 1997. Caspase-3-generated fragment of gelsolin: effector of morphological change in apoptosis. *Science* 278: 294-298.
247. Geng, Y. J., T. Azuma, J. X. Tang, J. H. Hartwig, M. Muszynski, Q. Wu, P. Libby, and D. J. Kwiatkowski. 1998. Caspase-3-induced gelsolin fragmentation contributes to actin cytoskeletal collapse, nucleolysis, and apoptosis of vascular smooth muscle cells exposed to proinflammatory cytokines. *Eur. J. Cell Biol.* 77: 294-302.
248. Koya, R. C., H. Fujita, S. Shimizu, M. Ohtsu, M. Takimoto, Y. Tsujimoto, and N. Kuzumaki. 2000. Gelsolin inhibits apoptosis by blocking mitochondrial membrane potential loss and cytochrome c release. *J. Biol. Chem.* 275: 15343-15349.
249. Chhabra, D., N. J. Nosworthy, and C. G. dos Remedios. 2005. The N-terminal fragment of gelsolin inhibits the interaction of DNase I with isolated actin, but not with the cofilin-actin complex. *Proteomics.* 5: 3131-3136.
250. Azuma, T., K. Koths, L. Flanagan, and D. Kwiatkowski. 2000. Gelsolin in complex with phosphatidylinositol 4,5-bisphosphate inhibits caspase-3 and -9 to retard apoptotic progression. *J. Biol. Chem.* 275: 3761-3766.
251. Winston, J. S., H. L. Asch, P. J. Zhang, S. B. Edge, A. Hyland, and B. B. Asch. 2001. Downregulation of gelsolin correlates with the progression to breast carcinoma. *Breast Cancer Res. Treat.* 65: 11-21.
252. Lee, H. K., D. Driscoll, H. Asch, B. Asch, and P. J. Zhang. 1999. Downregulated gelsolin expression in hyperplastic and neoplastic lesions of the prostate. *Prostate* 40: 14-19.
253. Gay, F., Y. Estornes, J. C. Saurin, M. O. Joly-Pharaboz, E. Friederich, J. Y. Scoazec, and J. Abello. 2008. In colon carcinogenesis, the cytoskeletal protein gelsolin is down-regulated during the transition from adenoma to carcinoma. *Hum. Pathol.* 39: 1420-1430.
254. Shieh, D. B., I. W. Chen, T. Y. Wei, C. Y. Shao, H. J. Chang, C. H. Chung, T. Y. Wong, and Y. T. Jin. 2006. Tissue expression of gelsolin in oral

- carcinogenesis progression and its clinicopathological implications. *Oral Oncol.* 42: 599-606.
255. Sagawa, N., H. Fujita, Y. Banno, Y. Nozawa, H. Katoh, and N. Kuzumaki. 2003. Gelsolin suppresses tumorigenicity through inhibiting PKC activation in a human lung cancer cell line, PC10. *Br. J. Cancer* 88: 606-612.
 256. Tanaka, H., R. Shirkoohi, K. Nakagawa, H. Qiao, H. Fujita, F. Okada, J. Hamada, S. Kuzumaki, M. Takimoto, and N. Kuzumaki. 2006. siRNA gelsolin knockdown induces epithelial-mesenchymal transition with a cadherin switch in human mammary epithelial cells. *Int. J. Cancer* 118: 1680-1691.
 257. Musse, A. A., E. Polverini, R. Raijmakers, and G. Harauz. 2008. Kinetics of human peptidylarginine deiminase 2 (hPAD2)--reduction of Ca²⁺ dependence by phospholipids and assessment of proposed inhibition by paclitaxel side chains. *Biochem. Cell Biol.* 86: 437-447.
 258. van Beers, J. J., C. M. Schwarte, J. Stammen-Vogelzangs, E. Oosterink, B. Bozic, and G. J. Pruijn. 2013. The rheumatoid arthritis synovial fluid citrullinome reveals novel citrullinated epitopes in apolipoprotein E, myeloid nuclear differentiation antigen, and beta-actin. *Arthritis Rheum.* 65: 69-80.
 259. Luo, Y., B. Knuckley, Y. H. Lee, M. R. Stallcup, and P. R. Thompson. 2006. A fluoroacetamide-based inactivator of protein arginine deiminase 4: design, synthesis, and in vitro and in vivo evaluation. *J. Am. Chem. Soc.* 128: 1092-1093.
 260. Knuckley, B., Y. Luo, and P. R. Thompson. 2008. Profiling Protein Arginine Deiminase 4 (PAD4): a novel screen to identify PAD4 inhibitors. *Bioorg. Med. Chem.* 16: 739-745.
 261. Barry, O. P., D. Pratico, R. C. Savani, and G. A. FitzGerald. 1998. Modulation of monocyte-endothelial cell interactions by platelet microparticles. *J Clin. Invest* 102: 136-144.
 262. Cestari, I., E. Ansa-Addo, P. Deolindo, J. M. Inal, and M. I. Ramirez. 2012. Trypanosoma cruzi immune evasion mediated by host cell-derived microvesicles. *J. Immunol.* 188: 1942-1952.
 263. Verbovetski, I., H. Bychkov, U. Trahtemberg, I. Shapira, M. Hareuveni, O. Ben-Tal, I. Kutikov, O. Gill, and D. Mevorach. 2002. Opsonization of apoptotic cells by autologous iC3b facilitates clearance by immature dendritic cells, down-regulates DR and CD86, and up-regulates CC chemokine receptor 7. *J. Exp. Med.* 196: 1553-1561.
 264. Chen, X., K. Doffek, S. L. Sugg, and J. Shilyansky. 2004. Phosphatidylserine regulates the maturation of human dendritic cells. *J. Immunol.* 173: 2985-2994.
 265. Morelli, A. E., A. T. Larregina, W. J. Shufesky, A. F. Zahorchak, A. J. Logar, G. D. Papworth, Z. Wang, S. C. Watkins, L. D. Falo, Jr., and A. W. Thomson. 2003. Internalization of circulating apoptotic cells by splenic

- marginal zone dendritic cells: dependence on complement receptors and effect on cytokine production. *Blood* 101: 611-620.
266. Gaither, T. A., C. H. Hammer, and M. M. Frank. 1979. Studies of the molecular mechanisms of C3b inactivation and a simplified assay of beta 1H and the C3b inactivator (C3bINA). *J. Immunol.* 123: 1195-1204.
267. Mevorach, D., J. O. Mascarenhas, D. Gershov, and K. B. Elkon. 1998. Complement-dependent clearance of apoptotic cells by human macrophages. *J. Exp. Med.* 188: 2313-2320.
268. Steinman, R. M., S. Turley, I. Mellman, and K. Inaba. 2000. The induction of tolerance by dendritic cells that have captured apoptotic cells. *J. Exp. Med.* 191: 411-416.
269. Steinman, R. M., and M. C. Nussenzweig. 2002. Avoiding horror autotoxicus: the importance of dendritic cells in peripheral T cell tolerance. *Proc. Natl. Acad. Sci. U. S. A* 99: 351-358.
270. Liu, C., S. Yu, K. Zinn, J. Wang, L. Zhang, Y. Jia, J. C. Kappes, S. Barnes, R. P. Kimberly, W. E. Grizzle, and H. G. Zhang. 2006. Murine mammary carcinoma exosomes promote tumor growth by suppression of NK cell function. *J. Immunol.* 176: 1375-1385.
271. Szajnik, M., M. Czystowska, M. J. Szczepanski, M. Mandapathil, and T. L. Whiteside. 2010. Tumor-derived microvesicles induce, expand and up-regulate biological activities of human regulatory T cells (Treg). *PLoS. One.* 5: e11469.
272. Wieckowski, E. U., C. Visus, M. Szajnik, M. J. Szczepanski, W. J. Storkus, and T. L. Whiteside. 2009. Tumor-derived microvesicles promote regulatory T cell expansion and induce apoptosis in tumor-reactive activated CD8+ T lymphocytes. *J. Immunol.* 183: 3720-3730.
273. Yu, S., C. Liu, K. Su, J. Wang, Y. Liu, L. Zhang, C. Li, Y. Cong, R. Kimberly, W. E. Grizzle, C. Falkson, and H. G. Zhang. 2007. Tumor exosomes inhibit differentiation of bone marrow dendritic cells. *J. Immunol.* 178: 6867-6875.
274. Stahl, A. L., L. Sartz, and D. Karpman. 2011. Complement activation on platelet-leukocyte complexes and microparticles in enterohemorrhagic *Escherichia coli*-induced hemolytic uremic syndrome. *Blood* 117: 5503-5513.
275. Gasser, O., and J. A. Schifferli. 2004. Activated polymorphonuclear neutrophils disseminate anti-inflammatory microparticles by ectocytosis. *Blood* 104: 2543-2548.
276. Akbari, O., and D. T. Umetsu. 2005. Role of regulatory dendritic cells in allergy and asthma. *Curr. Allergy Asthma Rep.* 5: 56-61.